

Towards a new classification of galaxies: principal component analysis of CALIFA circular velocity curves

V. Kalinova^{1,2*}, D. Colombo^{1,2}, E. Rosolowsky¹, R. Kannan³, L. Galbany⁴,
 R. García-Benito⁵, R. González Delgado⁵, S. F. Sánchez⁶, T. Ruiz-Lara^{7,8,9,10},
 J. Méndez-Abreu¹¹, C. Catalán-Torrecilla¹², L. Sánchez-Menguiano^{5,7},
 A. de Lorenzo-Cáceres^{7,11}, L. Costantin¹³, E. Florido^{7,8}, K. Kodaira²,
 R. A. Marino¹⁴, R. Láska¹⁵, J. Bland-Hawthorn¹⁶

¹ Department of Physics 4-181 CCIS, University of Alberta, Edmonton AB T6G 2E1, Canada

² Max Planck Institute for Radio Astronomy, Auf dem Hügel 69, D-53121 Bonn, Germany

³ Department of Physics, Kavli Institute for Astrophysics & Space Research, Massachusetts Institute of Technology, Cambridge, MA 02139, USA

⁴ PITT PACC, Department of Physics and Astronomy, University of Pittsburgh, Pittsburgh, PA 15260, USA

⁵ Instituto de Astrofísica de Andalucía, CSIC, Apartado de correos 3004, E-18080 Granada, Spain

⁶ Instituto de Astronomía, Universidad Nacional Autónoma de México, A.P. 70-264, 04510 México, D.F., México

⁷ Departamento de Física Teórica y del Cosmos, Universidad de Granada, Campus de Fuentenueva, E-18071 Granada, Spain

⁸ Instituto Carlos I de Física Teórica y Computacional, Universidad de Granada, E-18071 Granada, Spain

⁹ Instituto de Astrofísica de Canarias, Calle Vía Láctea s/n, E-38205 La Laguna, Tenerife, Spain

¹⁰ Departamento de Astrofísica, Universidad de La Laguna, E-38200 La Laguna, Tenerife, Spain

¹¹ School of Physics and Astronomy, University of St. Andrews, SUPA, North Haugh, St. Andrews, KY16 9SS, UK

¹² Departamento de Astrofísica y CC. de la Atmósfera, Universidad Complutense de Madrid, E-28040 Madrid, Spain

¹³ Dipartimento di Fisica e Astronomia 'G. Galilei', Università di Padova, vicolo dell'Osservatorio 3, I-35122 Padova, Italy

¹⁴ Department of Physics, Institute for Astronomy, ETH Zürich, CH-8093 Zürich, Switzerland

¹⁵ Finnish Centre for Astronomy with ESO (FINCA), University of Turku, Väistöläntie 20, FI-21500 Kaarina, Finland

¹⁶ Sydney Institute for Astronomy, School of Physics A28, University of Sydney, NSW 2006, Australia

Accepted 2017 April 8. Received 2017 April 4; in original form 2016 December 12

ABSTRACT

We present a galaxy classification system for 238 (E1–Sdm) CALIFA (Calar Alto Legacy Integral Field Area) galaxies based on the shapes and amplitudes of their circular velocity curves (CVCs). We infer the CVCs from the de-projected surface brightness of the galaxies, after scaling by a constant mass-to-light ratio based on stellar dynamics - solving axisymmetric Jeans equations via fitting the second velocity moment $V_{\text{rms}} = \sqrt{V^2 + \sigma^2}$ of the stellar kinematics. We use principal component analysis (PCA) applied to the CVC shapes to find characteristic features and use a k -means classifier to separate circular curves into classes. This objective classification method identifies four different classes, which we name slow-rising (SR), flat (FL), round-peaked (RP) and sharp-peaked (SP) circular curves.

SR are typical for low-mass, late-type (Sb–Sdm), young, faint, metal-poor and disc-dominated galaxies. SP are typical for high-mass, early-type (E1–E7), old, bright, metal-rich and bulge-dominated galaxies. FL and RP appear presented by galaxies with intermediate mass, age, luminosity, metallicity, bulge-to-disk ratio and morphologies (E4-S0a, Sa-Sbc). The discrepancy mass factor, $f_d = 1 - M_*/M_{\text{dyn}}$, have the largest value for SR and SP classes (~ 74 per cent and ~ 71 per cent, respectively) in contrast to the FL and RP classes (with ~ 59 per cent and ~ 61 per cent, respectively). Circular curve classification presents an alternative to typical morphological classification and appears more tightly linked to galaxy evolution.

Key words: methods: data analysis – methods: statistical – galaxies: evolution – galaxies: kinematics and dynamics – galaxies: structure

1 INTRODUCTION

Circular velocity curves (CVCs) are considered one of the best tools to trace the mass distribution of galaxies. Since the earliest studies (Rubin, Ford & Thonnard 1980; Bosma 1981; Persic & Salucci 1988), the non-Keplerian shape of the curves implied that the mass derived with this technique was much higher than the total luminous mass (accounting for stars and gas). This inconsistency suggested that a significant fraction of galaxies is dark matter (hereafter DM), which becomes progressively more dominant towards the outskirts of the galaxies (Persic & Salucci 1988; Broeils 1992).

Moreover, the shape and the amplitude of CVCs¹ are both closely related to the gravitational potential of the galaxy, and therefore, can be used to obtain important information about the different components of the galaxies (Noordermeer et al. 2007).

In almost all disc galaxies, the stellar disc contribution can be scaled to explain all features of the observed CVCs out to ~ 2 disc scale lengths (e.g., Kalnajs 1983; Palunas & Williams 2000). This indicates that the total mass density and luminous mass density are closely connected (e.g., Sancisi 2004; Swaters et al. 2009).

There are several indications that the *shape* of the CVC, in addition to its overall amplitude, is connected to galaxy properties and possibly evolution. Rubin et al. (1985) pointed out that, within the same morphological type, spiral galaxies show a progression of central velocity gradients and maximum circular velocities with increasing absolute luminosities. The correlation between the light distribution and the inner rise of the CVCs is well known for spiral galaxies (e.g., Kent 1987; Corradi & Capaccioli 1990). Swaters et al. (2009) have found that dwarf galaxies with a central concentration of light also have CVCs that rise more steeply in the centre than the CVCs of dwarf galaxies that do not have a central concentration of light. They observed a correlation between the light distribution and the inner CVC shape, as seen in both spiral and late-type dwarf galaxies, implying that galaxies with stronger central concentrations of light also have higher central mass densities. This correlation suggests that the luminous mass dominates the gravitational potential in the central regions, even in low surface brightness (SB) dwarf galaxies.

Avila-Reese, Firmani & Zavala (2002) discuss the shapes and decomposition of CVCs of galaxies formed within growing cold dark matter haloes. They find that CVC shape correlates mainly with the SB, the luminous mass fraction, and the bulge fraction of the galaxies. Further, the galaxy's SB scales with the bulge-to-disc (B/D) ratio, and a steeper slope of decline from a high peak in the CVC. Their high-SB models can be maximal discs only when the haloes have a shallow core. The low-SB models possess sub-maximal discs containing DM (Sackett 1997).

The shape and the amplitude of the CVCs reflect the mass distribution of both luminous matter and DM in galaxies (e.g., Zasov & Kyazumov 1983; Corradi & Capaccioli 1990; Swaters et al. 2009; Martinsson et al. 2013). The next step is to classify the CVCs by common properties and try to draw global conclusions for the internal structure of the galaxies, formation and evolution, through studying large data sets with diversity in morphological types.

¹ When we discuss HI 21-cm CVCs in the paper, we usually refer to their rotation curve, i.e., azimuthal velocity V_ϕ . We use this approximation here since for cold gas it is valid $V_c \approx V_\phi$, where the vertical component of the velocity is negligible (Binney & Merrifield 1998).

There is a suite of dynamics-based classification schemes already present in the literature. We describe several of these approaches below, focusing on those studies with similar data, approaches or outcomes that are relevant to this work. For example, classification of HI 21-cm CVCs was proposed by Sofue et al. (1999) using a large sample of Sb–Sc galaxies. They observe a steep nuclear rise of galaxy CVC and conclude that is a universal property for massive Sb and Sc galaxies, regardless of the existence of a bar and morphological peculiarities. However, less massive galaxies tend to show a rigid-body rise. They classify the observed CVCs into the following three types, according to their behaviour in the central regions. *Central Peak* type: CVC attains a sharp maximum near the centre at $R \sim 100$ –500 pc, followed by a dip at ~ 1 kpc, then by a broad maximum of the disc component (e.g., Milky Way). *No-Central Peak* type: The CVC rises steeply at the center, followed immediately by a flat part. *Rigid-body* type: the CVC increases mildly from the centre in a rigid-body fashion within the central 1 kpc. This type is found in less massive Sc-type galaxies and it has been already reported by Casertano & van Gorkom (1991).

Wakamatsu (1976) proposes a two-dimensional classification of 22 disc galaxies using their optical and/or HI 21-cm CVCs. For the goal, Wakamatsu (1976) use two independent parameters: k ($= V_{\max}^2/r_{\max}$) and \mathcal{M} (mass of galaxy within Holmberg's radius; Holmberg 1958), where k is the centrifugal force at the radius r_{\max} and maximum value of the circular velocity, V_{\max} . The parameter k is found to be correlated with the morphological type (decreasing from early-type to late-type galaxies) and the mass ratio of the bulge to the disc, but not correlated with \mathcal{M} . Using dynamical properties of the 22 galaxies, they also find that late-type galaxies have systematically larger angular momenta and smaller rotational energies in comparison to early-type galaxies.

Shostak (1977) shows a relation between a galaxy's Hubble type and the shape of its HI profile. They find a type progression from Sbc to Irr, where the CVC (represented by two linear sections) turnover radius increases relative to the full width at half-maximum (FWHM) of HI line. They find that Sbc galaxies have CVCs that rise three to five times faster, relatively to their HI radii, than those of irregular galaxies. This indicates a greater degree of central mass concentration in the earlier types.

Biviano et al. (1991) find a significant correlation between the velocity gradients of 94 spiral galaxies and their arm classes (as given by Elmegreen & Elmegreen 1982), where galaxies with steeper curves tend to have a flocculent arm structure, and galaxies with flatter curves tend to have a grand design morphology. This result is consistent with the predictions of density wave theory for the formation of the spiral structure (Lin & Shu 1964).

Keel (1993) classifies a set of spiral galaxies in pairs regarding their velocity structure in a few major classes. *Normal* – galaxies with quickly rising velocity from the nucleus to a flat plateau; *Solid-body* (or linear) – galaxies with solid-body rotation, sometimes extended over the entire measured area; *Slow* – non-rotating or slow-rotating galaxies with total amplitudes no greater than 50 km s^{-1} despite elongated shapes and fairly high luminosities; *Dist* – galaxies with disturbed or asymmetric velocity patterns. Enhanced star formation is found for galaxies with large areas of solid-body rotation and for galaxies with more general kinds of disturbed velocity structure, with the highest levels occurring in a set of galaxies distinguished by anomalously small overall velocity amplitude.

Chattopadhyay & Chattopadhyay (2006) carry out an objective classification of four samples of spiral galaxies having extended CVCs beyond the optical radius. A multivariate statistical analysis

(namely, principal component analysis, PCA) shows that about 96% of the total variation is due to two components, one being the combination of absolute blue magnitude and maximum velocity beyond the optical region and the other being the central density of the halo. On the basis of PCA, a Fundamental Plane has been constructed that reduces the scatter in the Tully–Fisher relation up to 16%. A multiple stepwise regression analysis of the variation of the overall shape of the CVCs shows that it is mainly determined by the central SB, while the shape purely in the outer part of the galaxy (beyond the optical radius) is mainly determined by the size of the galactic disc.

Márquez & Moles (1999) also apply PCA to the properties of 22 isolated spiral galaxies and found a tight correlation between the B/D ratio of the galaxies and the gradient of the solid-body rotation region of the optical rotation curve, G . This parameter is defined as $G = (v_G^{ob}/\sin i)/r_G$, where r_G (in kpc) is the radius of the inner region of solid-body rotation, v_G^{ob} (in km s^{-1}) is the observed velocity amplitude at r_G and i is the galaxy disc inclination. Furthermore, they found that their sample of isolated galaxies can be described by two eigenvectors representing 95 % of the total variance: a scale parameter set by the size of the galaxy (or the total luminosity or the total mass) and the B/D ratio (or the G parameter).

Wiegert & English (2014) present a kinematic classification of 79 non-interacting spiral galaxies using their neutral hydrogen (HI) CVCs. Their method employs a simple parametrized form for the CVC to derive the three parameters: the maximum rotational velocity, the turnover radius, and a measure of the slope of the CVC beyond the turnover radius. Wiegert & English (2014) also use the statistical hierarchical clustering method to guide their division of the resultant 3D distribution of galaxies into five classes. The class that contains galaxies with the largest rotational velocities has a mean morphological type of Sb/Sbc while the other classes tend to later types. They confirm correlations between increasing maximum rotational velocity and the following observed properties such as increasing brightness in the B -band, increasing size of the optical disc (D_{25}) and increasing star formation rate. The analysis also suggests that lower velocities are associated with a higher ratio of the HI mass over the dynamical mass.

Other classification approaches have been forwarded in various studies (Spitzer & Baade 1951; van den Bergh 1976; Poggianti et al. 1999) and modern observations are providing reason to raise the question of galaxy classification again (e.g., Bertin 2000, section 18.2). For example, the recent study of 260 early-type galaxies (E/S0) by Cappellari et al. (2011) as part of ATLAS^{3D} project gives an overview of the limitations of the classic Hubble (1936) tuning-fork diagram. They show, instead, the usefulness of a scheme similar to the one proposed by van den Bergh (1976) to properly understand the morphology of early-type galaxies. The authors consider two classes of objects: (i) slow rotators, which are consistent with being genuinely elliptical-like objects with intrinsic ellipticity $\epsilon \gtrsim 0.4$; and (ii) the fast rotators, which are generally flatter than $\epsilon \lesssim 0.4$ and are morphologically similar to spiral galaxies, or in some cases to flat ellipticals with discy isophotes, and span the same full range of bulge sizes of spirals. They argued for a revised comb-shaped scheme to represent the morphology of nearby galaxies, which overcomes the limitations of the tuning-fork diagram.

Despite the rich previous literature, most past work has relied on CVCs to infer other galaxy properties, using by-eye classification schemes, or simple approximations to CVC shapes. In this work, we use PCA to fully describe the shape and amplitude of the CVCs across its full extent. This work uses CVCs derived from the stellar disc, in contrast with most of previous work that usually re-

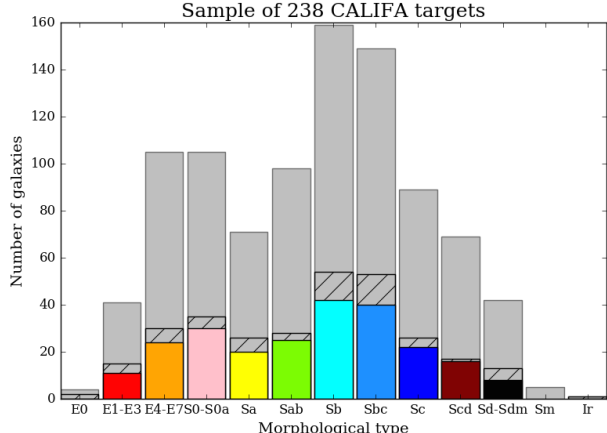


Figure 1. Distribution of our 238 galaxy sub-sample through Hubble type (colour) compared with CALIFA mother sample of 939 targets (grey, Walcher et al. 2014) and with stellar kinematics galaxy sample of 300 galaxies (hatched lines, Falcón-Barroso et al. 2017). The sub-sample of 238 targets well represents through morphology both CALIFA mother sample and stellar kinematics sample.

lies on interstellar medium (ISM) tracers, typically HI 21-cm data. This allows us to study the internal structure of the galaxies from all Hubble types (E1–Sdm), since not all galaxies contain significant amount of neutral gas (Longair 2008). In addition, stellar dynamics is more sensitive to dynamically hot stellar components like bulges and may provide a tighter connection to the evolution of the galaxies.

We introduce the data and sample, needed to probe the shape and amplitude of the galaxy circular curves in Section 2. Section 3 describes the analysis approach used in our study - dynamical modelling, PCA applied to circular curves and k -means statistics. We propose a CVC classification of our sample of galaxies in Section 4, and examine a possible genesis of the proposed CVC classes in Section 5. The main uncertainties of our results are discussed in Section 6. An example application of our classification is presented in Section 7, and we make our conclusions in Section 8.

2 SAMPLE AND DATA

2.1 Sample selection

We select our galaxies from the sample of Falcón-Barroso et al. (2017), who provide reliable stellar kinematics of 300 galaxies from the Calar Alto Legacy Intergal Field Area (CALIFA) survey² (Sánchez et al. 2012) observed until 2014 June. From the original sample of 300 galaxies, we discard galaxy mergers and those cases where the dynamical models of the galaxies were not of sufficient quality for our study (see Section 3.1). The final sub-sample consists of 238 CALIFA targets with various masses and morphologies from elliptical (E1) to late-type (Sdm) galaxies. The distribution of the Hubble type (in colour) for the 238 CALIFA galaxies sample is shown in Fig. 1, which is compared with CALIFA mother sample of 939 targets (grey; Walcher et al. 2014) and with stellar kinematics galaxy sample of 300 galaxies (hatched lines; Falcón-Barroso et al. 2017). The sub-sample of 238 targets well represents through

² <http://califa.caha.es/>

Hubble sequence both the CALIFA mother sample and stellar kinematics sample. The morphology of all CALIFA galaxies has been defined after visual examination by several members of the CALIFA team. We refer the reader to Walcher et al. (2014) for further details related to the selection procedure and statistical properties of the CALIFA mother sample³.

2.2 Stellar kinematics and imaging

The observations of the 238 CALIFA galaxies have been made by using the integral-field spectroscopic instrument PMAS (Roth et al. 2005) in PPaK mode (Verheijen et al. 2004), mounted on the 3.5 m telescope at the Calar Alto Observatory.

To obtain well resolved stellar kinematics for these galaxies, Falcón-Barroso et al. (2017) used the mid-resolution prism data (V1200 with $R \sim 1650$) having the coverage of the nominal wavelength range 3850–4600 Å at an FWHM spectral resolution of ~ 2.3 Å, i.e., $\sigma \sim 85$ km s $^{-1}$ and a $74'' \times 64''$ hexagonal field of view (FoV). The exposure time per pointing has been fixed to 1800 s, split into two or three individual exposures (Sánchez et al. 2012; Husemann et al. 2013; García-Benito et al. 2015). The stellar kinematics used in this study is based on data from CALIFA v1.4 reduction pipeline (Sánchez et al. 2012; Husemann et al. 2013; García-Benito et al. 2015). Falcón-Barroso et al. (2017) extracted the stellar kinematic maps from the CALIFA data cubes using the PPXF fitting procedure (Cappellari & Emsellem 2004) with a subset of ~ 300 stars from the INDO-US (Valdes et al. 2004) spectral templates library. In the case the full library is applied, the stellar kinematic results will be reproducible (see section 4 of their paper). Furthermore, Falcón-Barroso et al. (2017) spatially binned the data cube using the Voronoi 2D binning algorithm of Cappellari & Copin (2003) to obtain signal-to-noise ratio of ~ 20 and, hence, reliable stellar kinematics. For most of the galaxies, the FoV covers a radial extent R_{\max} of one to two times of the galaxy’s half-light radius, R_e (see Table 1 of Falcón-Barroso et al. 2017). We also calculate the systemic velocity of the 238 CALIFA galaxies (V_{sys}) as the median value of the velocity field (see Tables B1–B6).

To obtain the SB of the 238 CALIFA galaxies, we use the r -band photometric images from the Sloan Digital Sky Survey⁴ (SDSS; York et al. 2000) using Data Release 12⁵ (DR12; Alam et al. 2015), which have already been flux calibrated and sky subtracted.

3 ANALYSIS

In this paper, we aim to explore a new classification method based on the dynamics of the 238 CALIFA galaxies given their V and σ stellar kinematic maps and photometric images. We use the maps and the images of the galaxies to construct a reliable dynamical model and derive the CVCs. We then use the suite of 238 CVCs to define a basis set of generalized circular curve components using PCA. These basis curves are used to project the CVCs into a basis space, where each curve can be represented by a linear combination of the basis set. We use two-dimensional k -means clustering

³ The sample characterization tables (e.g., morphological type, effective radius, etc.) from Walcher et al. (2014) can be found here: http://www.caha.es/CALIFA/public_html/?q=content/sample-characterization-tables

⁴ <http://www.sdss.org/>

⁵ <http://data.sdss3.org/>

of points in the space of the two main components of the PCA to define four classes of CVCs, providing a new galaxy classification framework.

3.1 JAM-MCMC CVC derivation

To reliably derive the total CVCs of our sample of galaxies from the CALIFA stellar kinematic fields, we use the axisymmetric Jeans anisotropic multi-Gaussian expansion (JAM; Cappellari 2008) dynamical model with the basic assumptions of a constant velocity anisotropy in the meridional plane $\beta_z = 1 - \sigma_z^2/\sigma_R^2$ and a constant mass-to-light ratio $(M/L)_{\text{dyn}}$ of the galaxies. We obtain the values of these two parameters by fitting the observed second-order velocity moment $V_{\text{rms}}^2 = V^2 + \sigma^2$ using the PYTHON version of the JAM⁶ method. Further, we apply a Markov chain Monte Carlo (MCMC) technique to constrain the parameter space in JAM model (Cappellari 2008) between the two fitting parameters – β_z and $(M/L)_{\text{dyn}}$ (see Kalinova et al. 2017). We also symmetrized our observed V_{rms}^2 fields before applying JAM-MCMC code in order to reduce outliers in the data (see Cappellari et al. 2015). In this case, our χ^2 -statistics for fitting the V_{rms}^2 field will be less influenced by a few deviant values. This is especially important when one applies MCMC analysis.

Due to the large computational expense of evaluating JAM-MCMC model, we run the code with only 30 walkers, though the model still converged with only 30 steps for burn-in phase and 80 steps for sampling. The prior distributions of the parameters were taken to be uniform with, e.g., $\beta_z \in [-1, 1]$ and $(M/L)_{\text{dyn}} \in [0, 20] M_\odot/L_\odot$. For the calculation of the dynamical models, we fixed the inclination i of the galaxies to the photometric value, estimated from the ellipticity (ϵ) of the galaxies using equation 1 in Kalinova et al. (2017, where ϵ is the average ellipticity, determined from `findgalaxy` python procedure of Cappellari 2002). For those galaxies where the calculated photometric inclination was below the minimum allowed multi-Gaussian expansion (MGE) inclination (i^{MGE}) of JAM approach (see section 2.2.2 in Cappellari 2002), we adopt $i = i^{MGE}$ (see Tables B1–B6).

In Appendix A, Figs A1–A8, we present the second moment maps $V_{\text{rms}} = \sqrt{V^2 + \sigma^2}$ of the data ($V_{\text{rms}}^{\text{OBS}}$; first columns) and the best-fitting models of the JAM-MCMC method ($V_{\text{rms}}^{\text{MOD}}$; second columns) with overplotted fluxes and MGE contours, respectively. The third columns correspond to the residual field between the observed and modelled V_{rms} maps, where $RES = |1 - (V_{\text{rms}, \text{OBS}}/V_{\text{rms}, \text{MOD}})|$. On average, the median value of the residual maps $RES \sim 0.10$ for most of the 238 CALIFA galaxies, which corresponds to around 10 per cent error. We initially discarded galaxies with not well-defined minima of the prior chain distributions for the parameters β_z or $(M/L)_{\text{dyn}}$ (see section 4.3.2 and appendix B of Kalinova et al. 2017 for examples).

Next, we derived the CVCs of the 238 CALIFA galaxies by applying Poisson’s equation to the best fitting gravitational potential and calculating $V_c^2 = R \frac{\partial \Phi}{\partial R}|_{z=0}$. We calculate the $\Phi(R, z)$ through the MGE method (MGE; Monnet, Bacon & Emsellem 1992; Emsellem, Monnet & Bacon 1994). It describes the observed SB of the galaxies as a sum of N Gaussian components, which also allows us to reproduce the photometry of the galaxies in detail,

$$I(x', y') = \sum_{j=0}^N I_{0,j} \exp \left\{ -\frac{1}{2\xi_j'^2} \left[x'^2 + \frac{y'^2}{q_j'^2} \right] \right\}, \quad (1)$$

⁶ <http://purl.org/cappellari/software>

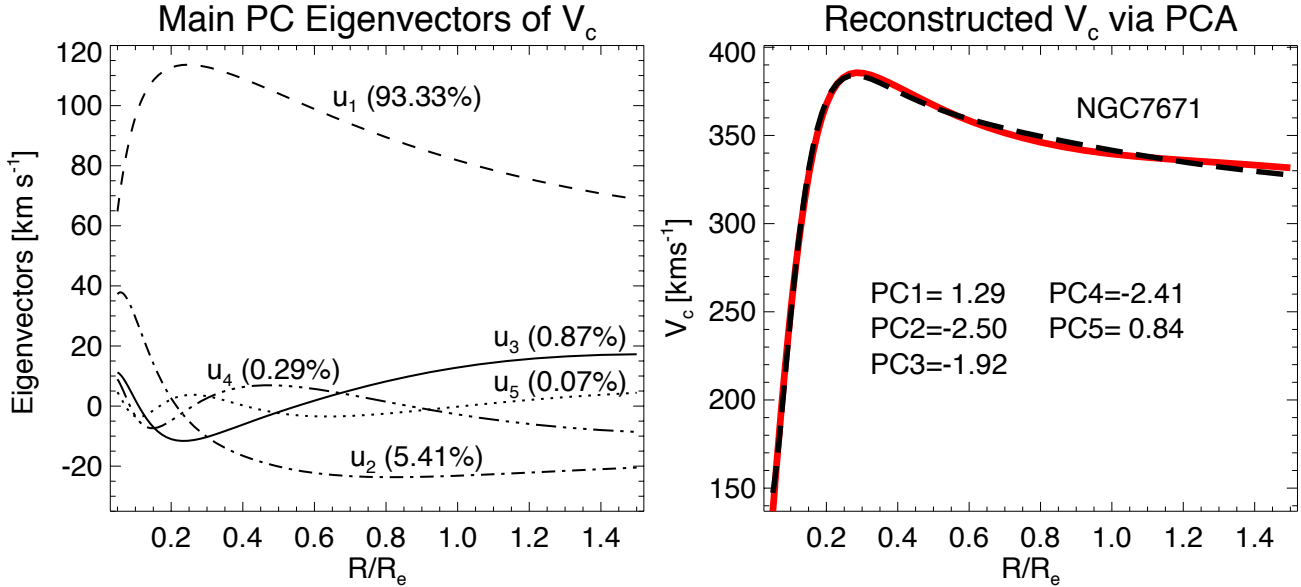


Figure 2. PCA. *Left:* the main five principal component eigenvectors \mathbf{u} , needed to reconstruct the CVCs of the 238 CALIFA galaxies shown with the corresponding fraction of power in that component. *Right:* example of the reconstructed circular velocity (red curve) of the galaxy NGC7671 after applying PCA, where V_c (black dashed curve) is the linear combination between the five main PC eigenvectors \mathbf{u} and projections PC_i .

where $I_{0,j}$ is the central SB, ξ'_j is the dispersion along the major x' -axis and q'_j is the flattening. The intrinsic dispersion and flattening, ξ_j and q_j , are related to their observed (i.e., plane-of-sky) quantities, as

$$\xi_j = \xi'_j \quad \text{and} \quad q'^2_j = \cos^2 i + q_j^2 \sin^2 i, \quad (2)$$

where the inclination i ranges from $i = 0^\circ$ for face-on viewing to $i = 90^\circ$ for edge-on viewing.

We apply the MGE fitting method to the r -band SDSS images using the software implementation of Cappellari (2002). We also take into account the point spread function (PSF) convolution, where the median PSF FWHM is 1.3 arcsec for the r -band SDSS images. The resulting analytically deconvolved MGE model for each galaxy was corrected for extinction as given by NASA/IPAC Extragalactic Database⁷ (NED). It was converted to an SB in solar units assuming the r -band absolute magnitude for the Sun of $M_{r,\odot} = 4.68$ mag (table 1.3 of Sparke & Gallagher 2007). Additionally, we adopt the ‘bulge-disc decomposition’ keyword in the software implementation of Cappellari (2002) when performing the MGE fits. In this case, the Gaussians were separated into two groups, where each of them described more efficiently the bulge and disc of the spiral/lenticular galaxies, or the nuclear disk of the ellipticals. The MGE fit parameters are listed in Appendix E.

The MGE parametrization can be deprojected analytically into an intrinsic luminosity density $\nu(R, z)$ when the viewing direction is given. Furthermore, the calculation of v_{los}^2 reduces from the (numerical) evaluation of a triple integral to a straightforward single integral (Cappellari 2008, equation 27). Similarly, the gravitational potential $\Phi(R, z)$ can be calculated by means of one-dimensional integral (Emsellem, Monnet & Bacon 1994, equation 39).

⁷ The NASA/IPAC Extragalactic Database (NED) is operated by the Jet Propulsion Laboratory, California Institute of Technology, under contract with the National Aeronautics and Space Administration, (<https://ned.ipac.caltech.edu/>)

Given the latter, the circular velocity from the JAM model in the equatorial plane then follows upon (numerical) evaluation of

$$v_{c,\text{JAM}}^2(R) = \sum_{j=0}^N \frac{2G L_j (M/L)_j}{\sqrt{2\pi} \xi_j} \frac{R^2}{\xi_j^2} \times \int_0^1 \exp \left\{ -\frac{u^2 R^2}{2\xi_j^2} \right\} \frac{u^2 du}{\sqrt{1 - (1 - q_j^2)u^2}}, \quad (3)$$

where $L_j \equiv 2\pi \xi_j^2 q'_j I_{0,j}$ and $(M/L)_j$ are the total luminosity and the mass-to-light ratio of the j th Gaussian. Since we assume that mass follows light in our dynamical model, $(M/L)_j$ is the same for all Gaussians, i.e., $(M/L)_{\text{dyn}} = (M/L)_j$ (see section 3.2 of Kalinova et al. 2017).

3.2 Principal Component Analysis

A common criticism of the visual classifications in general is that the criteria for assigning galaxies to classes are subjective, leading to different observers assigning galaxies to different classes. To develop an objective classification scheme, we use PCA (Pearson 1901) applied to the CVCs to classify the 238 E1–Sdm galaxies by their dynamics. PCA is a powerful approach to identify patterns in broad range of data, and expressing the data in such a way as to highlight their similarities and differences (e.g., Shlens 2014).

PCA operates by constructing a covariance matrix between data sets, diagonalizing that matrix and using the resulting eigenvectors as a basis set for the new space. We normalize the radial coordinate to the effective radius R_e and interpolate each circular curve V_c to a common radial sampling, using 50 points spanning $R/R_e \in [0, 1.5]$.

We construct a covariance between the j th and k th sample on the velocity curve as

$$\sigma_{jk} = \sum_i (v_{c,i}(R_j) - \bar{V}_c)(v_{c,i}(R_k) - \bar{V}_c), \quad (4)$$

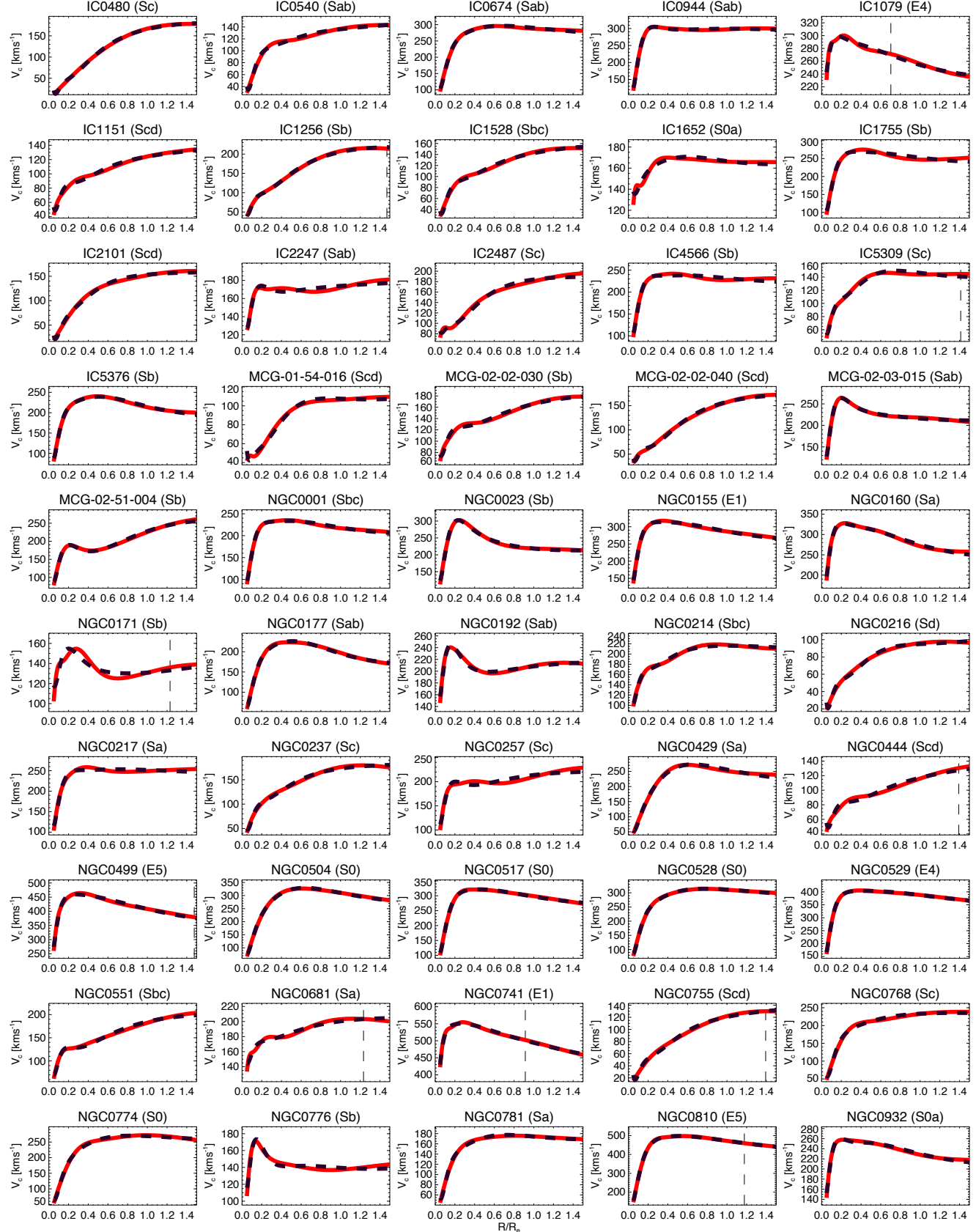


Figure 3. CVCs V_c of the 238 CALIFA galaxies (red curve), normalized to the effective radius (R_e) and their reconstruction (thick black dashed curve) from applying PCA, which is the linear combination between the five main PC eigenvectors \mathbf{u} and five main PC projections \mathbf{PC}_i . The vertical thin dashed line indicates the maximum radial extent of our observations in the cases where the data do not cover all $R < 1.5R_e$.

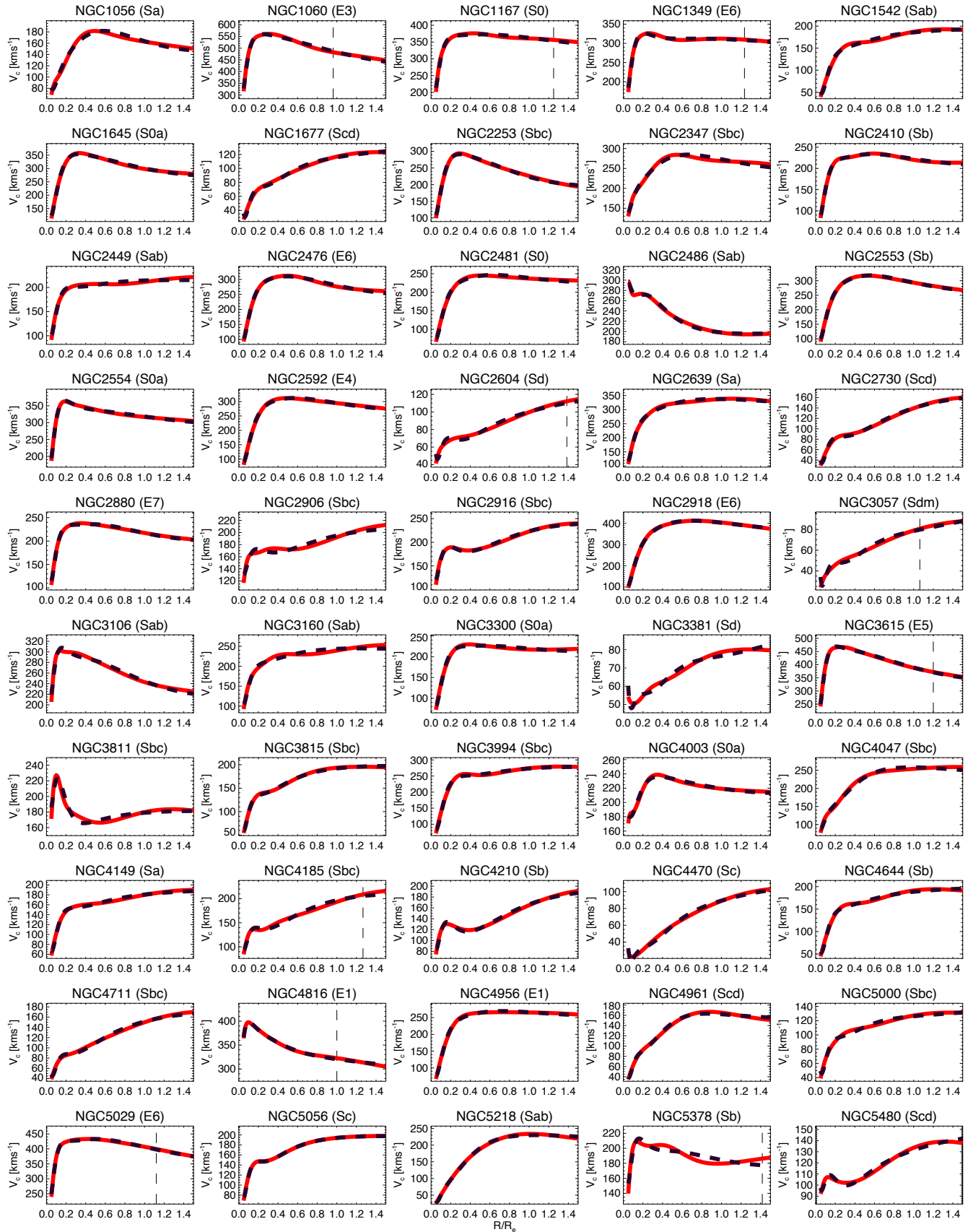
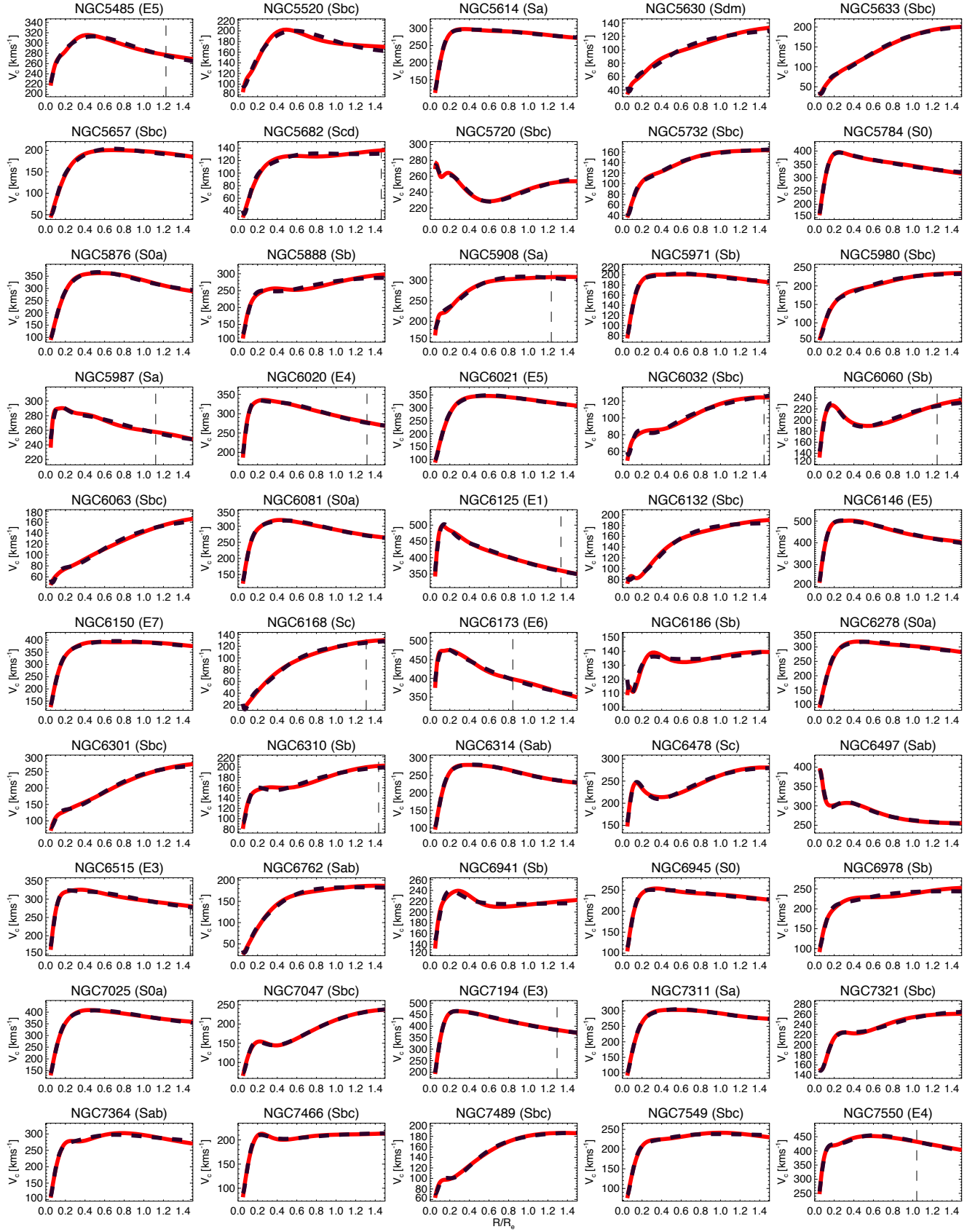


Figure 3. – continuation

**Figure 3.** – continuation

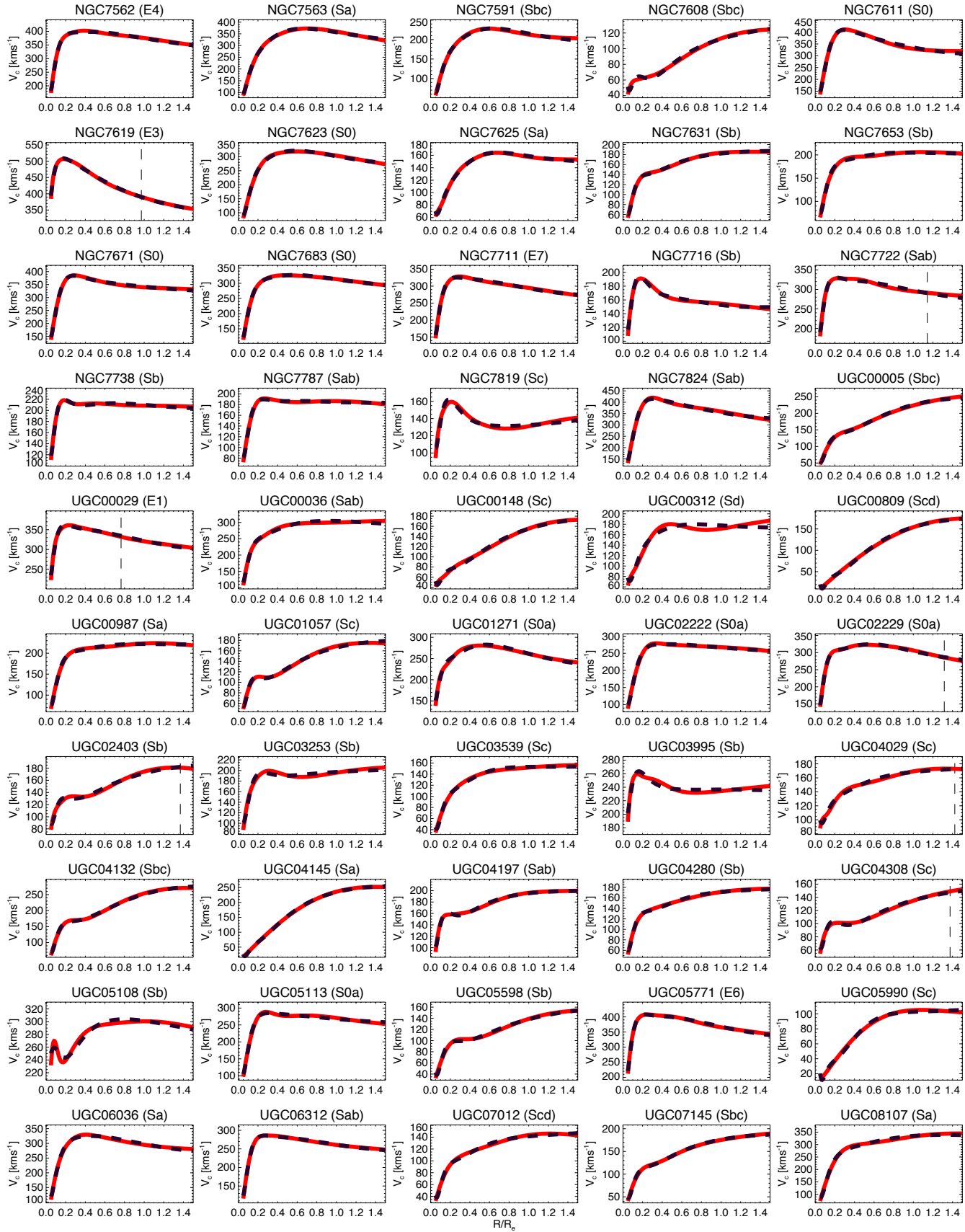
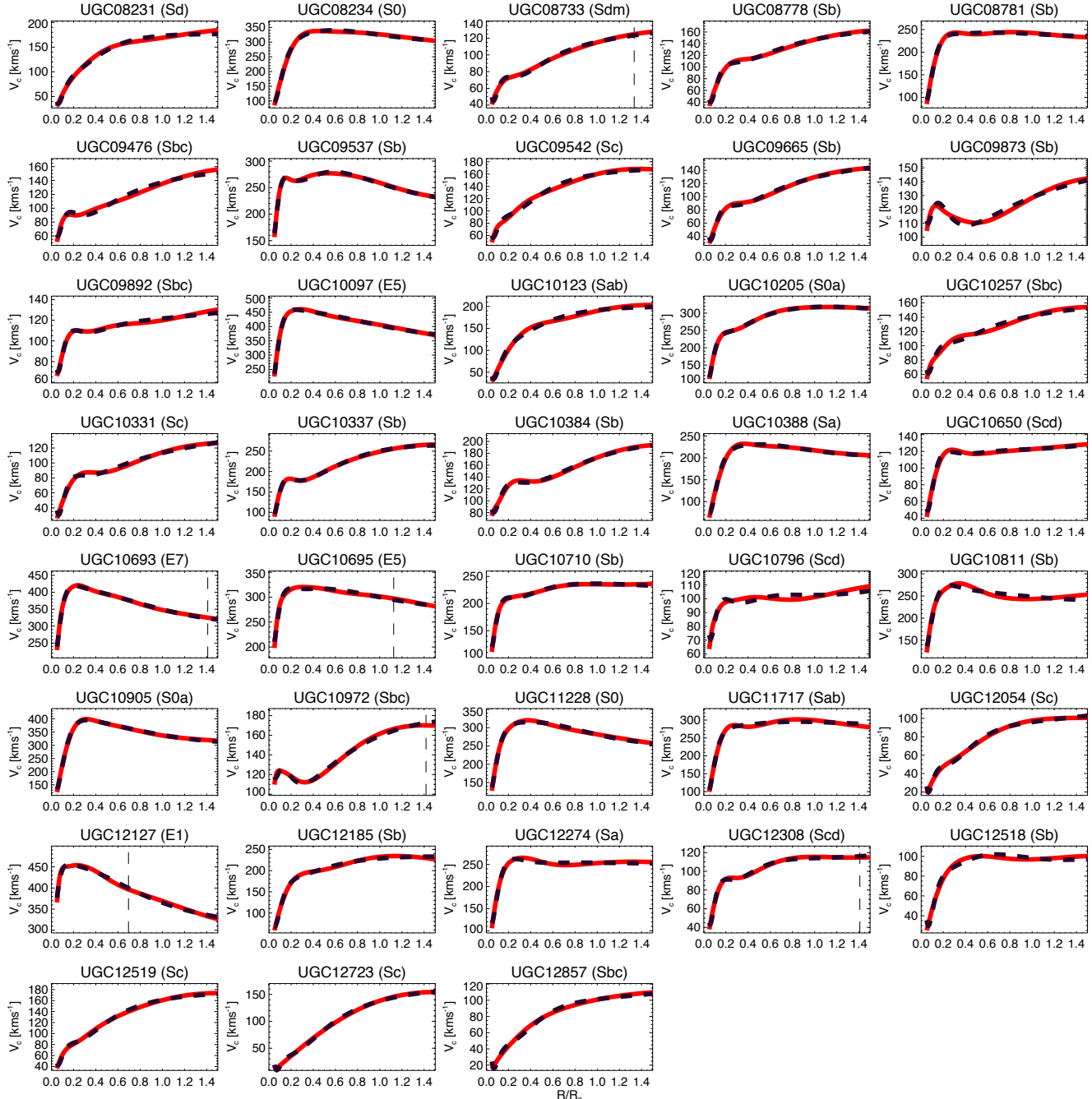


Figure 3. – continuation

**Figure 3.** – continuation

where the sum is carried out over the sample of galaxies $N = 238$ and \bar{V}_c is the mean circular speed for all galaxies across the whole sample. Note that, in our application of PCA, we do not subtract the mean of each circular curve but rather the mean of this sample (for our sample $\bar{V}_c = 196.336 \text{ km s}^{-1}$). Such a formulation is needed in the cases where we are trying to develop a representative basis (Koch 2013). We diagonalize the covariance matrix, obtaining a set of N eigenvectors (\mathbf{u}_n) and the eigenvalues represent the relative power of those eigenvectors in describing the population.

Fig. 2, left-hand panel, shows the first five principal component (PC) eigenvectors \mathbf{u} , needed to reconstruct the CVCs of the 238

galaxies shown with the corresponding fraction of the power in that eigenvector. The first dominant feature of the 238 CVCs is shown by the first eigenvector \mathbf{u}_1 with 93.33 per cent (long-dashed line). Eigenvectors \mathbf{u}_2 to \mathbf{u}_5 contain 5.41 per cent, 0.87 per cent, 0.29 per cent and 0.07 per cent of the power respectively. The reconstructed circular velocities, using the five eigenvectors and five principal components, contain 99.97 per cent of the total information of the 238 CVCs.

In Fig. 2, right-hand panel, we show an example of reconstructed circular velocity ($V_{c,\text{rec}}$) of the galaxy NGC 7671 (red curve) after applying PCA. $V_{c,\text{rec}}$ (black dashed curve) is the linear com-

bination between the five main PC eigenvectors \mathbf{u} and five projections PC_i , adding the mean value \bar{V}_c of the circular velocities calculated among all 238 galaxies:

$$V_{c,\text{rec}} = (\text{PC}_1\mathbf{u}_1 + \text{PC}_2\mathbf{u}_2 + \text{PC}_3\mathbf{u}_3 + \text{PC}_4\mathbf{u}_4 + \text{PC}_5\mathbf{u}_5) + \bar{V}_c. \quad (5)$$

For this galaxy, the projections are $\text{PC}_1 = +1.29$, $\text{PC}_2 = -2.50$, $\text{PC}_3 = -1.92$, $\text{PC}_4 = -2.41$, $\text{PC}_5 = +0.84$.

In Fig. 3, we show the reconstructed circular velocities of the 238 CALIFA galaxies. The fits are nearly perfect for all galaxies. The five main PC eigenvectors and the five main projections PC_i are listed in Appendices C and D, respectively.

3.3 k -means clustering

With the eigenvector decomposition, each circular curve can now be represented in a reduced-dimensionality space as the PC projections required for a reconstruction. We use k -means clustering to identify classes within that space. The k -means clustering approach is a vector classification method (MacQueen 1967) based on Lloyd's algorithm (Lloyd 1982). It is commonly used in data mining due to its simplicity (for a review of clustering methods see Everitt 1993; Jain, Murty & Flynn 1999). The k -means clustering method partitions n observations into k clusters in which each observation belongs to the cluster with the nearest mean, considered as the “centroid” (prototype) of the cluster. Given k , the method optimizes, by several iterations, the mean positions that minimize intracluster variation and maximize intercluster variation. The final result is a partitioning of the data space to regions based on the closest mean. We use the IDL implementation of k -means algorithm: the CLUSTER_WTS⁸ task calculates the weights and the centres of the clusters, and the CLUSTER⁹ task defines the final clusters based on those weights.

In Fig. 4, we present the k -means clustering applied to the first and second PCs of our circular curves. In k -means clustering, the choice of clusters k is established by the user, though some algorithmic approaches exist (e.g., Everitt 1993). In our case of the 238 galaxies, we choose $k = 4$, because we visually see four distinct sets of CVC shapes that appear to represent a useful classification approach. Additionally, our choice is guided by the general k -means heuristic method for determining the maximum number of the clusters within a given data set: the square root of the number of data points (N) divided by two (Kodinariya & Makwana 2013), i.e., $k \approx \sqrt{N/2}$, where $N = 238$ for our sample, and the calculated maximum number of clusters is $k \approx 11$. Thus, our choice for $k = 4$ is also consistent with this rule. For our CVCs classification, like other schemes for galaxy classification, the circular curves form a continuum of different shapes and there will be always borderline cases (see Fig. 5). We have experimented with variation of both the numbers of PCs included and the number of clusters. We settle on two components and four clusters and arrive at the groupings shown in Fig. 7, which form a basis for classification. However, PCA also provides dimensionality reduction, which enables the continuum of galaxy properties to be quantified.

⁸ https://www.harrisgeospatial.com/docs/clust_wts.html

⁹ https://www.harrisgeospatial.com/docs/cluster.html#C_854643309_862474

4 TOWARDS A NEW CLASSIFICATION OF GALAXIES

4.1 Shape of the CVCs across Hubble sequence

In the left-hand panel of Fig. 4, we show the two projections of the PCA to the stellar circular curve of the 238 E1–Sdm galaxies (Section 3.2) with colour coding corresponding to the morphological types of the galaxies. The right-hand panel shows the cluster labels that are derived after applying the two-dimensional k -means clustering technique, considering the projection of the two main PC Eigenvectors, plotted in the panels. The colour coding and symbols correspond to the four CVC groups identified by this method. Given the appearance of these four classes, we describe them as: *slow-rising* (SR, black filled pentagons), *flat* (FL, blue filled squares), *round-peaked* (RP, green filled circles), and *sharp-peaked* (SP, red filled triangles).

To investigate the properties of the four classes, in Fig. 6, first row, we plot together the CVCs from each class (from left-to the right-hand panel): SR-CVCs (black curves), FL-CVCs (blue curves), RP-CVCs (green curves) and SP-CVCs (red curves). In the second row of Fig. 6, we calculate the mean prototype circular curve, which corresponds to the mean value of the CVCs at each k -means cluster group, in order for each class to obtain a representative shape and amplitude of the CVCs. The shaded band represents the standard variation of the CVCs within the cluster group. To contrast the CVC and photometric (Hubble) classification, we use the last row of Fig. 6 to show the CVCs from each class with corresponding colour representing the morphology of the galaxies. The SR-CVCs have a clear connection to late-type spirals (Sb–Sdm), and the SP-CVCs to early-type galaxies (E1–E7). However, the other two CVC classes are represented by galaxies with different morphologies. Interestingly, the lenticular galaxies fall mainly in one category – RP class.

In Fig. 7 (left), we combine the four prototype curves together to compare their typical shapes and amplitudes. SP-CVCs have the highest and the SR-CVCs have the lowest amplitude. Furthermore, the SR-CVCs and FL-CVCs have tighter mass range than RP-CVCs and SP-CVCs.

We modelled the CVCs of our galaxies with a maximum extent to $1.5R_e$ since most of the galaxies appear to reach their flat (asymptotic) circular speed (V_F) at this radius. This allowed us to represent the normalized prototype curves V_c/V_F in the right-hand panel of Fig. 7, where we can more clearly see the shape of the peak of the CVCs (absent, anaemic/flat, round or sharp).

Additionally, we note that the different prototype curves differ in the steepness of the rising central parts ($\sim 0.1R_e$) and the declining of the outer parts ($\sim 1.5R_e$). The dashed line correspond to unity of the ratio V_c/V_F for guiding the eye.

4.2 CVC classes – main features

After analysing the shape and amplitude of the CVCs of the 238 (E1–Sdm) galaxies, we list the main properties of the four new CVC classes (see Figs 7 and 8).

Slow-rising (SR): the circular velocity increases monotonically without a peak in the centre. This class consists mostly of late-type spiral galaxies (Sb–Sdm). The typical amplitude of CVCs reaches $\sim 150 \text{ km s}^{-1}$.

Flat (FL): the circular velocity is approximately constant throughout the whole galaxy. This class is represented mostly by early-type spiral galaxies (Sab–Sbc). The average amplitude of CVCs reaches $\sim 210 \text{ km s}^{-1}$.

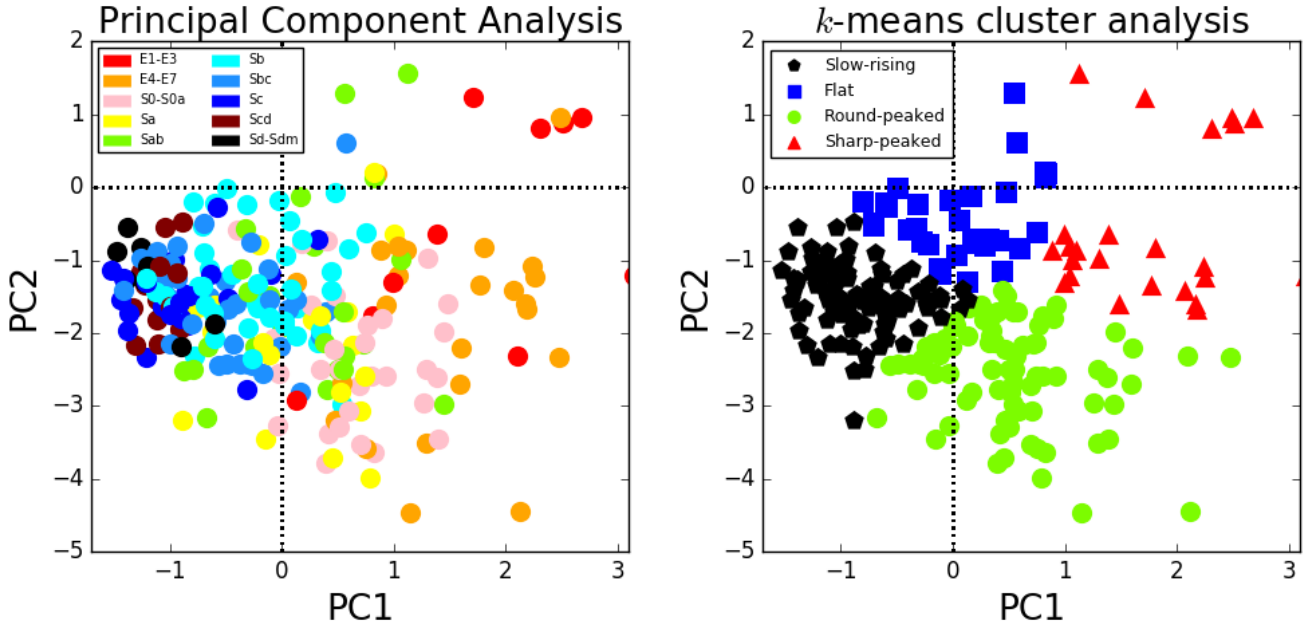


Figure 4. PCA of the 238 galaxies. *Left:* PC projections for each circular curve coded by Hubble type. *Right:* applied *k*-means clustering method on the two PC projections carrying ~ 99 per cent of the power, where the colour coding corresponds to the proposed four groups of galaxies.

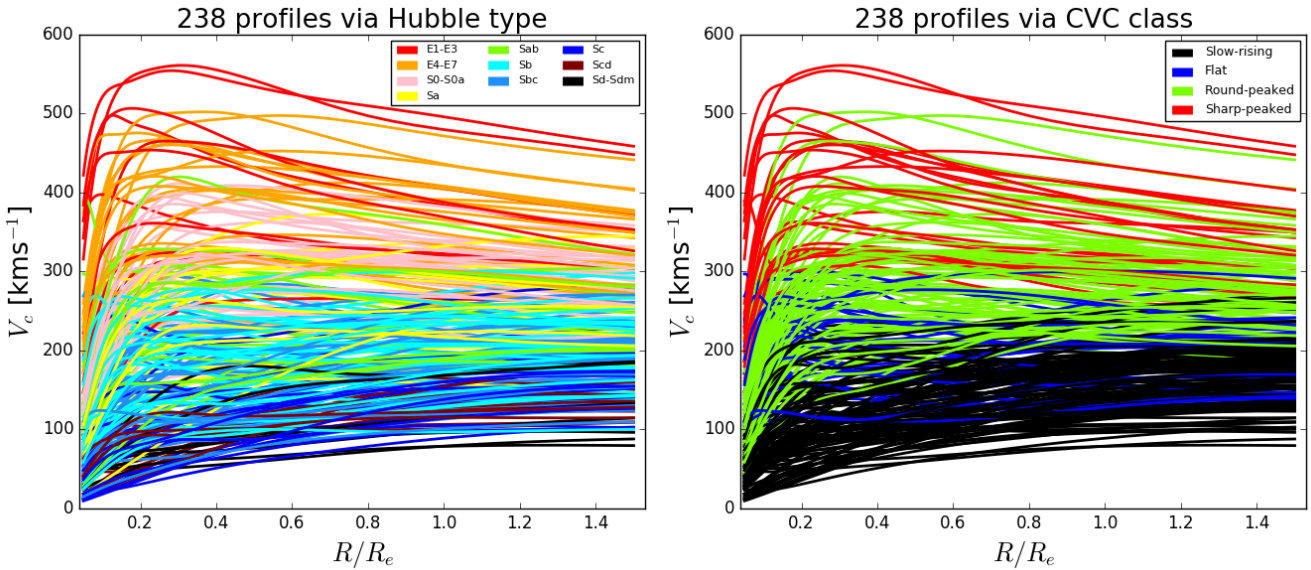


Figure 5. CVCs of the 238 (E1–Sdm) CALIFA galaxies colour coded by morphological type (left) and CVC class (right). CVCs form a continuum of different shapes, amplitudes and slopes. Thus, there will be always borderline cases for our CVC classification like other schemes for galaxy classification (Section 3.3).

Round-peaked (RP): the circular velocity rises steeply and has a round peak, gradually changing to the flat part of the CVC at radius $\sim 0.5R_e$. This class is represented by early-type galaxies and early-type spiral galaxies (E4–S0a, Sa–Sbc). The average amplitude of CVCs reaches $\sim 300 \text{ km s}^{-1}$.

Sharp-peaked (SP): the circular velocity rises steeply and has a sharp peak, making a sudden change to the flat part of the CVC at radius $\sim 0.2R_e$. This class is dominated by early-type galaxies (E1–E7). The average amplitude of CVCs reaches $\sim 400 \text{ km s}^{-1}$.

In general, the SR class is mostly represented by late-type galaxies, while the SP class is represented by early-type galaxies. FL- and RP-CVCs include galaxies with a wide-range of morphologies.

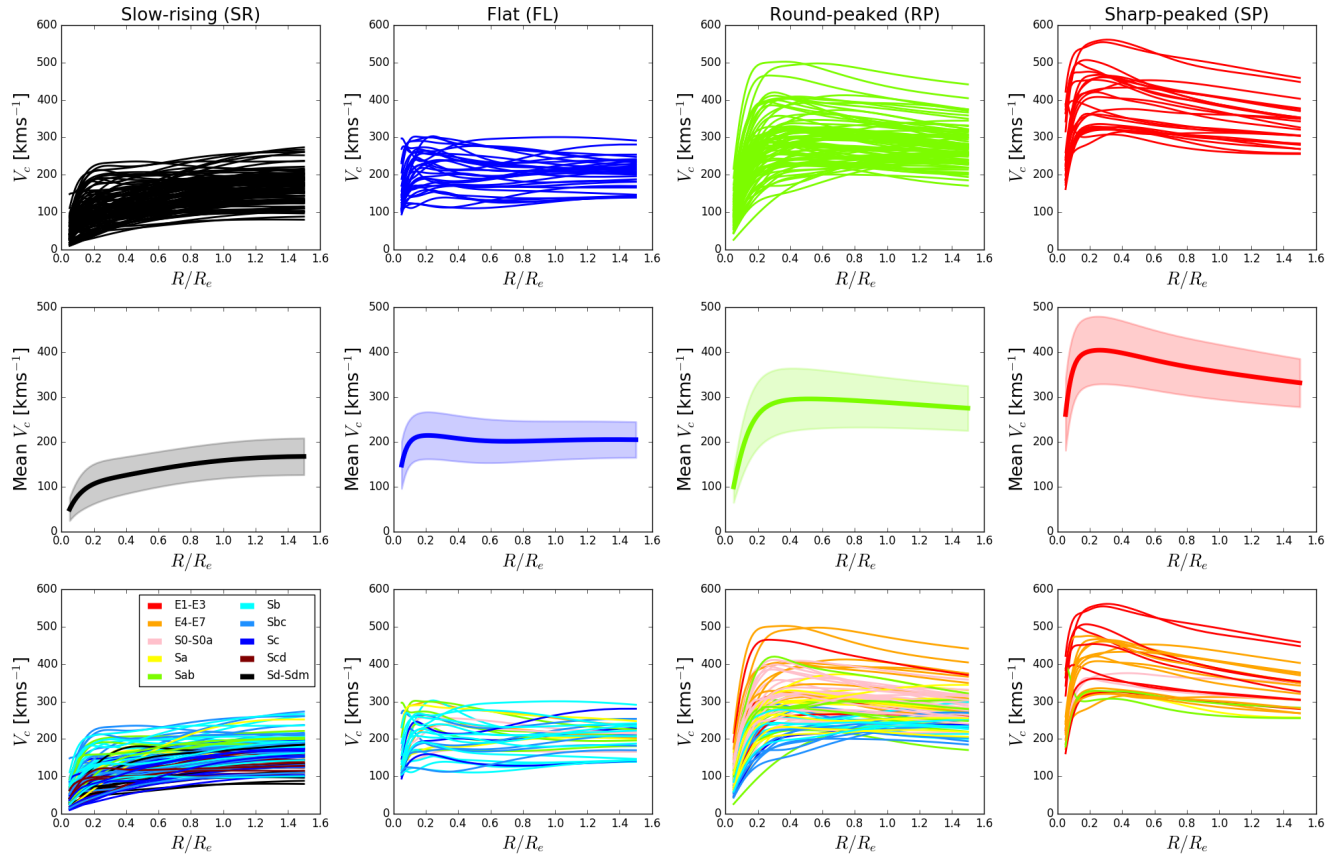


Figure 6. PCA of the 238 galaxies. *First row:* CVCs of the four groups classified using the k -means clustering method (Section 3.3). *Second row:* prototype circular curve, which corresponds to the mean CVC of each k -means cluster group with the corresponding uncertainty band. *Third row:* V_c from each k -means cluster group, where the colour coding corresponds to the morphology of the galaxies.

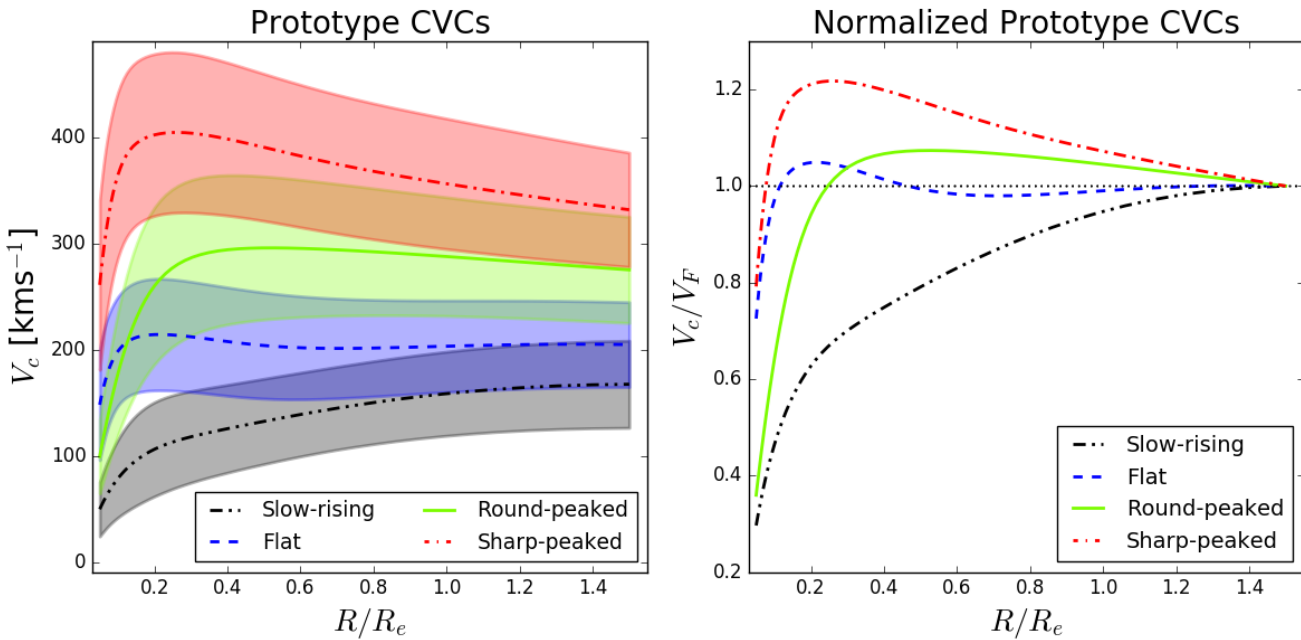


Figure 7. CVC classification of the 238 galaxies. *Left:* prototype (mean) circular curve, which corresponds to the CVC at center of each k -means cluster group. *Right:* normalized (on the flat/asymptotic circular speed) prototype curve for each k -means cluster group.

4.3 Global properties of the galaxies through CVC Class

To understand how the CVCs of the galaxies are shaped at different stage of their evolution, we explore further the relation between the CVC class properties and fundamental galaxy parameters.

In Fig. 9, we plot vertical box-and-whisker diagrams of the four CVC classes with different colour (SR—black, FL—blue, RP—green, SP—red). Box plots are a convenient way to graphically represent groups of numerical data through their quartiles of the distribution (Tukey 1977). The lines extending vertically from the boxes, called whiskers (shown with dashed line in Fig. 9), indicate variability outside the upper and lower quartiles (i.e., box-and-whisker diagram). In this descriptive statistics, the outliers are plotted as individual points (crosses in our case), where the spacings between the different parts of the box indicate the degree of dispersion (spread) and skewness in the data. The median values of the distributions are indicated by the white lines in the box plots. The box contains 50 per cent of the data. In the case of a normal distribution, this corresponds to two times the median absolute deviation of the distribution, where the extent of the whisker corresponds to approximately 3σ (σ being the standard deviation). The numbers of the galaxies, included in the statistics of the box-and-whisker diagrams, are printed with the label "stat" in each panel.

In panels ‘A–D’ of Fig. 9, we explore the photometric galaxy properties: the effective radius (R_e) corresponds to the radius, which contains half of the total light of the galaxies and it is measured via growth curve analysis as described in Walcher et al. (2014); the total luminosity (L_{tot}) is obtained from the r -band SDSS (DR12; Alam et al. 2015) images via MGE method (see Section 3); the bulge-to-total flux (B/T) ratio and disc-to-total luminosity (D/T) ratio are calculated by Méndez-Abreu et al. (2017) from r -band SDSS (DR7; Abazajian et al. 2009) images.

In panels ‘E–H’ of Fig. 9, we explore the stellar population properties, taken from González Delgado et al. (2015): the stellar surface-mass-density, μ_* (within half-light radius) is extinction corrected; the total stellar mass (M_*) is calculated using Chabrier initial mass function (IMF); the age (Age) and the metallicity (Z) of the galaxies are light-weighted and mass-weighted within half-light radius, respectively. González Delgado et al. (2015) apply the fossil record method based on spectral synthesis techniques to derive these physical properties for each spatial resolution element of the integral field unit (IFU).

In panels ‘I–L’ of Fig. 9, we explore the kinematic properties of the galaxies. One of them is the mean value of the de-projected rotational velocity of the galaxies v_ϕ , calculated within half-light radius ($R = 0.5R_e$). It is expressed as $v_\phi = v_{\text{los}} / \sin(i)$, where i is the inclination of the galaxies and v_{los} is the line-of-sight velocity derived via kinemetry procedure of Krajnović et al. (2006). Further, the mean value of the line-of-sight velocity dispersion (σ_{los}) is taken within an aperture of half-light radius ($R = 0.5R_e$). The ratio $v_\phi/\sigma_{\text{los}}$ aims to reflect the ordered-over-random motion of the galaxies in their central parts.

However, a more robust representation of the latter parameter is the specific angular momentum λ_{R_e} , which is integrated within one effective radius ($R = 1.0R_e$, reached by most of our galaxies) as follows:

$$\lambda_R = \frac{\sum_{i=0}^{N_p} F_i R_i |V_i|}{\sum_{i=0}^{N_p} F_i R_i \sqrt{V_i^2 + \sigma_i^2}} \quad (6)$$

where F_i, R_i, V_i and σ_i are the flux, circular radius, velocity and

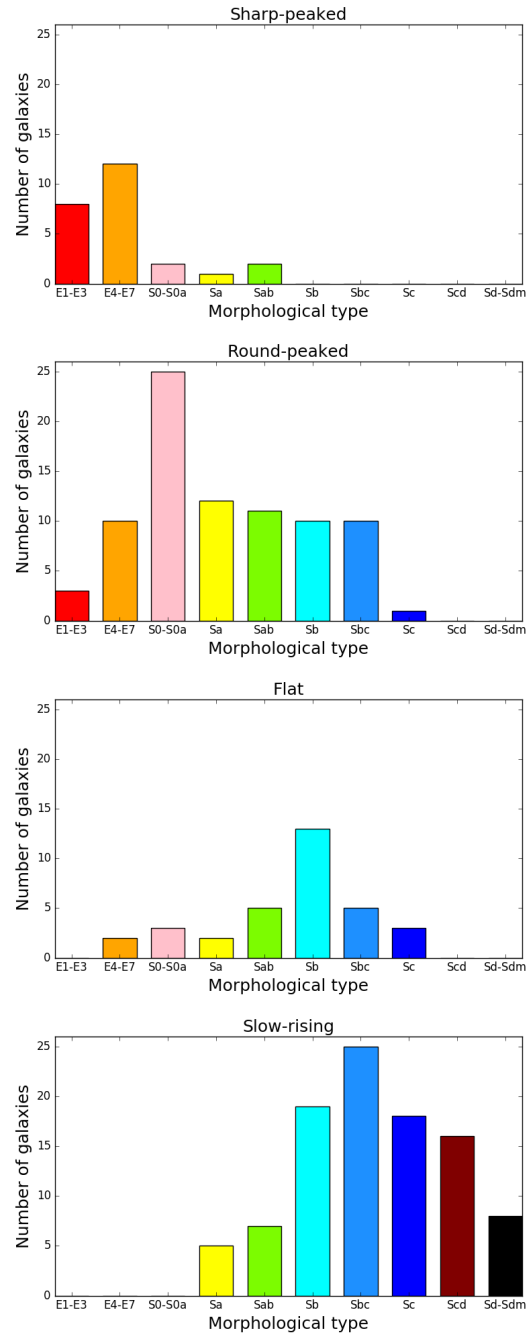


Figure 8. Distribution of the CVC classes by morphology. SP-CVCs are mostly presented by early-type galaxies, while SR-CVCs are mainly presented by late-type spiral galaxies. RP-CVCs and FL-CVCs are presented by various morphologies.

velocity dispersion of the i -th spatial bin, the sum running on the N_p bins (Emsellem et al. 2007).

In panels ‘M–P’ of Fig. 9, we explore the dynamical properties: the maximum circular velocity ($V_{c,\text{max}}$) is the circular velocity of the galaxy with the largest amplitude up to $1.5R_e$; the total dynamical mass $M_{\text{dyn}}^{\text{tot}}$ is calculated as the multiplication between the total luminosity of the galaxies (L_{tot}), derived via MGE method, and the dynamical mass-to-light ratio (M/L)_{dyn}, obtained from JAM-MCMC approach (see Section 3.1); the discrepancy factor

$f_d = 1 - (M_{*,pop}^{tot}/M_{dyn}^{tot})$, showing the relation between the total stellar and dynamical masses as a fraction value.

The maximum circular velocity, the total r -band luminosity, total stellar mass, total dynamical mass, age, metallicity and B/T ratio increase gradually in order: SR, FL, RP, SP. This means that galaxies with SR-CVCs are low-mass, faint, young, metal-poor with small bulges in comparison with the other CVC classes, and in particular with SP class, which is the most massive, bright, old, metal-rich with almost 100 per cent B/T ratio. Instead, the D/T ratio decreases with increasing CVC class.

The stellar surface mass density of the galaxies (μ_*) also increases with CVC class, but it saturates to $\log \mu_* \sim 2.7 M_\odot \text{ pc}^{-2}$ for RP and SP classes. They have the highest and approximately identical median values of the distribution. Interestingly, the median of the distribution for the galaxy effective radius (half-light radius) show that SP- and FL-CVCs have the largest effective radii in contrast to SR- and RP-CVCs.

The random motion of the galaxy σ_{los} increases with CVC class. Instead, the ordered motion v_ϕ increases with CVC class up to the RP-CVCs, and then decreases for SP class. The value of v_ϕ/σ better represents which of the motions of the stars in the galaxies (ordered or random) mostly contribute in the total potential of the galaxy and shape the CVC. For example, FL-CVCs are mostly shaped by the ordered motions, instead SP-CVCs are shaped by the random motions. The angular momentum of the galaxies λ_R shows similar trend. SL, FL and RP class are fast rotators, while SP are slow rotators.

The dynamical mass-to-light ratio, $(M/L)_{dyn}$, is lowest for FL-CVCs, and larger for SR, RP and SP classes. The discrepancy mass factor ($f_d = 1 - M_*/M_{dyn}$) follows similar trend: SR and SP class have the largest value (with 74 per cent and 71 per cent, respectively) in contrast to the FL and RP class (with 59 per cent and 61 per cent, respectively). The large value of f_d might be due to the uncounted gas fraction (most likely for late-types), variation of the IMF or a large DM content in the galaxies.

5 DISCUSSION

Every classification scheme focuses on certain properties of the objects, and consider some features as primary and others as secondary. In our study, the primary focus of the CVC classification scheme is the shape and amplitude of the CVC, tracing the total potential of the galaxies. We aim to understand if the CVC encodes some important information about galaxy's internal structure and merging history. We use stellar dynamics to explore the potential of the galaxies from early- to late-types with one approach, which give us the great opportunity to study this problem uniformly.

5.1 The new classification scheme

The Hubble sequence (Hubble 1936) is the original classification of galaxies, based on their photometric morphology. Morphological classification has good utility and clearly groups galaxies with similar properties. However, the Hubble sequence is only tenuously connected to the long-term evolutionary processes that govern galaxies. A galaxy's morphology is set by its recent star formation history and gas content. For example, elliptical and dwarf spheroidal look morphologically similar but have different formation histories (e.g., Kormendy & Bender 2012). In contrast, the stellar kinematics are intimately connected to the galactic potential

and are thought to probe a longer evolutionary history. Thus, identifying a CVC classification scheme for galaxies will likely highlight different physical features than morphological classifications. Our classification scheme is an effort in this direction.

We have used PCA analysis for dimensionality reduction and k -means clustering to group the circular curves into four distinct groups. The choice of four clusters, while only weakly preferred by clustering metrics, is guided by the visual distinction of four different families of circular curves regarding their shape (see Fig. 5). The four families serve as a useful representation, but we stress that *there is a continuum of CVC types*. This continuum is quantitatively described by the projections, PC_i .

Two features distinguish this approach from past efforts. First, we use detailed stellar dynamical modelling using the JAM model, which capture the dynamical signatures of both hot and cold stellar components. Secondly, we use a non-parametric approach to generate a classification based on the circular curves. Since a small basis set can reconstruct ~ 99.97 per cent of the informative content of a wide variety of circular curves, this indicates the power of the PCA analysis when derived from a large observational set. However, the main features of our sample of galaxies (~ 99 per cent) are contained in the first two PCs; thus we apply k -means method only in the two-dimensional parameter space of PC1 and PC2.

The first five PC eigenvectors \mathbf{u}_i represent an excellent vector base for reconstruction of the CVCs (see Figs 2 and 3). The main eigenvectors appear similar to the classical CVC decomposition on individual radial velocity contributions of the components: bulge, disc, gas, DM halo, etc. (e.g., van Albada & Sancisi 1986). In upcoming papers, we will explore if such physical connection exists.

Further, our proposed classification shows very promising relations with the fundamental properties of the galaxies (see Fig. 9). SR-CVCs are represented by young, late-type spirals (Sc–Sdm), low-mass, faint, low-metallicity galaxies with small bulges, effective radius, stellar-mass-surface density and maximum circular velocity. The SR class is one of the extremes in our classification, where the other extreme is the SP class, represented by elliptical (E1–E7), old, high-mass, bright, high-metallicity galaxies with large bulge/spheroid, large effective radius, stellar mass surface density and maximum circular velocity. SR- and SP-CVCs are the most separate groups in our two-dimensional PC clustering space (see Fig. 4) and opposite in most of the explored galaxy properties. On the other hand, SR and SP classes are characterized by similar small rotation and large dark matter contents in comparison with the other two classes, FL- and RP-CVCs.

In Fig. 9 we see that FL-CVCs and RP-CVCs appear to be intermediate CVC classes. By properties distributions, FL class appears close to SR class, while RP appears close to SP. This is also the case in the PC clustering space, where SR and FL have mostly negative values of the PC projections, while RP and SP have mostly positive values (see Fig. 4).

In short, by looking at the shape and the amplitude of the CVCs, it appears possible to guess the properties of the galaxies.

5.2 Link to galaxy evolution: CVC classes on the mass-size plane

CVCs trace the total potential of the galaxies, and potentially incorporate all information about their single constituents: stars, gas and DM. In Fig. 9, we found that the properties of the galaxies are connected to the shape and the amplitude of their CVCs. There-

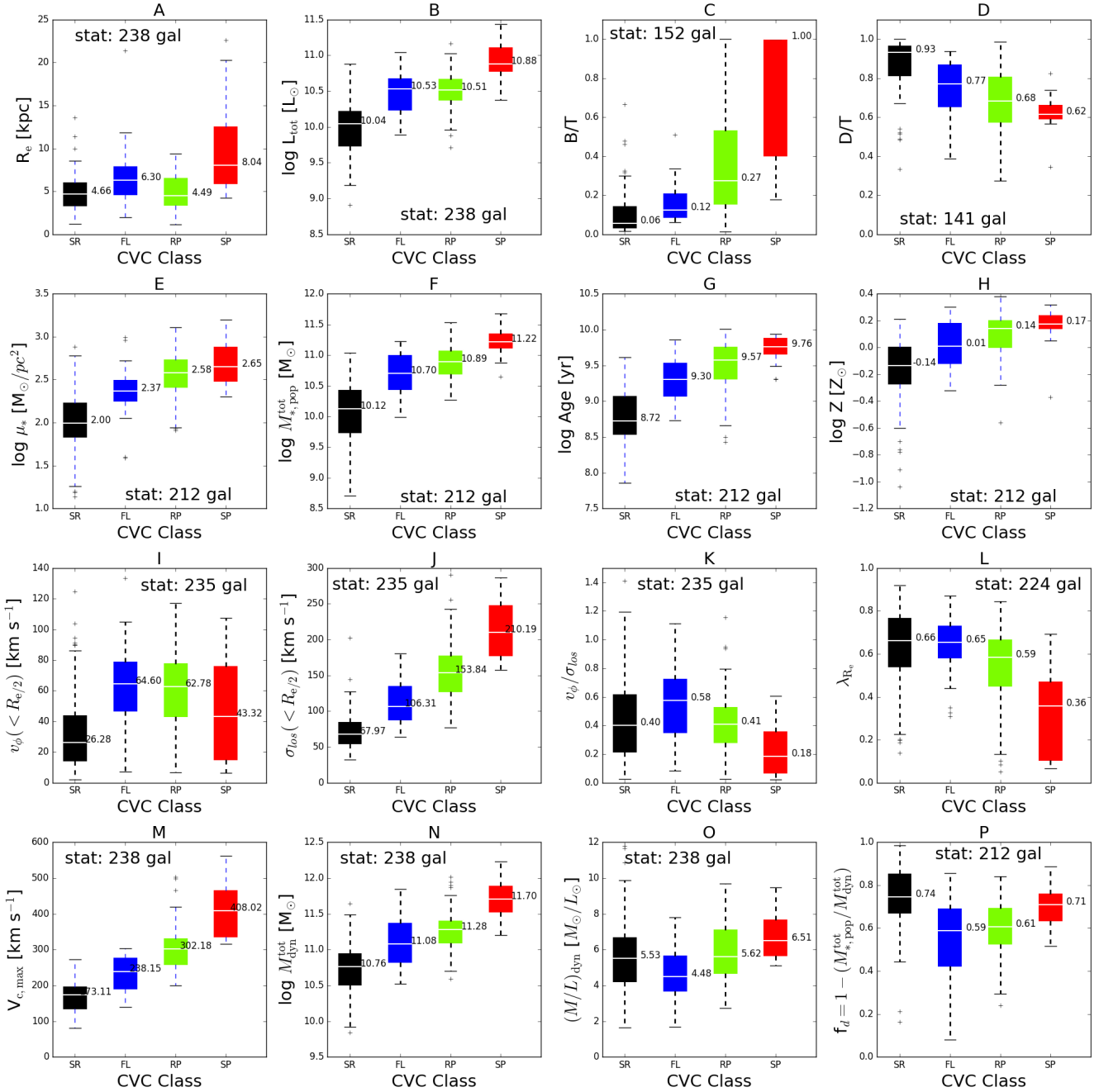


Figure 9. Box-and-whisker diagram of fundamental galaxy properties through CVC class (see Section 4.3). The white lines and the numbers represent the median value of the distributions for each class (SR-red, FL-blue, RP-green, and SP-red). The box contains 50 per cent of the data. In the case of a normal distribution this corresponds to two times the median absolute deviation of the distribution, where the extent of the whisker (dashed lines) corresponds to approximately 3σ (σ being the standard deviation). The numbers of the galaxies, participating in the statistics of the box-and-whisker diagrams, are printed with the label ‘stat’ in each panel (note here that for panels C and D, biases might occur due to the lower number of galaxies). We find several global correlations: SR-CVCs are typical for low-mass, young, faint, metal-poor, disc-dominated galaxies with large value of the discrepancy mass factor ($f_d \sim 74$ per cent); SP-CVCs are typical for high-mass, old, bright, metal-rich, bulge-dominated galaxies with also significant value of the discrepancy mass factor ($f_d \sim 71$ per cent); FL-CVCs and RP-CVCs appear presented by galaxies with intermediate mass, age, luminosity, metallicity, bulge-to-disc ratio, and value of the discrepancy mass factor ($f_d \sim 59$ per cent and $f_d \sim 61$ per cent, respectively). These relations suggest that CVCs can be used as a reliable classifier for studying the formation and evolution of the galaxies (see Section 5).

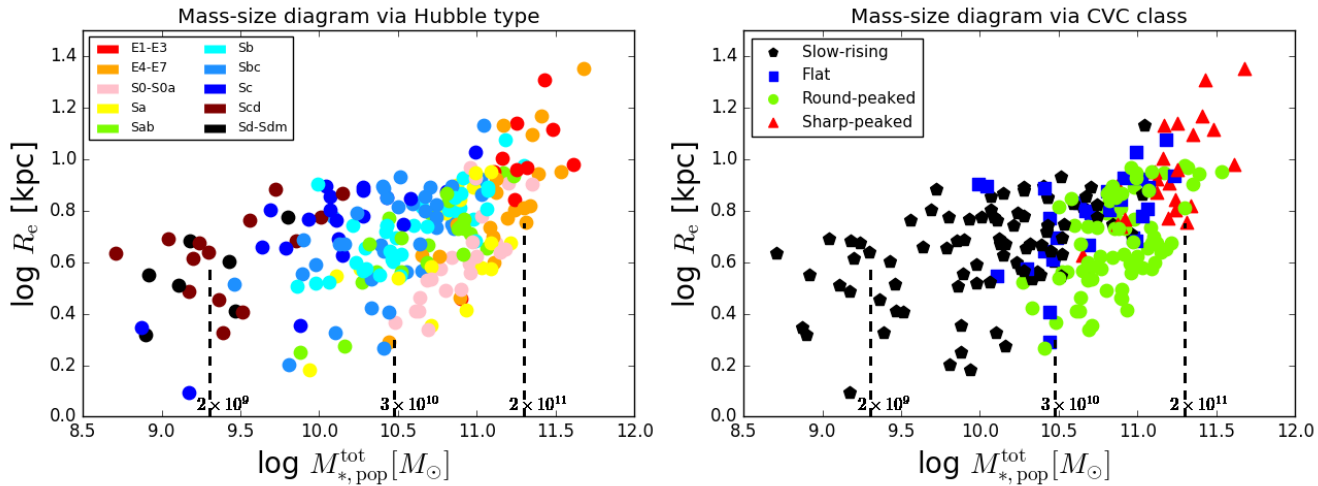


Figure 10. Mass-size (MS) plane of the 238 (E1-Sdm) CALIFA galaxies via Hubble type (left) and CVC class (right). The dashed lines indicate the three characteristic stellar masses in the MS diagram of Cappellari et al. (2013): below around 2×10^9 the MS is populated by no regular early-type galaxies; around 3×10^{10} the early-type galaxies reach their minimum size and maximum stellar density before a sudden change in the slope at larger masses; below 2×10^{11} the MS is mostly populated by fast rotators and rarely by slow rotators; above 2×10^{11} there are no spiral galaxies and MS is dominated by round and triaxial slow rotators. The distribution of our 238 CALIFA galaxies on the MS diagram via Hubble type (left) fit well to these three domains of characteristic masses, described in Cappellari et al. (2013). Galaxies with SR-CVCs occupy the MS diagram below around $M_{*,\text{pop}}^{\text{tot}} \approx 3 \times 10^{10}$, FL-CVCs and RP-CVCs – mainly the domain between $M_{*,\text{pop}}^{\text{tot}} \approx 3 \times 10^{10}$ and $M_{*,\text{pop}}^{\text{tot}} \approx 2 \times 10^{11}$, whereas SP-CVCs – mainly above $M_{*,\text{pop}}^{\text{tot}} \approx 2 \times 10^{11}$. This indicates that the shape and the amplitude of the galaxies are tightly linked to galaxy evolutional processes (see Section 5.2).

fore, the galaxy evolution should, somehow, be related to the new classification scheme.

The relation between the total stellar mass M_*^{tot} and the effective radius R_e of the galaxies is called mass-size (MS) diagram, and it is often used to probe galaxy evolution (e.g., Cappellari et al. 2013; van Dokkum et al. 2015; Cappellari 2016). Through this diagram, fig.29 of Cappellari (2016) summarizes the possible evolutionary scenario for present-day early-type galaxies. Cappellari (2016) discuss two channels of galaxy evolution. In the first one, galaxies grow through gas accretion or gas rich minor mergers, where the star-forming discs are the progenitors of the fast rotators early-type galaxies, and with the increase in mass the bulge grows. The second channel is dominated by mostly dry mergers, which move galaxies on the MS diagram by increasing their size proportionally to the stellar mass. This scenario is also postulated by van Dokkum et al. (2015), who explore the MS diagram of galaxies from $z \sim 3$ to $z \sim 0$. They conclude that star-forming galaxies grow mostly in mass with the gradual increase in their stellar density. Once galaxies reach a threshold of their velocity dispersion or stellar density, they tend to quench due to AGN feedback or other processes. The possible growth of the quenching galaxies goes through dry merging with consequent steepness of the MS diagram.

To study how our findings may be connected with these galaxy evolution theories, in Fig. 10, we investigate the local MS diagram, $(M_{*,\text{pop}}^{\text{tot}}, R_e)$, for our sample through Hubble type (left) and CVC class (right). The total stellar mass ($M_{*,\text{pop}}^{\text{tot}}$) of the galaxies is taken from González Delgado et al. (2015), while the effective radius (R_e), measured in r -band SDSS photometry, comes from Walcher et al. (2014). We overplot three dashed lines, corresponding to the characteristic stellar masses in the MS diagram of Cappellari et al. (2013). In their fig.9, Cappellari et al. (2013) show that the MS diagram is populated by no regular early-type galaxies below $\approx 2 \times 10^9 M_\odot$, while around $3 \times 10^{10} M_\odot$ the early-type galax-

ies reach their minimum size and maximum stellar density. After this characteristic mass, MS relation becomes suddenly steeper at larger stellar masses. The MS diagram is mostly populated by fast rotators and rarely by slow rotators below $2 \times 10^{11} M_\odot$; however above $2 \times 10^{11} M_\odot$ is mainly presented by round and triaxial slow rotators with the absence of spiral galaxies.

The distribution of our 238 CALIFA galaxies on the MS diagram via Hubble type, in Fig. 10 (left), fits well to these three domains of characteristic masses, described in Cappellari et al. (2013). Galaxies with SR-CVCs occupy the MS diagram below $M_{*,\text{pop}}^{\text{tot}} \approx 3 \times 10^{10} M_\odot$, FL-CVCs and RP-CVCs mainly cover the mass range between $M_{*,\text{pop}}^{\text{tot}} \approx 3 \times 10^{10} M_\odot$ and $M_{*,\text{pop}}^{\text{tot}} \approx 2 \times 10^{11} M_\odot$, and SP-CVCs mostly populate above $M_{*,\text{pop}}^{\text{tot}} \approx 2 \times 10^{11} M_\odot$.

Our results appear complementary to the MS diagram presented in figs 9 and 14 of Cappellari et al. (2013). They show that the growth of bulge makes the galaxy old and red with increasing dynamical mass-to-light ratio. This is in agreement with our results in panels C, G, H and O of Fig. 9. Furthermore, they discussed that the spiral galaxies do not populate the region of the MS diagram above the characteristic mass $\gtrsim 2 \times 10^{11} M_\odot$, and the (M_*, R_e) relation become steeper from late-type galaxies to early-type galaxies. We see the same trends through Hubble type for our sample in Fig. 10 (left-hand panel). In addition to the classical Hubble type study of the MS diagram, we illustrate how the galaxy potential, shape and amplitude of the CVC transform on this diagram in the right-hand panel of Fig. 10 with symbols corresponding to the different CVC classes. Interestingly, the CVC classes transit in the sequence SR-FL-RP-SP from left to right on the MS plane, which represents the direction of growing of the amplitude and steepness of the CVCs. Those two characteristics of the CVCs may represent the mass increase and bulge growth of the galaxies, respectively (e.g., Márquez & Moles 1999). Therefore, the CVC sequence matches

closely with the direction of the galaxy evolution through Hubble type according to Cappellari et al. (2013) and Cappellari (2016).

A similar galaxy evolution scenario is proposed by Combes (2009), where the bar-bulge cycle drives the local processes (e.g. secular evolution) in the spiral galaxies, which are considered the progenitors of the early-type galaxies via sequences of minor and major mergers. Additionally, Khochfar & Silk (2006) shows that bulges might grow from the local or global instabilities of the disc through secular evolution or minor mergers, respectively, which can drive the gas to the centre and form new stars. This scenario is further supported by González Delgado et al. (2015), where CALIFA galaxies are described to grow from inside out.

The properties of our four CVC classes can also be linked to recent results from hydrodynamical simulations. In particular, Tonini et al. (2016) present four channels of galaxy evolution. The first channel of their galaxy evolution scheme is presented by a smooth accretion of gas in the DM halo potential, where the stellar disc is growing inside out regulated by local star formation and stellar feedback without formation of bulge. This channel can be related to the SR-CVCs class of the faint, young, metal-poor, bulge-less with low stellar surface mass density CALIFA galaxies (see panels B, C, D, E, G, H of Fig. 9).

The second channel is presented by disk perturbations from chaotic gas accretion with high infall rates or gas-rich minor mergers provide large supplies of gas, which sinks towards the galaxy centre and a violent burst of star formation occurs. This channel can be associated with FL or RP class, which show intermediate properties' values in Fig. 9. These galaxies already have well-formed bulge and disc, and are characterized by intermediate age and metallicity, significant rotation and stellar surface mass density (see panels C, D, E, G, H of Fig. 9). For those galaxies, the discrepancy mass factor f_d is the lowest, which might indicate high star-forming galaxies (see panel P of Fig. 9).

The third channel is presented by minor mergers of satellites that overtake the disruptive force of the central galaxy's DM halo. In the case of early-type galaxies, there is a formation of a merger-driven bulge with the formation of the new stellar material in shells around it. However, in the case of a disc-dominated galaxy, there is a formation of an instability-driven bulge with the formation of new starburst in its regions. This channel can be associated with RP or SP classes. These galaxies have big spread in the B/T and D/T ratios (panels C and D), which might be the result of previous minor mergers. Additionally, those are the CVC classes dominating the MS relation on the steepness massive end with the largest dynamical masses, dynamical mass-to-light ratios, maximum velocities, which galaxies are also oldest, richest of metals, with the highest stellar surface mass density (see panels M, N, O, E, G, H of Fig. 9).

The fourth channel is presented by major mergers, where the two colliding galaxies have similar masses. These galaxies are completely pressure supported with the formation of merger-driven bulge. The final equilibrium of the new system depends on the overall gravitational potential. This channel can be presented by the SP class, which is presented by bright, old, metal-rich, pressure-supported, slow-rotating galaxies with the highest stellar mass surface density (see panels B, E, G, H, I, J, K, L of Fig. 9), which might indicate those previous major mergers.

Furthermore, Wang et al. (2015), using hydrodynamical simulations for studying the inefficiency of galaxy formation across cosmic time, found various shapes of the rotation curves of the galaxies with changing halo mass, which represent a gradual transition, similar to our finding in Fig 5. They also show similar group of shapes and amplitudes of the circular curves as the shapes and amp-

itudes of our four CVC classes (fig.8 of their paper), which correspond to four different DM halo masses, i.e., the lowest halo masses $M_{halo} < 2 \times 10^{10} M_\odot$ have CVCs that rise relatively steeply. When the halo masses increase, the CVCs rise more slowly, and vice-versa, galaxies with halo masses $\approx 6 \times 10^{11} M_\odot$ show steeply rising CVCs with growth of high central peak. Therefore, our CVC classes are expected to be also linked to the DM halo mass of the galaxies, which we expect to increase with CVC class in the sequence SR-FL-RP-SP.

Because the above considerations argue that evolutionary processes will leave a signature both on the spatial mass distributions of the disc and on resulting stellar motions, a CVC classification scheme can be well motivated. Fortunately, this idea is presented at the advent of a large number of IFU studies of galaxies of all types and can be further extended. The integral-field surveys such as CALIFA (Sánchez et al. 2012), VENGA (VIRUS-P Exploration of Nearby Galaxies, Blanc et al. 2010), SAMI (Sydney-AAO Multi-object Integral Field Spectrograph, Croom et al. 2012) and MANGA (Mapping Nearby Galaxies, Bundy et al. 2015) provide or will provide large statistical samples, a variety of FoV and spatial resolutions. This will give the opportunity to further investigate the mass distribution of galaxies with different morphologies and kinematics.

The interpretation of the MS relation (Fig. 10) and the box-and-whisker diagrams (Fig. 9), in the context of the current galaxy evolutionary theories, encourage us to explore the possibility if the CVC classification scheme could be a *dynamical evolution sequence of the galaxies* in the direction SR-FL-RP-SP. In upcoming papers, we intend to explore the properties of the CVC classes in relation to the ISM – star formation and gas content of the galaxies (e.g., Kalinova, Colombo & Rosolowsky 2016; Bolatto et al. 2017), as well as the radial acceleration traced by the CVCs (e.g., McGaugh, Lelli & Schombert 2016), which will shed more light on a possible dynamical evolution of the galaxies.

6 CAVEATS

(i) *Sample.* In our study, the selected galaxies cover a variety of morphological types and balance the number of early- versus late-type galaxies, as well as covering a wide range of masses. However, we still might expect a bias in our results due to either our selection criteria, or the CALIFA mother sample selection criteria (see Walcher et al. 2014). Additionally, given the data-based nature of the classifier, increasing the sample size would bring this CVC-based classification scheme into clarity and possibly provide a clearer distinction among the proposed CVC classes.

(ii) *Dynamical modelling assumptions.* A significant limitation of our work stems from the adopted assumptions in JAM dynamical model. We rely on two fundamental assumptions: constant mass-to-light ratio $(M/L)_{dyn}$ and constant velocity anisotropy $\beta_z = 1 - \sigma_z^2/\sigma_R^2$. While more general techniques exist, such as Schwarzschild's orbit superposition method (Schwarzschild 1979), JAM represents the best available compromise between physical accuracy in deriving stellar dynamics and computational efficiency for a large sample. The remain long-standing uncertainties in the dynamical modelling since we do not have good knowledge about the gradient of the mass-to-light ratio and the velocity anisotropy in the different types of galaxies, which might affect the shape and the amplitude of our derived 238 CVCs. Once more extended studies address these issues, as well as a set of gas dynamical properties are derived for a large sample of galaxies (e.g. the EDGE sample;

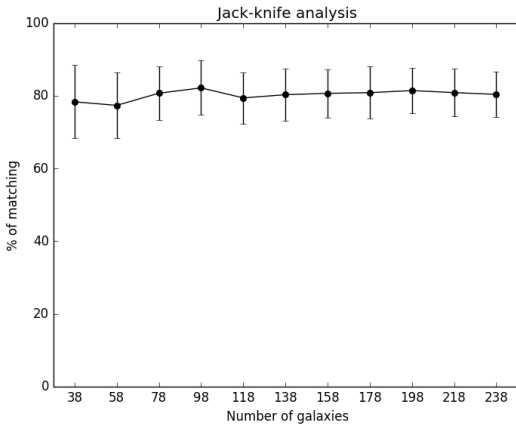


Figure 11. The results of a jack-knife technique, which probes the stability of the classification through a cross-validation approach: we select a sub-sample from the original set and carry out a complete analysis including PCA decomposition of the rotation curves and the k -means separation into classes. On the x -axis, we plot the number of the sub-samples drawn from the original set of 238 galaxies, while the y -axis corresponds to the matching of the original classification in per cent (see Section 6).

Bolatto et al. 2017), the classification should be repeated using improved approaches. In addition, the combination of different kinematical tracers (e.g., stars, CO, HI) may provide better constraints on galaxies’ potential without heavy computational cost (e.g., Cappellari et al. 2011, 2015), but large, matched samples of gas and stellar dynamics need to be explored (Kalinova et al., in preparation).

(iii) *Radial extent of the observations.* For several galaxies of our sample (e.g., IC 1079, NGC 0171, NGC 6173), the stellar kinematics does not reach $R/R_e = 1.5$. In this case, the extrapolations of the CVCs based on the $(M/L)_{\text{dyn}}$ can be uncertain. Further, we have experimented with classifying the CVCs using smaller sections of R/R_e . In general, the classification becomes noisier; however, since most of the classification power comes from the structure of the inner circular curve, the same basic results remain visible. The utility of a new approach remains high, and this method can be updated as a larger sample becomes available.

(iv) *Validation of PCA and k -means analyses.* Both the size and galaxy content of the sample will influence both the PCA representation and any classification of the CVCs based on this scheme. Since the categories are not clearly defined in the PC space (Fig. 4), there will naturally be uncertainty in any division into categories. We stress that the PCA provides a reduced-dimensionality summary of the CVC data, and the proposed classification is a part of a continuum.

We have assessed the stability of our classification using a cross-validation technique. We select a sub-sample from the original set and carry out a complete analysis including PCA decomposition of the CVCs and the k -means separation into classes. We find that the primary uncertainty in the classification results from the k -means algorithm. Since the exact solution to the problem requires intensive computation, heuristic approaches to approximate a near-optimal solution are typically employed. These approximate approaches result in a set of galaxies potentially being classified differently on different runs of the algorithm. As a first test, we run the algorithm 100 times on the full set of 238 galaxies, which results in the same categorizations for $\sim 80\%$ of the galaxies on av-

erage, with the $\sim 20\%$ representing a systematic error imparted by the k -means approach.

Next, we complete the full categorization algorithm on smaller subsets of the original galaxies to assess how sample size and membership affect the classification. In Fig. 11, we plot the fraction of galaxies that maintain their original classifications as the sample size is changed. For each sample size, we draw a sub-sample of that size 20 times from the parent sample, identify the PC representation of the CVC and classify the galaxies using k -means with $k = 4$ groups. We calculate the fraction of galaxies that retain their original classification. Fig. 11 shows that there remains some uncertainty in the classification, even for numbers approaching that of the original sample. We note that the classifications of the SR- and SP-CVCs tend to be more stable in their classification when compared to the RP- and FL-CVCs.

While there are some uncertainties, the stability of the method is encouraging, particularly when applying a coarse machine learning approach to a relatively small sample size. The uncertainty appears to be driven primarily by the lack of clear divisions between categories, which reflects the continuous nature of the underlying galactic population. While separating the sample into four categories provides a useful means of simply describing the dynamical properties of the galaxy, there may ultimately be more utility in using the PCs themselves as a measure of the dynamical properties of the system.

7 APPLICATION

Our analysis provides promising results in the classification of the galaxies based on their total potential using their CVC based on stellar dynamics. The sample we used is variable via morphology and large enough to be used as a classifier for future studies, especially for a single CVC or small samples of galaxies.

The practical way to classify a single galaxy is to use the five main PC eigenvectors (as shown in the left-hand panel of Fig. 2), and estimate the new first five PC projections for the new galaxy. Note that the CVC decomposition can be done after subtracting the mean circular velocity of our sample ($\bar{V}_c = 196.336 \text{ km s}^{-1}$, Section 3.2). Next, the derived first two main PC projections (PC1 and PC2) are the only values necessary to define the CVC class of the new galaxy using the k -means clustering of our sample in the right-hand panel of Fig. 4. After overplotting the two new PC projections in the (PC1, PC2) parameter space of our sample, the minimum distance to the closest k -means center will define the CVC class of the new galaxy. We provide a python script with an example for the application of our PC-classifier on the link <https://github.com/Astroua/DynClass>.

8 CONCLUSION

In this study, we derive the total CVCs of 238 (E1–Sdm) CALIFA galaxies. The shapes of the CVCs are given by the light profiles of the galaxies (via MGE model), where the amplitudes of the CVCs are given by the value of the dynamical mass-to-light ratio $(M/L)_{\text{dyn}}$, derived through fitting the stellar kinematics and solving the Jeans equations in the axisymmetric case via JAM-MCMC method (Section 3).

We investigate the maximum circular velocities (i.e., amplitude) and qualitative shape of circular curves through Hubble sequence using PCA and k -means clustering technique. We distin-

guish four main CVC classes: (1) in the SL class, the circular velocity increases monotonically with the absence of a peak in the centres and mostly represented by late-type spiral galaxies (Sb–Sdm) with the average amplitude of CVCs reaching $\sim 150 \text{ km s}^{-1}$. (2) FL-CVCs have an anaemic peak in the centres or approximately constant circular velocity within the whole galaxy and include most of the early-type spiral galaxies (Sab–Sbc). The average amplitude of CVCs for FL galaxies is $\sim 210 \text{ km s}^{-1}$. (3) RP-CVCs have a steeply rising central CVC with a round peak, gradually changing to the flat part of the CVC at radius $\sim 0.5R_e$. This group mostly includes late-type ellipticals (E4–E7), lenticular galaxies (S0–S0a) and early-type spirals (Sa–Sbc) with average amplitude of CVCs $\sim 300 \text{ km s}^{-1}$. Finally, SP-CVCs are steeply increasing in the centre with a sharp peak, which changes abruptly to the flat part of the CVC at radius $\sim 0.2R_e$. This class is mostly represented by early-type (E1–E7), similar to the RP galaxies. The average amplitude of CVCs reaches $\sim 400 \text{ km s}^{-1}$.

In general, the SR class is represented by late-type, low-mass, young, faint, metal-poor and disc-dominated galaxies, while SP class is represented by early-type, high-mass, old, bright, metal-rich and bulge-dominated galaxies. FL and RP are represented by galaxies with various morphologies and intermediate values of mass, age, luminosity, metallicity and B/D ratio.

CVC-based classifications provide a view on galaxy potential that is complementary to morphological schemes. Our study provides a step forward in the empirical constraints on current and future theoretical models of galaxy evolution across a wide range of galaxy morphological types and masses. This approach provides a good way to reduce the complexity present in optical IFU studies of galaxies into a manageable descriptor of galaxy dynamics.

The following data products of the 238 (E1–Sdm) galaxies will be made available to the community at the CALIFA website, <http://califa.caha.es/?q=content/science-dataproducts>: the basic properties of the galaxies from Appendix B; the five main PC eigenvectors from Appendix C; the five main projection PC_i from Appendix D; the MGE models from Appendix E; the CVC models and their uncertainties from the online material.

ACKNOWLEDGEMENTS

This study makes use of the data provided by the Calar Alto Legacy Integral Field Area (CALIFA) survey (<http://califa.caha.es>). Based on observations collected at the Centro Astronómico Hispano Alemán (CAHA) at Calar Alto, operated jointly by the Max-Planck-Institut für Astronomie and the Instituto de Astrofísica de Andalucía (CSIC). CALIFA is the first legacy survey being performed at Calar Alto. The CALIFA collaboration would like to thank the IAA-CSIC and MPIA-MPG as major partners of the observatory, and CAHA itself, for the unique access to telescope time and support in manpower and infrastructures. The CALIFA collaboration also thanks the CAHA staff for the dedication to this project.

We are grateful to the anonymous referees for their constructive comments, which helped us to substantially improve the manuscript. VK acknowledges Glenn van de Ven, Jesús Falcón-Barroso, and Mariya Lyubenova for the relevant discussions. VK is supported by the Avadh Bhatia Fellowship at the University of Alberta. VK, DC and ER are supported by a Discovery Grant from NSERC of Canada. DC acknowledges support by the Deutsche Forschungsgemeinschaft, DFG through project number SFB956C.

LG is supported in part by the US National Science Foundation under Grant AST-1311862. LSM thanks support from the Spanish *Ministerio de Economía y Competitividad (MINECO)* via grant AYA2012-31935. RGD and RGB are supported by the Spanish Ministerio de Ciencia e Innovación under grant AYA2010-15081 and AyA2014-57490-P. SFS thanks the CONACYT-125180 and DGAPA-IA100815 projects for providing him support in this study. EF acknowledges support from MINECO and JA grants, AYA2014-53506-P and FQM-108. RAM acknowledges support by the Swiss National Science Foundation. JM-A acknowledge support from the European Research Council Starting Grant (SED-Morph; PI: V. Wild).

This research has made use of the NASA/IPAC Extragalactic Database (NED), which is operated by the Jet Propulsion Laboratory, California Institute of Technology, under contract with the National Aeronautics and Space Administration

Funding for the Sloan Digital Sky Survey IV has been provided by the Alfred P. Sloan Foundation, the U.S. Department of Energy Office of Science, and the Participating Institutions. SDSS-IV acknowledges support and resources from the Center for High-Performance Computing at the University of Utah. The SDSS web site is www.sdss.org.

SDSS-IV is managed by the Astrophysical Research Consortium for the Participating Institutions of the SDSS Collaboration including the Brazilian Participation Group, the Carnegie Institution for Science, Carnegie Mellon University, the Chilean Participation Group, the French Participation Group, Harvard-Smithsonian Center for Astrophysics, Instituto de Astrofísica de Canarias, The Johns Hopkins University, Kavli Institute for the Physics and Mathematics of the Universe (IPMU)/University of Tokyo, Lawrence Berkeley National Laboratory, Leibniz Institut für Astrophysik Potsdam (AIP), Max-Planck-Institut für Astronomie (MPIA Heidelberg), Max-Planck-Institut für Astrophysik (MPA Garching), Max-Planck-Institut für Extraterrestrische Physik (MPE), National Astronomical Observatory of China, New Mexico State University, New York University, University of Notre Dame, Observatório Nacional/MCTI, the Ohio State University, Pennsylvania State University, Shanghai Astronomical Observatory, United Kingdom Participation Group, Universidad Nacional Autónoma de México, University of Arizona, University of Colorado Boulder, University of Oxford, University of Portsmouth, University of Utah, University of Virginia, University of Washington, University of Wisconsin, Vanderbilt University, and Yale University.

This research made use of ASTROPY (<http://www.astropy.org>), a community-developed core PYTHON package for Astronomy (Astropy Collaboration et al. 2013).

References

- Abazajian K. N. et al., 2009, ApJS, 182, 543
- Alam S. et al., 2015, ApJS, 219, 12
- Astropy Collaboration et al., 2013, A&A, 558, A33
- Avila-Reese V., Firmani C., Zavala J., 2002, in Astronomical Society of the Pacific Conference Series, Vol. 282, Galaxies: the Third Dimension, Rosada M., Binette L., Arias L., eds., p. 137
- Bertin G., 2000, Dynamics of Galaxies, Cambridge, UK: Cambridge University Press, ISBN 0521472628
- Binney J., Merrifield M., 1998, Galactic Astronomy, Princeton University Press, Princeton, NJ
- Biviano A., Girardi M., Giuricin G., Mardirossian F., Mezzetti M., 1991, ApJ, 376, 458

- Blanc G. A. et al., 2010, in Astronomical Society of the Pacific Conference Series, Vol. 432, New Horizons in Astronomy: Frank N. Bash Symposium 2009, Stanford L. M., Green J. D., Hao L., Mao Y., eds., p. 180
- Bolatto A. D. et al., 2017, ApJ, preprint (arXiv: 1704.02504)
- Bosma A., 1981, AJ, 86, 1791
- Broeils A. H., 1992, A&A, 256, 19
- Bundy K. et al., 2015, ApJ, 798, 7
- Cappellari M., 2002, MNRAS, 333, 400
- Cappellari M., 2008, MNRAS, 390, 71
- Cappellari M., 2016, ARA&A, 54, 597
- Cappellari M., Copin Y., 2003, MNRAS, 342, 345
- Cappellari M., Emsellem E., 2004, PASP, 116, 138
- Cappellari M. et al., 2011, MNRAS, 413, 813
- Cappellari M. et al., 2013, MNRAS, 432, 1862
- Cappellari M. et al., 2015, ApJ, 804, L21
- Casertano S., van Gorkom J. H., 1991, AJ, 101, 1231
- Chattopadhyay T., Chattopadhyay A. K., 2006, AJ, 131, 2452
- Combes F., 2009, *Mysteries of Galaxy Formation*, Springer, Berlin
- Corradi R. L. M., Capaccioli M., 1990, A&A, 237, 36
- Croom S. M. et al., 2012, MNRAS, 421, 872
- de Vaucouleurs G., de Vaucouleurs A., Corwin, Jr. H. G., Buta R. J., Paturel G., Fouqué P., 1991, *Third Reference Catalogue of Bright Galaxies*. Volume I: Explanations and references. Volume II: Data for galaxies between 0^h and 12^h . Volume III: Data for galaxies between 12^h and 24^h . Springer, New York, NY
- Elmegreen D. M., Elmegreen B. G., 1982, MNRAS, 201, 1021
- Emsellem E. et al., 2007, MNRAS, 379, 401
- Emsellem E., Monnet G., Bacon R., 1994, A&A, 285, 723
- Everitt B. S., 1993, *Cluster Analysis*. New York: Halsted Press, ISBN 0-470-22043-0
- Falcón-Barroso J. et al., 2017, A&A, 597, A48
- García-Benito R. et al., 2015, A&A, 576, A135
- González Delgado R. M. et al., 2015, A&A, 581, A103
- Holmberg E., 1958, *Meddelanden fran Lunds Astronomiska Observatorium Serie II*, 136, 1
- Hubble E. P., 1936, *The Realm of the Nebulae*, New Haven: Yale University Press
- Husemann B. et al., 2013, A&A, 549, A87
- Jain A. K., Murty M. N., Flynn P. J., 1999, ACM Comput. Surv., 31, 264
- Kalinova V., Colombo D., Rosolowsky E., 2016, in IAU Symposium, Vol. 315, *From Interstellar Clouds to Star-Forming Galaxies: Universal Processes?*, Jablonka P., André P., van der Tak F., eds., p. E39
- Kalinova V., van de Ven G., Lyubenova M., Falcón-Barroso J., Colombo D., Rosolowsky E., 2017, MNRAS, 464, 1903
- Kalnajs A. J., 1983, in IAU Symposium, Vol. 100, *Internal Kinematics and Dynamics of Galaxies*, Athanassoula E., ed., pp. 109–115
- Keel W. C., 1993, AJ, 106, 1771
- Kent S. M., 1987, AJ, 93, 816
- Khochfar S., Silk J., 2006, MNRAS, 370, 902
- Koch I., 2013, *Analysis of Multivariate and High-Dimensional Data*. Cambridge University Press, Cambridge Books Online
- Kodinariya T. M., Makwana D. P. R., 2013, Int. J. Adv. Res. Comput. Sci. Manage. Stud., 1, 90
- Kormendy J., Bender R., 2012, ApJS, 198, 2
- Krajnović D., Cappellari M., de Zeeuw P. T., Copin Y., 2006, MNRAS, 366, 787
- Lin C. C., Shu F. H., 1964, ApJ, 140, 646
- Lloyd S., 1982, IEEE Transactions on Information Theory, 28, 129
- Longair M. S., 2008, *Galaxy Formation*, Berlin: Springer, ISBN 978-3-540-73477-2
- MacQueen J., 1967, in *Proceedings of the Fifth Berkeley Symposium on Mathematical Statistics and Probability*, Volume 1: Statistics, University of California Press, Berkeley, Calif., pp. 281–297
- Márquez I., Moles M., 1999, A&A, 344, 421
- Martinsson T. P. K., Verheijen M. A. W., Westfall K. B., Bershady M. A., Andersen D. R., Swaters R. A., 2013, A&A, 557, A131
- McGaugh S. S., Lelli F., Schombert J. M., 2016, Physical Review Letters, 117, 201101
- Méndez-Abreu J. et al., 2017, A&A, 598, A32
- Monnet G., Bacon R., Emsellem E., 1992, A&A, 253, 366
- Noordermeer E., van der Hulst J. M., Sancisi R., Swaters R. S., van Albada T. S., 2007, MNRAS, 376, 1513
- Palunas P., Williams T. B., 2000, AJ, 120, 2884
- Pearson K., 1901, On Lines and Planes of Closest Fit to Systems of Points in Space, *Philosophical Magazine*, 2 (11): 559–572
- Persic M., Salucci P., 1988, MNRAS, 234, 131
- Poggianti B. M., Smail I., Dressler A., Couch W. J., Barger A. J., Butcher H., Ellis R. S., Oemler, Jr. A., 1999, ApJ, 518, 576
- Roth M. M. et al., 2005, PASP, 117, 620
- Rubin V. C., Burstein D., Ford, Jr. W. K., Thonnard N., 1985, ApJ, 289, 81
- Rubin V. C., Ford W. K. J., Thonnard N., 1980, ApJ, 238, 471
- Sackett P. D., 1997, ApJ, 483, 103
- Sánchez S. F. et al., 2012, A&A, 538, A8
- Sancisi R., 2004, in IAU Symposium, Vol. 220, *Dark Matter in Galaxies*, Ryder S., Pisano D., Walker M., Freeman K., eds., p. 233
- Schwarzschild M., 1979, ApJ, 232, 236
- Shlens J., 2014, preprint, (arXiv: 1404.1100)
- Shostak G. S., 1977, A&A, 58, L31
- Sofue Y., Tutui Y., Honma M., Tomita A., Takamiya T., Koda J., Takeda Y., 1999, ApJ, 523, 136
- Sparke L. S., Gallagher, III J. S., 2007, *Galaxies in the Universe: An Introduction*. Cambridge University Press
- Spitzer, Jr. L., Baade W., 1951, ApJ, 113, 413
- Swaters R. A., Sancisi R., van Albada T. S., van der Hulst J. M., 2009, A&A, 493, 871
- Tonini C., Mutch S. J., Croton D. J., Wyithe J. S. B., 2016, MNRAS, 459, 4109
- Tukey J. W., 1977, *Exploratory data analysis*, Exploratory data analysis. Reading, PA: Addison-Wesley
- Valdes F., Gupta R., Rose J. A., Singh H. P., Bell D. J., 2004, ApJS, 152, 251
- van Albada T. S., Sancisi R., 1986, *Philosophical Transactions of the Royal Society of London Series A*, 320, 447
- van den Bergh S., 1976, ApJ, 206, 883
- van Dokkum P. G. et al., 2015, ApJ, 813, 23
- Verheijen M. A. W., Bershady M. A., Andersen D. R., Swaters R. A., Westfall K., Kelz A., Roth M. M., 2004, *Astronomische Nachrichten*, 325, 151
- Wakamatsu K.-I., 1976, PASJ, 28, 397
- Walcher C. J. et al., 2014, A&A, 569, A1
- Wang L., Dutton A. A., Stinson G. S., Macciò A. V., Penzo C., Kang X., Keller B. W., Wadsley J., 2015, MNRAS, 454, 83
- Wiegert T., English J., 2014, New Astronomy, 26, 40
- York D. G. et al., 2000, AJ, 120, 1579
- Zasov A. V., Kyazumov G. A., 1983, Soviet Ast., 27, 384

APPENDIX A: SECOND VELOCITY MOMENT MAPS

For our sample of 238 (E1-Sdm) galaxies, in Figs A1-A8, the first and second columns show the second moment maps $V_{\text{rms}} = \sqrt{V^2 + \sigma^2}$ of the data and the model with overplotted flux and MGE contours, respectively. The third columns correspond to the residual field between the observed and modelled V_{rms} maps, where $RES = |1 - (V_{\text{rms},\text{OBS}}/V_{\text{rms},\text{MOD}})|$ and \bar{RES} is the median value of the residual field. We observed that on average the median of the residual $\bar{RES} \sim 0.10$ for the 238 CALIFA galaxies, corresponding to 10 per cent error.

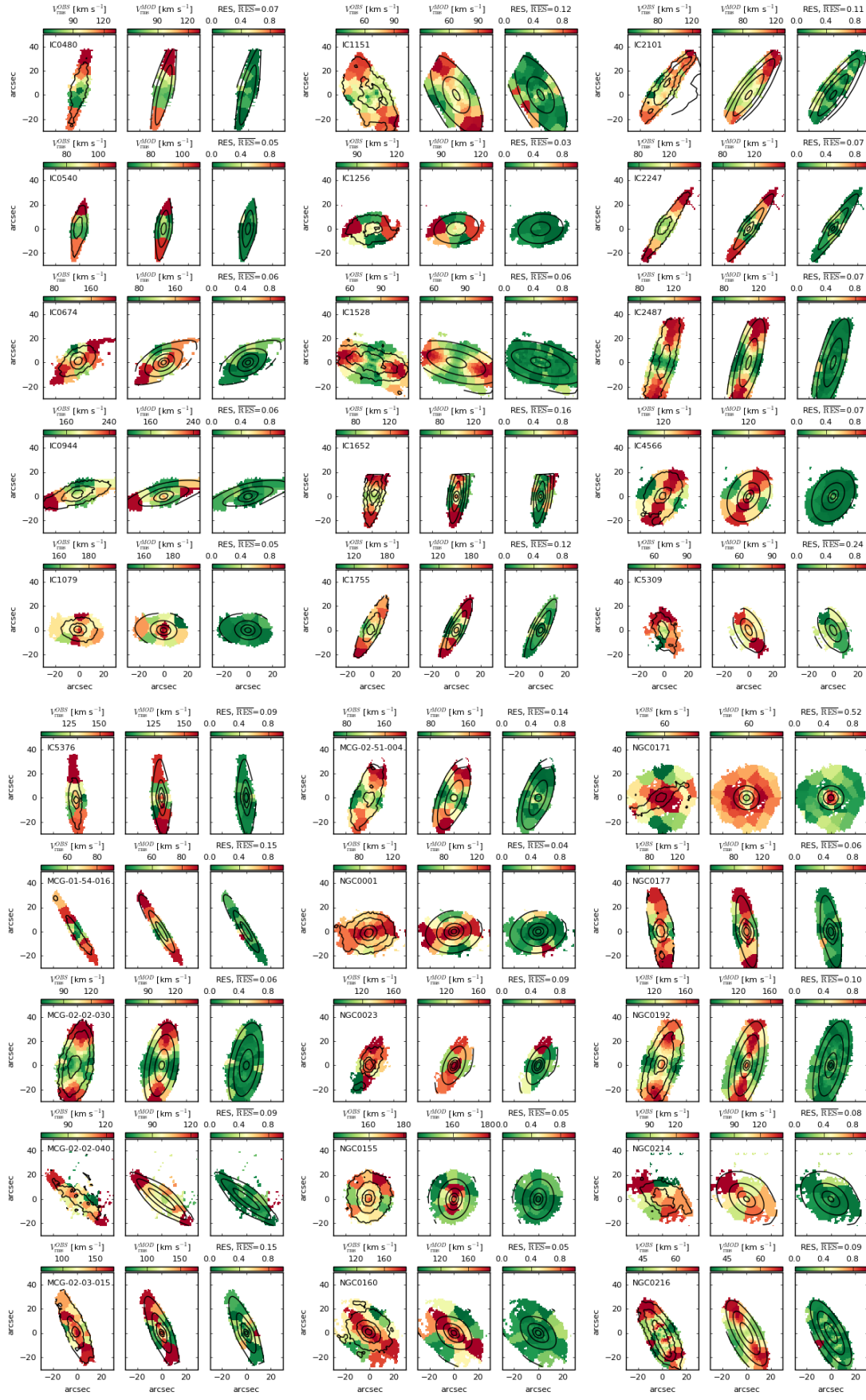


Figure A1. Second moment maps $V_{\text{rms}} = \sqrt{V^2 + \sigma^2}$ of the data and the model, and residual maps of our sample of 238 (E1–Sdm) galaxies.

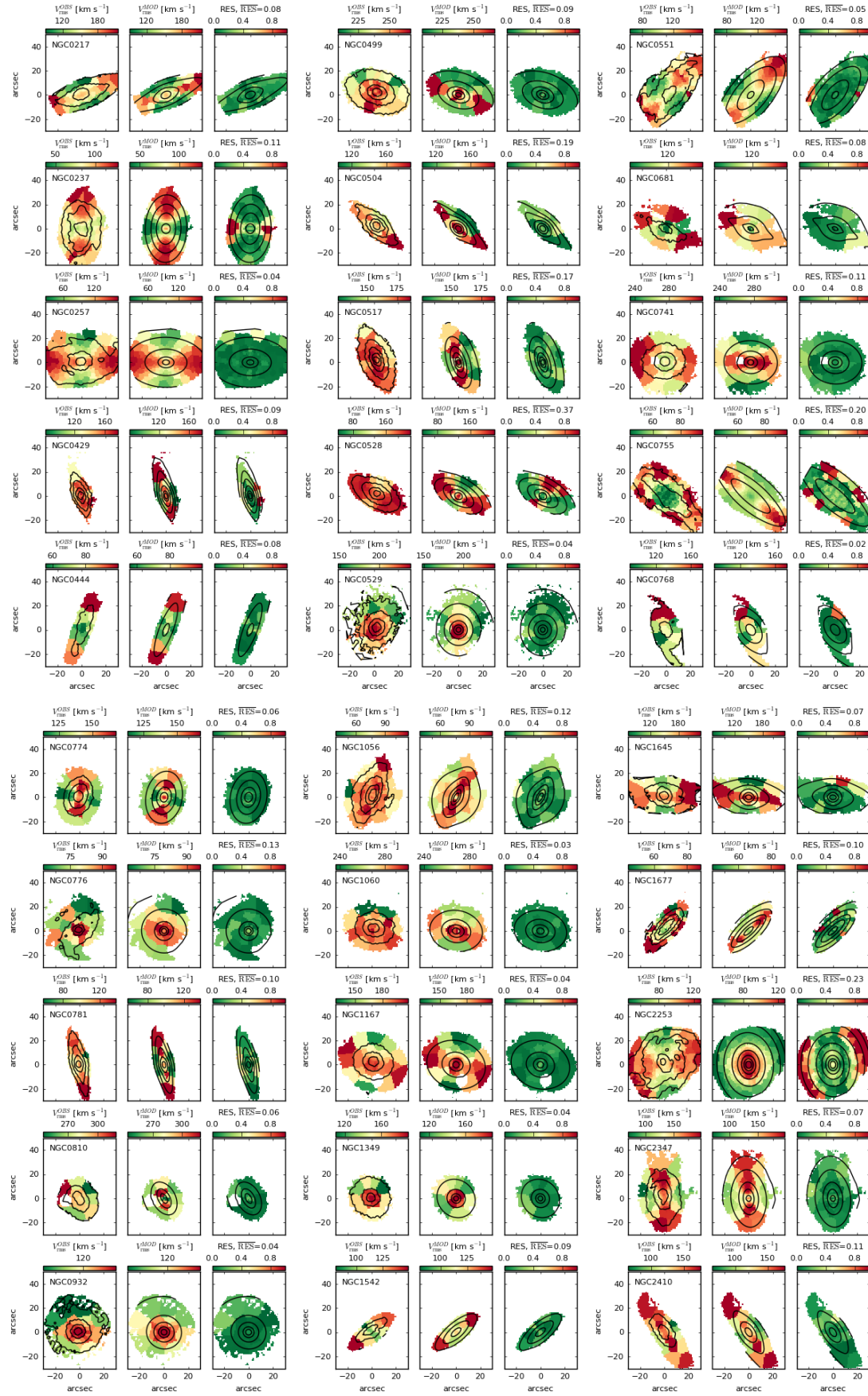


Figure A2. Second moment maps $V_{\text{rms}} = \sqrt{V^2 + \sigma^2}$ of the data and the model, and residual maps of our sample of 238 (E1–Sdm) galaxies.

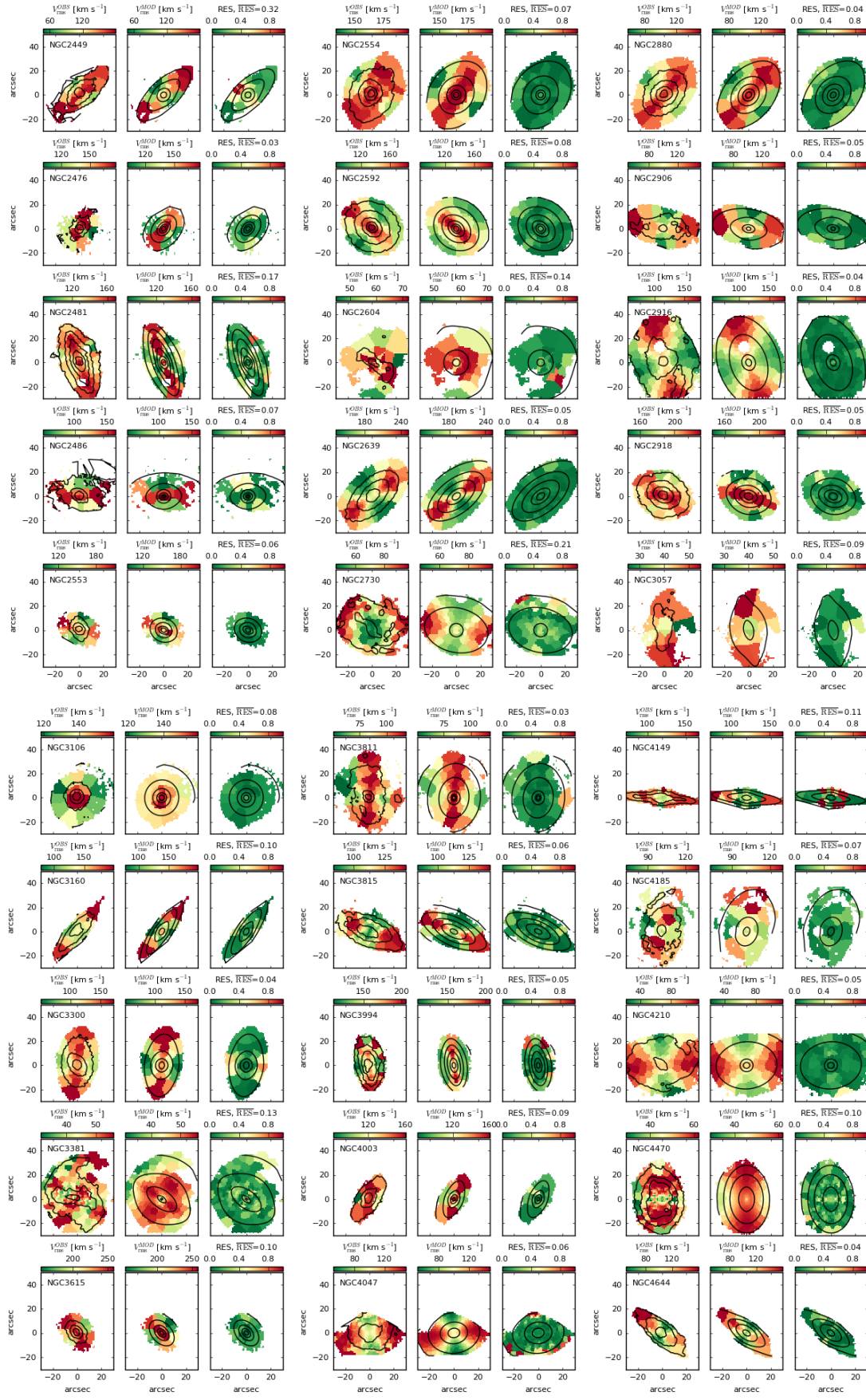


Figure A3. Second moment maps $V_{\text{rms}} = \sqrt{V^2 + \sigma^2}$ of the data and the model, and residual maps of our sample of 238 (E1–Sdm) galaxies.

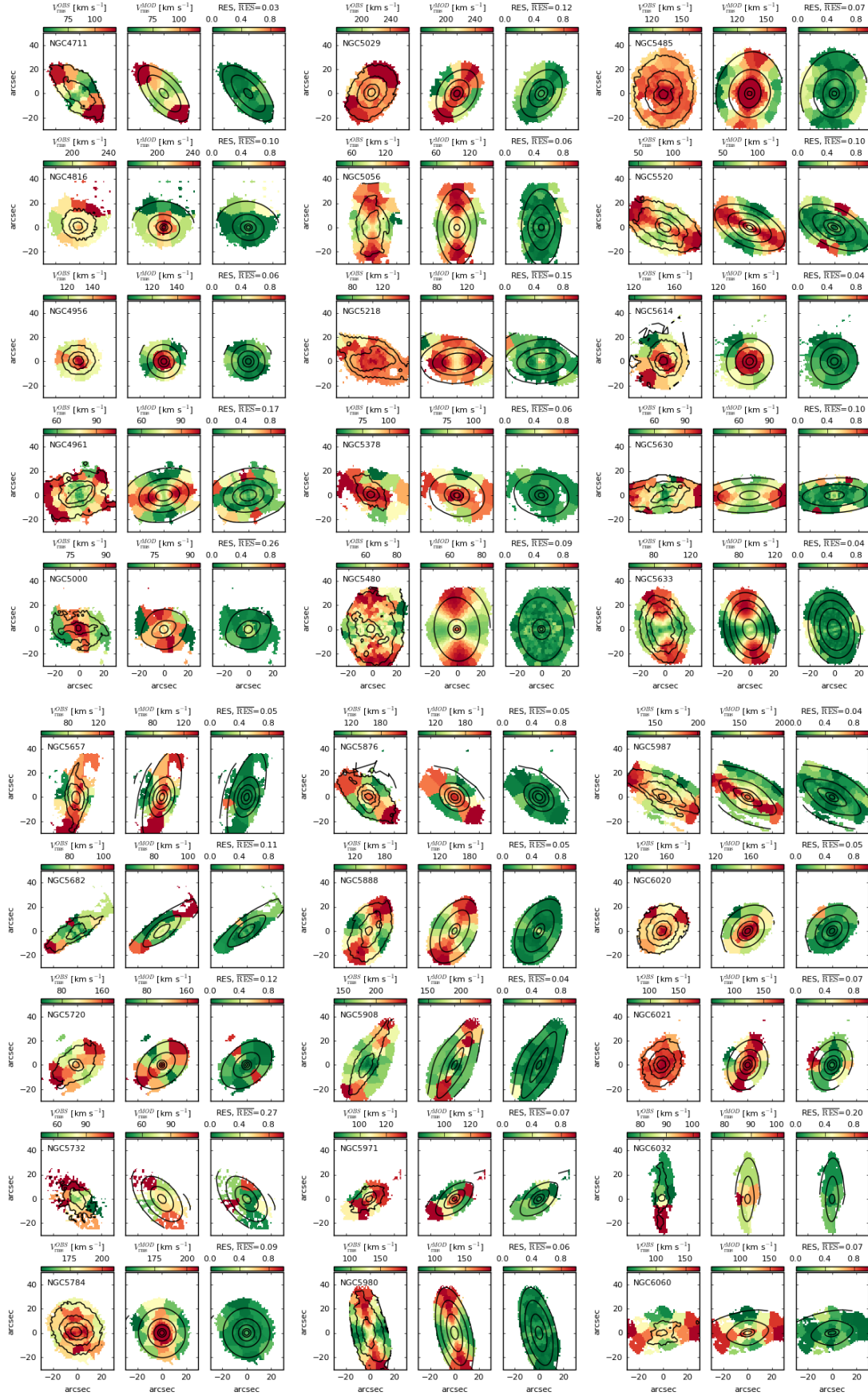


Figure A4. Second moment maps $V_{\text{rms}} = \sqrt{V^2 + \sigma^2}$ of the data and the model, and residual maps of our sample of 238 (E1–Sdm) galaxies.

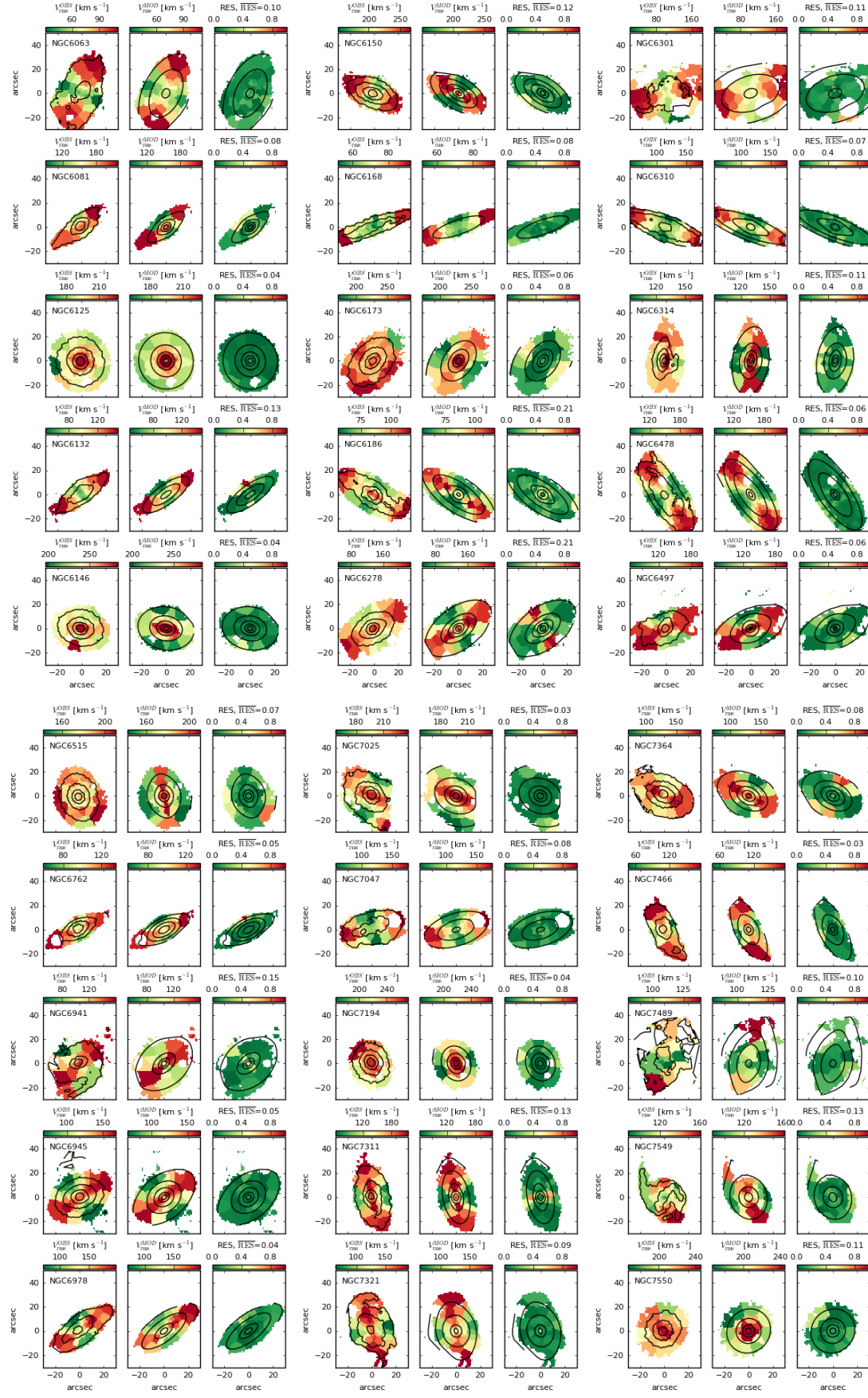


Figure A5. Second moment maps $V_{\text{rms}} = \sqrt{V^2 + \sigma^2}$ of the data and the model, and residual maps of our sample of 238 (E1–Sdm) galaxies.

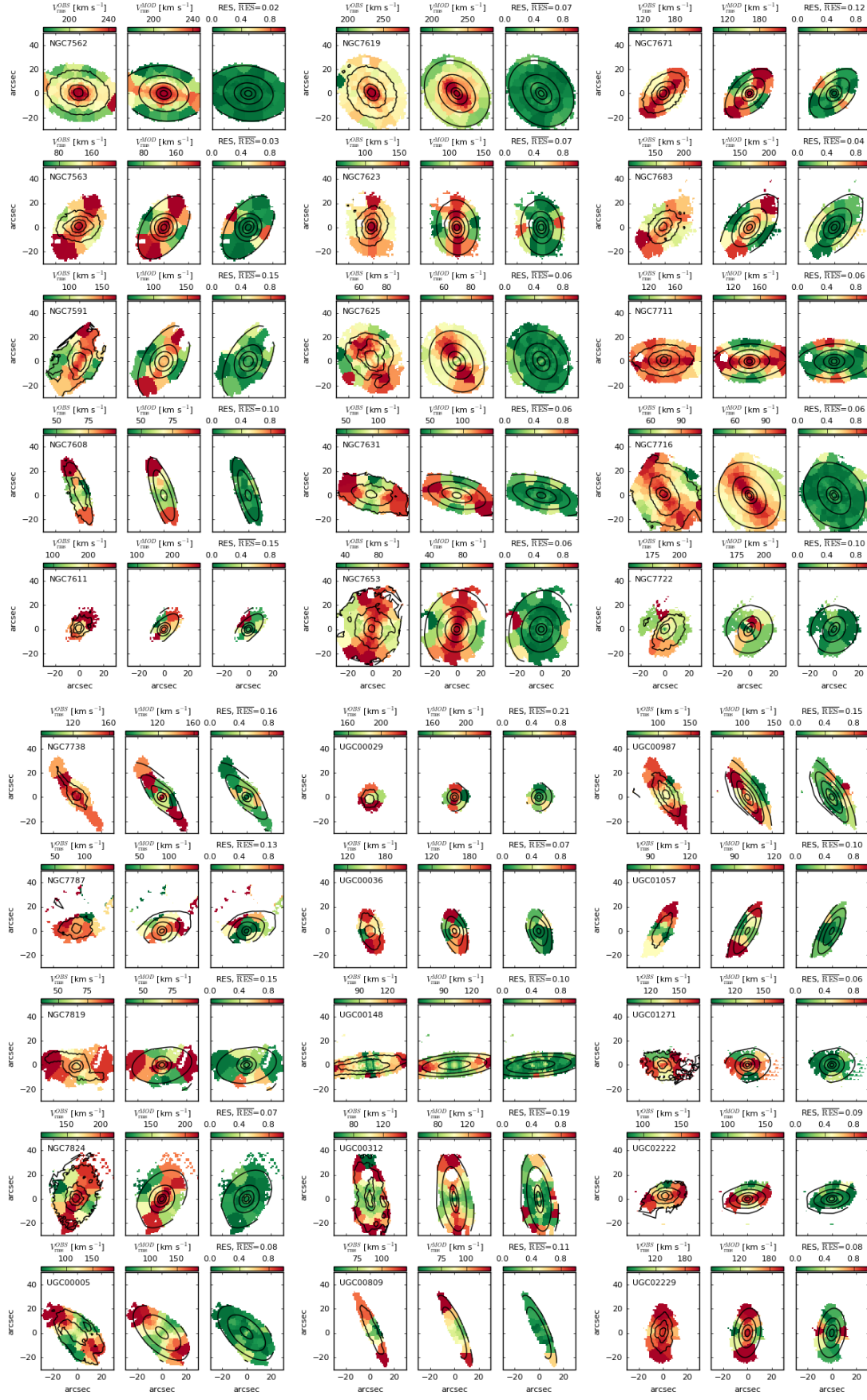


Figure A6. Second moment maps $V_{\text{rms}} = \sqrt{V^2 + \sigma^2}$ of the data and the model, and residual maps of our sample of 238 (E1–Sdm) galaxies.

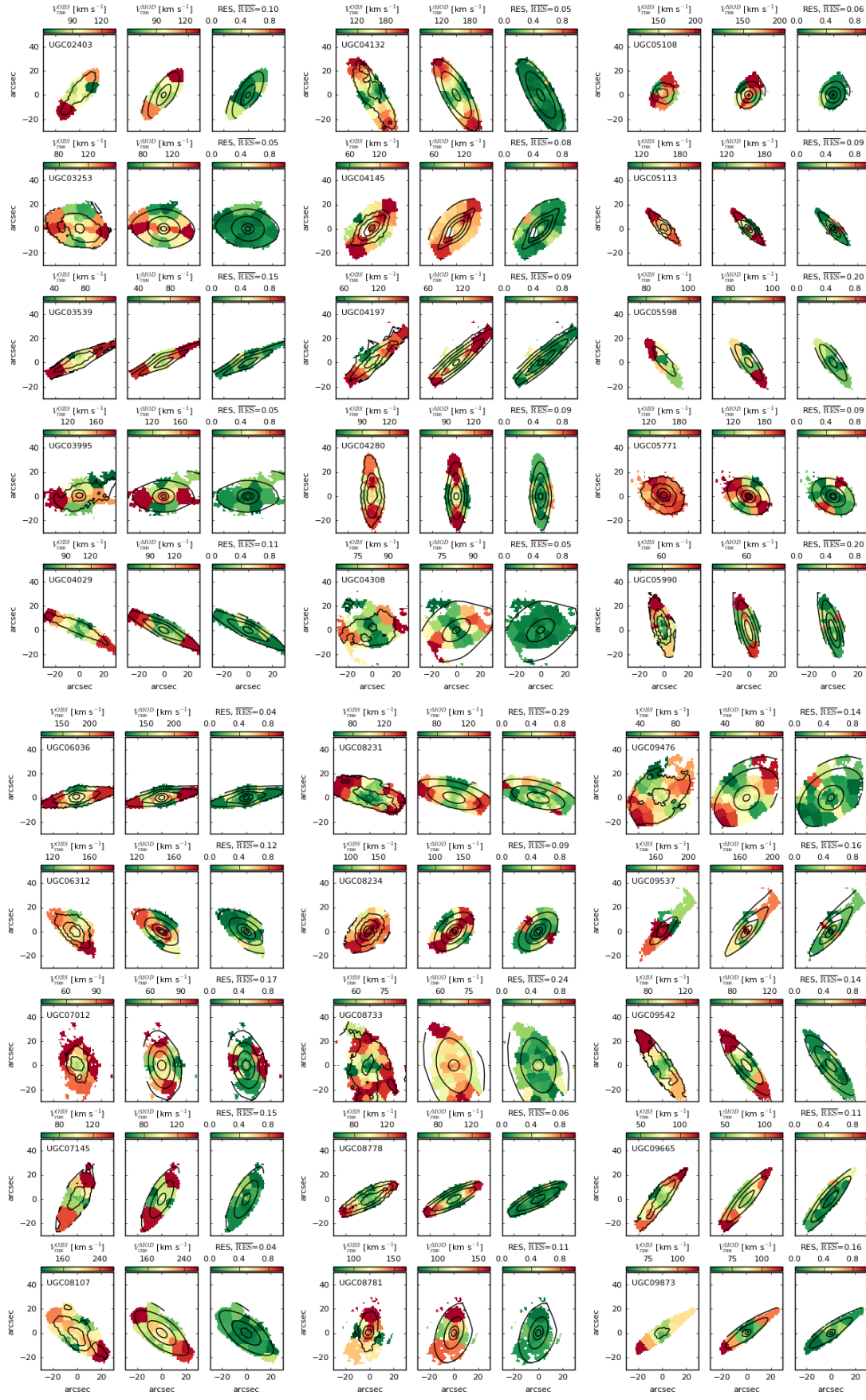


Figure A7. Second moment maps $V_{\text{rms}} = \sqrt{V^2 + \sigma^2}$ of the data and the model, and residual maps of our sample of 238 (E1–Sdm) galaxies.

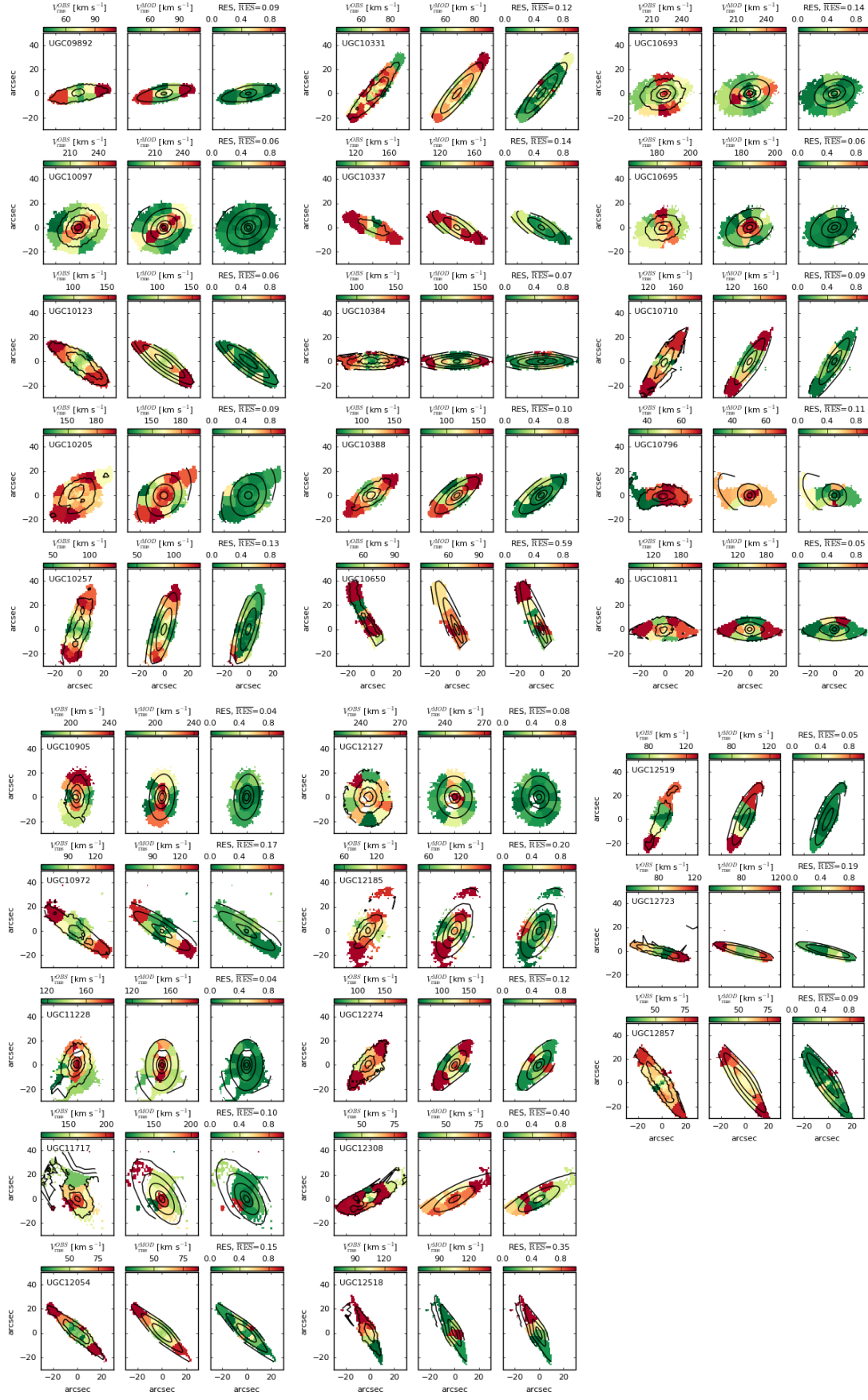


Figure A8. Second moment maps $V_{\text{rms}} = \sqrt{V^2 + \sigma^2}$ of the data and the model, and residual maps of our sample of 238 (E1–Sdm) galaxies.

**APPENDIX B: BASIC PROPERTIES OF THE 238 CALIFA
GALAXIES**

In Tables B1–B6, we present basic properties of the 238 (E1–Sdm) CALIFA galaxies from the literature and our own measurements.

Table B1. Properties of the 238 (E1–Sdm) CALIFA galaxies. Columns list (1) galaxy identifier, (2) Hubble type based on by-eye morphological classification from Walcher et al. (2014), (3) Hubble Flow (Galactocentric) distances from NED (using Hubble constant of $H_0=73 \text{ km sec}^{-1} \text{ Mpc}^{-1}$), calculated from the weighted mean radial velocities of the radio and optical redshifts, corrected to the Galactic standard of rest (GSR) from the RC3 (Third Reference Catalogue of Bright Galaxies) as described in de Vaucouleurs et al. (1991, section 3.10c, page 54). (4) and (5) Average photometric position angle and ellipticity from *r*-band SDSS (DR12) images with typical uncertainty of 5° – 10° and 5 per cent, respectively, using `findgalaxy` PYTHON procedure of Cappellari 2002. (6) From the axial ratio of the galaxies ($q = 1 - \epsilon$, where ϵ is the average ellipticity of the galaxy, determined from `findgalaxy`), we calculated the inclination (i) assuming $q_o = 0.2$ for the intrinsic axial ratio of the galaxies (Section 3.1). (7) Effective (half-light) radius measured via growth curve analysis (Walcher et al. 2014). (8) Radial extent of the stellar kinematic data in arcseconds (Falcón-Barroso et al. 2017). (9) Radial extent of the stellar kinematic data in terms of effective radius. (10) Systemic velocity of the galaxies with a typical uncertainty of 5 km s^{-1} , measured as the median value of the velocity field (Section 2.2). (11) and (12) The medians of the posterior distributions of the dynamical mass-to-light ratios and azimuthal velocity anisotropies, respectively, from JAM-MCMC model. The uncertainties are estimated as the 25th and 75th percentiles of the data corresponding to the median absolute deviation (Section 3.1). (13) CVC (circular velocity curve) class of the 238 (E1–Sdm) galaxies, where 0 – Slow rising (SR); 1 – Flat (FL); 2 – Round-peaked (RP); 3 – Sharp-peaked (SP).

Galaxy (1)	Type (2)	Dist Mpc (3)	PA (°) (4)	ϵ (5)	i (°) (6)	R_e (arcsec) (7)	R_{\max} (arcsec) (8)	R_{\max}/R_e (9)	V_{sys} (km s $^{-1}$) (10)	$(M/L)_{\text{dyn}}$ (11)	β_z (12)	CVC class (13)
IC0480	Sc	62	167	0.80	84	24	38	1.6	4597	$11.661^{+0.069}_{-0.073}$	$0.362^{+0.009}_{-0.012}$	0
IC0540	Sab	26	172	0.78	81	14	27	1.9	2095	$8.582^{+0.054}_{-0.047}$	$0.390^{+0.009}_{-0.011}$	0
IC0674	Sab	103	119	0.60	69	9	36	4.0	7459	$6.439^{+0.024}_{-0.022}$	$-0.451^{+0.021}_{-0.020}$	2
IC0944	Sab	96	105	0.66	75	19	37	1.9	6974	$8.054^{+0.025}_{-0.021}$	$0.440^{+0.004}_{-0.005}$	2
IC1079	E4	119	83	0.50	71	37	26	0.7	8631	$6.306^{+0.025}_{-0.023}$	$0.320^{+0.004}_{-0.005}$	1
IC1151	Scd	31	29	0.57	68	22	37	1.7	2158	$5.420^{+0.034}_{-0.032}$	$0.211^{+0.018}_{-0.029}$	0
IC1256	Sb	67	99	0.37	51	17	25	1.5	4691	$5.852^{+0.040}_{-0.038}$	$0.598^{+0.006}_{-0.010}$	0
IC1528	Sbc	53	74	0.57	68	23	41	1.8	3741	$3.582^{+0.021}_{-0.014}$	$0.402^{+0.010}_{-0.015}$	0
IC1652	S0a	73	171	0.78	78	11	26	2.4	5040	$2.959^{+0.013}_{-0.012}$	$0.456^{+0.009}_{-0.017}$	1
IC1755	Sb	110	155	0.75	78	11	31	2.8	7889	$7.108^{+0.021}_{-0.021}$	$0.281^{+0.010}_{-0.018}$	2
IC2101	Scd	61	145	0.76	80	25	44	1.8	4445	$5.773^{+0.044}_{-0.039}$	$0.601^{+0.005}_{-0.008}$	0
IC2247	Sab	58	145	0.77	81	21	41	2.0	4230	$7.787^{+0.035}_{-0.035}$	$0.480^{+0.011}_{-0.016}$	1
IC2487	Sc	58	164	0.74	76	25	40	1.6	4284	$7.423^{+0.026}_{-0.041}$	$0.610^{+0.007}_{-0.011}$	0
IC4566	Sb	81	151	0.38	53	15	27	1.8	5523	$5.556^{+0.030}_{-0.016}$	$-0.681^{+0.035}_{-0.030}$	2
IC5309	Sc	60	27	0.54	64	17	24	1.4	4153	$4.163^{+0.046}_{-0.037}$	$0.420^{+0.013}_{-0.019}$	0
IC5376	Sb	72	3	0.73	80	16	36	2.2	4975	$7.894^{+0.035}_{-0.035}$	$0.516^{+0.006}_{-0.008}$	2
MCG-01-54-016	Scd	42	31	0.74	80	24	38	1.6	2915	$10.861^{+0.172}_{-0.186}$	$0.818^{+0.011}_{-0.015}$	0
MCG-02-02-030	Sb	49	170	0.57	69	19	38	2.0	3482	$3.686^{+0.066}_{-0.013}$	$0.478^{+0.006}_{-0.010}$	0
MCG-02-02-040	Scd	50	51	0.63	81	20	34	1.7	3458	$7.080^{+0.064}_{-0.050}$	$0.569^{+0.005}_{-0.007}$	0
MCG-02-03-015	Sab	80	22	0.73	76	12	37	3.1	5773	$4.886^{+0.021}_{-0.029}$	$0.450^{+0.008}_{-0.015}$	1
MCG-02-51-004	Sb	79	160	0.63	69	17	34	2.0	5587	$6.556^{+0.018}_{-0.020}$	$0.259^{+0.010}_{-0.013}$	0
NGC0001	Sbc	65	105	0.31	47	12	30	2.5	4498	$3.129^{+0.020}_{-0.014}$	$0.163^{+0.012}_{-0.012}$	0
NGC0023	Sb	65	157	0.33	63	17	26	1.5	4570	$1.801^{+0.034}_{-0.018}$	$0.519^{+0.011}_{-0.023}$	1
NGC0155	E1	86	170	0.18	48	15	25	1.7	6182	$4.534^{+0.018}_{-0.016}$	$0.342^{+0.006}_{-0.010}$	2
NGC0160	Sa	74	51	0.47	59	22	35	1.6	5183	$5.868^{+0.034}_{-0.016}$	$0.494^{+0.004}_{-0.006}$	3
NGC0171	Sb	54	84	0.04	23	26	32	1.2	3879	$1.683^{+0.034}_{-0.012}$	$0.457^{+0.035}_{-0.194}$	1
NGC0177	Sab	53	190	0.75	77	13	37	2.8	3810	$5.498^{+0.023}_{-0.026}$	$0.079^{+0.011}_{-0.013}$	2
NGC0192	Sab	58	166	0.57	72	22	39	1.8	4192	$3.791^{+0.011}_{-0.009}$	$0.507^{+0.005}_{-0.011}$	1
NGC0214	Sbc	64	52	0.29	56	18	31	1.7	4501	$2.608^{+0.015}_{-0.013}$	$-0.030^{+0.024}_{-0.019}$	0
NGC0216	Sd	21	208	0.65	73	20	35	1.8	1544	$3.301^{+0.039}_{-0.039}$	$0.559^{+0.014}_{-0.017}$	0
NGC0217	Sa	55	113	0.76	79	23	41	1.8	3989	$5.593^{+0.016}_{-0.014}$	$0.349^{+0.004}_{-0.006}$	2
NGC0237	Sc	58	178	0.38	52	15	35	2.3	4125	$2.732^{+0.017}_{-0.015}$	$0.595^{+0.009}_{-0.024}$	0
NGC0257	Sc	74	89	0.38	52	21	40	1.9	5273	$3.448^{+0.012}_{-0.010}$	$0.056^{+0.016}_{-0.030}$	1
NGC0429	Sa	78	14	0.72	78	6	29	4.8	5650	$3.948^{+0.029}_{-0.018}$	$0.432^{+0.006}_{-0.008}$	2
NGC0444	Scd	68	159	0.76	78	23	32	1.4	4770	$6.327^{+0.065}_{-0.052}$	$0.694^{+0.009}_{-0.017}$	0
NGC0499	E5	62	71	0.34	54	21	31	1.5	4359	$6.672^{+0.100}_{-0.029}$	$0.727^{+0.002}_{-0.013}$	3
NGC0504	S0	60	48	0.66	76	8	30	3.8	4236	$7.243^{+0.020}_{-0.020}$	$0.122^{+0.006}_{-0.007}$	2
NGC0517	S0	60	17	0.52	66	10	34	3.4	4122	$5.136^{+0.042}_{-0.023}$	$0.712^{+0.002}_{-0.006}$	2
NGC0528	S0	68	58	0.49	61	12	28	2.3	4773	$5.408^{+0.017}_{-0.015}$	$0.517^{+0.005}_{-0.012}$	2
NGC0529	E4	68	179	0.18	35	12	37	3.1	4791	$5.811^{+0.022}_{-0.014}$	$0.063^{+0.013}_{-0.014}$	2
NGC0551	Sbc	73	140	0.62	67	19	44	2.3	5124	$4.714^{+0.032}_{-0.021}$	$0.388^{+0.007}_{-0.023}$	0

Table B2. Properties of the 238 (E1–Sdm) CALIFA galaxies. Columns list (1) galaxy identifier, (2) Hubble type based on by-eye morphological classification from Walcher et al. (2014), (3) Hubble Flow (Galactocentric) distances from NED (using Hubble constant of $H_0=73 \text{ km sec}^{-1} \text{ Mpc}^{-1}$), calculated from the weighted mean radial velocities of the radio and optical redshifts, corrected to the Galactic standard of rest (GSR) from the RC3 (Third Reference Catalogue of Bright Galaxies) as described in de Vaucouleurs et al. (1991, section 3.10c, page 54). (4) and (5) Average photometric position angle and ellipticity from *r*-band SDSS (DR12) images with typical uncertainty of $5^\circ\text{--}10^\circ$ and 5 per cent, respectively, using `findgalaxy` PYTHON procedure of Cappellari 2002. (6) From the axial ratio of the galaxies ($q = 1 - \epsilon$, where ϵ is the average ellipticity of the galaxy, determined from `findgalaxy`), we calculated the inclination (i) assuming $q_o = 0.2$ for the intrinsic axial ratio of the galaxies (Section 3.1). (7) Effective (half-light) radius measured via growth curve analysis (Walcher et al. 2014). (8) Radial extent of the stellar kinematic data in arcseconds (Falcón-Barroso et al. 2017). (9) Radial extent of the stellar kinematic data in terms of effective radius. (10) Systemic velocity of the galaxies with a typical uncertainty of 5 km s^{-1} , measured as the median value of the velocity field (Section 2.2). (11) and (12) The medians of the posterior distributions of the dynamical mass-to-light ratios and azimuthal velocity anisotropies, respectively, from JAM-MCMC model. The uncertainties are estimated as the 25th and 75th percentiles of the data corresponding to the median absolute deviation (Section 3.1). (13) CVC (circular velocity curve) class of the 238 (E1–Sdm) galaxies, where 0 – Slow rising (SR); 1 – Flat (FL); 2 – Round-peaked (RP); 3 – Sharp-peaked (SP).

Galaxy (1)	Type (2)	Dist Mpc (3)	PA (°) (4)	ϵ (5)	i (°) (6)	R_e (arcsec) (7)	R_{\max} (arcsec) (8)	R_{\max}/R_e (9)	V_{sys} (km s $^{-1}$) (10)	$(M/L)_{\text{dyn}}$ (11)	β_z (12)	CVC class (13)
NGC0681	Sa	24	67	0.32	86	30	37	1.2	1743	$6.745^{+0.050}_{-0.041}$	$-0.010^{+0.010}_{-0.011}$	1
NGC0741	E1	77	86	0.21	38	35	32	0.9	5524	$8.999^{+0.024}_{-0.021}$	$0.265^{+0.007}_{-0.009}$	3
NGC0755	Scd	23	49	0.67	76	28	39	1.4	1655	$4.933^{+0.044}_{-0.042}$	$0.447^{+0.009}_{-0.011}$	0
NGC0768	Sc	97	35	0.55	67	15	34	2.3	6898	$7.081^{+0.041}_{-0.036}$	$0.093^{+0.014}_{-0.014}$	2
NGC0774	S0	64	169	0.18	49	12	26	2.2	4595	$4.691^{+0.027}_{-0.013}$	$0.554^{+0.005}_{-0.008}$	2
NGC0776	Sb	69	67	0.05	29	19	32	1.7	4866	$1.976^{+0.020}_{-0.015}$	$-0.334^{+0.084}_{-0.089}$	1
NGC0781	Sa	49	12	0.71	79	8	32	4.0	3482	$2.738^{+0.011}_{-0.010}$	$0.413^{+0.005}_{-0.009}$	0
NGC0810	E5	106	28	0.32	61	17	20	1.2	7716	$12.168^{+0.047}_{-0.058}$	$0.275^{+0.007}_{-0.008}$	2
NGC0932	S0a	57	71	0.10	29	18	33	1.8	4066	$3.314^{+0.014}_{-0.010}$	$0.036^{+0.026}_{-0.034}$	1
NGC1056	Sa	22	154	0.32	70	14	37	2.6	1556	$3.115^{+0.029}_{-0.018}$	$0.252^{+0.008}_{-0.016}$	0
NGC1060	E3	72	81	0.17	42	27	26	1.0	5132	$5.797^{+0.043}_{-0.024}$	$0.788^{+0.002}_{-0.008}$	3
NGC1167	S0	69	73	0.18	38	24	30	1.2	4885	$5.198^{+0.016}_{-0.015}$	$0.591^{+0.003}_{-0.008}$	3
NGC1349	E6	90	43	0.14	32	17	21	1.2	6525	$5.395^{+0.031}_{-0.034}$	$0.440^{+0.012}_{-0.032}$	3
NGC1542	Sab	50	130	0.54	70	15	23	1.5	3687	$5.259^{+0.046}_{-0.033}$	$0.776^{+0.004}_{-0.007}$	0
NGC1645	S0a	66	85	0.59	66	13	39	3.0	4749	$6.579^{+0.017}_{-0.015}$	$-0.050^{+0.007}_{-0.010}$	2
NGC1677	Scd	36	133	0.73	77	12	29	2.4	2725	$4.317^{+0.060}_{-0.053}$	$0.465^{+0.015}_{-0.025}$	0
NGC2253	Sbc	50	5	0.25	41	15	36	2.4	3527	$9.701^{+0.067}_{-0.043}$	$0.815^{+0.001}_{-0.001}$	2
NGC2347	Sbc	62	5	0.38	56	18	42	2.3	4408	$4.306^{+0.021}_{-0.032}$	$0.599^{+0.005}_{-0.024}$	2
NGC2410	Sb	64	34	0.71	76	21	37	1.8	4638	$5.487^{+0.018}_{-0.016}$	$0.205^{+0.010}_{-0.012}$	2
NGC2449	Sab	66	134	0.56	66	16	33	2.1	4842	$4.078^{+0.014}_{-0.011}$	$-0.095^{+0.013}_{-0.018}$	0
NGC2476	E6	51	140	0.28	51	9	22	2.4	3628	$4.097^{+0.026}_{-0.023}$	$0.398^{+0.009}_{-0.021}$	2
NGC2481	S0	29	20	0.50	74	9	34	3.8	2147	$4.241^{+0.016}_{-0.013}$	$0.447^{+0.004}_{-0.035}$	2
NGC2486	Sab	63	93	0.42	56	15	29	1.9	4602	$5.837^{+0.034}_{-0.032}$	$-0.019^{+0.028}_{-0.031}$	1
NGC2553	Sb	64	65	0.46	61	9	19	2.1	4622	$7.403^{+0.035}_{-0.035}$	$-0.264^{+0.017}_{-0.016}$	2
NGC2554	S0a	56	146	0.35	49	19	38	2.0	4064	$5.097^{+0.013}_{-0.010}$	$-0.029^{+0.006}_{-0.008}$	3
NGC2592	E4	26	49	0.20	51	9	28	3.1	1937	$6.868^{+0.013}_{-0.013}$	$-0.029^{+0.006}_{-0.007}$	2
NGC2604	Sd	28	179	0.08	22	26	36	1.4	2048	$4.619^{+0.047}_{-0.044}$	$0.552^{+0.024}_{-0.034}$	0
NGC2639	Sa	46	128	0.38	61	17	38	2.2	3149	$4.334^{+0.011}_{-0.023}$	$0.579^{+0.003}_{-0.020}$	2
NGC2730	Scd	51	77	0.23	49	24	39	1.6	3762	$4.926^{+0.045}_{-0.031}$	$0.377^{+0.015}_{-0.021}$	0
NGC2880	E7	22	140	0.36	54	18	36	2.0	1553	$4.365^{+0.010}_{-0.008}$	$0.032^{+0.006}_{-0.008}$	1
NGC2906	Sbc	28	81	0.45	58	19	33	1.7	2110	$5.364^{+0.021}_{-0.018}$	$0.390^{+0.010}_{-0.014}$	1
NGC2916	Sbc	50	18	0.36	56	26	40	1.5	3678	$4.480^{+0.010}_{-0.009}$	$-0.403^{+0.022}_{-0.019}$	1
NGC2918	E6	93	74	0.34	53	12	28	2.3	6653	$6.008^{+0.018}_{-0.015}$	$0.424^{+0.003}_{-0.006}$	2
NGC3057	Sdm	23	191	0.38	81	32	34	1.1	1508	$6.614^{+0.107}_{-0.101}$	$-0.307^{+0.036}_{-0.046}$	0
NGC3106	Sab	84	169	0.01	25	21	32	1.5	6111	$4.023^{+0.014}_{-0.014}$	$0.017^{+0.033}_{-0.034}$	1
NGC3160	Sab	95	148	0.68	75	15	36	2.4	6777	$8.517^{+0.039}_{-0.046}$	$0.488^{+0.007}_{-0.010}$	2
NGC3300	S0a	41	174	0.45	59	13	32	2.5	2989	$4.728^{+0.021}_{-0.013}$	$0.027^{+0.010}_{-0.014}$	2
NGC3381	Sd	22	54	0.13	63	24	42	1.8	1594	$2.305^{+0.034}_{-0.027}$	$0.350^{+0.010}_{-0.012}$	0
NGC3615	E5	91	42	0.40	53	15	18	1.2	6581	$5.669^{+0.039}_{-0.028}$	$0.572^{+0.006}_{-0.013}$	3
NGC3811	Sbc	43	174	0.29	48	21	39	1.9	3064	$3.817^{+0.014}_{-0.012}$	$0.120^{+0.013}_{-0.013}$	1

Table B3. Properties of the 238 (E1–Sdm) CALIFA galaxies. Columns list (1) galaxy identifier, (2) Hubble type based on by-eye morphological classification from Walcher et al. (2014), (3) Hubble Flow (Galactocentric) distances from NED (using Hubble constant of $H_0=73 \text{ km sec}^{-1} \text{ Mpc}^{-1}$), calculated from the weighted mean radial velocities of the radio and optical redshifts, corrected to the Galactic standard of rest (GSR) from the RC3 (Third Reference Catalogue of Bright Galaxies) as described in de Vaucouleurs et al. (1991, section 3.10c, page 54). (4) and (5) Average photometric position angle and ellipticity from *r*-band SDSS (DR12) images with typical uncertainty of 5° – 10° and 5 per cent, respectively, using `findgalaxy` PYTHON procedure of Cappellari 2002. (6) From the axial ratio of the galaxies ($q = 1 - \epsilon$, where ϵ is the average ellipticity of the galaxy, determined from `findgalaxy`), we calculated the inclination (i) assuming $q_o = 0.2$ for the intrinsic axial ratio of the galaxies (Section 3.1). (7) Effective (half-light) radius measured via growth curve analysis (Walcher et al. 2014). (8) Radial extent of the stellar kinematic data in arcseconds (Falcón-Barroso et al. 2017). (9) Radial extent of the stellar kinematic data in terms of effective radius. (10) Systemic velocity of the galaxies with a typical uncertainty of 5 km s^{-1} , measured as the median value of the velocity field (Section 2.2). (11) and (12) The medians of the posterior distributions of the dynamical mass-to-light ratios and azimuthal velocity anisotropies, respectively, from JAM-MCMC model. The uncertainties are estimated as the 25th and 75th percentiles of the data corresponding to the median absolute deviation (Section 3.1). (13) CVC (circular velocity curve) class of the 238 (E1–Sdm) galaxies, where 0 – Slow rising (SR); 1 – Flat (FL); 2 – Round-peaked (RP); 3 – Sharp-peaked (SP).

Galaxy (1)	Type (2)	Dist Mpc (3)	PA (°) (4)	ϵ (5)	i (°) (6)	R_e (arcsec) (7)	R_{\max} (arcsec) (8)	R_{\max}/R_e (9)	V_{sys} (km s $^{-1}$) (10)	$(M/L)_{\text{dyn}}$ (11)	β_z (12)	CVC class (13)
NGC3815	Sbc	50	65	0.57	71	14	34	2.4	3655	$5.177^{+0.021}_{-0.019}$	$0.257^{+0.007}_{-0.009}$	0
NGC3994	Sbc	42	8	0.44	68	9	26	2.9	3115	$5.358^{+0.034}_{-0.027}$	$0.441^{+0.006}_{-0.010}$	2
NGC4003	S0a	89	159	0.36	64	14	22	1.6	6499	$4.037^{+0.025}_{-0.021}$	$0.557^{+0.008}_{-0.031}$	1
NGC4047	Sbc	48	97	0.19	38	16	33	2.1	3381	$3.801^{+0.025}_{-0.017}$	$0.699^{+0.006}_{-0.019}$	2
NGC4149	Sa	43	84	0.73	81	18	36	2.0	3030	$6.325^{+0.033}_{-0.029}$	$0.405^{+0.010}_{-0.017}$	0
NGC4185	Sbc	53	164	0.34	52	30	38	1.3	3831	$5.304^{+0.033}_{-0.020}$	$0.398^{+0.009}_{-0.016}$	0
NGC4210	Sb	39	95	0.26	43	21	36	1.7	2694	$4.544^{+0.016}_{-0.014}$	$-0.447^{+0.044}_{-0.046}$	0
NGC4470	Sc	31	1	0.32	71	15	33	2.2	2309	$1.636^{+0.024}_{-0.015}$	$0.001^{+0.019}_{-0.021}$	0
NGC4644	Sb	69	56	0.67	76	12	29	2.4	4933	$6.180^{+0.037}_{-0.021}$	$-0.680^{+0.033}_{-0.033}$	0
NGC4711	Sbc	56	42	0.47	67	17	33	1.9	4027	$4.202^{+0.019}_{-0.018}$	$0.128^{+0.010}_{-0.014}$	0
NGC4816	E1	95	79	0.27	52	30	30	1.0	6813	$9.178^{+0.024}_{-0.024}$	$0.430^{+0.004}_{-0.004}$	3
NGC4956	E1	66	38	0.12	30	9	21	2.3	4683	$2.730^{+0.011}_{-0.009}$	$-0.138^{+0.025}_{-0.024}$	2
NGC4961	Scd	35	100	0.33	49	15	33	2.2	2549	$5.201^{+0.036}_{-0.035}$	$0.632^{+0.007}_{-0.010}$	0
NGC5000	Sbc	77	115	0.29	63	16	30	1.9	5586	$2.499^{+0.015}_{-0.014}$	$0.365^{+0.008}_{-0.012}$	0
NGC5029	E6	121	146	0.37	51	25	28	1.1	8563	$9.458^{+0.026}_{-0.025}$	$0.326^{+0.005}_{-0.005}$	3
NGC5056	Sc	77	181	0.48	63	15	38	2.5	5534	$4.376^{+0.016}_{-0.012}$	$-0.182^{+0.017}_{-0.019}$	0
NGC5218	Sab	42	95	0.33	57	18	36	2.0	2906	$4.542^{+0.042}_{-0.018}$	$0.768^{+0.002}_{-0.006}$	2
NGC5378	Sb	43	77	0.25	42	24	34	1.4	2925	$5.601^{+0.028}_{-0.025}$	$0.612^{+0.004}_{-0.013}$	1
NGC5480	Scd	27	186	0.19	46	25	41	1.6	1906	$2.780^{+0.025}_{-0.018}$	$0.430^{+0.014}_{-0.022}$	0
NGC5485	E5	28	171	0.24	45	31	38	1.2	1902	$6.688^{+0.017}_{-0.019}$	$0.522^{+0.003}_{-0.010}$	3
NGC5520	Sbc	27	64	0.50	61	12	34	2.8	1879	$4.934^{+0.023}_{-0.019}$	$0.330^{+0.009}_{-0.014}$	0
NGC5614	Sa	54	133	0.19	36	18	35	1.9	3818	$3.792^{+0.015}_{-0.013}$	$0.008^{+0.013}_{-0.012}$	2
NGC5630	Sdm	38	93	0.66	75	22	38	1.7	2642	$5.803^{+0.043}_{-0.038}$	$0.198^{+0.023}_{-0.026}$	0
NGC5633	Sbc	34	193	0.33	49	13	35	2.7	2333	$3.157^{+0.021}_{-0.027}$	$0.596^{+0.010}_{-0.084}$	0
NGC5657	Sbc	54	165	0.62	71	10	39	3.9	3881	$4.961^{+0.017}_{-0.016}$	$-0.177^{+0.014}_{-0.014}$	2
NGC5682	Scd	33	129	0.65	77	26	38	1.5	2278	$13.554^{+0.158}_{-0.142}$	$0.501^{+0.014}_{-0.020}$	0
NGC5720	Sbc	108	131	0.31	49	16	27	1.7	7687	$5.211^{+0.017}_{-0.019}$	$0.059^{+0.011}_{-0.013}$	1
NGC5732	Sbc	53	39	0.47	60	14	32	2.3	3768	$5.972^{+0.064}_{-0.055}$	$0.317^{+0.017}_{-0.020}$	0
NGC5784	S0	75	190	0.31	59	13	29	2.2	5418	$6.000^{+0.013}_{-0.011}$	$-0.035^{+0.004}_{-0.005}$	2
NGC5876	S0a	47	50	0.58	67	12	31	2.6	3274	$9.370^{+0.023}_{-0.025}$	$0.094^{+0.005}_{-0.008}$	2
NGC5888	Sb	121	152	0.39	68	16	31	1.9	8583	$5.749^{+0.013}_{-0.011}$	$-0.888^{+0.060}_{-0.023}$	2
NGC5908	Sa	47	154	0.56	81	34	42	1.2	3327	$8.192^{+0.020}_{-0.016}$	$-0.026^{+0.006}_{-0.005}$	2
NGC5971	Sb	61	131	0.55	68	12	27	2.2	3385	$6.655^{+0.047}_{-0.033}$	$0.429^{+0.006}_{-0.008}$	0
NGC5980	Sbc	57	193	0.62	71	17	40	2.4	4045	$4.474^{+0.022}_{-0.014}$	$0.401^{+0.008}_{-0.012}$	2
NGC5987	Sa	44	61	0.61	75	33	37	1.1	2994	$6.452^{+0.024}_{-0.014}$	$0.308^{+0.004}_{-0.006}$	1
NGC6020	E4	60	133	0.29	50	19	25	1.3	4272	$6.520^{+0.037}_{-0.027}$	$0.417^{+0.005}_{-0.008}$	3
NGC6021	E5	66	156	0.30	48	9	27	3.0	4698	$6.203^{+0.029}_{-0.025}$	$0.475^{+0.003}_{-0.005}$	2
NGC6032	Sbc	60	179	0.48	76	27	39	1.4	4331	$3.198^{+0.063}_{-0.028}$	$0.757^{+0.004}_{-0.018}$	0
NGC6060	Sb	62	100	0.58	65	28	35	1.2	4407	$4.937^{+0.020}_{-0.017}$	$0.325^{+0.010}_{-0.021}$	1
NGC6063	Sbc	40	155	0.45	59	20	36	1.8	2853	$5.875^{+0.025}_{-0.025}$	$-0.073^{+0.025}_{-0.031}$	0

Table B4. Properties of the 238 (E1–Sdm) CALIFA galaxies. Columns list (1) galaxy identifier, (2) Hubble type based on by-eye morphological classification from Walcher et al. (2014), (3) Hubble Flow (Galactocentric) distances from NED (using Hubble constant of $H_0=73 \text{ km sec}^{-1} \text{ Mpc}^{-1}$), calculated from the weighted mean radial velocities of the radio and optical redshifts, corrected to the Galactic standard of rest (GSR) from the RC3 (Third Reference Catalogue of Bright Galaxies) as described in de Vaucouleurs et al. (1991, section 3.10c, page 54). (4) and (5) Average photometric position angle and ellipticity from r -band SDSS (DR12) images with typical uncertainty of 5° – 10° and 5 per cent, respectively, using `findgalaxy` PYTHON procedure of Cappellari 2002. (6) From the axial ratio of the galaxies ($q = 1 - \epsilon$, where ϵ is the average ellipticity of the galaxy, determined from `findgalaxy`), we calculated the inclination (i) assuming $q_o = 0.2$ for the intrinsic axial ratio of the galaxies (Section 3.1). (7) Effective (half-light) radius measured via growth curve analysis (Walcher et al. 2014). (8) Radial extent of the stellar kinematic data in arcseconds (Falcón-Barroso et al. 2017). (9) Radial extent of the stellar kinematic data in terms of effective radius. (10) Systemic velocity of the galaxies with a typical uncertainty of 5 km s^{-1} , measured as the median value of the velocity field (Section 2.2). (11) and (12) The medians of the posterior distributions of the dynamical mass-to-light ratios and azimuthal velocity anisotropies, respectively, from JAM-MCMC model. The uncertainties are estimated as the 25th and 75th percentiles of the data corresponding to the median absolute deviation (Section 3.1). (13) CVC (circular velocity curve) class of the 238 (E1–Sdm) galaxies, where 0 – Slow rising (SR); 1 – Flat (FL); 2 – Round-peaked (RP); 3 – Sharp-peaked (SP).

Galaxy (1)	Type (2)	Dist Mpc (3)	PA (°) (4)	ϵ (5)	i (°) (6)	R_e (arcsec) (7)	R_{\max} (arcsec) (8)	R_{\max}/R_e (9)	V_{sys} (km s $^{-1}$) (10)	$(M/L)_{\text{dyn}}$ (11)	β_z (12)	CVC class (13)
NGC6081	S0a	72	129	0.60	71	12	30	2.5	5073	$6.046^{+0.025}_{-0.022}$	$0.197^{+0.008}_{-0.012}$	2
NGC6125	E1	69	199	0.04	26	21	28	1.3	4678	$6.507^{+0.018}_{-0.012}$	$0.389^{+0.006}_{-0.008}$	3
NGC6132	Sbc	69	126	0.66	72	14	31	2.2	4911	$5.884^{+0.025}_{-0.027}$	$0.384^{+0.011}_{-0.018}$	0
NGC6146	E5	123	79	0.35	49	15	26	1.7	8700	$5.968^{+0.018}_{-0.018}$	$0.270^{+0.005}_{-0.006}$	2
NGC6150	E7	122	58	0.46	61	11	29	2.6	8645	$6.897^{+0.019}_{-0.019}$	$0.633^{+0.002}_{-0.005}$	2
NGC6168	Sc	36	109	0.77	77	26	34	1.3	2539	$7.706^{+0.078}_{-0.070}$	$0.548^{+0.017}_{-0.017}$	0
NGC6173	E6	122	145	0.39	53	38	32	0.8	8694	$6.146^{+0.017}_{-0.017}$	$0.544^{+0.002}_{-0.004}$	3
NGC6186	Sb	42	55	0.36	69	20	35	1.8	2937	$2.341^{+0.014}_{-0.012}$	$0.218^{+0.013}_{-0.019}$	1
NGC6278	S0a	41	126	0.45	57	11	33	3.0	2869	$5.284^{+0.015}_{-0.017}$	$0.517^{+0.003}_{-0.008}$	2
NGC6301	Sbc	117	108	0.42	57	24	39	1.6	8219	$5.787^{+0.017}_{-0.014}$	$-0.119^{+0.014}_{-0.017}$	0
NGC6310	Sb	50	248	0.72	76	23	33	1.4	3393	$6.152^{+0.022}_{-0.022}$	$0.347^{+0.012}_{-0.026}$	0
NGC6314	Sab	93	171	0.44	60	12	37	3.1	6548	$3.258^{+0.020}_{-0.013}$	$0.712^{+0.003}_{-0.006}$	2
NGC6478	Sc	96	215	0.58	69	23	38	1.7	6701	$5.026^{+0.012}_{-0.014}$	$0.612^{+0.005}_{-0.012}$	1
NGC6497	Sab	87	114	0.45	61	13	34	2.6	5981	$5.385^{+0.012}_{-0.013}$	$-0.199^{+0.010}_{-0.013}$	3
NGC6515	E3	97	193	0.33	62	19	28	1.5	6764	$5.769^{+0.021}_{-0.019}$	$0.163^{+0.004}_{-0.006}$	3
NGC6762	Sab	43	118	0.70	78	9	31	3.4	2932	$4.733^{+0.016}_{-0.021}$	$0.120^{+0.008}_{-0.011}$	0
NGC6941	Sb	87	131	0.28	53	20	32	1.6	6171	$4.154^{+0.013}_{-0.010}$	$-0.270^{+0.020}_{-0.022}$	1
NGC6945	S0	54	129	0.33	55	13	31	2.4	3750	$3.622^{+0.011}_{-0.008}$	$-0.326^{+0.013}_{-0.014}$	2
NGC6978	Sb	84	128	0.62	70	18	34	1.9	5876	$5.003^{+0.011}_{-0.014}$	$0.380^{+0.007}_{-0.008}$	2
NGC7025	S0a	71	66	0.31	46	13	31	2.4	4916	$5.381^{+0.014}_{-0.010}$	$0.033^{+0.007}_{-0.011}$	2
NGC7047	Sbc	82	108	0.52	61	18	29	1.6	5729	$4.719^{+0.021}_{-0.022}$	$0.230^{+0.013}_{-0.023}$	0
NGC7194	E3	113	20	0.31	47	17	22	1.3	8037	$7.426^{+0.036}_{-0.027}$	$0.117^{+0.007}_{-0.012}$	2
NGC7311	Sa	64	11	0.46	61	12	37	3.1	4474	$2.752^{+0.011}_{-0.011}$	$0.294^{+0.011}_{-0.028}$	2
NGC7321	Sbc	100	15	0.34	56	15	32	2.1	7060	$4.272^{+0.015}_{-0.010}$	$-0.634^{+0.031}_{-0.020}$	0
NGC7364	Sab	68	62	0.34	49	12	32	2.7	4797	$3.906^{+0.013}_{-0.016}$	$0.758^{+0.003}_{-0.013}$	2
NGC7466	Sbc	106	206	0.58	67	13	31	2.4	7417	$5.280^{+0.016}_{-0.017}$	$0.087^{+0.015}_{-0.017}$	0
NGC7489	Sbc	88	169	0.43	67	20	39	2.0	6170	$3.516^{+0.022}_{-0.016}$	$0.134^{+0.011}_{-0.018}$	0
NGC7549	Sbc	67	196	0.58	72	20	34	1.7	4616	$7.854^{+0.042}_{-0.038}$	$-0.514^{+0.019}_{-0.015}$	2
NGC7550	E4	72	138	0.08	22	24	25	1.0	5029	$7.122^{+0.024}_{-0.023}$	$0.318^{+0.014}_{-0.016}$	3
NGC7562	E4	51	83	0.35	66	20	36	1.8	3588	$5.285^{+0.028}_{-0.012}$	$0.220^{+0.003}_{-0.005}$	2
NGC7563	Sa	59	146	0.40	55	9	31	3.4	4310	$6.571^{+0.015}_{-0.015}$	$0.048^{+0.006}_{-0.006}$	2
NGC7591	Sbc	70	151	0.49	62	16	33	2.1	4950	$3.785^{+0.012}_{-0.012}$	$-0.048^{+0.011}_{-0.011}$	2
NGC7608	Sbc	50	18	0.71	75	20	33	1.6	3522	$4.043^{+0.033}_{-0.039}$	$0.734^{+0.007}_{-0.014}$	0
NGC7611	S0	47	136	0.49	63	11	21	1.9	3204	$7.129^{+0.068}_{-0.062}$	$0.086^{+0.017}_{-0.019}$	2
NGC7619	E3	54	42	0.16	47	35	34	1.0	3732	$5.679^{+0.016}_{-0.013}$	$0.366^{+0.003}_{-0.008}$	3
NGC7623	S0	53	7	0.27	44	10	31	3.1	3660	$4.314^{+0.013}_{-0.030}$	$0.714^{+0.002}_{-0.008}$	2
NGC7625	Sa	25	211	0.10	41	14	34	2.4	1615	$2.273^{+0.020}_{-0.017}$	$0.510^{+0.011}_{-0.109}$	0
NGC7631	Sb	54	76	0.60	68	17	33	1.9	3706	$4.150^{+0.012}_{-0.010}$	$0.179^{+0.015}_{-0.018}$	0
NGC7653	Sb	61	167	0.17	35	12	38	3.2	4239	$2.832^{+0.019}_{-0.011}$	$-0.730^{+0.071}_{-0.068}$	0
NGC7671	S0	59	136	0.38	56	11	26	2.4	3885	$6.004^{+0.017}_{-0.014}$	$0.311^{+0.006}_{-0.009}$	2

Table B5. Properties of the 238 (E1–Sdm) CALIFA galaxies. Columns list (1) galaxy identifier, (2) Hubble type based on by-eye morphological classification from Walcher et al. (2014), (3) Hubble Flow (Galactocentric) distances from NED (using Hubble constant of $H_0=73 \text{ km sec}^{-1} \text{ Mpc}^{-1}$), calculated from the weighted mean radial velocities of the radio and optical redshifts, corrected to the Galactic standard of rest (GSR) from the RC3 (Third Reference Catalogue of Bright Galaxies) as described in de Vaucouleurs et al. (1991, section 3.10c, page 54). (4) and (5) Average photometric position angle and ellipticity from *r*-band SDSS (DR12) images with typical uncertainty of 5° – 10° and 5 per cent, respectively, using `findgalaxy` PYTHON procedure of Cappellari 2002. (6) From the axial ratio of the galaxies ($q = 1 - \epsilon$, where ϵ is the average ellipticity of the galaxy, determined from `findgalaxy`), we calculated the inclination (i) assuming $q_o = 0.2$ for the intrinsic axial ratio of the galaxies (Section 3.1). (7) Effective (half-light) radius measured via growth curve analysis (Walcher et al. 2014). (8) Radial extent of the stellar kinematic data in arcseconds (Falcón-Barroso et al. 2017). (9) Radial extent of the stellar kinematic data in terms of effective radius. (10) Systemic velocity of the galaxies with a typical uncertainty of 5 km s^{-1} , measured as the median value of the velocity field (Section 2.2). (11) and (12) The medians of the posterior distributions of the dynamical mass-to-light ratios and azimuthal velocity anisotropies, respectively, from JAM-MCMC model. The uncertainties are estimated as the 25th and 75th percentiles of the data corresponding to the median absolute deviation (Section 3.1). (13) CVC (circular velocity curve) class of the 238 (E1–Sdm) galaxies, where 0 – Slow rising (SR); 1 – Flat (FL); 2 – Round-peaked (RP); 3 – Sharp-peaked (SP).

Galaxy (1)	Type (2)	Dist Mpc (3)	PA (°) (4)	ϵ (5)	i (°) (6)	R_e (arcsec) (7)	R_{\max} (arcsec) (8)	R_{\max}/R_e (9)	V_{sys} (km s $^{-1}$) (10)	$(M/L)_{\text{dyn}}$ (11)	β_z (12)	CVC class (13)
NGC7683	S0	53	141	0.48	62	14	33	2.4	3725	$5.646^{+0.018}_{-0.021}$	$0.309^{+0.006}_{-0.018}$	2
NGC7711	E7	58	92	0.58	65	15	42	2.8	4049	$4.564^{+0.019}_{-0.011}$	$0.345^{+0.004}_{-0.013}$	2
NGC7716	Sb	37	35	0.19	55	21	38	1.8	2565	$2.485^{+0.007}_{-0.007}$	$-0.176^{+0.012}_{-0.019}$	1
NGC7722	Sab	57	148	0.19	54	21	24	1.1	4024	$6.660^{+0.030}_{-0.030}$	$0.102^{+0.010}_{-0.012}$	3
NGC7738	Sb	94	43	0.37	72	14	37	2.6	6708	$3.685^{+0.019}_{-0.020}$	$0.508^{+0.008}_{-0.041}$	1
NGC7787	Sab	93	115	0.48	62	11	23	2.1	6622	$5.480^{+0.048}_{-0.048}$	$-0.100^{+0.022}_{-0.021}$	0
NGC7819	Sc	70	100	0.40	54	23	37	1.6	4908	$3.754^{+0.021}_{-0.019}$	$0.175^{+0.023}_{-0.025}$	1
NGC7824	Sab	86	146	0.35	54	11	38	3.5	6071	$6.052^{+0.031}_{-0.027}$	$0.250^{+0.011}_{-0.017}$	2
UGC00005	Sbc	101	227	0.49	65	16	33	2.1	7166	$5.291^{+0.015}_{-0.014}$	$-0.626^{+0.032}_{-0.020}$	2
UGC00029	E1	123	172	0.26	45	17	13	0.8	8687	$7.690^{+0.073}_{-0.066}$	$-0.504^{+0.063}_{-0.056}$	3
UGC00036	Sab	88	17	0.59	66	10	20	2.0	6249	$7.877^{+0.029}_{-0.032}$	$-0.099^{+0.013}_{-0.013}$	2
UGC00148	Sc	60	95	0.66	76	20	36	1.8	4148	$4.755^{+0.041}_{-0.035}$	$0.705^{+0.006}_{-0.016}$	0
UGC00312	Sd	61	8	0.56	75	20	38	1.9	4288	$8.364^{+0.064}_{-0.057}$	$-0.357^{+0.030}_{-0.035}$	0
UGC00809	Scd	60	22	0.79	78	20	36	1.8	4154	$13.184^{+0.101}_{-0.098}$	$0.532^{+0.008}_{-0.010}$	0
UGC00987	Sa	66	31	0.69	75	12	34	2.8	4615	$4.650^{+0.028}_{-0.017}$	$0.262^{+0.011}_{-0.016}$	2
UGC01057	Sc	89	152	0.69	77	14	27	1.9	6308	$5.074^{+0.034}_{-0.038}$	$0.420^{+0.009}_{-0.012}$	0
UGC01271	S0a	71	101	0.42	60	9	29	3.2	5017	$4.959^{+0.035}_{-0.030}$	$-0.423^{+0.031}_{-0.028}$	2
UGC02222	S0a	71	98	0.56	66	10	23	2.3	4949	$5.060^{+0.024}_{-0.019}$	$0.314^{+0.007}_{-0.011}$	2
UGC02229	S0a	100	172	0.38	59	19	25	1.3	7219	$8.181^{+0.031}_{-0.027}$	$0.597^{+0.004}_{-0.005}$	2
UGC02403	Sb	57	150	0.62	70	19	26	1.4	4144	$4.777^{+0.040}_{-0.037}$	$0.569^{+0.008}_{-0.010}$	0
UGC03253	Sb	59	84	0.36	62	15	33	2.2	4093	$5.915^{+0.022}_{-0.019}$	$-0.455^{+0.024}_{-0.020}$	0
UGC03539	Sc	47	117	0.78	84	20	38	1.9	3257	$11.785^{+0.090}_{-0.090}$	$-0.555^{+0.058}_{-0.060}$	0
UGC03995	Sb	64	90	0.53	62	25	39	1.6	4746	$5.642^{+0.023}_{-0.025}$	$0.345^{+0.007}_{-0.009}$	1
UGC04029	Sc	60	63	0.80	81	26	37	1.4	4411	$7.837^{+0.045}_{-0.037}$	$0.394^{+0.009}_{-0.018}$	0
UGC04132	Sbc	71	29	0.71	76	22	35	1.6	5111	$7.697^{+0.029}_{-0.019}$	$0.024^{+0.011}_{-0.016}$	2
UGC04145	Sa	62	138	0.48	81	9	29	3.2	4609	$7.279^{+0.028}_{-0.030}$	$0.077^{+0.009}_{-0.007}$	0
UGC04197	Sab	61	131	0.74	82	18	41	2.3	4490	$7.807^{+0.026}_{-0.022}$	$0.303^{+0.012}_{-0.013}$	0
UGC04280	Sb	49	1	0.68	75	11	36	3.3	3512	$5.942^{+0.023}_{-0.029}$	$0.291^{+0.009}_{-0.010}$	0
UGC04308	Sc	48	125	0.23	58	24	33	1.4	3538	$4.002^{+0.030}_{-0.030}$	$-0.404^{+0.040}_{-0.037}$	0
UGC05108	Sb	110	151	0.56	64	9	19	2.1	8001	$7.372^{+0.039}_{-0.039}$	$-0.337^{+0.015}_{-0.016}$	1
UGC05113	S0a	95	41	0.71	78	8	22	2.8	6752	$5.324^{+0.024}_{-0.024}$	$0.510^{+0.006}_{-0.008}$	2
UGC05598	Sb	76	36	0.73	76	15	27	1.8	5597	$5.574^{+0.071}_{-0.057}$	$0.713^{+0.007}_{-0.012}$	0
UGC05771	E6	102	57	0.31	47	12	27	2.2	7360	$7.771^{+0.034}_{-0.032}$	$0.501^{+0.004}_{-0.009}$	3
UGC05990	Sc	21	16	0.70	78	12	33	2.8	1566	$8.605^{+0.137}_{-0.114}$	$0.656^{+0.010}_{-0.011}$	0
UGC06036	Sa	89	100	0.74	81	11	38	3.5	6492	$7.644^{+0.017}_{-0.017}$	$0.005^{+0.008}_{-0.007}$	2
UGC06312	Sab	85	56	0.62	68	13	29	2.2	6295	$7.055^{+0.028}_{-0.025}$	$0.370^{+0.005}_{-0.006}$	2
UGC07012	Scd	42	10	0.47	58	14	30	2.1	3070	$6.506^{+0.061}_{-0.052}$	$0.289^{+0.020}_{-0.027}$	0
UGC07145	Sbc	91	152	0.62	69	16	32	2.0	6562	$7.018^{+0.059}_{-0.051}$	$0.744^{+0.004}_{-0.010}$	0
UGC08107	Sa	115	52	0.62	72	16	33	2.1	8220	$12.324^{+0.039}_{-0.047}$	$0.390^{+0.006}_{-0.007}$	2
UGC08231	Sd	35	75	0.63	71	19	33	1.7	2482	$19.564^{+0.171}_{-0.170}$	$0.249^{+0.017}_{-0.023}$	0

Table B6. Properties of the 238 (E1–Sdm) CALIFA galaxies. Columns list (1) galaxy identifier, (2) Hubble type based on by-eye morphological classification from Walcher et al. (2014), (3) Hubble Flow (Galactocentric) distances from NED (using Hubble constant of $H_0=73 \text{ km sec}^{-1} \text{ Mpc}^{-1}$), calculated from the weighted mean radial velocities of the radio and optical redshifts, corrected to the Galactic standard of rest (GSR) from the RC3 (Third Reference Catalogue of Bright Galaxies) as described in de Vaucouleurs et al. (1991, section 3.10c, page 54). (4) and (5) Average photometric position angle and ellipticity from r -band SDSS (DR12) images with typical uncertainty of 5° – 10° and 5 per cent, respectively, using `findgalaxy` PYTHON procedure of Cappellari 2002. (6) From the axial ratio of the galaxies ($q = 1 - \epsilon$, where ϵ is the average ellipticity of the galaxy, determined from `findgalaxy`), we calculated the inclination (i) assuming $q_o = 0.2$ for the intrinsic axial ratio of the galaxies (Section 3.1). (7) Effective (half-light) radius measured via growth curve analysis (Walcher et al. 2014). (8) Radial extent of the stellar kinematic data in arcseconds (Falcón-Barroso et al. 2017). (9) Radial extent of the stellar kinematic data in terms of effective radius. (10) Systemic velocity of the galaxies with a typical uncertainty of 5 km s^{-1} , measured as the median value of the velocity field (Section 2.2). (11) and (12) The medians of the posterior distributions of the dynamical mass-to-light ratios and azimuthal velocity anisotropies, respectively, from JAM-MCMC model. The uncertainties are estimated as the 25th and 75th percentiles of the data corresponding to the median absolute deviation (Section 3.1). (13) CVC (circular velocity curve) class of the 238 (E1–Sdm) galaxies, where 0 – Slow rising (SR); 1 – Flat (FL); 2 – Round-peaked (RP); 3 – Sharp-peaked (SP).

Galaxy (1)	Type (2)	Dist Mpc (3)	PA (°) (4)	ϵ (5)	i (°) (6)	R_e (arcsec) (7)	R_{\max} (arcsec) (8)	R_{\max}/R_e (9)	V_{sys} (km s $^{-1}$) (10)	$(M/L)_{\text{dyn}}$ (11)	β_z (12)	CVC class (13)
UGC08234	S0	113	134	0.40	55	8	24	3.0	8043	$3.166^{+0.021}_{-0.013}$	$0.565^{+0.004}_{-0.020}$	2
UGC08733	Sdm	33	195	0.42	64	30	40	1.3	2329	$9.708^{+0.080}_{-0.075}$	$0.528^{+0.009}_{-0.010}$	0
UGC08778	Sb	46	117	0.74	78	15	27	1.8	3235	$5.848^{+0.036}_{-0.029}$	$0.362^{+0.013}_{-0.015}$	0
UGC08781	Sb	104	161	0.42	59	15	29	1.9	7554	$4.789^{+0.036}_{-0.027}$	$0.289^{+0.008}_{-0.010}$	2
UGC09476	Sbc	46	130	0.34	49	21	40	1.9	3247	$3.754^{+0.016}_{-0.018}$	$0.111^{+0.033}_{-0.036}$	0
UGC09537	Sb	122	139	0.76	82	20	40	2.0	8778	$6.438^{+0.040}_{-0.029}$	$0.659^{+0.005}_{-0.005}$	1
UGC09542	Sc	76	40	0.69	73	21	37	1.8	5412	$6.245^{+0.040}_{-0.037}$	$0.788^{+0.004}_{-0.008}$	0
UGC09665	Sb	37	140	0.76	80	18	33	1.8	2524	$6.302^{+0.050}_{-0.038}$	$0.285^{+0.025}_{-0.031}$	0
UGC09873	Sb	79	125	0.77	78	21	33	1.6	5587	$7.666^{+0.056}_{-0.054}$	$0.427^{+0.020}_{-0.019}$	1
UGC09892	Sbc	80	101	0.74	77	16	26	1.6	5632	$4.904^{+0.037}_{-0.028}$	$-0.083^{+0.046}_{-0.048}$	0
UGC10097	E5	84	125	0.14	51	14	27	1.9	5912	$6.390^{+0.016}_{-0.015}$	$0.415^{+0.004}_{-0.005}$	3
UGC10123	Sab	54	53	0.72	79	18	31	1.7	3723	$8.337^{+0.037}_{-0.041}$	$0.476^{+0.008}_{-0.011}$	0
UGC10205	S0a	92	152	0.41	54	19	35	1.8	6500	$8.828^{+0.019}_{-0.023}$	$0.055^{+0.008}_{-0.008}$	2
UGC10257	Sbc	54	164	0.76	77	20	38	1.9	3826	$6.514^{+0.040}_{-0.037}$	$0.531^{+0.016}_{-0.024}$	0
UGC10331	Sc	64	141	0.77	78	19	41	2.2	4447	$4.990^{+0.073}_{-0.103}$	$0.776^{+0.006}_{-0.038}$	0
UGC10337	Sb	121	56	0.54	72	17	26	1.5	8685	$6.969^{+0.027}_{-0.044}$	$0.869^{+0.001}_{-0.011}$	0
UGC10384	Sb	69	91	0.76	79	11	35	3.2	4935	$6.230^{+0.042}_{-0.038}$	$0.505^{+0.013}_{-0.019}$	0
UGC10388	Sa	65	129	0.68	73	11	28	2.5	4600	$6.253^{+0.024}_{-0.019}$	$0.292^{+0.008}_{-0.009}$	2
UGC10650	Scd	42	202	0.77	83	23	43	1.9	2999	$13.753^{+0.306}_{-0.281}$	$0.798^{+0.008}_{-0.007}$	0
UGC10693	E7	117	109	0.34	49	22	31	1.4	8259	$5.434^{+0.028}_{-0.024}$	$0.774^{+0.002}_{-0.008}$	3
UGC10695	E5	116	116	0.42	55	24	27	1.1	8156	$7.652^{+0.028}_{-0.026}$	$0.390^{+0.005}_{-0.007}$	3
UGC10710	Sb	117	148	0.74	78	20	36	1.8	8239	$8.040^{+0.035}_{-0.028}$	$0.568^{+0.007}_{-0.011}$	0
UGC10796	Scd	45	236	0.44	57	20	32	1.6	3060	$6.207^{+0.098}_{-0.109}$	$0.293^{+0.021}_{-0.028}$	0
UGC10811	Sb	122	90	0.65	71	12	29	2.4	8581	$8.154^{+0.046}_{-0.043}$	$-0.313^{+0.023}_{-0.026}$	2
UGC10905	S0a	110	173	0.47	69	15	25	1.7	7679	$6.456^{+0.017}_{-0.020}$	$0.203^{+0.005}_{-0.004}$	2
UGC10972	Sbc	66	57	0.62	77	24	34	1.4	4617	$5.231^{+0.028}_{-0.023}$	$0.612^{+0.006}_{-0.016}$	1
UGC11228	S0	82	178	0.31	59	12	33	2.8	5745	$4.673^{+0.031}_{-0.016}$	$0.439^{+0.004}_{-0.009}$	2
UGC11717	Sab	89	213	0.57	65	17	39	2.3	6181	$9.592^{+0.080}_{-0.066}$	$0.607^{+0.005}_{-0.006}$	2
UGC12054	Sc	31	47	0.78	83	15	33	2.2	2039	$7.214^{+0.106}_{-0.128}$	$0.140^{+0.036}_{-0.041}$	0
UGC12127	E1	116	185	0.15	44	36	25	0.7	8169	$7.714^{+0.052}_{-0.033}$	$0.444^{+0.005}_{-0.005}$	3
UGC12185	Sb	94	153	0.48	60	12	33	2.8	6518	$4.967^{+0.032}_{-0.027}$	$0.584^{+0.006}_{-0.017}$	2
UGC12274	Sa	108	142	0.58	66	17	27	1.6	7553	$6.030^{+0.033}_{-0.032}$	$0.529^{+0.007}_{-0.015}$	2
UGC12308	Scd	33	119	0.80	79	27	38	1.4	2204	$12.393^{+0.139}_{-0.119}$	$0.655^{+0.008}_{-0.010}$	0
UGC12518	Sb	40	25	0.75	80	17	34	2.0	3740	$3.869^{+0.952}_{-0.127}$	$0.905^{+0.004}_{-0.024}$	0
UGC12519	Sc	62	157	0.70	81	21	34	1.6	4325	$5.886^{+0.049}_{-0.047}$	$-0.188^{+0.025}_{-0.029}$	0
UGC12723	Sc	77	76	0.83	82	17	27	1.6	5400	$9.874^{+0.081}_{-0.090}$	$0.588^{+0.016}_{-0.023}$	0
UGC12857	Sbc	36	34	0.74	82	19	36	1.9	2466	$4.287^{+0.051}_{-0.049}$	$0.554^{+0.014}_{-0.031}$	0

APPENDIX C: MAIN PC EIGENVECTORS OF THE 238 CVCS

In Table C1, we present the five main PC eigenvectors as a common basis of the 238 CVCs (columns: 2, 3, 4, 5 and 6); see Fig. 2 and Section 3.2. We normalize the radius R of the CVCs to the effective radius of the galaxies, R_e (column 1). We use 50 points spanning $R/R_e \in [0, 1.5]$. We logarithmically sample the normalized radius since the CVCs vary much more in the centre than in their outer parts.

Table C1. Main PC eigenvectors of the 238 CVCs

Normalized PC radius R/R_e (1)	Main PC eigenvectors of the 238 CVCs				
	\mathbf{u}_1 (2)	\mathbf{u}_2 (3)	\mathbf{u}_3 (4)	\mathbf{u}_4 (5)	\mathbf{u}_5 (6)
0.05	64.76932	37.259213	11.21853	8.9489543	4.6411178
0.054	68.055877	37.676725	10.948696	8.2453302	3.9447158
0.057	71.360914	37.860693	10.536666	7.3751072	3.1373666
0.062	74.666903	37.79002	9.9738811	6.3419901	2.2366909
0.066	77.955658	37.448003	9.255452	5.1579907	1.2700509
0.071	81.208198	36.823327	8.3807879	3.8442673	0.27449214
0.076	84.404509	35.910691	7.3539918	2.4312438	-0.70464477
0.081	87.523333	34.710926	6.1840008	0.95782335	-1.6166277
0.087	90.542206	33.230662	4.8844873	-0.53034653	-2.4096168
0.093	93.437834	31.481733	3.4735645	-1.9834188	-3.0357776
0.1	96.186956	29.480676	1.9734466	-3.3503051	-3.4563487
0.107	98.767639	27.248632	0.41017445	-4.5815536	-3.6456969
0.115	101.16079	24.81173	-1.1865335	-5.6317402	-3.5936475
0.123	103.35157	22.201673	-2.7834851	-6.4613244	-3.3059167
0.132	105.33025	19.455889	-4.3446576	-7.0383221	-2.8030829
0.142	107.09223	16.616691	-5.83257	-7.3401554	-2.1187458
0.152	108.63717	13.729172	-7.2103017	-7.3556303	-1.2973089
0.163	109.96751	10.838253	-8.443638	-7.0864419	-0.39138065
0.174	111.08682	7.9855522	-9.5028233	-6.5475253	0.54139922
0.187	111.9985	5.2068615	-10.36366	-5.7659212	1.4420876
0.2	112.70507	2.5307238	-11.008105	-4.7784258	2.2543876
0.215	113.20818	-0.021777731	-11.424611	-3.628653	2.9282843
0.23	113.50901	-2.4363144	-11.608392	-2.3641805	3.4229664
0.247	113.60883	-4.7042019	-11.561535	-1.0341945	3.7089523
0.265	113.50953	-6.8213952	-11.292886	0.31222026	3.769558
0.284	113.21381	-8.7878239	-10.817487	1.627416	3.6018536
0.304	112.7253	-10.607081	-10.155462	2.8664942	3.2171157
0.326	112.04845	-12.28619	-9.3303486	3.9889544	2.640534
0.349	111.18832	-13.835095	-8.3670289	4.9605188	1.9099085
0.374	110.15019	-15.265495	-7.2896241	5.75468	1.0731298
0.401	108.93919	-16.588888	-6.1197481	6.3532541	0.18453767
0.43	107.5604	-17.814046	-4.8753713	6.7456375	-0.69945797
0.461	106.01947	-18.944648	-3.5702978	6.9270234	-1.5248958
0.494	104.32389	-19.977969	-2.2141963	6.8964496	-2.2442446
0.53	102.48434	-20.905308	-0.81308321	6.6555928	-2.8193531
0.568	100.51531	-21.714176	0.62961878	6.2088247	-3.2231187
0.608	98.434589	-22.391575	2.1114059	5.5643904	-3.4398877
0.652	96.261432	-22.927287	3.6284619	4.7359681	-3.4648218
0.699	94.014357	-23.316129	5.1733235	3.7437964	-3.3026104
0.749	91.709379	-23.558792	6.7330028	2.6147314	-2.9658773
0.803	89.359544	-23.661338	8.288097	1.3811375	-2.4736442
0.861	86.975896	-23.633893	9.8130658	0.078952947	-1.849921
0.923	84.569475	-23.489183	11.277512	-1.2544409	-1.1224072
0.989	82.153758	-23.241346	12.648154	-2.5820091	-0.32111982
1.06	79.746783	-22.905296	13.891131	-3.8682639	0.52307182
1.136	77.372457	-22.496554	14.974439	-5.0799294	1.3799602
1.218	75.060533	-22.031309	15.870277	-6.1863094	2.2212881
1.306	72.845036	-21.526336	16.557231	-7.1595417	3.0216525
1.399	70.761173	-20.998587	17.022091	-7.974969	3.7589679
1.5	68.841272	-20.464343	17.261184	-8.6117751	4.4146419

**APPENDIX D: THE FIVE MAIN PROJECTIONS PC_I OF
THE 238 CVCS**

In Tables D1–D5, we present the five main projections PC_i of the CVCs for each of the 238 (E1–Sdm) CALIFA galaxies as described in Section 3.2. Using the linear combination between those five projections PC_i and the five main PC vectors, plus adding the mean value \bar{V}_c of the 238 CVCs, we are able to reconstruct well all CVCs of our sample (see also Fig. 3 and equation 5).

Table D1. The five main projections PC_i of the 238 CVCs.

Galaxy (1)	PC1 (2)	PC2 (3)	PC3 (4)	PC4 (5)	PC5 (6)
IC0480	-1.20926	-2.3276	0.79536	-1.35533	-1.45758
IC0540	-1.0277	-1.65598	-1.3821	-1.15281	-0.449284
IC0674	0.409293	-2.77205	-0.482785	-0.747374	-0.628182
IC0944	0.723189	-2.14871	-1.0831	-2.88036	0.103113
IC1079	0.841509	0.195445	-0.612319	-0.398093	-1.05088
IC1151	-1.09668	-1.18971	-1.06528	-1.23835	-1.00047
IC1256	-0.780024	-2.31828	1.0241	-2.00657	-1.61986
IC1528	-1.06868	-1.71063	-0.832056	-1.55337	-0.656684
IC1652	-0.399075	-0.587136	-0.819743	0.0887954	-0.519594
IC1755	0.319741	-2.12241	-1.78489	-1.30644	-0.330496
IC2101	-1.10349	-2.14584	-0.356404	-0.668677	-1.34662
IC2247	-0.326579	-0.569163	-0.998491	-1.3598	-0.65643
IC2487	-0.7437	-1.56494	0.786716	-0.642283	-1.65642
IC4566	0.143066	-1.65649	-1.52814	-1.70792	-0.975006
IC5309	-0.861252	-1.4714	-1.22377	-0.535366	-2.40962
IC5376	-0.00336622	-1.90825	-2.0792	-0.546939	-1.85613
MCG-01-54-016	-1.26462	-1.16168	-0.966791	0.0883945	-1.88919
MCG-02-02-030	-0.74409	-1.35248	-0.449203	-1.70031	-0.128108
MCG-02-02-040	-1.12141	-1.81402	0.506846	-1.54051	-1.59858
MCG-02-03-015	0.284227	-0.810432	-2.37091	-2.84387	-1.05553
MCG-02-51-004	-0.222262	-1.64179	0.0107271	-4.22379	1.09131
NGC0001	0.0590133	-1.663	-1.97393	-1.40448	-1.40828
NGC0023	0.443446	-1.15225	-3.70625	-2.50189	1.17438
NGC0155	0.806298	-1.76249	-1.64517	-1.54686	-1.36864
NGC0160	0.997055	-0.64756	-1.72468	-1.26951	-2.04502
NGC0171	-0.600168	-0.213682	-1.90794	-1.14194	0.0927998
NGC0177	-0.242677	-2.18961	-2.42122	0.320728	-1.67213
NGC0192	0.166642	-0.132587	-1.08111	-3.16354	-1.02631
NGC0214	-0.226703	-1.54425	-0.0834138	-1.19997	-1.8465
NGC0216	-1.38734	-1.25915	-1.52472	-0.727423	-1.86062
NGC0217	0.274476	-1.81879	-1.11533	-1.805	-0.435183
NGC0237	-0.84227	-1.88684	-0.205547	-1.45908	-1.28688
NGC0257	-0.101976	-1.1933	-0.705063	-2.51945	-0.676655
NGC0429	-0.149136	-3.44591	-0.393745	1.22482	-2.22765
NGC0444	-1.14733	-1.08421	-1.1132	-1.31008	-0.482442
NGC0499	2.25356	-1.22882	-0.392556	-1.36232	-1.31672
NGC0504	0.391501	-3.77708	-0.293322	0.772278	-1.78642
NGC0517	0.696317	-2.71926	-1.73005	-1.03803	-0.50969
NGC0528	0.421842	-3.37503	-0.0295673	-0.865415	-0.820105
NGC0529	1.5928	-2.69623	-0.639182	-2.30655	-0.826763
NGC0551	-0.650087	-1.50068	-0.0254303	-2.48497	-1.04241
NGC0681	-0.211422	-0.785398	0.0452183	-0.881701	-0.394939
NGC0741	3.31104	-0.0460114	1.97253	-0.162111	0.0313921
NGC0755	-1.33352	-1.65394	-0.661884	-1.17364	-1.2099
NGC0768	-0.319662	-2.77593	-0.338327	-1.08984	0.167925
NGC0774	-0.0371416	-3.26697	-0.103042	-0.429948	-0.599349
NGC0776	-0.488312	-0.018084	-1.80124	-1.94228	-2.27739
NGC0781	-0.625485	-1.97724	-1.47397	-0.650459	-1.15739
NGC0810	2.12353	-4.44166	-0.30524	-1.2928	0.255498
NGC0932	0.403977	-0.725801	-1.6333	-1.51453	-2.38971
NGC1056	-0.597191	-1.61349	-1.48216	0.935024	-1.71221

Table D2. The five main projections PC_i of the 238 CVCs.

Galaxy (1)	PC1 (2)	PC2 (3)	PC3 (4)	PC4 (5)	PC5 (6)
NGC1060	3.14852	-1.20864	-0.33093	-1.89527	-1.45218
NGC1167	1.48641	-1.59929	0.173107	-1.84505	-1.09924
NGC1349	1.03684	-1.20366	-0.461765	-2.77004	-0.905643
NGC1542	-0.65718	-2.18568	-0.857595	-1.31328	0.0514257
NGC1645	0.924748	-2.59453	-2.65253	-0.797754	0.236382
NGC1677	-1.22476	-1.33862	-1.1884	-1.34635	-1.34623
NGC2253	0.391909	-1.69758	-3.62714	-0.686867	-0.722437
NGC2347	0.338657	-2.0277	0.204938	0.373939	-1.96271
NGC2410	0.015673	-1.83271	-1.69969	-1.35327	-1.68101
NGC2449	-0.115256	-1.48962	-0.970933	-1.87502	-0.689973
NGC2476	0.536627	-2.68001	-1.84769	-0.360344	-1.18392
NGC2481	-0.0299444	-2.54517	-1.2607	-0.630674	-0.649462
NGC2486	0.555538	1.29881	-0.790794	1.03536	2.4756
NGC2553	0.539209	-2.96772	-1.27083	-0.0851655	-1.39875
NGC2554	1.30283	-0.962678	-1.24524	-3.05613	-2.01115
NGC2592	0.47325	-3.18959	-1.15446	-0.233936	-0.468901
NGC2604	-1.26277	-0.829645	-1.26636	-1.42856	-0.984058
NGC2639	0.701131	-3.0644	0.65683	-1.61775	-0.78759
NGC2730	-1.11375	-1.53485	-0.571618	-2.2206	-0.294456
NGC2880	0.133457	-1.30168	-1.88764	-1.27788	-1.83529
NGC2906	-0.277558	-0.754825	-0.109797	-1.86315	-0.298498
NGC2916	-0.123477	-1.11497	0.222431	-2.99827	-0.370833
NGC2918	1.14822	-4.45705	0.632056	-0.365575	-0.788331
NGC3057	-1.47475	-0.88222	-1.62413	-1.05265	-1.33162
NGC3106	0.826744	0.126182	-1.4728	-0.776833	-2.55434
NGC3160	0.013251	-1.90649	-0.225168	-1.72557	-0.713456
NGC3300	-0.0698678	-2.06551	-1.7395	-1.19746	-0.229852
NGC3381	-1.38387	-0.545028	-1.58721	-0.354488	-1.11364
NGC3615	2.23241	-1.07155	-1.68654	-2.25966	-2.55642
NGC3811	-0.0807657	0.628409	-0.128984	-1.84056	-2.31545
NGC3815	-0.589177	-1.82769	-0.33038	-1.99619	-1.65024
NGC3994	0.169504	-2.80224	-0.56651	-2.01865	1.21709
NGC4003	0.179141	-0.770381	-0.59803	0.53172	0.849872
NGC4047	-0.166514	-2.55476	1.13155	-0.475375	-2.25634
NGC4149	-0.55653	-1.64648	-1.06817	-1.91999	-0.49263
NGC4185	-0.506522	-1.28953	0.422828	-2.26548	-1.29101
NGC4210	-0.696877	-0.899789	-0.19917	-3.12556	-0.607097
NGC4470	-1.52534	-1.14175	-0.878827	-0.833444	-1.07501
NGC4644	-0.598155	-2.0802	-0.894709	-1.59717	-0.155306
NGC4711	-1.01796	-1.50683	-0.208537	-2.09663	-1.06802
NGC4816	1.70659	1.2395	1.04209	-0.0435526	0.425543
NGC4956	0.125409	-2.92302	-0.834996	-0.822844	-0.114177
NGC4961	-0.909017	-1.93505	-0.539806	-0.566348	-2.9985
NGC5000	-1.04415	-1.28577	-1.398	-1.16529	-1.13803
NGC5029	2.06655	-1.41662	0.193125	-1.91201	-2.84009
NGC5056	-0.48565	-1.52834	-0.327255	-2.1092	-2.05446
NGC5218	-0.675768	-3.15847	1.10512	-0.314519	-2.44868
NGC5378	-0.0223568	-0.17787	-1.38833	-1.219	-1.85529
NGC5480	-0.887018	-0.477911	-0.572379	-1.34536	-1.1238
NGC5485	0.885995	-0.863803	0.00398722	0.660348	-1.04989
NGC5520	-0.415538	-1.58961	-1.2535	1.08169	-1.62206

Table D3. The five main projections PC_i of the 238 CVCs.

Galaxy (1)	PC1 (2)	PC2 (3)	PC3 (4)	PC4 (5)	PC5 (6)
NGC5614	0.626909	-2.15989	-1.37688	-1.95352	-0.759416
NGC5630	-1.22364	-1.30351	-0.805675	-1.03281	-1.16507
NGC5633	-1.00172	-2.15113	0.692719	-2.12723	-0.488874
NGC5657	-0.492301	-2.42364	-1.23416	-0.124995	-1.24796
NGC5682	-1.01703	-1.64883	-1.74058	-0.593311	-0.870584
NGC5720	0.572892	0.602459	0.918431	-0.638802	2.77394
NGC5732	-0.898305	-1.78692	-0.79812	-1.45943	-1.18247
NGC5784	1.44617	-1.98282	-2.07935	-2.70938	-0.751516
NGC5876	0.827159	-3.63918	-1.33785	0.622526	-1.45295
NGC5888	0.345202	-1.96351	-0.0116483	-2.9603	0.530924
NGC5908	0.580897	-1.70357	1.86103	-0.450364	-1.59016
NGC5971	-0.234269	-1.60258	-1.80396	-1.33797	-1.32671
NGC5980	-0.379456	-2.42495	-0.066242	-1.72009	-0.246283
NGC5987	0.825058	0.202409	-0.0197113	-0.4315	-1.11461
NGC6020	1.10619	-0.863381	-1.32647	-1.47519	-2.44128
NGC6021	0.75056	-3.57711	-0.735847	-0.294582	-0.526381
NGC6032	-1.12095	-0.870351	-1.0976	-1.59065	-1.18814
NGC6060	0.0652768	-0.454215	-0.62023	-3.71057	-0.0419281
NGC6063	-1.08955	-1.39203	-0.0150701	-1.73812	-0.67609
NGC6081	0.744095	-2.13503	-1.59998	-0.954489	-1.89919
NGC6125	2.51513	0.889342	-0.308561	-1.95412	-2.97736
NGC6132	-0.798896	-1.56309	0.830146	-0.408422	-1.58356
NGC6146	2.47239	-2.32306	-1.56287	-2.38165	-1.90229
NGC6150	1.29296	-3.50879	0.223116	-1.72499	-0.444164
NGC6168	-1.37067	-1.72106	-0.618762	-0.917962	-1.35513
NGC6173	2.4895	0.951474	0.349885	-0.38986	-0.578864
NGC6186	-0.70412	-0.523137	-1.20044	-0.0438859	0.47021
NGC6278	0.5913	-3.06759	-1.21877	-0.675217	-0.233788
NGC6301	-0.437515	-2.14835	1.90313	-2.93975	-0.336462
NGC6310	-0.445764	-1.19929	-0.581098	-2.46027	-0.404885
NGC6314	0.377287	-2.12739	-2.17955	-0.871077	-1.38105
NGC6478	0.322259	-0.705531	0.971574	-4.24043	-1.54252
NGC6497	1.1269	1.56045	1.6568	3.56648	3.21273
NGC6515	0.991123	-1.3043	-1.24659	-1.94864	-2.06186
NGC6762	-0.881306	-2.50781	-0.0972395	-0.401164	-1.40666
NGC6941	0.177489	-0.718485	-1.39284	-1.9978	-0.00824516
NGC6945	0.255424	-1.61691	-1.66164	-1.68237	-1.11491
NGC6978	0.0227149	-1.89752	-0.397437	-1.88286	-0.497865
NGC7025	1.39389	-3.44742	-0.763846	-0.86445	-0.589905
NGC7047	-0.48258	-1.66649	0.320467	-3.86304	0.447648
NGC7194	2.10062	-2.30269	-1.84827	-2.45428	-1.22815
NGC7311	0.518819	-2.80461	-1.20811	-0.928716	-0.716494
NGC7321	0.12649	-1.53494	0.490853	-1.31074	1.86042
NGC7364	0.557072	-2.31453	-0.741403	-2.14695	-2.00103
NGC7466	-0.110419	-1.54346	-1.5577	-2.56754	-0.394559
NGC7489	-0.777748	-1.51366	0.584255	-1.49091	-2.2348
NGC7549	-0.013092	-2.17648	-0.984777	-1.818	-0.692386
NGC7550	2.18375	-1.6648	1.29361	-1.71546	-3.90838
NGC7562	1.60219	-2.20663	-0.782445	-2.15979	-1.66792
NGC7563	0.785775	-3.98466	0.287908	0.102194	-2.1711
NGC7591	-0.264197	-2.432	-1.26894	-0.0198076	-1.88376

Table D4. The five main projections PC_i of the 238 CVCs.

Galaxy (1)	PC1 (2)	PC2 (3)	PC3 (4)	PC4 (5)	PC5 (6)
NGC7608	-1.25382	-0.974813	-0.655114	-1.49076	-1.4333
NGC7611	1.38192	-2.60431	-2.99434	-1.35975	0.980652
NGC7619	2.67635	0.96161	-0.541645	-0.394273	-0.367046
NGC7623	0.506492	-3.29185	-0.991882	-0.0626366	-1.09721
NGC7625	-0.753266	-1.65591	-1.07167	0.326613	-1.41829
NGC7631	-0.613771	-1.7269	-0.741237	-1.8912	-1.29132
NGC7653	-0.304786	-1.92099	-1.19279	-1.4258	-0.709507
NGC7671	1.28804	-2.50376	-1.92126	-2.40655	0.843059
NGC7683	0.799171	-2.59421	-1.01781	-1.41289	-1.15274
NGC7711	0.925026	-1.60574	-1.65224	-1.84335	-1.23785
NGC7716	-0.308364	-0.226569	-2.2927	-1.94909	-1.69735
NGC7722	1.06193	-0.979749	-1.10416	-1.88796	-1.93734
NGC7738	0.0336331	-0.937297	-1.37609	-2.24552	-2.13936
NGC7787	-0.305826	-1.43139	-1.9494	-1.84802	-0.788726
NGC7819	-0.58144	-0.269941	-2.16629	-1.80617	-0.450127
NGC7824	1.44191	-2.97776	-2.5445	-1.4094	0.947523
UGC00005	-0.562864	-2.44482	0.882002	-2.67218	0.0905813
UGC00029	1.38817	-0.632478	-0.581561	-1.58943	-1.60693
UGC00036	0.500905	-2.48737	0.309335	-1.82194	-1.5261
UGC00148	-1.06812	-1.63918	0.283095	-1.6438	-0.533773
UGC00312	-0.606696	-1.87013	-0.923356	0.20359	-0.303226
UGC00809	-1.30326	-2.15657	0.749096	-1.68255	-0.988628
UGC00987	-0.172349	-2.13615	-1.10264	-1.58724	-0.493098
UGC01057	-0.833112	-1.47802	-0.24579	-2.42167	-1.58075
UGC01271	0.477361	-1.48872	-0.726871	-0.213719	-2.42679
UGC02222	0.347309	-2.5012	-1.49554	-1.26473	0.286401
UGC02229	0.897063	-1.80358	-0.994325	-1.68955	-3.05358
UGC02403	-0.645573	-1.11054	-0.25598	-1.9803	-0.730478
UGC03253	-0.213947	-1.31896	-1.37795	-1.93616	-0.0537322
UGC03539	-0.89508	-1.80346	-1.14041	-0.867211	-1.33255
UGC03995	0.474327	-0.0702206	-0.401241	-1.71494	-0.648783
UGC04029	-0.634351	-1.19482	-0.418676	-0.561495	-0.391212
UGC04132	-0.298852	-2.41825	1.06062	-3.52727	0.247902
UGC04145	-0.88732	-3.18494	2.47724	-1.82675	-1.16889
UGC04197	-0.367152	-1.11075	-0.20997	-2.05196	-1.89764
UGC04280	-0.683564	-1.62057	-0.910266	-1.71303	-1.13216
UGC04308	-0.962203	-0.988778	-0.864225	-2.10756	-0.887249
UGC05108	0.748679	-0.619859	2.47141	0.946725	-1.62914
UGC05113	0.466305	-2.22344	-1.84701	-1.91937	-0.173713
UGC05598	-1.03932	-1.49279	-1.03799	-2.03769	-0.157719
UGC05771	1.76954	-1.34517	-0.850302	-2.17789	-2.30426
UGC05990	-1.44234	-1.54689	-1.00317	-0.398566	-2.17121
UGC06036	0.736569	-2.58025	-1.63428	-0.715293	-0.74499
UGC06312	0.543326	-1.69868	-1.90135	-1.93157	-1.23111
UGC07012	-1.00155	-1.63583	-1.13029	-1.21017	-1.1714
UGC07145	-0.801511	-1.86991	-0.293473	-1.97158	-0.953033
UGC08107	0.456131	-3.70777	0.798667	-1.80536	1.23986
UGC08231	-0.902553	-2.17499	-0.227133	-0.914167	-1.36939
UGC08234	0.697236	-3.53237	-0.906581	-0.396873	0.101844
UGC08733	-1.19376	-1.08321	-0.968352	-1.39974	-1.24759
UGC08778	-0.972854	-1.6397	-0.986926	-1.82459	-0.198743

Table D5. The five main projections PC_i of the 238 CVCs.

Galaxy (1)	PC1 (2)	PC2 (3)	PC3 (4)	PC4 (5)	PC5 (6)
UGC08781	0.129011	-2.03356	-1.45934	-1.8092	-0.53345
UGC09476	-1.00204	-1.04906	-0.557631	-2.02659	-1.29871
UGC09537	0.594893	-0.83711	-0.833453	-1.22542	-4.1369
UGC09542	-0.917297	-1.56885	-0.119025	-1.19161	-1.37776
UGC09665	-1.13236	-1.43426	-1.02951	-1.87287	-0.529737
UGC09873	-0.798433	-0.205172	-0.87993	-1.47617	-0.474682
UGC09892	-0.936655	-0.803293	-1.59138	-1.25113	-0.994022
UGC10097	2.17048	-1.59701	-1.1101	-2.46573	-1.84765
UGC10123	-0.78853	-2.49877	-0.0889768	-0.994331	-0.338527
UGC10205	0.510202	-2.4934	1.08186	-2.61422	-2.32096
UGC10257	-0.941415	-1.24607	-0.773566	-1.30932	-0.527751
UGC10331	-1.20751	-1.30369	-1.48972	-1.66741	-0.283607
UGC10337	-0.112275	-1.78647	0.948613	-3.40711	-1.52422
UGC10384	-0.703524	-1.34828	-0.203839	-1.9664	1.02627
UGC10388	-0.114117	-2.28869	-1.98973	-0.645969	-0.264282
UGC10650	-0.939656	-1.16788	-2.19008	-1.47155	-0.6418
UGC10693	1.80447	-0.818887	-1.51373	-1.93755	-1.92207
UGC10695	1.04318	-0.807674	-0.337421	-1.302	-1.72437
UGC10710	0.0822857	-1.38522	-0.341625	-1.96588	-1.92577
UGC10796	-1.03984	-0.550743	-1.87062	-0.87959	-1.26422
UGC10811	0.441968	-1.40624	-1.71174	-1.82401	-0.21878
UGC10905	1.26279	-2.96128	-2.51871	-1.11793	0.87601
UGC10972	-0.702804	-0.4874	0.351719	-1.62141	-0.957344
UGC11228	0.763098	-1.89596	-1.9166	-1.05657	-1.48065
UGC11717	0.545557	-2.48664	-0.819629	-2.37346	-0.673287
UGC12054	-1.41809	-1.24747	-1.28259	-1.00902	-1.82222
UGC12127	2.31114	0.814716	0.00545966	0.478953	-0.782018
UGC12185	-0.269127	-2.35725	-0.41775	-1.81632	-0.350056
UGC12274	0.343704	-1.75987	-1.38584	-2.2932	0.0435052
UGC12308	-1.09323	-1.07904	-1.7085	-1.34418	-1.93308
UGC12518	-1.2169	-1.24586	-2.26026	-0.472193	-1.30585
UGC12519	-0.99504	-1.74992	0.0775947	-1.602	-1.56866
UGC12723	-1.37479	-1.9558	0.318592	-1.50003	-1.16429
UGC12857	-1.4187	-1.41638	-1.12355	-0.794839	-1.60526

**APPENDIX E: MULTI-GAUSSIAN EXPANSION (MGE)
MODELS OF THE 238 CALIFA GALAXIES**

We present tables with the parameters of the multi-Gaussian expansion (MGE) models for each galaxy from our sample of 238 (E1–Sdm) CALIFA targets, where $I_{0,j}$ is the central surface brightness (SB), ξ'_j is the dispersion along the major x' -axis, and q' is the flattening of the each Gaussian.

Table E1. Multi-Gaussian Expansion (MGE) models of the 238 (E1-Sdm) galaxies.

j	IC0480			IC0540			IC0674			IC0944		
	$I_{0,j}$	ξ'_j	q'									
	($L_\odot \text{ pc}^{-2}$)	(arcsec)		($L_\odot \text{ pc}^{-2}$)	(arcsec)		($L_\odot \text{ pc}^{-2}$)	(arcsec)		($L_\odot \text{ pc}^{-2}$)	(arcsec)	
1	62.93	13.82	0.317	404.89	2.25	0.161	416.95	0.39	0.360	1213.04	1.90	0.664
2	79.19	18.30	0.118	418.59	2.33	0.501	1345.07	1.07	0.743	272.39	4.43	0.664
3	11.40	33.62	0.317	144.61	7.35	0.501	35.47	1.78	0.360	95.99	10.72	0.265
4	32.52	33.62	0.118	50.26	11.47	0.501	707.17	2.55	0.743	13.65	14.47	0.664
5	173.52	15.37	0.161	201.76	6.79	0.743	113.91	17.93	0.265
6	33.18	33.79	0.161	26.21	12.04	0.360	6.88	33.99	0.664
7	47.27	25.40	0.360	33.45	33.99	0.265
	IC1079			IC1151			IC1256			IC1528		
j	$I_{0,j}$	ξ'_j	q'									
	($L_\odot \text{ pc}^{-2}$)	(arcsec)		($L_\odot \text{ pc}^{-2}$)	(arcsec)		($L_\odot \text{ pc}^{-2}$)	(arcsec)		($L_\odot \text{ pc}^{-2}$)	(arcsec)	
	1301.28	1.44	0.763	330.60	1.21	0.379	196.84	1.50	1.000	314.57	3.34	0.479
2	390.77	4.19	0.763	281.02	3.48	0.379	24.42	5.03	1.000	162.31	14.68	0.371
3	19.29	5.20	0.333	103.32	9.99	0.700	159.20	11.00	0.637	36.27	27.81	0.479
4	79.92	12.47	0.763	61.68	24.57	0.379	34.70	25.21	0.637	30.88	30.70	0.371
5	22.45	19.48	0.333	0.49	34.25	0.700
6	11.88	54.24	0.333	41.62	34.25	0.379
7	9.31	54.24	0.763
	IC1652			IC1755			IC2101			IC2247		
j	$I_{0,j}$	ξ'_j	q'									
	($L_\odot \text{ pc}^{-2}$)	(arcsec)		($L_\odot \text{ pc}^{-2}$)	(arcsec)		($L_\odot \text{ pc}^{-2}$)	(arcsec)		($L_\odot \text{ pc}^{-2}$)	(arcsec)	
	5051.79	0.39	0.685	1106.35	1.07	0.702	129.91	6.77	0.479	4415.87	0.39	0.164
2	1196.96	1.58	0.685	643.15	2.44	0.702	121.66	19.58	0.180	381.81	1.49	0.785
3	387.05	3.41	0.685	26.15	5.34	0.702	23.00	20.15	0.479	933.29	1.53	0.164
4	240.93	8.01	0.213	74.81	9.92	0.220	36.55	30.58	0.180	89.66	2.79	0.785
5	217.78	15.39	0.213	169.81	16.93	0.220	73.26	4.84	0.785
6	8.10	25.01	0.685	6.10	22.63	0.702	216.35	5.08	0.164
7	24.63	25.01	0.213	183.29	18.57	0.164
8	5.09	34.00	0.785
9	24.13	34.00	0.164
	IC2487			IC4566			IC5309			IC5376		
j	$I_{0,j}$	ξ'_j	q'									
	($L_\odot \text{ pc}^{-2}$)	(arcsec)		($L_\odot \text{ pc}^{-2}$)	(arcsec)		($L_\odot \text{ pc}^{-2}$)	(arcsec)		($L_\odot \text{ pc}^{-2}$)	(arcsec)	
	551.49	1.14	0.371	820.25	1.18	0.719	442.38	1.36	0.447	815.69	1.56	0.630
2	77.68	6.84	0.371	575.58	1.77	0.719	218.09	4.87	0.447	276.55	3.22	0.630
3	109.11	8.43	0.241	336.43	4.11	0.605	111.10	5.03	0.537	537.49	5.41	0.180
4	149.47	23.34	0.241	131.69	12.24	0.719	88.68	12.41	0.537	27.66	9.02	0.630
5	11.34	30.60	0.371	25.74	27.87	0.719	35.31	27.54	0.447	10.80	16.69	0.630
6	64.94	20.66	0.180
7	25.09	33.63	0.180
8	6.04	33.63	0.630

Table E2. Multi-Gaussian Expansion (MGE) models of the 238 (E1-Sdm) galaxies.

<i>j</i>	MCG-01-54-016			MCG-02-02-030			MCG-02-02-040			MCG-02-03-015		
	$I_{0,j}$	ξ'_j	q'									
	($L_\odot \text{ pc}^{-2}$)	(arcsec)		($L_\odot \text{ pc}^{-2}$)	(arcsec)		($L_\odot \text{ pc}^{-2}$)	(arcsec)		($L_\odot \text{ pc}^{-2}$)	(arcsec)	
1	273.14	0.94	0.191	741.18	0.85	0.674	278.37	1.34	0.167	2041.22	0.94	0.737
2	123.02	8.03	0.187	621.77	2.68	0.674	96.56	6.28	0.167	2611.65	1.28	0.244
3	57.84	22.98	0.187	19.15	7.47	0.674	50.90	13.21	0.508	536.10	2.24	0.737
4	289.54	14.97	0.355	203.01	16.77	0.167	56.42	5.35	0.737
5	19.45	24.93	0.674	21.96	23.37	0.508	47.41	5.44	0.737
6	32.21	27.78	0.355	245.57	7.89	0.244
7	114.63	22.51	0.244
8	2.67	25.98	0.737
MCG-02-51-004												
<i>j</i>	NGC0001			NGC0023			NGC0155					
	$I_{0,j}$	ξ'_j	q'									
	($L_\odot \text{ pc}^{-2}$)	(arcsec)		($L_\odot \text{ pc}^{-2}$)	(arcsec)		($L_\odot \text{ pc}^{-2}$)	(arcsec)		($L_\odot \text{ pc}^{-2}$)	(arcsec)	
1	804.23	1.63	1.000	1301.76	1.18	0.688	6868.74	1.92	0.460	2031.77	1.10	0.836
2	3.96	15.33	1.000	1477.89	1.24	0.933	2736.30	2.90	0.761	185.24	1.94	0.675
3	236.74	16.98	0.368	514.59	2.53	0.933	356.40	14.19	0.460	489.95	2.24	0.675
4	454.44	3.46	0.688	52.24	19.34	0.761	476.79	3.05	0.836
5	214.99	6.77	0.933	21.24	44.80	0.761	220.38	4.59	0.675
6	82.77	12.46	0.688	110.26	8.49	0.675
7	33.88	27.91	0.688	103.29	12.02	0.836
8	5.97	16.97	0.675
9	27.84	33.70	0.836
NGC0160												
<i>j</i>	NGC0171			NGC0177			NGC0192					
	$I_{0,j}$	ξ'_j	q'									
	($L_\odot \text{ pc}^{-2}$)	(arcsec)		($L_\odot \text{ pc}^{-2}$)	(arcsec)		($L_\odot \text{ pc}^{-2}$)	(arcsec)		($L_\odot \text{ pc}^{-2}$)	(arcsec)	
1	1361.69	1.02	0.976	1489.78	1.28	0.921	1449.94	1.86	0.735	4321.61	1.34	0.308
2	749.37	1.57	0.524	654.19	4.12	0.921	385.03	4.44	0.735	1612.89	2.36	0.614
3	574.72	2.42	0.976	62.61	22.04	0.921	361.62	4.86	0.237	184.78	4.08	0.614
4	501.06	2.82	0.524	59.80	25.94	1.000	1.75	17.70	0.735	327.59	16.10	0.308
5	81.28	5.71	0.976	96.61	28.21	0.237	14.77	22.84	0.614
6	295.34	6.90	0.524	27.77	36.57	0.308
7	36.03	9.80	0.976	14.56	36.57	0.614
8	72.08	33.83	0.524
NGC0214												
<i>j</i>	NGC0216			NGC0217			NGC0237					
	$I_{0,j}$	ξ'_j	q'									
	($L_\odot \text{ pc}^{-2}$)	(arcsec)		($L_\odot \text{ pc}^{-2}$)	(arcsec)		($L_\odot \text{ pc}^{-2}$)	(arcsec)		($L_\odot \text{ pc}^{-2}$)	(arcsec)	
1	1325.82	0.65	0.888	295.85	2.19	0.299	1307.83	1.73	0.687	340.06	0.97	1.000
2	389.20	1.48	0.888	245.22	5.83	0.360	863.17	4.10	0.687	432.82	2.23	1.000
3	886.47	2.06	0.566	185.51	12.05	0.299	114.24	9.92	0.687	282.05	9.40	0.611
4	58.04	3.04	0.888	120.24	16.45	0.360	114.76	17.17	0.204	61.00	13.17	0.611
5	434.54	7.27	0.566	33.75	33.66	0.360	204.69	29.71	0.204	1.65	28.03	1.000
6	149.72	9.67	0.888	36.52	44.63	0.204	27.02	28.03	0.611
7	92.74	23.90	0.566	7.08	44.63	0.687
8	46.18	24.78	0.888

Table E3. Multi-Gaussian Expansion (MGE) models of the 238 (E1-Sdm) galaxies.

j	NGC0257			NGC0429			NGC0444			NGC0499		
	$I_{0,j}$	ξ'_j	q'	$I_{0,j}$	ξ'_j	q'	$I_{0,j}$	ξ'_j	q'	$I_{0,j}$	ξ'_j	q'
	($L_\odot \text{ pc}^{-2}$)	(arcsec)		($L_\odot \text{ pc}^{-2}$)	(arcsec)		($L_\odot \text{ pc}^{-2}$)	(arcsec)		($L_\odot \text{ pc}^{-2}$)	(arcsec)	
1	1457.57	1.53	0.671	3246.45	1.47	0.221	169.66	1.08	0.371	4082.86	1.06	0.719
2	490.95	4.22	0.671	2219.39	1.92	0.510	129.74	3.59	0.371	1836.50	1.98	0.719
3	51.29	17.87	0.671	424.35	5.44	0.510	17.44	8.62	0.371	886.93	3.62	0.595
4	102.00	19.28	0.613	228.43	9.58	0.221	55.51	22.52	0.215	668.59	4.95	0.719
5	29.95	30.60	0.613	2.59	26.32	0.510	9.51	23.26	0.371	265.45	10.33	0.595
6	37.48	26.32	0.221	23.06	28.82	0.215	101.50	21.12	0.595
7	29.62	21.28	0.719
8	21.09	50.43	0.719
NGC0504			NGC0517			NGC0528			NGC0529			
j	$I_{0,j}$	ξ'_j	q'	$I_{0,j}$	ξ'_j	q'	$I_{0,j}$	ξ'_j	q'	$I_{0,j}$	ξ'_j	q'
	($L_\odot \text{ pc}^{-2}$)	(arcsec)		($L_\odot \text{ pc}^{-2}$)	(arcsec)		($L_\odot \text{ pc}^{-2}$)	(arcsec)		($L_\odot \text{ pc}^{-2}$)	(arcsec)	
1	1023.80	1.09	0.772	4639.72	1.21	0.564	1503.76	1.48	1.000	3315.24	0.94	1.000
2	1570.22	1.83	0.772	1515.73	2.45	0.564	433.42	2.62	1.000	1295.95	1.35	0.858
3	622.51	3.01	0.772	457.46	4.68	0.409	565.58	4.91	0.494	1611.77	2.24	1.000
4	281.44	4.94	0.772	62.46	6.34	0.564	287.06	11.57	0.494	556.74	4.73	1.000
5	118.42	15.17	0.244	278.35	7.06	0.409	28.98	32.84	0.494	128.58	6.90	0.858
6	9.77	27.92	0.772	109.04	15.06	0.409	168.26	12.39	0.858
7	31.08	27.92	0.244	6.32	32.16	0.409	32.29	36.91	0.858
8	22.58	32.16	0.564
NGC0551			NGC0681			NGC0741			NGC0755			
j	$I_{0,j}$	ξ'_j	q'	$I_{0,j}$	ξ'_j	q'	$I_{0,j}$	ξ'_j	q'	$I_{0,j}$	ξ'_j	q'
	($L_\odot \text{ pc}^{-2}$)	(arcsec)		($L_\odot \text{ pc}^{-2}$)	(arcsec)		($L_\odot \text{ pc}^{-2}$)	(arcsec)		($L_\odot \text{ pc}^{-2}$)	(arcsec)	
1	596.19	1.46	0.631	2629.97	1.07	0.710	1994.17	0.91	0.830	140.08	4.72	0.249
2	97.21	3.82	0.631	671.25	3.74	0.710	2337.25	1.79	0.830	37.91	8.01	0.249
3	61.90	6.52	0.408	766.05	3.99	0.086	772.40	4.23	0.830	197.79	18.72	0.249
4	32.82	14.24	0.631	233.77	13.19	0.710	329.58	7.33	0.809	84.15	22.96	0.479
5	140.94	17.92	0.408	118.59	22.82	0.086	162.63	15.06	0.809	30.19	49.32	0.249
6	21.39	30.82	0.408	89.85	26.16	0.710	66.38	27.51	0.830
7	21.55	65.28	0.710	23.67	76.28	0.809
8	1.15	65.28	0.086
NGC0768			NGC0774			NGC0776			NGC0781			
j	$I_{0,j}$	ξ'_j	q'	$I_{0,j}$	ξ'_j	q'	$I_{0,j}$	ξ'_j	q'	$I_{0,j}$	ξ'_j	q'
	($L_\odot \text{ pc}^{-2}$)	(arcsec)		($L_\odot \text{ pc}^{-2}$)	(arcsec)		($L_\odot \text{ pc}^{-2}$)	(arcsec)		($L_\odot \text{ pc}^{-2}$)	(arcsec)	
1	405.78	2.54	0.717	825.79	2.13	0.871	1621.05	1.21	0.873	2175.73	0.91	0.205
2	29.69	4.05	0.394	391.58	2.24	0.653	922.31	1.73	1.000	2085.91	1.35	0.692
3	128.42	8.23	0.717	158.03	4.38	0.871	281.59	4.71	1.000	988.50	3.06	0.692
4	66.79	21.81	0.394	344.91	6.99	0.653	81.37	17.65	1.000	42.79	7.15	0.692
5	67.90	14.12	0.653	27.83	25.37	0.873	469.59	7.21	0.205
6	6.33	14.51	0.871	282.14	15.38	0.205
7	26.29	26.91	0.871	12.64	21.36	0.692
8	37.34	24.86	0.205

Table E4. Multi-Gaussian Expansion (MGE) models of the 238 (E1-Sdm) galaxies.

<i>j</i>	NGC0810			NGC0932			NGC1056			NGC1060		
	$I_{0,j}$	ξ'_j	q'	$I_{0,j}$	ξ'_j	q'	$I_{0,j}$	ξ'_j	q'	$I_{0,j}$	ξ'_j	q'
	($L_\odot \text{ pc}^{-2}$)	(arcsec)		($L_\odot \text{ pc}^{-2}$)	(arcsec)		($L_\odot \text{ pc}^{-2}$)	(arcsec)		($L_\odot \text{ pc}^{-2}$)	(arcsec)	
1	1175.94	2.27	0.488	1703.45	1.11	0.872	3709.09	0.66	0.351	2117.10	1.06	1.000
2	356.12	4.72	0.488	1857.41	1.61	0.972	462.74	3.07	0.958	2572.95	1.99	0.749
3	37.04	5.26	0.488	103.22	2.02	0.872	3033.90	3.26	0.351	1149.40	3.86	0.749
4	228.11	7.29	0.665	660.01	3.11	0.972	547.61	6.43	0.351	154.47	6.23	1.000
5	85.13	14.97	0.665	412.26	5.92	0.972	87.30	7.52	0.958	660.57	7.02	0.749
6	29.64	34.00	0.665	43.54	6.26	0.872	183.64	11.91	0.351	183.42	16.64	0.749
7	52.90	19.28	0.972	93.85	14.56	0.958	28.78	21.10	1.000
8	16.21	20.91	0.872	22.76	37.07	0.351	57.43	34.88	0.749
9	41.83	33.76	0.872	15.77	37.07	0.958	17.69	88.69	1.000
NGC1167			NGC1349			NGC1542			NGC1645			
<i>j</i>	$I_{0,j}$	ξ'_j	q'	$I_{0,j}$	ξ'_j	q'	$I_{0,j}$	ξ'_j	q'	$I_{0,j}$	ξ'_j	q'
	($L_\odot \text{ pc}^{-2}$)	(arcsec)		($L_\odot \text{ pc}^{-2}$)	(arcsec)		($L_\odot \text{ pc}^{-2}$)	(arcsec)		($L_\odot \text{ pc}^{-2}$)	(arcsec)	
	2370.58	1.17	1.000	1813.56	1.00	1.000	101.00	2.02	0.749	1395.48	1.34	1.000
2	488.56	2.39	0.787	326.21	1.16	0.845	747.44	2.67	0.346	1684.04	2.00	0.411
3	777.24	2.63	1.000	563.66	2.10	1.000	61.93	3.62	0.749	848.45	3.32	1.000
4	2.90	5.42	1.000	256.50	2.46	0.845	3.80	7.91	0.749	63.74	7.84	1.000
5	325.41	5.64	0.787	232.88	3.23	1.000	317.24	10.26	0.346	99.51	13.92	0.411
6	223.39	5.93	1.000	71.09	7.19	1.000	57.07	20.95	0.346	49.09	33.66	0.411
7	15.41	14.23	1.000	78.57	8.65	0.845	17.22	25.22	0.749
8	148.46	14.37	0.787	40.25	14.27	0.845
9	71.62	34.27	0.787	24.12	14.37	1.000
10	11.28	153.48	1.000	34.86	27.88	0.845
NGC1677			NGC2253			NGC2347			NGC2410			
<i>j</i>	$I_{0,j}$	ξ'_j	q'	$I_{0,j}$	ξ'_j	q'	$I_{0,j}$	ξ'_j	q'	$I_{0,j}$	ξ'_j	q'
	($L_\odot \text{ pc}^{-2}$)	(arcsec)		($L_\odot \text{ pc}^{-2}$)	(arcsec)		($L_\odot \text{ pc}^{-2}$)	(arcsec)		($L_\odot \text{ pc}^{-2}$)	(arcsec)	
	463.28	1.25	0.235	1022.30	1.72	0.770	954.58	0.39	1.000	1370.76	2.17	0.556
2	209.32	1.37	0.380	239.50	2.64	0.752	1600.21	0.99	1.000	459.99	6.54	0.556
3	203.40	3.01	0.380	214.19	3.34	0.770	174.83	2.06	1.000	94.64	23.28	0.246
4	316.49	8.12	0.235	123.10	6.25	0.752	918.30	4.83	0.558	13.99	33.08	0.556
5	126.15	11.39	0.380	25.72	15.73	0.770	50.25	9.24	1.000	48.63	38.41	0.246
6	22.10	24.62	0.380	202.21	13.73	0.558
7	8.60	28.38	1.000
8	37.90	31.79	0.558
NGC2449			NGC2476			NGC2481			NGC2486			
<i>j</i>	$I_{0,j}$	ξ'_j	q'	$I_{0,j}$	ξ'_j	q'	$I_{0,j}$	ξ'_j	q'	$I_{0,j}$	ξ'_j	q'
	($L_\odot \text{ pc}^{-2}$)	(arcsec)		($L_\odot \text{ pc}^{-2}$)	(arcsec)		($L_\odot \text{ pc}^{-2}$)	(arcsec)		($L_\odot \text{ pc}^{-2}$)	(arcsec)	
	591.57	0.90	1.000	4824.83	1.04	0.745	3573.53	1.01	0.772	11060.70	0.39	0.566
2	477.89	1.21	0.413	2082.27	2.38	0.745	3144.88	1.77	0.772	1506.20	0.87	0.971
3	838.79	1.80	1.000	521.56	2.92	0.634	1059.76	3.16	0.772	743.65	1.85	0.566
4	386.90	3.82	1.000	228.86	6.38	0.745	109.14	3.28	0.772	460.14	2.32	0.971
5	213.73	14.76	0.413	178.82	11.88	0.634	833.22	7.48	0.284	156.81	4.50	0.971
6	47.98	25.41	0.413	26.70	13.08	0.745	425.83	14.51	0.284	76.95	23.17	0.566
7	31.22	27.24	0.745	43.76	19.99	0.772
8	18.57	26.97	0.284

Table E5. Multi-Gaussian Expansion (MGE) models of the 238 (E1-Sdm) galaxies.

<i>j</i>	NGC2553			NGC2554			NGC2592			NGC2604		
	$I_{0,j}$	ξ'_j	q'	$I_{0,j}$	ξ'_j	q'	$I_{0,j}$	ξ'_j	q'	$I_{0,j}$	ξ'_j	q'
	($L_\odot \text{ pc}^{-2}$)	(arcsec)		($L_\odot \text{ pc}^{-2}$)	(arcsec)		($L_\odot \text{ pc}^{-2}$)	(arcsec)		($L_\odot \text{ pc}^{-2}$)	(arcsec)	
1	316.92	0.62	0.933	5075.34	1.34	0.996	4289.02	1.18	0.897	281.08	1.17	1.000
2	1767.05	1.12	0.933	479.98	1.75	0.737	2625.76	2.07	0.897	145.08	2.95	1.000
3	902.56	2.45	0.487	910.14	3.36	0.996	62.81	3.87	0.897	24.39	6.47	1.000
4	449.85	4.01	0.933	297.51	6.34	0.996	489.21	4.66	0.625	56.11	19.23	1.000
5	61.04	9.69	0.933	87.88	11.18	0.737	132.08	5.55	0.897	24.99	33.55	0.930
6	21.14	12.39	0.487	142.43	17.89	0.737	140.19	8.13	0.625
7	32.85	27.58	0.487	37.60	44.82	0.737	194.36	10.72	0.897
8	24.04	23.51	0.625
9	25.27	25.69	0.897
NGC2639			NGC2730			NGC2880			NGC2906			
<i>j</i>	$I_{0,j}$	ξ'_j	q'	$I_{0,j}$	ξ'_j	q'	$I_{0,j}$	ξ'_j	q'	$I_{0,j}$	ξ'_j	q'
	($L_\odot \text{ pc}^{-2}$)	(arcsec)		($L_\odot \text{ pc}^{-2}$)	(arcsec)		($L_\odot \text{ pc}^{-2}$)	(arcsec)		($L_\odot \text{ pc}^{-2}$)	(arcsec)	
1	2361.01	1.31	0.685	175.80	2.70	1.000	3516.34	1.23	0.853	2066.02	0.77	1.000
2	1431.59	2.86	0.685	72.50	21.66	0.660	884.83	1.59	0.588	1181.45	1.27	0.533
3	798.53	4.23	0.491	11.69	24.91	1.000	2151.17	2.57	0.853	610.17	3.18	0.533
4	133.08	6.19	0.685	680.67	4.54	0.853	248.29	4.35	1.000
5	707.44	10.69	0.491	509.62	7.46	0.853	287.99	17.92	0.533
6	36.70	20.12	0.685	12.28	18.84	0.853	7.10	21.66	1.000
7	179.95	20.79	0.491	142.65	21.71	0.588	35.86	29.67	0.533
8	26.53	44.93	0.685	21.93	48.22	0.588
9	10.38	48.22	0.853
NGC2916			NGC2918			NGC3057			NGC3106			
<i>j</i>	$I_{0,j}$	ξ'_j	q'	$I_{0,j}$	ξ'_j	q'	$I_{0,j}$	ξ'_j	q'	$I_{0,j}$	ξ'_j	q'
	($L_\odot \text{ pc}^{-2}$)	(arcsec)		($L_\odot \text{ pc}^{-2}$)	(arcsec)		($L_\odot \text{ pc}^{-2}$)	(arcsec)		($L_\odot \text{ pc}^{-2}$)	(arcsec)	
1	980.55	1.23	0.914	774.48	1.67	0.603	71.71	1.56	0.664	1905.09	1.12	0.904
2	410.54	2.51	0.557	897.12	1.92	1.000	55.24	4.25	0.664	988.58	1.75	1.000
3	398.51	2.77	0.914	501.10	3.96	0.603	8.48	9.62	0.664	189.33	3.31	0.904
4	126.34	5.64	0.914	148.94	4.87	1.000	25.90	18.68	0.161	309.81	3.42	1.000
5	137.95	20.22	0.557	265.80	7.07	0.603	16.62	21.87	0.664	12.39	6.34	1.000
6	54.85	20.47	0.914	88.86	10.20	1.000	26.08	35.01	0.664	152.65	6.85	0.904
7	38.24	37.15	0.557	40.73	16.03	0.603	74.51	15.43	1.000
8	19.77	33.54	0.603	23.88	37.16	1.000
9	6.03	33.54	1.000
NGC3160			NGC3300			NGC3381			NGC3615			
<i>j</i>	$I_{0,j}$	ξ'_j	q'	$I_{0,j}$	ξ'_j	q'	$I_{0,j}$	ξ'_j	q'	$I_{0,j}$	ξ'_j	q'
	($L_\odot \text{ pc}^{-2}$)	(arcsec)		($L_\odot \text{ pc}^{-2}$)	(arcsec)		($L_\odot \text{ pc}^{-2}$)	(arcsec)		($L_\odot \text{ pc}^{-2}$)	(arcsec)	
1	599.95	1.02	0.265	1260.32	1.23	1.000	2917.76	0.39	0.928	4267.69	1.08	0.600
2	248.44	1.29	0.710	1208.38	2.08	0.519	179.23	0.93	0.928	936.73	1.85	0.728
3	347.27	3.12	0.710	687.06	3.34	1.000	120.48	1.45	0.449	1150.37	2.36	0.600
4	171.10	12.92	0.265	169.89	5.79	1.000	242.59	3.93	0.449	442.08	4.29	0.600
5	3.56	23.44	0.710	206.48	16.69	0.519	118.74	12.41	0.449	305.66	5.09	0.728
6	38.54	23.44	0.265	3.19	33.75	1.000	54.34	17.51	0.928	109.28	8.85	0.600
7	27.38	33.75	0.519	33.75	30.55	0.928	66.00	11.53	0.728
8	49.83	17.77	0.600
9	21.43	43.73	0.600

Table E6. Multi-Gaussian Expansion (MGE) models of the 238 (E1-Sdm) galaxies.

<i>j</i>	NGC3811			NGC3815			NGC3994			NGC4003		
	$I_{0,j}$	ξ'_j	q'									
	($L_\odot \text{ pc}^{-2}$)	(arcsec)		($L_\odot \text{ pc}^{-2}$)	(arcsec)		($L_\odot \text{ pc}^{-2}$)	(arcsec)		($L_\odot \text{ pc}^{-2}$)	(arcsec)	
1	710.09	0.93	0.932	1138.99	1.40	0.529	4748.50	1.31	0.602	3821.92	0.42	0.947
2	4045.09	1.13	0.675	244.46	5.35	0.529	671.72	4.04	0.602	339.47	1.65	0.947
3	513.49	3.14	0.932	115.61	6.90	0.324	571.59	7.53	0.379	650.42	2.17	0.444
4	121.30	14.24	0.675	132.88	9.41	0.529	16.83	9.43	0.379	343.99	2.88	0.947
5	63.01	16.21	0.932	117.02	15.95	0.324	163.56	9.76	0.602	170.22	5.75	0.444
6	22.80	37.40	0.675	8.64	24.82	0.529	94.27	11.96	0.379	118.82	13.28	0.444
7	25.22	25.56	0.529	26.53	27.92	0.602	21.23	22.26	0.444
8	15.85	22.26	0.947
	NGC4047			NGC4149			NGC4185			NGC4210		
<i>j</i>	$I_{0,j}$	ξ'_j	q'									
	($L_\odot \text{ pc}^{-2}$)	(arcsec)		($L_\odot \text{ pc}^{-2}$)	(arcsec)		($L_\odot \text{ pc}^{-2}$)	(arcsec)		($L_\odot \text{ pc}^{-2}$)	(arcsec)	
1	907.61	0.99	0.792	1319.49	1.72	0.170	119.66	0.62	0.622	594.80	1.37	0.732
2	533.36	4.20	0.792	134.97	2.14	0.845	223.26	1.88	0.787	520.49	2.13	1.000
3	229.68	6.35	0.788	316.03	3.24	0.845	288.04	2.14	0.622	33.59	12.33	1.000
4	276.94	14.38	0.788	65.57	7.59	0.845	131.68	6.90	0.787	140.66	21.84	0.732
5	25.37	37.06	0.788	346.28	16.49	0.170	90.48	27.66	0.622
6	10.07	23.38	0.845	15.21	40.65	0.787
7	42.22	27.83	0.170
	NGC4470			NGC4644			NGC4711			NGC4816		
<i>j</i>	$I_{0,j}$	ξ'_j	q'									
	($L_\odot \text{ pc}^{-2}$)	(arcsec)		($L_\odot \text{ pc}^{-2}$)	(arcsec)		($L_\odot \text{ pc}^{-2}$)	(arcsec)		($L_\odot \text{ pc}^{-2}$)	(arcsec)	
1	589.91	0.39	0.679	761.65	1.72	0.573	404.32	1.40	0.569	1558.69	0.70	0.612
2	154.65	4.23	0.331	265.08	6.97	0.573	103.61	4.22	0.569	1830.95	1.15	0.873
3	391.50	12.35	0.679	73.26	21.84	0.244	135.18	14.02	0.391	80.62	1.96	0.612
4	33.85	27.88	0.679	4.27	23.30	0.573	93.56	17.76	0.569	484.31	2.37	0.873
5	102.83	4.28	0.612
6	166.46	5.90	0.873
7	24.63	13.27	0.612
8	55.67	17.74	0.873
9	15.38	59.32	0.612
	NGC4956			NGC4961			NGC5000			NGC5029		
<i>j</i>	$I_{0,j}$	ξ'_j	q'									
	($L_\odot \text{ pc}^{-2}$)	(arcsec)		($L_\odot \text{ pc}^{-2}$)	(arcsec)		($L_\odot \text{ pc}^{-2}$)	(arcsec)		($L_\odot \text{ pc}^{-2}$)	(arcsec)	
1	3256.75	1.23	1.000	285.62	1.53	0.653	272.64	1.03	1.000	135.19	1.23	0.655
2	355.51	1.64	0.869	350.60	6.68	0.653	293.95	2.55	1.000	1176.67	1.50	0.826
3	1174.79	2.60	1.000	67.18	20.26	0.662	1.49	4.06	0.452	417.24	2.94	0.826
4	461.84	5.37	1.000	90.59	9.41	0.452	56.05	5.50	0.655
5	71.81	6.44	0.869	71.39	13.58	1.000	173.54	6.17	0.826
6	140.25	10.86	1.000	11.62	33.24	1.000	14.24	9.53	0.826
7	47.81	11.24	0.869	90.66	13.24	0.655
8	29.51	27.89	0.869	28.96	37.07	0.655

Table E7. Multi-Gaussian Expansion (MGE) models of the 238 (E1-Sdm) galaxies.

	NGC5056			NGC5218			NGC5378			NGC5480		
j	$I_{0,j}$ ($\text{L}_\odot \text{pc}^{-2}$)	ξ'_j (arcsec)	q'	$I_{0,j}$ ($\text{L}_\odot \text{pc}^{-2}$)	ξ'_j (arcsec)	q'	$I_{0,j}$ ($\text{L}_\odot \text{pc}^{-2}$)	ξ'_j (arcsec)	q'	$I_{0,j}$ ($\text{L}_\odot \text{pc}^{-2}$)	ξ'_j (arcsec)	q'
1	902.38	1.19	1.000	160.93	4.32	0.551	1304.94	1.31	0.745	3071.30	0.41	0.694
2	198.84	5.28	1.000	528.92	9.22	0.551	474.77	2.24	0.745	1483.65	1.17	1.000
3	101.77	11.79	0.455	82.36	21.83	0.551	375.79	5.46	0.767	434.51	1.92	1.000
4	11.17	20.67	1.000	32.89	27.79	0.820	22.28	17.70	0.767	204.72	3.72	1.000
5	48.10	26.37	0.455	54.67	31.78	0.745	199.21	18.24	0.694
6	24.61	33.20	1.000
	NGC5485			NGC5520			NGC5614			NGC5630		
j	$I_{0,j}$ ($\text{L}_\odot \text{pc}^{-2}$)	ξ'_j (arcsec)	q'	$I_{0,j}$ ($\text{L}_\odot \text{pc}^{-2}$)	ξ'_j (arcsec)	q'	$I_{0,j}$ ($\text{L}_\odot \text{pc}^{-2}$)	ξ'_j (arcsec)	q'	$I_{0,j}$ ($\text{L}_\odot \text{pc}^{-2}$)	ξ'_j (arcsec)	q'
1	3976.91	0.67	1.000	2609.40	0.48	1.000	3109.54	1.65	1.000	198.76	1.18	0.483
2	2671.89	1.68	1.000	1946.43	2.97	0.481	543.80	3.24	1.000	131.24	4.99	0.483
3	644.21	5.71	0.712	70.59	3.36	1.000	450.05	3.27	0.842	36.12	14.96	0.271
4	250.23	9.76	1.000	144.62	4.77	1.000	544.93	7.75	1.000	51.07	18.19	0.483
5	208.68	9.87	0.712	151.41	9.03	0.481	110.58	23.10	0.842	62.23	28.87	0.271
6	25.89	20.80	1.000	5.67	14.57	1.000	17.54	55.95	0.842	4.18	33.64	0.483
7	93.16	26.42	0.712	105.25	16.79	0.481
8	23.00	72.22	0.712	32.54	30.71	0.481
	NGC5633			NGC5657			NGC5682			NGC5720		
j	$I_{0,j}$ ($\text{L}_\odot \text{pc}^{-2}$)	ξ'_j (arcsec)	q'	$I_{0,j}$ ($\text{L}_\odot \text{pc}^{-2}$)	ξ'_j (arcsec)	q'	$I_{0,j}$ ($\text{L}_\odot \text{pc}^{-2}$)	ξ'_j (arcsec)	q'	$I_{0,j}$ ($\text{L}_\odot \text{pc}^{-2}$)	ξ'_j (arcsec)	q'
1	249.63	1.02	1.000	1033.07	1.59	0.330	141.34	3.86	0.229	4160.82	0.49	0.662
2	354.86	2.03	1.000	764.26	2.53	0.714	109.90	6.66	0.512	989.96	1.33	1.000
3	5.48	7.30	1.000	352.08	5.83	0.714	10.63	26.90	0.512	316.26	2.39	1.000
4	573.69	10.86	0.651	48.89	26.93	0.330	49.21	26.90	0.229	98.06	12.31	0.662
5	18.43	14.19	1.000	4.40	30.75	0.714	30.03	25.30	0.662
6	32.80	27.88	0.651
	NGC5732			NGC5784			NGC5876			NGC5888		
j	$I_{0,j}$ ($\text{L}_\odot \text{pc}^{-2}$)	ξ'_j (arcsec)	q'	$I_{0,j}$ ($\text{L}_\odot \text{pc}^{-2}$)	ξ'_j (arcsec)	q'	$I_{0,j}$ ($\text{L}_\odot \text{pc}^{-2}$)	ξ'_j (arcsec)	q'	$I_{0,j}$ ($\text{L}_\odot \text{pc}^{-2}$)	ξ'_j (arcsec)	q'
1	375.58	1.69	0.708	4540.08	1.22	1.000	2355.55	1.76	0.838	926.69	1.20	0.630
2	111.95	6.04	0.708	764.65	2.50	1.000	983.12	4.33	0.838	535.11	2.85	0.630
3	60.50	7.02	0.502	440.35	5.69	1.000	16.17	15.04	0.838	72.47	9.95	0.385
4	22.59	13.25	0.708	73.31	15.20	1.000	72.78	32.02	0.401	22.17	15.61	0.385
5	63.26	19.06	0.502	5.28	23.11	0.515	137.86	17.08	0.630
6	14.31	37.01	1.000
7	9.43	37.01	0.515

Table E8. Multi-Gaussian Expansion (MGE) models of the 238 (E1-Sdm) galaxies.

<i>j</i>	NGC5908			NGC5971			NGC5980			NGC5987		
	$I_{0,j}$	ξ'_j	q'	$I_{0,j}$	ξ'_j	q'	$I_{0,j}$	ξ'_j	q'	$I_{0,j}$	ξ'_j	q'
	($L_\odot \text{ pc}^{-2}$)	(arcsec)		($L_\odot \text{ pc}^{-2}$)	(arcsec)		($L_\odot \text{ pc}^{-2}$)	(arcsec)		($L_\odot \text{ pc}^{-2}$)	(arcsec)	
1	1691.19	1.47	0.167	827.69	1.02	0.739	457.15	1.58	0.619	4154.75	1.23	0.695
2	943.11	1.63	0.697	171.41	1.65	0.379	662.30	3.03	0.619	1205.81	2.88	0.695
3	275.39	4.57	0.697	483.81	1.68	0.739	271.29	8.76	0.329	454.34	7.33	0.259
4	702.55	10.18	0.167	212.07	3.21	0.739	79.96	11.90	0.619	197.94	8.76	0.695
5	104.89	17.54	0.697	150.65	6.24	0.379	230.72	20.09	0.329	125.08	21.23	0.259
6	195.78	34.07	0.167	56.15	7.44	0.739	9.55	27.13	0.619	65.37	21.99	0.695
7	36.05	37.58	0.697	52.16	21.40	0.379	32.41	51.92	0.259
8	0.12	44.76	0.697	8.03	22.99	0.739	6.42	91.66	0.695
9	3.98	44.76	0.167	17.70	91.66	0.259
NGC6020			NGC6021			NGC6032			NGC6060			
<i>j</i>	$I_{0,j}$	ξ'_j	q'	$I_{0,j}$	ξ'_j	q'	$I_{0,j}$	ξ'_j	q'	$I_{0,j}$	ξ'_j	q'
	($L_\odot \text{ pc}^{-2}$)	(arcsec)		($L_\odot \text{ pc}^{-2}$)	(arcsec)		($L_\odot \text{ pc}^{-2}$)	(arcsec)		($L_\odot \text{ pc}^{-2}$)	(arcsec)	
1	1973.38	1.15	0.650	2486.67	1.20	0.932	344.45	1.40	0.604	896.91	1.49	0.423
2	1514.12	2.05	0.801	407.57	2.06	0.674	179.21	3.41	0.604	106.35	1.66	1.000
3	330.37	4.37	0.650	599.33	2.64	0.932	118.02	18.53	0.248	1107.46	2.80	0.423
4	256.21	6.66	0.801	343.90	4.50	0.674	37.06	27.55	0.604	146.27	5.22	1.000
5	41.17	11.11	0.650	120.42	6.76	0.932	133.20	26.15	0.423
6	77.65	14.18	0.801	88.47	12.14	0.674	34.51	39.48	0.423
7	19.71	42.67	0.650	24.92	30.80	0.674
NGC6063			NGC6081			NGC6125			NGC6132			
<i>j</i>	$I_{0,j}$	ξ'_j	q'	$I_{0,j}$	ξ'_j	q'	$I_{0,j}$	ξ'_j	q'	$I_{0,j}$	ξ'_j	q'
	($L_\odot \text{ pc}^{-2}$)	(arcsec)		($L_\odot \text{ pc}^{-2}$)	(arcsec)		($L_\odot \text{ pc}^{-2}$)	(arcsec)		($L_\odot \text{ pc}^{-2}$)	(arcsec)	
1	194.44	0.71	0.803	2864.93	1.03	0.327	4456.54	1.15	0.899	949.16	0.62	0.320
2	149.45	1.75	0.803	582.22	1.49	0.812	1192.82	2.48	0.899	268.63	4.36	0.357
3	61.13	5.07	0.803	1172.21	2.29	0.812	736.53	4.03	0.996	189.85	11.88	0.357
4	24.00	13.68	0.803	319.05	4.24	0.812	154.99	8.09	0.899	42.36	22.85	0.320
5	112.24	21.37	0.523	216.98	6.64	0.327	92.85	13.96	0.996
6	125.15	20.47	0.327	41.32	17.34	0.899
7	9.73	27.87	0.812	22.63	48.16	0.996
8	12.91	27.87	0.327
NGC6146			NGC6150			NGC6168			NGC6173			
<i>j</i>	$I_{0,j}$	ξ'_j	q'	$I_{0,j}$	ξ'_j	q'	$I_{0,j}$	ξ'_j	q'	$I_{0,j}$	ξ'_j	q'
	($L_\odot \text{ pc}^{-2}$)	(arcsec)		($L_\odot \text{ pc}^{-2}$)	(arcsec)		($L_\odot \text{ pc}^{-2}$)	(arcsec)		($L_\odot \text{ pc}^{-2}$)	(arcsec)	
1	3729.22	1.27	0.780	1575.29	1.06	0.681	71.55	7.91	0.289	2842.27	1.55	0.682
2	557.59	2.86	0.697	1057.84	2.29	0.681	85.26	20.43	0.263	751.33	3.50	0.682
3	438.82	3.13	0.780	311.97	5.95	0.483	39.31	30.16	0.263	362.52	6.86	0.682
4	352.33	4.76	0.780	140.24	11.09	0.483	43.30	7.30	0.682
5	102.45	6.02	0.697	14.41	23.24	0.681	103.12	19.61	0.623
6	127.68	12.81	0.780	21.63	23.24	0.483	20.83	58.09	0.623
7	24.87	13.45	0.697
8	22.96	40.60	0.697

Table E9. Multi-Gaussian Expansion (MGE) models of the 238 (E1-Sdm) galaxies.

j	NGC6186			NGC6278			NGC6301			NGC6310		
	$I_{0,j}$	ξ'_j	q'	$I_{0,j}$	ξ'_j	q'	$I_{0,j}$	ξ'_j	q'	$I_{0,j}$	ξ'_j	q'
	($L_\odot \text{ pc}^{-2}$)	(arcsec)		($L_\odot \text{ pc}^{-2}$)	(arcsec)		($L_\odot \text{ pc}^{-2}$)	(arcsec)		($L_\odot \text{ pc}^{-2}$)	(arcsec)	
1	5530.20	0.67	0.361	3313.01	1.30	0.884	173.80	1.52	0.551	724.83	1.48	0.773
2	1175.02	2.79	0.888	640.40	2.26	0.550	90.21	3.50	0.685	60.18	2.63	0.248
3	117.20	7.72	0.361	1576.68	2.50	0.884	30.85	10.42	0.685	301.58	3.67	0.773
4	234.81	17.12	0.361	677.42	6.79	0.550	73.95	22.30	0.551	243.98	19.65	0.248
5	32.20	25.63	0.888	151.71	23.19	0.550	15.48	30.59	0.685	27.70	30.58	0.248
6	7.83	30.59	0.551	7.01	30.58	0.773
NGC6314			NGC6478			NGC6497			NGC6515			
j	$I_{0,j}$	ξ'_j	q'	$I_{0,j}$	ξ'_j	q'	$I_{0,j}$	ξ'_j	q'	$I_{0,j}$	ξ'_j	q'
	($L_\odot \text{ pc}^{-2}$)	(arcsec)		($L_\odot \text{ pc}^{-2}$)	(arcsec)		($L_\odot \text{ pc}^{-2}$)	(arcsec)		($L_\odot \text{ pc}^{-2}$)	(arcsec)	
	1371.62	1.22	0.921	1601.84	1.56	0.366	19774.45	0.39	0.487	1937.50	1.29	1.000
2	792.20	1.27	0.506	451.40	1.58	0.798	825.78	1.17	1.000	350.51	2.76	1.000
3	926.12	2.07	0.506	169.68	3.17	0.366	615.85	2.45	0.487	102.56	4.10	0.469
4	668.34	4.17	0.506	100.51	4.48	0.798	419.38	3.20	1.000	222.17	4.39	1.000
5	96.62	5.80	0.921	226.73	18.03	0.366	90.39	6.41	1.000	60.47	7.71	0.469
6	73.91	7.70	0.506	28.95	33.79	0.366	112.59	20.53	0.487	77.17	10.93	1.000
7	77.32	16.95	0.506	3.51	33.79	0.798	38.60	16.64	0.469
8	21.52	30.68	0.506	13.56	37.18	0.469
9	5.61	30.68	0.921	13.64	37.18	1.000
NGC6762			NGC6941			NGC6945			NGC6978			
j	$I_{0,j}$	ξ'_j	q'	$I_{0,j}$	ξ'_j	q'	$I_{0,j}$	ξ'_j	q'	$I_{0,j}$	ξ'_j	q'
	($L_\odot \text{ pc}^{-2}$)	(arcsec)		($L_\odot \text{ pc}^{-2}$)	(arcsec)		($L_\odot \text{ pc}^{-2}$)	(arcsec)		($L_\odot \text{ pc}^{-2}$)	(arcsec)	
	1051.26	2.43	0.516	951.57	1.13	0.602	1544.84	1.02	0.570	886.09	1.26	0.614
2	587.21	6.93	0.516	471.61	1.42	0.972	1510.86	1.19	0.834	462.81	2.78	0.614
3	10.14	22.57	0.516	621.40	3.30	0.602	1024.20	2.05	0.570	314.84	5.10	0.342
4	46.62	29.61	0.219	68.63	8.96	0.602	899.83	2.86	0.834	47.05	14.92	0.614
5	43.98	19.29	0.602	469.46	6.74	0.834	167.53	15.74	0.342
6	31.21	20.24	0.972	89.70	20.32	0.570	44.15	30.58	0.342
7	28.12	33.24	0.602	10.41	37.19	0.570
8	15.57	37.19	0.834
NGC7025			NGC7047			NGC7194			NGC7311			
j	$I_{0,j}$	ξ'_j	q'	$I_{0,j}$	ξ'_j	q'	$I_{0,j}$	ξ'_j	q'	$I_{0,j}$	ξ'_j	q'
	($L_\odot \text{ pc}^{-2}$)	(arcsec)		($L_\odot \text{ pc}^{-2}$)	(arcsec)		($L_\odot \text{ pc}^{-2}$)	(arcsec)		($L_\odot \text{ pc}^{-2}$)	(arcsec)	
	2115.52	1.15	0.920	115.79	1.16	0.537	2296.58	1.50	0.846	3228.90	1.26	0.992
2	1188.62	2.04	0.744	1.86	1.40	0.537	82.19	1.91	0.726	2269.95	2.07	0.992
3	1157.08	2.66	0.920	610.36	2.07	0.484	712.44	3.39	0.846	1082.04	5.32	0.489
4	338.65	4.71	0.920	187.10	15.09	0.484	209.45	7.22	0.846	349.67	15.91	0.489
5	329.45	5.51	0.744	38.78	22.81	0.537	59.30	16.05	0.726	6.01	30.75	0.992
6	172.74	12.97	0.744	15.79	46.76	0.726	38.64	30.75	0.489
7	43.17	17.38	0.920
8	20.18	31.45	0.744
9	21.61	60.43	0.744

Table E10. Multi-Gaussian Expansion (MGE) models of the 238 (E1-Sdm) galaxies.

	NGC7321			NGC7364			NGC7466			NGC7489		
j	$I_{0,j}$ ($\text{L}_\odot \text{pc}^{-2}$)	ξ'_j (arcsec)	q'	$I_{0,j}$ ($\text{L}_\odot \text{pc}^{-2}$)	ξ'_j (arcsec)	q'	$I_{0,j}$ ($\text{L}_\odot \text{pc}^{-2}$)	ξ'_j (arcsec)	q'	$I_{0,j}$ ($\text{L}_\odot \text{pc}^{-2}$)	ξ'_j (arcsec)	q'
1	2182.33	0.39	0.558	340.73	1.17	1.000	1193.24	1.36	0.825	470.54	1.07	0.994
2	680.69	1.80	0.558	2724.63	1.33	0.658	163.99	5.29	0.825	4.56	2.83	0.390
3	356.47	2.32	0.963	217.75	2.87	1.000	57.69	14.98	0.392	43.89	4.25	0.390
4	225.77	7.17	0.963	276.85	3.76	0.658	48.43	23.03	0.392	95.90	8.64	0.994
5	86.35	17.77	0.558	582.00	5.76	0.658	98.84	13.81	0.390
6	11.81	27.61	0.963	132.38	14.03	0.658	16.21	26.34	0.994
7	13.65	27.64	0.558	28.42	33.77	0.658	35.07	30.63	0.390
	NGC7549			NGC7550			NGC7562			NGC7563		
j	$I_{0,j}$ ($\text{L}_\odot \text{pc}^{-2}$)	ξ'_j (arcsec)	q'	$I_{0,j}$ ($\text{L}_\odot \text{pc}^{-2}$)	ξ'_j (arcsec)	q'	$I_{0,j}$ ($\text{L}_\odot \text{pc}^{-2}$)	ξ'_j (arcsec)	q'	$I_{0,j}$ ($\text{L}_\odot \text{pc}^{-2}$)	ξ'_j (arcsec)	q'
1	446.86	2.03	0.960	3398.25	1.39	0.994	5005.28	1.55	0.766	1569.26	1.03	1.000
2	231.21	2.71	0.306	389.73	2.05	0.994	2010.08	3.69	0.766	291.40	1.30	0.575
3	144.33	3.90	0.960	693.97	4.61	0.994	619.75	9.10	0.766	759.36	1.71	1.000
4	153.49	10.18	0.960	228.32	9.13	0.931	102.74	20.38	0.766	850.14	3.06	0.575
5	36.07	40.41	0.306	115.16	17.88	0.931	55.60	27.46	0.402	810.54	4.42	1.000
6	23.06	47.71	0.931	26.98	48.82	0.766	87.42	23.61	0.575
7	11.82	48.82	0.402
	NGC7591			NGC7608			NGC7611			NGC7619		
j	$I_{0,j}$ ($\text{L}_\odot \text{pc}^{-2}$)	ξ'_j (arcsec)	q'	$I_{0,j}$ ($\text{L}_\odot \text{pc}^{-2}$)	ξ'_j (arcsec)	q'	$I_{0,j}$ ($\text{L}_\odot \text{pc}^{-2}$)	ξ'_j (arcsec)	q'	$I_{0,j}$ ($\text{L}_\odot \text{pc}^{-2}$)	ξ'_j (arcsec)	q'
1	470.47	1.72	0.469	283.52	0.92	0.742	4216.47	1.23	0.866	5294.95	1.12	0.811
2	395.81	2.65	0.908	11.95	1.19	0.260	1891.94	1.42	0.458	1233.11	1.82	0.680
3	613.99	4.72	0.908	95.39	2.15	0.742	255.59	1.96	0.866	2741.66	2.51	0.811
4	13.22	18.46	0.908	59.84	10.53	0.260	1920.49	2.63	0.866	444.97	4.32	0.680
5	76.51	18.73	0.469	129.46	17.79	0.260	329.34	13.30	0.458	501.50	5.55	0.680
6	28.22	37.04	0.469	24.84	22.94	0.260	44.34	30.59	0.458	326.66	6.80	0.811
7	5.86	22.94	0.742	228.12	8.40	0.680
8	263.94	14.21	0.811
9	80.49	34.91	0.811
10	18.03	94.15	0.811
	NGC7623			NGC7625			NGC7631			NGC7653		
j	$I_{0,j}$ ($\text{L}_\odot \text{pc}^{-2}$)	ξ'_j (arcsec)	q'	$I_{0,j}$ ($\text{L}_\odot \text{pc}^{-2}$)	ξ'_j (arcsec)	q'	$I_{0,j}$ ($\text{L}_\odot \text{pc}^{-2}$)	ξ'_j (arcsec)	q'	$I_{0,j}$ ($\text{L}_\odot \text{pc}^{-2}$)	ξ'_j (arcsec)	q'
1	188.29	0.99	0.719	1642.72	0.48	0.753	915.78	1.71	0.702	1262.52	1.00	0.986
2	2881.99	1.47	0.768	977.02	2.09	0.753	109.28	3.83	0.385	1408.72	1.89	0.986
3	1221.64	2.88	0.768	1097.15	4.83	0.753	220.79	8.29	0.385	125.87	5.41	0.816
4	124.89	4.59	0.768	39.58	5.60	0.996	86.37	8.50	0.702	188.21	6.48	0.986
5	367.11	5.40	0.719	260.98	14.52	0.753	147.60	22.95	0.385	78.28	8.64	0.816
6	89.42	7.38	0.719	65.68	22.68	0.996	92.01	21.24	0.816
7	55.61	8.72	0.768	1.07	25.21	0.986
8	43.68	16.70	0.719
9	35.81	30.64	0.719

Table E11. Multi-Gaussian Expansion (MGE) models of the 238 (E1-Sdm) galaxies.

j	NGC7671			NGC7683			NGC7711			NGC7716		
	$I_{0,j}$	ξ'_j	q'	$I_{0,j}$	ξ'_j	q'	$I_{0,j}$	ξ'_j	q'	$I_{0,j}$	ξ'_j	q'
	($L_\odot \text{ pc}^{-2}$)	(arcsec)		($L_\odot \text{ pc}^{-2}$)	(arcsec)		($L_\odot \text{ pc}^{-2}$)	(arcsec)		($L_\odot \text{ pc}^{-2}$)	(arcsec)	
1	3621.75	1.19	0.559	2738.97	1.28	0.735	3167.12	1.01	0.776	2103.31	1.13	0.863
2	2407.55	1.77	0.955	1366.39	2.44	0.735	303.84	1.13	0.431	1301.06	1.47	0.574
3	619.89	3.22	0.955	365.18	3.86	0.735	2464.53	1.87	0.776	890.10	2.29	0.574
4	25.16	7.30	0.955	114.56	5.19	0.471	748.74	3.17	0.776	1167.56	2.60	0.863
5	201.15	7.95	0.559	449.36	6.80	0.735	400.63	6.27	0.776	138.33	5.83	0.863
6	181.19	14.43	0.559	14.70	14.63	0.735	151.04	8.91	0.431	166.57	10.66	0.574
7	8.46	30.38	0.955	127.10	17.90	0.471	10.78	18.17	0.776	89.99	18.96	0.863
8	20.06	30.38	0.559	7.97	40.76	0.735	130.27	19.67	0.431	8.23	31.39	0.574
9	25.88	40.76	0.471	29.44	49.26	0.431	25.95	33.61	0.863
NGC7722			NGC7738			NGC7787			NGC7819			
j	$I_{0,j}$	ξ'_j	q'	$I_{0,j}$	ξ'_j	q'	$I_{0,j}$	ξ'_j	q'	$I_{0,j}$	ξ'_j	q'
	($L_\odot \text{ pc}^{-2}$)	(arcsec)		($L_\odot \text{ pc}^{-2}$)	(arcsec)		($L_\odot \text{ pc}^{-2}$)	(arcsec)		($L_\odot \text{ pc}^{-2}$)	(arcsec)	
1	1614.90	1.24	0.587	812.86	1.02	0.314	898.42	1.15	0.474	761.21	1.07	1.000
2	1306.66	2.16	0.587	1806.60	1.09	1.000	376.87	1.86	1.000	437.82	2.71	0.584
3	582.16	4.87	0.587	371.07	3.32	1.000	128.16	5.20	1.000	104.41	4.83	1.000
4	195.41	8.89	0.956	167.23	8.78	0.314	36.65	11.14	0.474	50.63	25.27	0.584
5	76.26	18.13	0.956	93.15	17.36	0.314	20.73	23.30	0.474
6	11.48	40.55	0.956	29.60	27.90	0.314
7	23.39	40.55	0.587	12.68	27.90	1.000
NGC7824			UGC00005			UGC00029			UGC00036			
j	$I_{0,j}$	ξ'_j	q'	$I_{0,j}$	ξ'_j	q'	$I_{0,j}$	ξ'_j	q'	$I_{0,j}$	ξ'_j	q'
	($L_\odot \text{ pc}^{-2}$)	(arcsec)		($L_\odot \text{ pc}^{-2}$)	(arcsec)		($L_\odot \text{ pc}^{-2}$)	(arcsec)		($L_\odot \text{ pc}^{-2}$)	(arcsec)	
1	759.65	1.22	0.954	13.88	0.81	0.554	1731.82	0.81	0.980	1519.03	0.83	0.412
2	2442.06	1.51	0.588	327.26	1.96	0.554	755.15	1.70	0.980	238.59	1.40	1.000
3	991.23	2.13	0.954	87.17	6.63	0.426	131.30	2.62	0.980	342.88	2.00	0.412
4	278.09	5.10	0.588	157.07	14.16	0.554	190.48	4.48	0.980	406.29	2.90	1.000
5	225.20	5.42	0.954	43.24	22.69	0.426	18.53	5.14	0.714	95.44	4.95	1.000
6	28.12	15.75	0.954	37.72	9.68	0.980	201.00	11.44	0.412
7	64.04	25.03	0.588	26.11	12.16	0.714	25.25	27.61	0.412
8	22.59	30.66	0.714
UGC00148			UGC00312			UGC00809			UGC00987			
j	$I_{0,j}$	ξ'_j	q'	$I_{0,j}$	ξ'_j	q'	$I_{0,j}$	ξ'_j	q'	$I_{0,j}$	ξ'_j	q'
	($L_\odot \text{ pc}^{-2}$)	(arcsec)		($L_\odot \text{ pc}^{-2}$)	(arcsec)		($L_\odot \text{ pc}^{-2}$)	(arcsec)		($L_\odot \text{ pc}^{-2}$)	(arcsec)	
1	321.47	0.89	0.241	364.41	0.88	0.266	77.40	14.85	0.263	1492.83	1.31	0.650
2	108.09	2.81	0.872	492.77	4.85	0.266	40.75	21.56	0.263	652.86	2.51	0.650
3	251.68	15.79	0.241	50.80	20.49	0.266	141.38	6.44	0.650
4	8.06	25.27	0.872	55.29	21.75	0.475	307.46	7.49	0.268
5	39.86	25.27	0.241	134.65	13.19	0.268
6	11.39	13.39	0.650
7	46.60	30.91	0.268

Table E12. Multi-Gaussian Expansion (MGE) models of the 238 (E1-Sdm) galaxies.

<i>j</i>	UGC01057			UGC01271			UGC02222			UGC02229		
	$I_{0,j}$	ξ'_j	q'									
	($L_\odot \text{ pc}^{-2}$)	(arcsec)		($L_\odot \text{ pc}^{-2}$)	(arcsec)		($L_\odot \text{ pc}^{-2}$)	(arcsec)		($L_\odot \text{ pc}^{-2}$)	(arcsec)	
1	636.26	1.30	0.400	3650.03	0.53	0.507	206.86	0.39	0.716	1035.69	1.63	0.524
2	126.65	8.12	0.400	1699.29	1.23	0.889	2988.24	1.32	0.716	392.45	3.73	0.680
3	101.35	8.26	0.223	522.71	2.31	0.507	588.20	3.01	0.716	163.35	8.86	0.524
4	49.05	14.48	0.400	647.88	3.37	0.889	274.27	7.07	0.404	36.76	25.35	0.524
5	39.91	22.27	0.223	123.73	8.49	0.889	118.59	7.76	0.716
6	40.71	21.85	0.507	4.33	21.92	0.716
7	1.54	23.02	0.889	55.32	21.92	0.404
8	9.10	23.02	0.507
	UGC02403			UGC03253			UGC03539			UGC03995		
<i>j</i>	$I_{0,j}$	ξ'_j	q'									
	($L_\odot \text{ pc}^{-2}$)	(arcsec)		($L_\odot \text{ pc}^{-2}$)	(arcsec)		($L_\odot \text{ pc}^{-2}$)	(arcsec)		($L_\odot \text{ pc}^{-2}$)	(arcsec)	
1	795.87	0.88	0.611	852.98	0.93	0.947	60.83	1.94	0.819	1406.44	0.94	0.466
2	511.62	2.29	0.611	398.45	2.07	0.465	192.53	2.87	0.123	1742.82	1.57	0.751
3	204.86	13.08	0.341	448.55	2.56	0.947	74.97	5.25	0.819	496.22	4.07	0.751
4	44.81	13.39	0.611	108.91	8.70	0.947	65.44	7.46	0.123	35.18	8.39	0.751
5	25.53	30.65	0.341	8.96	18.62	0.947	125.68	15.54	0.123	59.31	13.49	0.466
6	3.16	30.65	0.611	85.04	21.44	0.465	6.73	30.68	0.819	10.71	18.57	0.751
7	41.57	30.68	0.123	90.81	33.59	0.466
	UGC04029			UGC04132			UGC04145			UGC04197		
<i>j</i>	$I_{0,j}$	ξ'_j	q'									
	($L_\odot \text{ pc}^{-2}$)	(arcsec)		($L_\odot \text{ pc}^{-2}$)	(arcsec)		($L_\odot \text{ pc}^{-2}$)	(arcsec)		($L_\odot \text{ pc}^{-2}$)	(arcsec)	
1	480.90	0.91	0.610	627.88	2.56	0.359	563.46	5.56	0.546	789.88	1.06	0.774
2	85.07	3.06	0.610	260.13	15.00	0.359	260.23	9.64	0.157	209.09	2.33	0.774
3	117.63	4.57	0.610	69.08	28.88	0.247	22.52	14.95	0.157	24.46	6.35	0.774
4	24.73	7.85	0.610	49.98	23.50	0.546	315.97	9.01	0.149
5	145.95	17.26	0.160	164.69	21.14	0.149
6	7.09	33.57	0.610	37.85	28.41	0.149
7	44.53	33.57	0.160	6.17	30.47	0.774
	UGC04280			UGC04308			UGC05108			UGC05113		
<i>j</i>	$I_{0,j}$	ξ'_j	q'									
	($L_\odot \text{ pc}^{-2}$)	(arcsec)		($L_\odot \text{ pc}^{-2}$)	(arcsec)		($L_\odot \text{ pc}^{-2}$)	(arcsec)		($L_\odot \text{ pc}^{-2}$)	(arcsec)	
1	857.84	0.99	0.733	148.50	1.06	0.800	5737.47	0.39	0.450	4115.35	0.97	0.562
2	273.15	2.03	0.733	253.56	1.83	0.531	150.58	1.40	0.450	743.74	3.07	0.562
3	106.47	3.76	0.733	216.61	2.97	0.800	613.13	1.95	1.000	247.80	6.33	0.214
4	134.36	5.77	0.733	36.12	11.34	0.531	249.70	4.93	1.000	183.42	13.67	0.214
5	172.44	10.66	0.260	48.32	21.46	0.531	47.58	11.09	0.450	11.93	22.07	0.562
6	95.07	18.89	0.260	59.40	29.33	0.800	29.03	25.75	0.450	25.48	23.13	0.214
7	4.67	22.96	0.733

Table E13. Multi-Gaussian Expansion (MGE) models of the 238 (E1-Sdm) galaxies.

<i>j</i>	UGC05598			UGC05771			UGC05990			UGC06036		
	$I_{0,j}$	ξ'_j	q'	$I_{0,j}$	ξ'_j	q'	$I_{0,j}$	ξ'_j	q'	$I_{0,j}$	ξ'_j	q'
	($L_\odot \text{ pc}^{-2}$)	(arcsec)		($L_\odot \text{ pc}^{-2}$)	(arcsec)		($L_\odot \text{ pc}^{-2}$)	(arcsec)		($L_\odot \text{ pc}^{-2}$)	(arcsec)	
1	274.73	1.93	0.539	624.99	0.72	0.873	309.85	5.37	0.207	1151.88	0.94	0.790
2	46.27	2.03	0.242	1384.77	0.77	0.681	140.91	7.48	0.342	1145.73	1.87	0.790
3	34.94	9.39	0.539	1846.83	1.27	0.873	52.44	16.93	0.207	328.17	3.50	0.790
4	124.95	12.92	0.242	392.76	2.90	0.873	15.41	23.07	0.342	62.87	6.24	0.790
5	32.77	25.08	0.242	207.18	3.68	0.681	14.17	23.07	0.207	106.35	10.64	0.171
6	29.05	7.04	0.873	180.52	20.96	0.171
7	79.70	7.71	0.681	7.39	24.65	0.790
8	51.02	11.28	0.681
9	28.07	27.03	0.681
UGC06312			UGC07012			UGC07145			UGC08107			
<i>j</i>	$I_{0,j}$	ξ'_j	q'	$I_{0,j}$	ξ'_j	q'	$I_{0,j}$	ξ'_j	q'	$I_{0,j}$	ξ'_j	q'
	($L_\odot \text{ pc}^{-2}$)	(arcsec)		($L_\odot \text{ pc}^{-2}$)	(arcsec)		($L_\odot \text{ pc}^{-2}$)	(arcsec)		($L_\odot \text{ pc}^{-2}$)	(arcsec)	
1	2033.67	1.24	0.387	202.11	1.57	0.542	223.59	1.75	0.595	355.73	2.31	0.588
2	481.16	2.27	0.529	177.05	2.59	1.000	19.41	5.56	0.595	165.40	3.79	0.588
3	238.51	2.41	0.387	5.30	6.21	1.000	68.90	7.08	0.367	102.94	9.94	0.588
4	116.03	3.91	0.387	145.51	9.14	0.542	40.39	14.85	0.367	51.50	14.54	0.307
5	233.45	4.73	0.529	23.30	25.40	0.542	52.04	20.90	0.367	37.86	34.19	0.307
6	128.93	10.61	0.529	7.71	34.19	0.588
7	29.73	30.99	0.387
UGC08231			UGC08234			UGC08733			UGC08778			
<i>j</i>	$I_{0,j}$	ξ'_j	q'	$I_{0,j}$	ξ'_j	q'	$I_{0,j}$	ξ'_j	q'	$I_{0,j}$	ξ'_j	q'
	($L_\odot \text{ pc}^{-2}$)	(arcsec)		($L_\odot \text{ pc}^{-2}$)	(arcsec)		($L_\odot \text{ pc}^{-2}$)	(arcsec)		($L_\odot \text{ pc}^{-2}$)	(arcsec)	
1	62.24	2.01	0.337	3569.53	1.19	0.751	57.73	1.00	0.439	470.35	1.98	0.634
2	124.19	5.79	0.445	675.51	1.65	0.751	18.51	1.71	1.000	73.68	6.28	0.634
3	48.63	19.67	0.337	502.90	2.70	0.751	78.88	2.67	1.000	307.10	14.98	0.206
4	27.02	20.35	0.445	485.57	4.10	0.569	21.93	9.40	1.000	10.65	22.98	0.634
5	143.47	6.18	0.751	13.97	21.59	0.439
6	151.58	10.34	0.569	22.18	33.72	0.439
7	34.07	25.41	0.569	6.67	33.72	1.000
UGC08781			UGC09476			UGC09537			UGC09542			
<i>j</i>	$I_{0,j}$	ξ'_j	q'	$I_{0,j}$	ξ'_j	q'	$I_{0,j}$	ξ'_j	q'	$I_{0,j}$	ξ'_j	q'
	($L_\odot \text{ pc}^{-2}$)	(arcsec)		($L_\odot \text{ pc}^{-2}$)	(arcsec)		($L_\odot \text{ pc}^{-2}$)	(arcsec)		($L_\odot \text{ pc}^{-2}$)	(arcsec)	
1	644.65	1.40	0.759	57.45	1.33	1.000	2095.51	1.32	0.392	229.30	1.19	0.428
2	691.51	2.13	0.759	397.47	1.52	0.660	364.73	3.89	0.392	114.30	4.42	0.428
3	211.99	6.92	0.510	129.65	4.31	1.000	228.13	7.90	0.392	113.61	14.80	0.296
4	27.12	16.81	0.759	115.70	21.12	0.660	61.06	10.96	0.154	28.54	27.89	0.296
5	57.93	22.09	0.510	43.43	36.38	0.154
6	14.56	36.40	0.154
7	13.31	36.93	0.392

Table E14. Multi-Gaussian Expansion (MGE) models of the 238 (E1-Sdm) galaxies.

<i>j</i>	UGC09665			UGC09873			UGC09892			UGC10097		
	$I_{0,j}$	ξ'_j	q'	$I_{0,j}$	ξ'_j	q'	$I_{0,j}$	ξ'_j	q'	$I_{0,j}$	ξ'_j	q'
	($L_\odot \text{ pc}^{-2}$)	(arcsec)		($L_\odot \text{ pc}^{-2}$)	(arcsec)		($L_\odot \text{ pc}^{-2}$)	(arcsec)		($L_\odot \text{ pc}^{-2}$)	(arcsec)	
1	378.74	2.24	0.481	496.13	0.39	0.917	739.25	0.39	0.231	4872.94	0.94	0.927
2	56.10	10.74	0.481	187.98	0.88	0.917	174.38	1.14	0.625	1820.24	1.93	0.927
3	93.41	10.76	0.178	345.34	1.50	0.206	485.77	1.76	0.231	412.54	2.97	0.927
4	190.68	20.95	0.178	44.55	2.29	0.917	107.45	4.61	0.625	81.94	3.99	0.624
5	2.12	24.97	0.481	43.02	3.46	0.917	6.81	13.02	0.625	114.81	5.89	0.927
6	6.84	30.44	0.481	2.53	12.48	0.917	95.63	19.74	0.231	230.51	6.90	0.624
7	82.23	20.41	0.206	46.50	10.71	0.927
8	76.69	15.29	0.624
9	22.87	36.24	0.927
UGC10123			UGC10205			UGC10257			UGC10331			
<i>j</i>	$I_{0,j}$	ξ'_j	q'	$I_{0,j}$	ξ'_j	q'	$I_{0,j}$	ξ'_j	q'	$I_{0,j}$	ξ'_j	q'
	($L_\odot \text{ pc}^{-2}$)	(arcsec)		($L_\odot \text{ pc}^{-2}$)	(arcsec)		($L_\odot \text{ pc}^{-2}$)	(arcsec)		($L_\odot \text{ pc}^{-2}$)	(arcsec)	
1	242.12	3.90	0.361	736.84	1.55	1.000	376.73	1.01	0.396	357.06	2.78	0.247
2	173.83	4.34	0.190	17.51	2.40	1.000	257.84	3.44	0.396	131.12	15.03	0.247
3	58.76	12.49	0.361	205.23	6.32	1.000	1.01	4.14	0.396	30.11	29.95	0.207
4	224.98	15.24	0.190	82.70	14.02	0.643	13.83	13.23	0.396
5	24.00	23.91	0.361	28.32	27.78	0.643	138.43	15.72	0.226
6	3.39	27.78	1.000	42.01	29.61	0.226
UGC10337			UGC10384			UGC10388			UGC10650			
<i>j</i>	$I_{0,j}$	ξ'_j	q'	$I_{0,j}$	ξ'_j	q'	$I_{0,j}$	ξ'_j	q'	$I_{0,j}$	ξ'_j	q'
	($L_\odot \text{ pc}^{-2}$)	(arcsec)		($L_\odot \text{ pc}^{-2}$)	(arcsec)		($L_\odot \text{ pc}^{-2}$)	(arcsec)		($L_\odot \text{ pc}^{-2}$)	(arcsec)	
1	671.51	1.38	0.584	1521.21	0.39	0.196	1831.15	1.63	0.533	430.10	2.79	0.139
2	113.21	6.14	0.315	754.36	1.45	0.462	444.04	4.24	0.533	81.85	3.48	0.411
3	153.31	14.46	0.315	63.67	7.86	0.462	33.17	11.26	0.533	91.49	8.96	0.139
4	3.56	20.96	0.584	364.59	9.99	0.196	100.39	13.46	0.296	47.73	24.99	0.139
5	28.19	20.96	0.315	39.38	21.15	0.196	39.65	27.42	0.296	13.65	24.99	0.411
6	4.45	23.05	0.462
UGC10693			UGC10695			UGC10710			UGC10796			
<i>j</i>	$I_{0,j}$	ξ'_j	q'	$I_{0,j}$	ξ'_j	q'	$I_{0,j}$	ξ'_j	q'	$I_{0,j}$	ξ'_j	q'
	($L_\odot \text{ pc}^{-2}$)	(arcsec)		($L_\odot \text{ pc}^{-2}$)	(arcsec)		($L_\odot \text{ pc}^{-2}$)	(arcsec)		($L_\odot \text{ pc}^{-2}$)	(arcsec)	
1	1872.34	1.26	0.707	1068.26	1.18	0.700	620.69	1.23	0.218	325.56	0.71	0.998
2	1286.17	2.60	0.707	181.97	2.42	0.604	245.26	1.59	0.580	242.79	1.64	0.998
3	298.20	6.64	0.663	247.70	2.61	0.700	204.39	2.64	0.580	92.39	4.52	0.998
4	82.42	15.58	0.663	224.89	5.09	0.700	37.24	5.78	0.580	29.90	22.61	0.543
5	27.15	40.99	0.707	93.47	12.45	0.700	160.40	8.46	0.218	5.21	22.61	0.998
6	21.67	37.08	0.604	69.49	21.67	0.218
7	7.65	28.07	0.580
8	20.48	28.07	0.218

Table E15. Multi-Gaussian Expansion (MGE) models of the 238 (E1-Sdm) galaxies.

j	UGC10811			UGC10905			UGC10972			UGC11228			
	$I_{0,j}$	ξ'_j	q'	$I_{0,j}$	ξ'_j	q'	$I_{0,j}$	ξ'_j	q'	$I_{0,j}$	ξ'_j	q'	
	($L_\odot \text{ pc}^{-2}$)	(arcsec)		($L_\odot \text{ pc}^{-2}$)	(arcsec)		($L_\odot \text{ pc}^{-2}$)	(arcsec)		($L_\odot \text{ pc}^{-2}$)	(arcsec)		
1	1263.04	0.91	0.336	2354.99	1.96	0.617	737.84	0.71	0.882	2682.61	0.93	0.703	
2	621.93	1.99	1.000	49.16	4.49	0.357	466.79	1.15	0.233	1229.42	1.83	0.703	
3	29.79	5.46	1.000	472.88	4.59	0.617	237.91	2.06	0.882	841.74	2.67	0.703	
4	95.83	16.29	0.336	99.84	12.81	0.617	181.68	16.10	0.233	279.28	5.97	0.512	
5	19.42	23.00	0.336	32.41	15.36	0.357	47.78	33.61	0.233	77.57	10.84	0.703	
6	14.78	42.83	0.617	4.23	33.61	0.882	35.66	14.47	0.512	
7	12.16	42.83	0.357	27.91	27.23	0.703	
UGC11717			UGC12054			UGC12127			UGC12185				
j	$I_{0,j}$	ξ'_j	q'	$I_{0,j}$	ξ'_j	q'	$I_{0,j}$	ξ'_j	q'	$I_{0,j}$	ξ'_j	q'	
	($L_\odot \text{ pc}^{-2}$)	(arcsec)		($L_\odot \text{ pc}^{-2}$)	(arcsec)		($L_\odot \text{ pc}^{-2}$)	(arcsec)		($L_\odot \text{ pc}^{-2}$)	(arcsec)		
	1033.88	1.99	0.578	134.23	1.59	0.428	1163.95	0.99	1.000	317.91	1.28	0.495	
2	206.70	7.23	0.578	137.78	7.38	0.428	983.98	1.73	0.714	593.22	1.86	0.817	
3	39.27	7.26	0.437	16.15	18.42	0.428	609.77	3.11	1.000	278.14	7.52	0.495	
4	33.71	15.00	0.437	90.40	19.40	0.138	175.11	6.81	0.714	46.61	22.95	0.495	
5	35.77	25.74	0.437	8.49	25.36	0.138	83.51	7.22	1.000	
6	47.19	16.88	0.714	
7	28.17	18.69	1.000	
8	14.53	55.24	1.000	
UGC12274			UGC12308			UGC12518			UGC12519				
j	$I_{0,j}$	ξ'_j	q'	$I_{0,j}$	ξ'_j	q'	$I_{0,j}$	ξ'_j	q'	$I_{0,j}$	ξ'_j	q'	
	($L_\odot \text{ pc}^{-2}$)	(arcsec)		($L_\odot \text{ pc}^{-2}$)	(arcsec)		($L_\odot \text{ pc}^{-2}$)	(arcsec)		($L_\odot \text{ pc}^{-2}$)	(arcsec)		
	863.11	1.39	0.611	243.04	2.70	0.366	535.58	2.26	0.177	259.23	1.61	0.317	
2	155.28	2.32	0.413	74.38	11.35	0.366	14.88	2.36	1.000	97.61	5.54	0.317	
3	496.77	3.13	0.611	38.52	38.58	0.190	120.23	3.71	1.000	31.64	7.77	0.170	
4	84.75	9.69	0.413	1.87	40.25	0.366	315.85	5.01	0.177	102.37	14.52	0.170	
5	96.70	18.18	0.413	129.00	15.65	0.177	134.53	18.72	0.317	
6	8.21	24.04	1.000	
7	43.78	24.47	0.177	
UGC12723			UGC12857										
j	$I_{0,j}$	ξ'_j	q'	$I_{0,j}$	ξ'_j	q'	$I_{0,j}$	ξ'_j	q'	$I_{0,j}$	ξ'_j	q'	
	($L_\odot \text{ pc}^{-2}$)	(arcsec)		($L_\odot \text{ pc}^{-2}$)	(arcsec)		($L_\odot \text{ pc}^{-2}$)	(arcsec)		($L_\odot \text{ pc}^{-2}$)	(arcsec)		
	1	152.03	13.34	0.147	50.74	1.53	0.386	2	23.23	19.60	0.234	39.82	4.18
3	3	105.85	6.15	0.386	102.44	11.90	0.146
4	5	36.15	13.13	0.386	33.82	21.48	0.386
6	6	125.91	24.07	0.146	125.91	24.07	0.146
7	7

**APPENDIX F: CIRCULAR VELOCITY CURVES OF THE
238 CALIFA GALAXIES (ONLINE MATERIAL)**

In Table F1—Table F60, we present the circular velocity curves as a function of the sampling radius R , normalized on the effective radius R_e of the 238 CALIFA (E1–Sdm) galaxies from JAM-MCMC method together with their uncertainties, calculated from the 75th and 25th percentile of the distribution of the dynamical mass-to-light ratio $(M/L)_{\text{dyn}}$ (see Section 3.1).

Table F1. Circular velocity curves of the 238 (E1–Sdm) CALIFA galaxies with uncertainties corresponding to 75th and 25th percentiles of the data .

R/R_e	IC0480			IC0540			IC0674			IC0944		
	V_c	ΔV_c^{75th}	ΔV_c^{25th}									
0.05	12.51	0.03	0.04	29.17	0.09	0.08	94.59	0.17	0.16	116.85	0.18	0.15
0.054	13.31	0.04	0.04	31.04	0.09	0.08	100.18	0.18	0.17	124.58	0.19	0.16
0.057	14.18	0.04	0.04	33.04	0.10	0.09	105.97	0.19	0.18	132.73	0.21	0.17
0.062	15.12	0.04	0.05	35.19	0.11	0.09	111.97	0.20	0.19	141.30	0.22	0.18
0.066	16.14	0.05	0.05	37.49	0.12	0.10	118.16	0.22	0.20	150.26	0.23	0.19
0.071	17.24	0.05	0.05	39.95	0.12	0.11	124.56	0.23	0.21	159.62	0.25	0.20
0.076	18.42	0.05	0.06	42.56	0.13	0.12	131.15	0.24	0.22	169.34	0.26	0.22
0.081	19.69	0.06	0.06	45.32	0.14	0.12	137.96	0.25	0.23	179.39	0.28	0.23
0.087	21.06	0.06	0.06	48.25	0.15	0.13	144.98	0.27	0.25	189.73	0.30	0.24
0.093	22.53	0.07	0.07	51.34	0.16	0.14	152.23	0.28	0.26	200.30	0.31	0.26
0.1	24.11	0.07	0.07	54.59	0.17	0.15	159.73	0.29	0.27	211.01	0.33	0.27
0.107	25.80	0.08	0.08	57.99	0.18	0.16	167.48	0.31	0.29	221.77	0.35	0.28
0.115	27.62	0.08	0.09	61.54	0.19	0.17	175.48	0.32	0.30	232.47	0.36	0.30
0.123	29.56	0.09	0.09	65.23	0.21	0.18	183.71	0.34	0.31	242.98	0.38	0.31
0.132	31.64	0.09	0.10	69.04	0.22	0.19	192.14	0.35	0.33	253.15	0.40	0.32
0.142	33.86	0.10	0.11	72.95	0.23	0.20	200.69	0.37	0.34	262.81	0.41	0.34
0.152	36.24	0.11	0.11	76.93	0.24	0.21	209.28	0.38	0.36	271.81	0.43	0.35
0.163	38.78	0.11	0.12	80.97	0.26	0.22	217.81	0.40	0.37	279.96	0.44	0.36
0.174	41.49	0.12	0.13	85.00	0.27	0.23	226.15	0.41	0.39	287.12	0.45	0.37
0.187	44.38	0.13	0.14	89.01	0.28	0.25	234.17	0.43	0.40	293.14	0.46	0.38
0.2	47.47	0.14	0.15	92.92	0.29	0.26	241.75	0.44	0.41	297.94	0.47	0.38
0.215	50.75	0.15	0.16	96.69	0.31	0.27	248.79	0.46	0.42	301.48	0.47	0.39
0.23	54.24	0.16	0.17	100.25	0.32	0.28	255.21	0.47	0.43	303.81	0.48	0.39
0.247	57.95	0.17	0.18	103.54	0.33	0.29	260.95	0.48	0.44	305.02	0.48	0.39
0.265	61.88	0.18	0.19	106.51	0.34	0.29	266.01	0.49	0.45	305.31	0.48	0.39
0.284	66.05	0.19	0.21	109.10	0.34	0.30	270.42	0.50	0.46	304.92	0.48	0.39
0.304	70.45	0.21	0.22	111.28	0.35	0.31	274.27	0.50	0.47	304.12	0.48	0.39
0.326	75.10	0.22	0.23	113.03	0.36	0.31	277.66	0.51	0.47	303.14	0.47	0.39
0.349	79.99	0.24	0.25	114.37	0.36	0.32	280.71	0.51	0.48	302.18	0.47	0.39
0.374	85.12	0.25	0.26	115.34	0.36	0.32	283.51	0.52	0.48	301.34	0.47	0.39
0.401	90.48	0.27	0.28	116.03	0.37	0.32	286.15	0.52	0.49	300.66	0.47	0.39
0.43	96.07	0.28	0.30	116.55	0.37	0.32	288.62	0.53	0.49	300.09	0.47	0.38
0.461	101.87	0.30	0.32	117.04	0.37	0.32	290.87	0.53	0.50	299.55	0.47	0.38
0.494	107.85	0.32	0.34	117.63	0.37	0.32	292.82	0.54	0.50	298.98	0.47	0.38
0.53	113.99	0.34	0.35	118.45	0.37	0.33	294.36	0.54	0.50	298.32	0.47	0.38
0.568	120.24	0.35	0.37	119.58	0.38	0.33	295.38	0.54	0.50	297.58	0.47	0.38
0.608	126.56	0.37	0.39	121.07	0.38	0.33	295.80	0.54	0.50	296.82	0.46	0.38
0.652	132.89	0.39	0.41	122.88	0.39	0.34	295.62	0.54	0.50	296.12	0.46	0.38
0.699	139.15	0.41	0.43	124.99	0.39	0.35	294.88	0.54	0.50	295.59	0.46	0.38
0.749	145.26	0.43	0.45	127.30	0.40	0.35	293.69	0.54	0.50	295.34	0.46	0.38
0.803	151.14	0.45	0.47	129.72	0.41	0.36	292.20	0.54	0.50	295.42	0.46	0.38
0.861	156.68	0.46	0.49	132.17	0.42	0.37	290.59	0.53	0.49	295.85	0.46	0.38
0.923	161.77	0.48	0.50	134.54	0.43	0.37	289.02	0.53	0.49	296.57	0.46	0.38
0.989	166.32	0.49	0.52	136.75	0.43	0.38	287.62	0.53	0.49	297.49	0.47	0.38
1.06	170.23	0.50	0.53	138.72	0.44	0.38	286.43	0.52	0.49	298.48	0.47	0.38
1.136	173.41	0.51	0.54	140.41	0.44	0.39	285.43	0.52	0.49	299.39	0.47	0.38
1.218	175.80	0.52	0.55	141.75	0.45	0.39	284.53	0.52	0.48	300.07	0.47	0.38
1.306	177.36	0.52	0.55	142.73	0.45	0.39	283.59	0.52	0.48	300.41	0.47	0.39
1.399	178.11	0.52	0.55	143.31	0.45	0.40	282.46	0.52	0.48	300.30	0.47	0.39
1.5	178.08	0.52	0.55	143.51	0.45	0.40	280.99	0.51	0.48	299.67	0.47	0.38

Table F2. Circular velocity curves of the 238 (E1–Sdm) CALIFA galaxies with 75th and 25th percentile uncertainties.

R/R_e	IC1079			IC1151			IC1256			IC1528		
	V_c	ΔV_c^{75th}	ΔV_c^{25th}									
0.05	230.73	0.45	0.41	42.20	0.13	0.12	38.08	0.13	0.12	27.17	0.08	0.05
0.054	240.10	0.47	0.43	44.49	0.14	0.13	40.54	0.14	0.13	28.99	0.08	0.06
0.057	248.96	0.49	0.45	46.81	0.14	0.14	43.13	0.15	0.14	30.94	0.09	0.06
0.062	257.16	0.50	0.46	49.16	0.15	0.15	45.85	0.15	0.15	33.01	0.10	0.07
0.066	264.57	0.52	0.47	51.51	0.16	0.15	48.70	0.16	0.16	35.21	0.10	0.07
0.071	271.06	0.53	0.49	53.84	0.17	0.16	51.67	0.17	0.17	37.55	0.11	0.07
0.076	276.53	0.54	0.50	56.13	0.17	0.17	54.74	0.19	0.18	40.02	0.12	0.08
0.081	280.95	0.55	0.50	58.35	0.18	0.17	57.92	0.20	0.19	42.62	0.13	0.08
0.087	284.33	0.55	0.51	60.48	0.19	0.18	61.18	0.21	0.20	45.36	0.13	0.09
0.093	286.76	0.56	0.51	62.52	0.19	0.19	64.50	0.22	0.21	48.23	0.14	0.10
0.1	288.40	0.56	0.52	64.44	0.20	0.19	67.86	0.23	0.22	51.24	0.15	0.10
0.107	289.47	0.56	0.52	66.26	0.20	0.20	71.24	0.24	0.23	54.36	0.16	0.11
0.115	290.21	0.57	0.52	67.99	0.21	0.20	74.60	0.25	0.24	57.60	0.17	0.12
0.123	290.86	0.57	0.52	69.65	0.22	0.21	77.91	0.26	0.25	60.94	0.18	0.12
0.132	291.64	0.57	0.52	71.29	0.22	0.21	81.14	0.28	0.26	64.35	0.19	0.13
0.142	292.65	0.57	0.52	72.94	0.23	0.22	84.26	0.29	0.27	67.83	0.20	0.14
0.152	293.92	0.57	0.53	74.65	0.23	0.22	87.24	0.30	0.28	71.33	0.21	0.14
0.163	295.39	0.58	0.53	76.45	0.24	0.23	90.05	0.31	0.29	74.83	0.22	0.15
0.174	296.93	0.58	0.53	78.36	0.24	0.23	92.71	0.31	0.30	78.28	0.23	0.16
0.187	298.35	0.58	0.53	80.37	0.25	0.24	95.21	0.32	0.31	81.65	0.24	0.16
0.2	299.46	0.58	0.54	82.44	0.25	0.25	97.59	0.33	0.31	84.89	0.25	0.17
0.215	300.11	0.59	0.54	84.54	0.26	0.25	99.90	0.34	0.32	87.95	0.26	0.18
0.23	300.14	0.59	0.54	86.59	0.27	0.26	102.22	0.35	0.33	90.78	0.27	0.18
0.247	299.48	0.58	0.54	88.53	0.27	0.27	104.63	0.35	0.34	93.36	0.28	0.19
0.265	298.12	0.58	0.53	90.31	0.28	0.27	107.22	0.36	0.34	95.64	0.28	0.19
0.284	296.12	0.58	0.53	91.90	0.28	0.28	110.09	0.37	0.35	97.63	0.29	0.20
0.304	293.62	0.57	0.53	93.27	0.29	0.28	113.31	0.38	0.36	99.34	0.29	0.20
0.326	290.81	0.57	0.52	94.43	0.29	0.28	116.93	0.40	0.38	100.81	0.30	0.20
0.349	287.90	0.56	0.52	95.43	0.30	0.29	120.99	0.41	0.39	102.11	0.30	0.20
0.374	285.11	0.56	0.51	96.32	0.30	0.29	125.48	0.43	0.40	103.34	0.31	0.21
0.401	282.61	0.55	0.51	97.20	0.30	0.29	130.40	0.44	0.42	104.62	0.31	0.21
0.43	280.51	0.55	0.50	98.16	0.30	0.29	135.72	0.46	0.44	106.08	0.31	0.21
0.461	278.82	0.54	0.50	99.31	0.31	0.30	141.39	0.48	0.45	107.82	0.32	0.22
0.494	277.48	0.54	0.50	100.72	0.31	0.30	147.36	0.50	0.47	109.93	0.33	0.22
0.53	276.39	0.54	0.50	102.43	0.32	0.31	153.59	0.52	0.49	112.44	0.33	0.23
0.568	275.39	0.54	0.49	104.45	0.32	0.31	160.00	0.54	0.51	115.34	0.34	0.23
0.608	274.33	0.53	0.49	106.73	0.33	0.32	166.52	0.57	0.54	118.60	0.35	0.24
0.652	273.04	0.53	0.49	109.21	0.34	0.33	173.08	0.59	0.56	122.13	0.36	0.24
0.699	271.41	0.53	0.49	111.80	0.35	0.34	179.58	0.61	0.58	125.86	0.37	0.25
0.749	269.34	0.53	0.48	114.43	0.35	0.34	185.91	0.63	0.60	129.69	0.38	0.26
0.803	266.78	0.52	0.48	117.02	0.36	0.35	191.96	0.65	0.62	133.50	0.39	0.27
0.861	263.75	0.51	0.47	119.52	0.37	0.36	197.62	0.67	0.64	137.19	0.41	0.27
0.923	260.32	0.51	0.47	121.88	0.38	0.37	202.73	0.69	0.65	140.66	0.42	0.28
0.989	256.58	0.50	0.46	124.08	0.38	0.37	207.16	0.70	0.67	143.79	0.43	0.29
1.06	252.67	0.49	0.45	126.12	0.39	0.38	210.78	0.72	0.68	146.49	0.43	0.29
1.136	248.76	0.48	0.45	128.00	0.40	0.38	213.46	0.72	0.69	148.67	0.44	0.30
1.218	244.98	0.48	0.44	129.75	0.40	0.39	215.11	0.73	0.69	150.26	0.44	0.30
1.306	241.48	0.47	0.43	131.38	0.41	0.39	215.67	0.73	0.69	151.24	0.45	0.30
1.399	238.33	0.46	0.43	132.93	0.41	0.40	215.16	0.73	0.69	151.59	0.45	0.30
1.5	235.61	0.46	0.42	134.38	0.42	0.40	213.66	0.73	0.69	151.36	0.45	0.30

Table F3. Circular velocity curves of the 238 (E1–Sdm) CALIFA galaxies with 75th and 25th percentile uncertainties.

R/R_e	IC1652			IC1755			IC2101			IC2247		
	V_c	ΔV_c^{75th}	ΔV_c^{25th}									
0.05	125.06	0.27	0.25	93.51	0.14	0.14	18.42	0.07	0.06	125.15	0.28	0.28
0.054	129.23	0.28	0.26	99.72	0.15	0.14	19.66	0.07	0.06	126.20	0.29	0.29
0.057	132.97	0.29	0.26	106.27	0.16	0.15	21.01	0.08	0.07	127.68	0.29	0.29
0.062	136.22	0.30	0.27	113.16	0.17	0.16	22.45	0.08	0.07	129.68	0.29	0.30
0.066	138.91	0.30	0.28	120.39	0.18	0.17	23.99	0.09	0.08	132.23	0.30	0.30
0.071	140.99	0.31	0.28	127.95	0.19	0.19	25.65	0.10	0.09	135.29	0.31	0.31
0.076	142.47	0.31	0.28	135.82	0.20	0.20	27.43	0.10	0.09	138.79	0.31	0.32
0.081	143.37	0.31	0.28	143.99	0.21	0.21	29.33	0.11	0.10	142.60	0.32	0.32
0.087	143.76	0.32	0.29	152.41	0.23	0.22	31.35	0.12	0.11	146.60	0.33	0.33
0.093	143.77	0.32	0.29	161.06	0.24	0.23	33.52	0.13	0.11	150.65	0.34	0.34
0.1	143.56	0.32	0.29	169.87	0.25	0.25	35.83	0.13	0.12	154.63	0.35	0.35
0.107	143.30	0.31	0.28	178.79	0.27	0.26	38.28	0.14	0.13	158.41	0.36	0.36
0.115	143.16	0.31	0.28	187.73	0.28	0.27	40.90	0.15	0.14	161.86	0.37	0.37
0.123	143.31	0.31	0.28	196.61	0.29	0.29	43.67	0.16	0.15	164.90	0.37	0.38
0.132	143.85	0.32	0.29	205.34	0.31	0.30	46.62	0.18	0.16	167.42	0.38	0.38
0.142	144.84	0.32	0.29	213.80	0.32	0.31	49.73	0.19	0.17	169.38	0.38	0.39
0.152	146.27	0.32	0.29	221.89	0.33	0.32	53.02	0.20	0.18	170.74	0.39	0.39
0.163	148.10	0.33	0.29	229.50	0.34	0.33	56.48	0.21	0.19	171.54	0.39	0.39
0.174	150.27	0.33	0.30	236.53	0.35	0.34	60.13	0.23	0.20	171.83	0.39	0.39
0.187	152.69	0.34	0.30	242.91	0.36	0.35	63.94	0.24	0.22	171.73	0.39	0.39
0.2	155.24	0.34	0.31	248.59	0.37	0.36	67.93	0.26	0.23	171.38	0.39	0.39
0.215	157.84	0.35	0.31	253.56	0.38	0.37	72.07	0.27	0.24	170.94	0.39	0.39
0.23	160.37	0.35	0.32	257.83	0.38	0.37	76.37	0.29	0.26	170.53	0.39	0.39
0.247	162.73	0.36	0.32	261.47	0.39	0.38	80.79	0.30	0.27	170.25	0.39	0.39
0.265	164.83	0.36	0.33	264.56	0.39	0.38	85.32	0.32	0.29	170.17	0.39	0.39
0.284	166.60	0.37	0.33	267.19	0.40	0.39	89.92	0.34	0.30	170.27	0.39	0.39
0.304	167.99	0.37	0.33	269.45	0.40	0.39	94.57	0.36	0.32	170.50	0.39	0.39
0.326	168.99	0.37	0.34	271.38	0.41	0.39	99.23	0.37	0.34	170.81	0.39	0.39
0.349	169.62	0.37	0.34	272.96	0.41	0.40	103.85	0.39	0.35	171.11	0.39	0.39
0.374	169.92	0.37	0.34	274.14	0.41	0.40	108.37	0.41	0.37	171.33	0.39	0.39
0.401	169.97	0.37	0.34	274.81	0.41	0.40	112.76	0.42	0.38	171.42	0.39	0.39
0.43	169.85	0.37	0.34	274.88	0.41	0.40	116.96	0.44	0.40	171.34	0.39	0.39
0.461	169.64	0.37	0.34	274.23	0.41	0.40	120.93	0.45	0.41	171.07	0.39	0.39
0.494	169.41	0.37	0.34	272.82	0.41	0.40	124.63	0.47	0.42	170.60	0.39	0.39
0.53	169.19	0.37	0.34	270.69	0.40	0.39	128.05	0.48	0.43	169.97	0.39	0.39
0.568	168.98	0.37	0.34	267.91	0.40	0.39	131.19	0.49	0.44	169.24	0.38	0.39
0.608	168.76	0.37	0.34	264.66	0.39	0.38	134.07	0.50	0.45	168.50	0.38	0.38
0.652	168.50	0.37	0.33	261.16	0.39	0.38	136.74	0.51	0.46	167.86	0.38	0.38
0.699	168.17	0.37	0.33	257.67	0.38	0.37	139.25	0.52	0.47	167.47	0.38	0.38
0.749	167.77	0.37	0.33	254.42	0.38	0.37	141.69	0.53	0.48	167.42	0.38	0.38
0.803	167.32	0.37	0.33	251.63	0.38	0.36	144.12	0.54	0.49	167.80	0.38	0.38
0.861	166.86	0.37	0.33	249.42	0.37	0.36	146.59	0.55	0.50	168.63	0.38	0.38
0.923	166.44	0.37	0.33	247.87	0.37	0.36	149.10	0.56	0.50	169.90	0.39	0.39
0.989	166.10	0.37	0.33	246.98	0.37	0.36	151.62	0.57	0.51	171.51	0.39	0.39
1.06	165.87	0.36	0.33	246.72	0.37	0.36	154.07	0.58	0.52	173.36	0.39	0.39
1.136	165.75	0.36	0.33	247.02	0.37	0.36	156.33	0.59	0.53	175.31	0.40	0.40
1.218	165.72	0.36	0.33	247.81	0.37	0.36	158.28	0.60	0.54	177.20	0.40	0.40
1.306	165.74	0.36	0.33	249.00	0.37	0.36	159.77	0.60	0.54	178.87	0.41	0.41
1.399	165.76	0.36	0.33	250.49	0.37	0.36	160.67	0.60	0.54	180.18	0.41	0.41
1.5	165.71	0.36	0.33	252.18	0.38	0.37	160.86	0.61	0.54	180.98	0.41	0.41

Table F4. Circular velocity curves of the 238 (E1–Sdm) CALIFA galaxies with 75th and 25th percentile uncertainties.

R/R_e	IC2487			IC4566			IC5309			IC5376		
	V_c	ΔV_c^{75th}	ΔV_c^{25th}									
0.05	72.62	0.13	0.20	97.03	0.26	0.14	46.98	0.26	0.21	79.91	0.21	0.17
0.054	75.80	0.13	0.21	103.26	0.28	0.15	49.89	0.27	0.22	85.20	0.22	0.19
0.057	78.85	0.14	0.22	109.79	0.29	0.16	52.93	0.29	0.23	90.79	0.24	0.20
0.062	81.71	0.14	0.23	116.60	0.31	0.17	56.08	0.31	0.25	96.67	0.25	0.21
0.066	84.33	0.15	0.23	123.67	0.33	0.18	59.33	0.33	0.26	102.83	0.27	0.22
0.071	86.64	0.15	0.24	130.98	0.35	0.19	62.67	0.34	0.28	109.28	0.28	0.24
0.076	88.59	0.16	0.25	138.51	0.37	0.20	66.07	0.36	0.29	115.99	0.30	0.25
0.081	90.13	0.16	0.25	146.20	0.39	0.21	69.50	0.38	0.31	122.94	0.32	0.27
0.087	91.25	0.16	0.25	154.01	0.41	0.22	72.94	0.40	0.32	130.12	0.34	0.28
0.093	91.92	0.16	0.26	161.88	0.43	0.24	76.36	0.42	0.34	137.48	0.36	0.30
0.1	92.17	0.16	0.26	169.72	0.45	0.25	79.71	0.44	0.36	144.98	0.38	0.32
0.107	92.07	0.16	0.26	177.47	0.47	0.26	82.95	0.46	0.37	152.57	0.40	0.33
0.115	91.71	0.16	0.26	185.03	0.49	0.27	86.04	0.47	0.38	160.17	0.42	0.35
0.123	91.23	0.16	0.25	192.30	0.51	0.28	88.95	0.49	0.40	167.72	0.44	0.37
0.132	90.77	0.16	0.25	199.20	0.53	0.29	91.65	0.50	0.41	175.13	0.46	0.38
0.142	90.51	0.16	0.25	205.62	0.55	0.30	94.11	0.52	0.42	182.30	0.47	0.40
0.152	90.58	0.16	0.25	211.49	0.56	0.31	96.34	0.53	0.43	189.16	0.49	0.41
0.163	91.10	0.16	0.25	216.74	0.58	0.32	98.37	0.54	0.44	195.60	0.51	0.43
0.174	92.13	0.16	0.26	221.33	0.59	0.32	100.24	0.55	0.45	201.55	0.53	0.44
0.187	93.70	0.16	0.26	225.26	0.60	0.33	102.02	0.56	0.45	206.96	0.54	0.45
0.2	95.79	0.17	0.27	228.55	0.61	0.33	103.83	0.57	0.46	211.78	0.55	0.46
0.215	98.38	0.17	0.27	231.25	0.62	0.34	105.75	0.58	0.47	216.01	0.56	0.47
0.23	101.43	0.18	0.28	233.42	0.62	0.34	107.89	0.59	0.48	219.68	0.57	0.48
0.247	104.88	0.18	0.29	235.17	0.63	0.34	110.34	0.61	0.49	222.88	0.58	0.49
0.265	108.70	0.19	0.30	236.58	0.63	0.34	113.12	0.62	0.50	225.67	0.59	0.49
0.284	112.82	0.20	0.31	237.73	0.63	0.35	116.22	0.64	0.52	228.17	0.59	0.50
0.304	117.19	0.21	0.33	238.71	0.64	0.35	119.60	0.66	0.53	230.47	0.60	0.50
0.326	121.76	0.21	0.34	239.56	0.64	0.35	123.17	0.68	0.55	232.62	0.61	0.51
0.349	126.46	0.22	0.35	240.32	0.64	0.35	126.82	0.70	0.57	234.64	0.61	0.51
0.374	131.21	0.23	0.37	240.99	0.64	0.35	130.44	0.72	0.58	236.48	0.62	0.52
0.401	135.95	0.24	0.38	241.54	0.64	0.35	133.90	0.74	0.60	238.08	0.62	0.52
0.43	140.60	0.25	0.39	241.90	0.65	0.35	137.10	0.76	0.61	239.33	0.62	0.52
0.461	145.09	0.25	0.40	241.98	0.65	0.35	139.94	0.77	0.62	240.13	0.63	0.53
0.494	149.36	0.26	0.42	241.68	0.64	0.35	142.32	0.78	0.63	240.39	0.63	0.53
0.53	153.36	0.27	0.43	240.94	0.64	0.35	144.18	0.79	0.64	240.06	0.63	0.53
0.568	157.06	0.28	0.44	239.71	0.64	0.35	145.48	0.80	0.65	239.08	0.62	0.52
0.608	160.45	0.28	0.45	238.03	0.63	0.35	146.22	0.81	0.65	237.47	0.62	0.52
0.652	163.55	0.29	0.46	236.00	0.63	0.34	146.45	0.81	0.65	235.24	0.61	0.52
0.699	166.42	0.29	0.46	233.79	0.62	0.34	146.26	0.81	0.65	232.45	0.61	0.51
0.749	169.14	0.30	0.47	231.63	0.62	0.34	145.77	0.80	0.65	229.17	0.60	0.50
0.803	171.78	0.30	0.48	229.75	0.61	0.33	145.15	0.80	0.65	225.52	0.59	0.49
0.861	174.47	0.31	0.49	228.35	0.61	0.33	144.55	0.80	0.64	221.64	0.58	0.49
0.923	177.25	0.31	0.49	227.56	0.61	0.33	144.09	0.79	0.64	217.70	0.57	0.48
0.989	180.18	0.32	0.50	227.40	0.61	0.33	143.85	0.79	0.64	213.90	0.56	0.47
1.06	183.23	0.32	0.51	227.80	0.61	0.33	143.84	0.79	0.64	210.41	0.55	0.46
1.136	186.32	0.33	0.52	228.60	0.61	0.33	144.01	0.79	0.64	207.34	0.54	0.45
1.218	189.32	0.33	0.53	229.59	0.61	0.33	144.27	0.80	0.64	204.79	0.53	0.45
1.306	192.06	0.34	0.54	230.55	0.61	0.34	144.51	0.80	0.64	202.74	0.53	0.44
1.399	194.32	0.34	0.54	231.27	0.62	0.34	144.61	0.80	0.65	201.15	0.52	0.44
1.5	195.92	0.34	0.55	231.58	0.62	0.34	144.50	0.80	0.64	199.94	0.52	0.44

Table F5. Circular velocity curves of the 238 (E1–Sdm) CALIFA galaxies with 75th and 25th percentile uncertainties.

R/R_e	MCG-01-54-016			MCG-02-02-030			MCG-02-02-040			MCG-02-03-015		
	V_c	ΔV_c^{75th}	ΔV_c^{25th}									
0.05	41.83	0.33	0.36	64.64	0.13	0.11	30.89	0.14	0.11	120.34	0.26	0.35
0.054	43.21	0.34	0.37	67.89	0.13	0.12	32.65	0.15	0.11	128.02	0.27	0.38
0.057	44.43	0.35	0.38	71.14	0.14	0.13	34.47	0.15	0.12	136.04	0.29	0.40
0.062	45.48	0.36	0.39	74.36	0.15	0.13	36.33	0.16	0.13	144.40	0.31	0.42
0.066	46.32	0.36	0.40	77.51	0.15	0.14	38.22	0.17	0.13	153.06	0.33	0.45
0.071	46.94	0.37	0.40	80.57	0.16	0.14	40.12	0.18	0.14	161.99	0.34	0.47
0.076	47.32	0.37	0.41	83.51	0.16	0.15	42.01	0.19	0.15	171.13	0.36	0.50
0.081	47.48	0.37	0.41	86.31	0.17	0.15	43.87	0.20	0.16	180.44	0.38	0.53
0.087	47.44	0.37	0.41	88.96	0.18	0.16	45.67	0.21	0.16	189.82	0.40	0.56
0.093	47.24	0.37	0.41	91.47	0.18	0.16	47.40	0.21	0.17	199.20	0.42	0.58
0.1	46.97	0.37	0.40	93.85	0.19	0.17	49.03	0.22	0.17	208.45	0.44	0.61
0.107	46.70	0.37	0.40	96.13	0.19	0.17	50.54	0.23	0.18	217.46	0.46	0.64
0.115	46.54	0.37	0.40	98.37	0.19	0.17	51.91	0.23	0.18	226.09	0.48	0.66
0.123	46.57	0.37	0.40	100.62	0.20	0.18	53.16	0.24	0.19	234.18	0.50	0.69
0.132	46.86	0.37	0.40	102.93	0.20	0.18	54.28	0.24	0.19	241.59	0.51	0.71
0.142	47.47	0.37	0.41	105.35	0.21	0.19	55.30	0.25	0.20	248.14	0.53	0.73
0.152	48.41	0.38	0.42	107.90	0.21	0.19	56.28	0.25	0.20	253.70	0.54	0.74
0.163	49.67	0.39	0.43	110.57	0.22	0.20	57.27	0.26	0.20	258.15	0.55	0.76
0.174	51.25	0.40	0.44	113.33	0.22	0.20	58.36	0.26	0.21	261.39	0.56	0.77
0.187	53.12	0.42	0.46	116.13	0.23	0.21	59.62	0.27	0.21	263.38	0.56	0.77
0.2	55.25	0.44	0.48	118.89	0.23	0.21	61.13	0.28	0.22	264.14	0.56	0.77
0.215	57.63	0.45	0.50	121.53	0.24	0.21	62.94	0.28	0.22	263.72	0.56	0.77
0.23	60.23	0.48	0.52	123.96	0.24	0.22	65.11	0.29	0.23	262.28	0.56	0.77
0.247	63.04	0.50	0.54	126.12	0.25	0.22	67.63	0.31	0.24	259.98	0.55	0.76
0.265	66.02	0.52	0.57	127.93	0.25	0.23	70.51	0.32	0.25	257.06	0.55	0.75
0.284	69.15	0.55	0.60	129.37	0.26	0.23	73.71	0.33	0.26	253.74	0.54	0.74
0.304	72.40	0.57	0.62	130.43	0.26	0.23	77.21	0.35	0.27	250.24	0.53	0.73
0.326	75.74	0.60	0.65	131.15	0.26	0.23	80.98	0.37	0.29	246.75	0.53	0.72
0.349	79.12	0.62	0.68	131.59	0.26	0.23	84.99	0.38	0.30	243.39	0.52	0.71
0.374	82.50	0.65	0.71	131.88	0.26	0.23	89.21	0.40	0.32	240.23	0.51	0.70
0.401	85.82	0.68	0.74	132.13	0.26	0.23	93.62	0.42	0.33	237.28	0.51	0.70
0.43	89.03	0.70	0.77	132.52	0.26	0.23	98.19	0.44	0.35	234.53	0.50	0.69
0.461	92.08	0.73	0.79	133.18	0.26	0.24	102.90	0.46	0.37	231.96	0.49	0.68
0.494	94.90	0.75	0.82	134.23	0.27	0.24	107.71	0.49	0.38	229.57	0.49	0.67
0.53	97.44	0.77	0.84	135.75	0.27	0.24	112.60	0.51	0.40	227.37	0.48	0.67
0.568	99.65	0.79	0.86	137.78	0.27	0.24	117.55	0.53	0.42	225.42	0.48	0.66
0.608	101.49	0.80	0.87	140.31	0.28	0.25	122.55	0.55	0.44	223.75	0.48	0.66
0.652	102.96	0.81	0.89	143.28	0.28	0.25	127.57	0.58	0.45	222.39	0.47	0.65
0.699	104.07	0.82	0.90	146.64	0.29	0.26	132.59	0.60	0.47	221.34	0.47	0.65
0.749	104.85	0.83	0.90	150.30	0.30	0.27	137.60	0.62	0.49	220.55	0.47	0.65
0.803	105.38	0.83	0.91	154.17	0.30	0.27	142.57	0.64	0.51	219.95	0.47	0.65
0.861	105.75	0.84	0.91	158.14	0.31	0.28	147.45	0.67	0.52	219.42	0.47	0.64
0.923	106.07	0.84	0.91	162.11	0.32	0.29	152.19	0.69	0.54	218.85	0.47	0.64
0.989	106.42	0.84	0.92	165.94	0.33	0.29	156.71	0.71	0.56	218.15	0.46	0.64
1.06	106.86	0.84	0.92	169.52	0.33	0.30	160.90	0.73	0.57	217.21	0.46	0.64
1.136	107.43	0.85	0.93	172.70	0.34	0.31	164.64	0.74	0.59	215.97	0.46	0.63
1.218	108.07	0.85	0.93	175.34	0.35	0.31	167.81	0.76	0.60	214.39	0.46	0.63
1.306	108.72	0.86	0.94	177.33	0.35	0.31	170.25	0.77	0.61	212.48	0.45	0.62
1.399	109.25	0.86	0.94	178.53	0.35	0.32	171.86	0.78	0.61	210.27	0.45	0.62
1.5	109.53	0.87	0.94	178.86	0.35	0.32	172.52	0.78	0.61	207.85	0.44	0.61

Table F6. Circular velocity curves of the 238 (E1–Sdm) CALIFA galaxies with 75th and 25th percentile uncertainties.

R/R_e	MCG-02-51-004			NGC0001			NGC0023			NGC0155		
	V_c	ΔV_c^{75th}	ΔV_c^{25th}	V_c	ΔV_c^{75th}	ΔV_c^{25th}	V_c	ΔV_c^{75th}	ΔV_c^{25th}	V_c	ΔV_c^{75th}	ΔV_c^{25th}
0.05	78.16	0.11	0.12	88.85	0.28	0.20	112.32	1.06	0.55	134.64	0.27	0.23
0.054	83.28	0.12	0.13	94.69	0.30	0.21	119.82	1.13	0.59	143.13	0.29	0.25
0.057	88.66	0.12	0.14	100.84	0.32	0.22	127.75	1.21	0.63	151.99	0.30	0.26
0.062	94.30	0.13	0.14	107.29	0.34	0.24	136.09	1.28	0.67	161.18	0.32	0.28
0.066	100.19	0.14	0.15	114.04	0.36	0.25	144.85	1.37	0.71	170.68	0.34	0.29
0.071	106.32	0.15	0.16	121.08	0.38	0.27	154.03	1.45	0.76	180.45	0.36	0.31
0.076	112.66	0.16	0.17	128.38	0.40	0.28	163.60	1.54	0.80	190.43	0.38	0.33
0.081	119.19	0.17	0.18	135.92	0.43	0.30	173.54	1.64	0.85	200.55	0.40	0.34
0.087	125.87	0.18	0.19	143.66	0.45	0.32	183.81	1.73	0.90	210.74	0.42	0.36
0.093	132.65	0.19	0.20	151.55	0.47	0.34	194.36	1.83	0.95	220.89	0.44	0.38
0.1	139.47	0.20	0.21	159.53	0.50	0.35	205.12	1.94	1.01	230.92	0.46	0.40
0.107	146.26	0.21	0.22	167.53	0.53	0.37	216.01	2.04	1.06	240.69	0.48	0.41
0.115	152.93	0.22	0.23	175.46	0.55	0.39	226.93	2.14	1.11	250.11	0.50	0.43
0.123	159.37	0.22	0.24	183.22	0.57	0.41	237.76	2.24	1.17	259.04	0.52	0.44
0.132	165.49	0.23	0.25	190.71	0.60	0.42	248.34	2.34	1.22	267.39	0.54	0.46
0.142	171.16	0.24	0.26	197.81	0.62	0.44	258.51	2.44	1.27	275.07	0.55	0.47
0.152	176.26	0.25	0.27	204.40	0.64	0.45	268.08	2.53	1.32	282.01	0.57	0.48
0.163	180.66	0.25	0.28	210.38	0.66	0.47	276.87	2.61	1.36	288.19	0.58	0.49
0.174	184.26	0.26	0.28	215.63	0.68	0.48	284.67	2.69	1.40	293.61	0.59	0.50
0.187	186.96	0.26	0.29	220.10	0.69	0.49	291.28	2.75	1.43	298.32	0.60	0.51
0.2	188.70	0.27	0.29	223.75	0.70	0.50	296.53	2.80	1.46	302.39	0.61	0.52
0.215	189.47	0.27	0.29	226.58	0.71	0.50	300.27	2.83	1.47	305.90	0.61	0.53
0.23	189.31	0.27	0.29	228.67	0.72	0.51	302.41	2.86	1.48	308.92	0.62	0.53
0.247	188.32	0.27	0.29	230.13	0.72	0.51	302.94	2.86	1.49	311.50	0.62	0.53
0.265	186.65	0.26	0.29	231.11	0.72	0.51	301.90	2.85	1.48	313.65	0.63	0.54
0.284	184.52	0.26	0.28	231.80	0.73	0.51	299.43	2.83	1.47	315.37	0.63	0.54
0.304	182.17	0.26	0.28	232.36	0.73	0.52	295.73	2.79	1.45	316.62	0.63	0.54
0.326	179.84	0.25	0.28	232.91	0.73	0.52	291.04	2.75	1.43	317.36	0.64	0.54
0.349	177.76	0.25	0.27	233.52	0.73	0.52	285.63	2.70	1.40	317.59	0.64	0.55
0.374	176.10	0.25	0.27	234.17	0.73	0.52	279.72	2.64	1.37	317.33	0.64	0.54
0.401	175.02	0.25	0.27	234.79	0.74	0.52	273.51	2.58	1.34	316.60	0.63	0.54
0.43	174.59	0.25	0.27	235.27	0.74	0.52	267.14	2.52	1.31	315.47	0.63	0.54
0.461	174.89	0.25	0.27	235.49	0.74	0.52	260.74	2.46	1.28	314.00	0.63	0.54
0.494	175.94	0.25	0.27	235.32	0.74	0.52	254.43	2.40	1.25	312.23	0.63	0.54
0.53	177.77	0.25	0.27	234.71	0.74	0.52	248.34	2.34	1.22	310.21	0.62	0.53
0.568	180.38	0.25	0.28	233.61	0.73	0.52	242.62	2.29	1.19	307.96	0.62	0.53
0.608	183.76	0.26	0.28	232.06	0.73	0.52	237.42	2.24	1.17	305.52	0.61	0.52
0.652	187.88	0.26	0.29	230.12	0.72	0.51	232.83	2.20	1.14	302.91	0.61	0.52
0.699	192.71	0.27	0.29	227.91	0.71	0.51	228.93	2.16	1.12	300.19	0.60	0.52
0.749	198.17	0.28	0.30	225.57	0.71	0.50	225.72	2.13	1.11	297.42	0.60	0.51
0.803	204.21	0.29	0.31	223.23	0.70	0.50	223.18	2.11	1.10	294.64	0.59	0.51
0.861	210.71	0.30	0.32	221.03	0.69	0.49	221.23	2.09	1.09	291.90	0.58	0.50
0.923	217.57	0.31	0.33	219.05	0.69	0.49	219.80	2.08	1.08	289.22	0.58	0.50
0.989	224.64	0.32	0.34	217.30	0.68	0.48	218.77	2.07	1.07	286.59	0.57	0.49
1.06	231.76	0.33	0.35	215.77	0.68	0.48	218.01	2.06	1.07	283.94	0.57	0.49
1.136	238.75	0.34	0.37	214.39	0.67	0.48	217.38	2.05	1.07	281.20	0.56	0.48
1.218	245.39	0.35	0.38	213.04	0.67	0.47	216.73	2.05	1.06	278.29	0.56	0.48
1.306	251.46	0.35	0.38	211.64	0.66	0.47	215.90	2.04	1.06	275.10	0.55	0.47
1.399	256.72	0.36	0.39	210.10	0.66	0.47	214.73	2.03	1.05	271.59	0.54	0.47
1.5	260.92	0.37	0.40	208.36	0.65	0.46	213.08	2.01	1.05	267.74	0.54	0.46

Table F7. Circular velocity curves of the 238 (E1–Sdm) CALIFA galaxies with 75th and 25th percentile uncertainties.

R/R_e	NGC0160			NGC0171			NGC0177			NGC0192		
	V_c	ΔV_c^{75th}	ΔV_c^{25th}									
0.05	186.33	0.54	0.26	102.28	1.03	0.35	57.93	0.12	0.14	145.93	0.21	0.17
0.054	196.53	0.57	0.27	107.17	1.08	0.37	61.90	0.13	0.15	154.17	0.22	0.18
0.057	206.87	0.60	0.28	111.96	1.13	0.38	66.12	0.14	0.16	162.54	0.24	0.19
0.062	217.26	0.63	0.30	116.59	1.18	0.40	70.61	0.15	0.17	171.00	0.25	0.20
0.066	227.62	0.66	0.31	120.97	1.22	0.41	75.38	0.16	0.18	179.44	0.26	0.21
0.071	237.84	0.69	0.33	125.04	1.26	0.43	80.43	0.17	0.19	187.78	0.27	0.22
0.076	247.83	0.72	0.34	128.72	1.30	0.44	85.77	0.18	0.21	195.90	0.28	0.23
0.081	257.47	0.74	0.35	131.95	1.33	0.45	91.40	0.19	0.22	203.68	0.30	0.24
0.087	266.65	0.77	0.37	134.66	1.36	0.46	97.33	0.20	0.23	211.00	0.31	0.25
0.093	275.28	0.80	0.38	136.85	1.38	0.47	103.55	0.21	0.25	217.72	0.32	0.26
0.1	283.29	0.82	0.39	138.51	1.40	0.47	110.05	0.23	0.26	223.72	0.33	0.26
0.107	290.60	0.84	0.40	139.70	1.41	0.48	116.83	0.24	0.28	228.88	0.33	0.27
0.115	297.20	0.86	0.41	140.52	1.42	0.48	123.86	0.26	0.30	233.11	0.34	0.27
0.123	303.08	0.88	0.42	141.10	1.43	0.48	131.11	0.27	0.31	236.37	0.34	0.28
0.132	308.24	0.89	0.42	141.60	1.43	0.48	138.56	0.29	0.33	238.66	0.35	0.28
0.142	312.72	0.90	0.43	142.19	1.44	0.49	146.14	0.30	0.35	240.01	0.35	0.28
0.152	316.57	0.92	0.43	143.01	1.45	0.49	153.81	0.32	0.37	240.52	0.35	0.28
0.163	319.83	0.93	0.44	144.14	1.46	0.49	161.48	0.33	0.39	240.32	0.35	0.28
0.174	322.51	0.93	0.44	145.60	1.47	0.50	169.09	0.35	0.41	239.53	0.35	0.28
0.187	324.66	0.94	0.44	147.32	1.49	0.50	176.54	0.36	0.42	238.28	0.35	0.28
0.2	326.28	0.94	0.45	149.17	1.51	0.51	183.72	0.38	0.44	236.65	0.34	0.28
0.215	327.36	0.95	0.45	151.00	1.53	0.52	190.54	0.39	0.46	234.66	0.34	0.28
0.23	327.90	0.95	0.45	152.63	1.54	0.52	196.86	0.41	0.47	232.33	0.34	0.27
0.247	327.90	0.95	0.45	153.89	1.56	0.53	202.61	0.42	0.49	229.61	0.33	0.27
0.265	327.38	0.95	0.45	154.62	1.56	0.53	207.68	0.43	0.50	226.50	0.33	0.27
0.284	326.38	0.94	0.45	154.70	1.56	0.53	212.01	0.44	0.51	223.05	0.32	0.26
0.304	324.99	0.94	0.45	154.05	1.56	0.53	215.56	0.45	0.52	219.34	0.32	0.26
0.326	323.34	0.94	0.44	152.62	1.54	0.52	218.35	0.45	0.52	215.51	0.31	0.25
0.349	321.56	0.93	0.44	150.43	1.52	0.51	220.41	0.46	0.53	211.72	0.31	0.25
0.374	319.80	0.93	0.44	147.58	1.49	0.51	221.85	0.46	0.53	208.14	0.30	0.25
0.401	318.14	0.92	0.44	144.22	1.46	0.49	222.76	0.46	0.53	204.89	0.30	0.24
0.43	316.58	0.92	0.43	140.56	1.42	0.48	223.28	0.46	0.54	202.09	0.29	0.24
0.461	315.07	0.91	0.43	136.88	1.38	0.47	223.50	0.46	0.54	199.79	0.29	0.24
0.494	313.45	0.91	0.43	133.42	1.35	0.46	223.49	0.46	0.54	198.05	0.29	0.23
0.53	311.54	0.90	0.43	130.42	1.32	0.45	223.24	0.46	0.54	196.89	0.29	0.23
0.568	309.15	0.89	0.42	128.05	1.29	0.44	222.71	0.46	0.53	196.34	0.29	0.23
0.608	306.15	0.89	0.42	126.38	1.28	0.43	221.79	0.46	0.53	196.39	0.29	0.23
0.652	302.45	0.88	0.41	125.42	1.27	0.43	220.37	0.46	0.53	197.05	0.29	0.23
0.699	298.05	0.86	0.41	125.13	1.26	0.43	218.34	0.45	0.52	198.26	0.29	0.23
0.749	293.07	0.85	0.40	125.41	1.27	0.43	215.60	0.45	0.52	199.95	0.29	0.24
0.803	287.67	0.83	0.39	126.19	1.28	0.43	212.15	0.44	0.51	202.02	0.29	0.24
0.861	282.12	0.82	0.39	127.37	1.29	0.44	208.01	0.43	0.50	204.34	0.30	0.24
0.923	276.70	0.80	0.38	128.86	1.30	0.44	203.29	0.42	0.49	206.76	0.30	0.24
0.989	271.68	0.79	0.37	130.57	1.32	0.45	198.17	0.41	0.47	209.12	0.30	0.25
1.06	267.29	0.77	0.37	132.39	1.34	0.45	192.85	0.40	0.46	211.24	0.31	0.25
1.136	263.69	0.76	0.36	134.20	1.36	0.46	187.57	0.39	0.45	212.95	0.31	0.25
1.218	260.93	0.75	0.36	135.90	1.37	0.47	182.55	0.38	0.44	214.07	0.31	0.25
1.306	259.01	0.75	0.35	137.35	1.39	0.47	177.94	0.37	0.43	214.48	0.31	0.25
1.399	257.87	0.75	0.35	138.45	1.40	0.47	173.87	0.36	0.42	214.04	0.31	0.25
1.5	257.42	0.74	0.35	139.08	1.41	0.48	170.39	0.35	0.41	212.70	0.31	0.25

Table F8. Circular velocity curves of the 238 (E1–Sdm) CALIFA galaxies with 75th and 25th percentile uncertainties.

R/R_e	NGC0214			NGC0216			NGC0217			NGC0237		
	V_c	ΔV_c^{75th}	ΔV_c^{25th}									
0.05	97.44	0.28	0.25	18.76	0.10	0.10	103.70	0.15	0.13	40.95	0.12	0.11
0.054	101.92	0.30	0.26	19.81	0.10	0.11	110.26	0.16	0.14	43.50	0.13	0.12
0.057	106.34	0.31	0.27	20.95	0.11	0.11	117.11	0.17	0.15	46.16	0.14	0.12
0.062	110.68	0.32	0.29	22.18	0.12	0.12	124.23	0.18	0.16	48.94	0.15	0.13
0.066	114.92	0.34	0.30	23.49	0.13	0.13	131.60	0.19	0.17	51.82	0.16	0.14
0.071	119.04	0.35	0.31	24.89	0.14	0.14	139.19	0.20	0.18	54.80	0.17	0.15
0.076	123.04	0.36	0.32	26.36	0.15	0.15	146.95	0.21	0.19	57.86	0.18	0.16
0.081	126.93	0.37	0.33	27.92	0.16	0.16	154.84	0.23	0.20	60.99	0.18	0.17
0.087	130.73	0.38	0.34	29.56	0.17	0.17	162.80	0.24	0.21	64.17	0.19	0.17
0.093	134.48	0.39	0.35	31.26	0.18	0.18	170.75	0.25	0.22	67.39	0.20	0.18
0.1	138.22	0.40	0.36	33.03	0.19	0.19	178.63	0.26	0.23	70.63	0.21	0.19
0.107	141.96	0.42	0.37	34.85	0.20	0.20	186.34	0.27	0.24	73.87	0.22	0.20
0.115	145.73	0.43	0.38	36.73	0.21	0.21	193.79	0.28	0.25	77.09	0.23	0.21
0.123	149.53	0.44	0.39	38.63	0.22	0.22	200.91	0.29	0.26	80.28	0.24	0.22
0.132	153.32	0.45	0.40	40.56	0.23	0.24	207.62	0.30	0.27	83.43	0.25	0.23
0.142	157.04	0.46	0.41	42.49	0.25	0.25	213.84	0.31	0.27	86.55	0.26	0.24
0.152	160.62	0.47	0.42	44.42	0.26	0.26	219.55	0.32	0.28	89.62	0.27	0.24
0.163	163.97	0.48	0.42	46.34	0.27	0.27	224.72	0.33	0.29	92.66	0.28	0.25
0.174	167.02	0.49	0.43	48.22	0.28	0.28	229.38	0.33	0.29	95.68	0.29	0.26
0.187	169.69	0.50	0.44	50.07	0.29	0.29	233.57	0.34	0.30	98.69	0.30	0.27
0.2	171.94	0.50	0.44	51.87	0.30	0.30	237.38	0.35	0.30	101.68	0.31	0.28
0.215	173.76	0.51	0.45	53.65	0.31	0.31	240.89	0.35	0.31	104.65	0.32	0.28
0.23	175.18	0.51	0.45	55.41	0.32	0.33	244.16	0.36	0.31	107.60	0.33	0.29
0.247	176.26	0.52	0.46	57.17	0.33	0.34	247.23	0.36	0.32	110.50	0.34	0.30
0.265	177.13	0.52	0.46	58.97	0.34	0.35	250.10	0.36	0.32	113.32	0.34	0.31
0.284	177.94	0.52	0.46	60.82	0.35	0.36	252.72	0.37	0.32	116.06	0.35	0.32
0.304	178.85	0.52	0.46	62.76	0.37	0.37	255.00	0.37	0.33	118.71	0.36	0.32
0.326	180.05	0.53	0.47	64.81	0.38	0.38	256.80	0.37	0.33	121.26	0.37	0.33
0.349	181.67	0.53	0.47	66.97	0.39	0.39	258.03	0.38	0.33	123.76	0.38	0.34
0.374	183.80	0.54	0.48	69.24	0.40	0.41	258.61	0.38	0.33	126.25	0.38	0.34
0.401	186.48	0.55	0.48	71.59	0.42	0.42	258.51	0.38	0.33	128.79	0.39	0.35
0.43	189.66	0.55	0.49	73.98	0.43	0.44	257.76	0.38	0.33	131.47	0.40	0.36
0.461	193.24	0.57	0.50	76.37	0.45	0.45	256.47	0.37	0.33	134.35	0.41	0.37
0.494	197.08	0.58	0.51	78.73	0.46	0.46	254.81	0.37	0.33	137.49	0.42	0.37
0.53	201.02	0.59	0.52	81.01	0.47	0.48	252.98	0.37	0.32	140.92	0.43	0.38
0.568	204.90	0.60	0.53	83.19	0.48	0.49	251.19	0.37	0.32	144.65	0.44	0.39
0.608	208.55	0.61	0.54	85.25	0.50	0.50	249.62	0.36	0.32	148.62	0.45	0.40
0.652	211.82	0.62	0.55	87.17	0.51	0.51	248.41	0.36	0.32	152.79	0.46	0.42
0.699	214.57	0.63	0.55	88.96	0.52	0.52	247.63	0.36	0.32	157.06	0.48	0.43
0.749	216.69	0.63	0.56	90.61	0.53	0.53	247.28	0.36	0.32	161.32	0.49	0.44
0.803	218.10	0.64	0.56	92.14	0.54	0.54	247.31	0.36	0.32	165.45	0.50	0.45
0.861	218.77	0.64	0.57	93.54	0.55	0.55	247.64	0.36	0.32	169.29	0.51	0.46
0.923	218.75	0.64	0.57	94.80	0.55	0.56	248.21	0.36	0.32	172.73	0.52	0.47
0.989	218.11	0.64	0.56	95.88	0.56	0.56	248.94	0.36	0.32	175.60	0.53	0.48
1.06	217.00	0.63	0.56	96.76	0.56	0.57	249.78	0.36	0.32	177.78	0.54	0.48
1.136	215.59	0.63	0.56	97.37	0.57	0.57	250.67	0.37	0.32	179.14	0.54	0.49
1.218	214.07	0.63	0.55	97.67	0.57	0.57	251.59	0.37	0.32	179.59	0.55	0.49
1.306	212.62	0.62	0.55	97.61	0.57	0.57	252.51	0.37	0.32	179.10	0.54	0.49
1.399	211.33	0.62	0.55	97.19	0.57	0.57	253.40	0.37	0.32	177.65	0.54	0.48
1.5	210.28	0.61	0.54	96.39	0.56	0.57	254.20	0.37	0.32	175.31	0.53	0.48

Table F9. Circular velocity curves of the 238 (E1–Sdm) CALIFA galaxies with 75th and 25th percentile uncertainties.

R/R_e	NGC0257			NGC0429			NGC0444			NGC0499		
	V_c	ΔV_c^{75th}	ΔV_c^{25th}									
0.05	99.80	0.18	0.15	44.18	0.16	0.10	42.88	0.22	0.17	259.73	1.94	0.56
0.054	105.89	0.19	0.16	47.23	0.17	0.11	45.03	0.23	0.18	273.82	2.05	0.59
0.057	112.20	0.20	0.17	50.49	0.18	0.11	47.17	0.24	0.19	288.06	2.15	0.62
0.062	118.69	0.21	0.18	54.00	0.19	0.12	49.29	0.25	0.20	302.31	2.26	0.65
0.066	125.33	0.22	0.19	57.75	0.21	0.13	51.35	0.26	0.21	316.46	2.37	0.68
0.071	132.08	0.24	0.20	61.75	0.22	0.14	53.35	0.27	0.22	330.34	2.47	0.71
0.076	138.86	0.25	0.21	66.03	0.24	0.15	55.25	0.28	0.23	343.79	2.57	0.74
0.081	145.62	0.26	0.22	70.60	0.25	0.16	57.05	0.29	0.23	356.66	2.67	0.76
0.087	152.28	0.27	0.23	75.47	0.27	0.17	58.73	0.30	0.24	368.78	2.76	0.79
0.093	158.74	0.28	0.24	80.66	0.29	0.18	60.30	0.31	0.25	380.04	2.84	0.81
0.1	164.90	0.29	0.24	86.17	0.31	0.20	61.76	0.31	0.25	390.33	2.92	0.84
0.107	170.66	0.30	0.25	92.03	0.33	0.21	63.15	0.32	0.26	399.61	2.99	0.86
0.115	175.92	0.31	0.26	98.24	0.35	0.22	64.49	0.33	0.26	407.88	3.05	0.87
0.123	180.58	0.32	0.27	104.80	0.38	0.24	65.85	0.34	0.27	415.22	3.11	0.89
0.132	184.56	0.33	0.27	111.74	0.40	0.25	67.26	0.34	0.28	421.74	3.15	0.90
0.142	187.82	0.34	0.28	119.05	0.43	0.27	68.78	0.35	0.28	427.58	3.20	0.92
0.152	190.33	0.34	0.28	126.74	0.46	0.29	70.43	0.36	0.29	432.91	3.24	0.93
0.163	192.14	0.34	0.28	134.78	0.49	0.31	72.23	0.37	0.30	437.85	3.27	0.94
0.174	193.34	0.34	0.29	143.19	0.52	0.33	74.15	0.38	0.30	442.47	3.31	0.95
0.187	194.05	0.35	0.29	151.92	0.55	0.35	76.18	0.39	0.31	446.79	3.34	0.96
0.2	194.47	0.35	0.29	160.96	0.58	0.37	78.25	0.40	0.32	450.77	3.37	0.97
0.215	194.77	0.35	0.29	170.25	0.62	0.39	80.31	0.41	0.33	454.35	3.40	0.97
0.23	195.13	0.35	0.29	179.75	0.65	0.41	82.31	0.42	0.34	457.44	3.42	0.98
0.247	195.66	0.35	0.29	189.40	0.68	0.43	84.17	0.43	0.35	460.01	3.44	0.99
0.265	196.42	0.35	0.29	199.09	0.72	0.45	85.85	0.44	0.35	462.00	3.46	0.99
0.284	197.37	0.35	0.29	208.73	0.75	0.47	87.30	0.45	0.36	463.41	3.47	0.99
0.304	198.42	0.35	0.29	218.21	0.79	0.50	88.51	0.45	0.36	464.20	3.47	0.99
0.326	199.45	0.36	0.30	227.38	0.82	0.52	89.47	0.46	0.37	464.34	3.47	0.99
0.349	200.31	0.36	0.30	236.10	0.85	0.54	90.20	0.46	0.37	463.79	3.47	0.99
0.374	200.87	0.36	0.30	244.21	0.88	0.55	90.76	0.46	0.37	462.51	3.46	0.99
0.401	201.05	0.36	0.30	251.54	0.91	0.57	91.21	0.47	0.37	460.48	3.44	0.99
0.43	200.82	0.36	0.30	257.93	0.93	0.59	91.67	0.47	0.38	457.73	3.42	0.98
0.461	200.21	0.36	0.30	263.23	0.95	0.60	92.22	0.47	0.38	454.35	3.40	0.97
0.494	199.31	0.36	0.30	267.33	0.97	0.61	92.96	0.47	0.38	450.47	3.37	0.96
0.53	198.28	0.35	0.29	270.15	0.98	0.61	93.98	0.48	0.39	446.26	3.34	0.96
0.568	197.31	0.35	0.29	271.64	0.98	0.62	95.32	0.49	0.39	441.89	3.30	0.95
0.608	196.64	0.35	0.29	271.85	0.98	0.62	96.98	0.49	0.40	437.51	3.27	0.94
0.652	196.45	0.35	0.29	270.88	0.98	0.62	98.97	0.50	0.41	433.22	3.24	0.93
0.699	196.91	0.35	0.29	268.87	0.97	0.61	101.24	0.52	0.42	429.07	3.21	0.92
0.749	198.09	0.35	0.29	266.04	0.96	0.60	103.75	0.53	0.43	425.05	3.18	0.91
0.803	200.01	0.36	0.30	262.65	0.95	0.60	106.48	0.54	0.44	421.12	3.15	0.90
0.861	202.61	0.36	0.30	258.95	0.94	0.59	109.38	0.56	0.45	417.19	3.12	0.89
0.923	205.77	0.37	0.31	255.20	0.92	0.58	112.42	0.57	0.46	413.17	3.09	0.89
0.989	209.33	0.37	0.31	251.64	0.91	0.57	115.55	0.59	0.47	408.94	3.06	0.88
1.06	213.13	0.38	0.32	248.45	0.90	0.56	118.74	0.61	0.49	404.42	3.02	0.87
1.136	216.99	0.39	0.32	245.72	0.89	0.56	121.92	0.62	0.50	399.56	2.99	0.86
1.218	220.71	0.39	0.33	243.49	0.88	0.55	125.03	0.64	0.51	394.39	2.95	0.84
1.306	224.09	0.40	0.33	241.70	0.87	0.55	127.96	0.65	0.53	388.95	2.91	0.83
1.399	226.92	0.40	0.34	240.24	0.87	0.55	130.62	0.67	0.54	383.35	2.87	0.82
1.5	229.02	0.41	0.34	238.95	0.86	0.54	132.89	0.68	0.55	377.64	2.82	0.81

Table F10. Circular velocity curves of the 238 (E1–Sdm) CALIFA galaxies with 75th and 25th percentile uncertainties.

R/R_e	NGC0504			NGC0517			NGC0528			NGC0529		
	V_c	ΔV_c^{75th}	ΔV_c^{25th}									
0.05	66.61	0.09	0.09	100.08	0.41	0.22	76.92	0.12	0.10	159.40	0.31	0.20
0.054	71.21	0.10	0.10	106.86	0.44	0.23	82.18	0.13	0.11	169.71	0.33	0.21
0.057	76.12	0.11	0.11	114.05	0.47	0.25	87.77	0.13	0.12	180.53	0.35	0.22
0.062	81.35	0.11	0.11	121.65	0.50	0.27	93.70	0.14	0.13	191.82	0.37	0.24
0.066	86.91	0.12	0.12	129.68	0.53	0.28	99.97	0.15	0.14	203.59	0.39	0.25
0.071	92.83	0.13	0.13	138.13	0.56	0.30	106.61	0.16	0.14	215.78	0.41	0.27
0.076	99.10	0.14	0.14	147.01	0.60	0.32	113.60	0.17	0.15	228.35	0.44	0.28
0.081	105.75	0.15	0.15	156.30	0.64	0.34	120.96	0.19	0.16	241.24	0.46	0.30
0.087	112.79	0.16	0.16	166.00	0.68	0.37	128.68	0.20	0.17	254.37	0.49	0.31
0.093	120.21	0.17	0.17	176.06	0.72	0.39	136.75	0.21	0.19	267.64	0.51	0.33
0.1	128.02	0.18	0.18	186.47	0.76	0.41	145.15	0.22	0.20	280.95	0.54	0.35
0.107	136.23	0.19	0.19	197.16	0.81	0.43	153.86	0.24	0.21	294.16	0.57	0.36
0.115	144.82	0.20	0.20	208.07	0.85	0.46	162.85	0.25	0.22	307.13	0.59	0.38
0.123	153.78	0.22	0.22	219.13	0.90	0.48	172.08	0.26	0.23	319.70	0.61	0.39
0.132	163.09	0.23	0.23	230.23	0.94	0.51	181.49	0.28	0.25	331.72	0.64	0.41
0.142	172.73	0.24	0.24	241.27	0.99	0.53	191.01	0.29	0.26	343.02	0.66	0.42
0.152	182.65	0.26	0.26	252.10	1.03	0.55	200.57	0.31	0.27	353.47	0.68	0.44
0.163	192.82	0.27	0.27	262.59	1.07	0.58	210.07	0.32	0.29	362.95	0.70	0.45
0.174	203.16	0.29	0.29	272.57	1.11	0.60	219.43	0.34	0.30	371.37	0.71	0.46
0.187	213.62	0.30	0.30	281.88	1.15	0.62	228.53	0.35	0.31	378.69	0.73	0.47
0.2	224.11	0.32	0.32	290.36	1.19	0.64	237.27	0.36	0.32	384.91	0.74	0.48
0.215	234.55	0.33	0.33	297.88	1.22	0.66	245.54	0.38	0.33	390.09	0.75	0.48
0.23	244.84	0.35	0.34	304.32	1.24	0.67	253.26	0.39	0.34	394.31	0.76	0.49
0.247	254.88	0.36	0.36	309.62	1.27	0.68	260.36	0.40	0.35	397.70	0.76	0.49
0.265	264.58	0.37	0.37	313.75	1.28	0.69	266.81	0.41	0.36	400.38	0.77	0.49
0.284	273.85	0.39	0.39	316.79	1.30	0.70	272.60	0.42	0.37	402.47	0.77	0.50
0.304	282.58	0.40	0.40	318.85	1.30	0.70	277.76	0.43	0.38	404.06	0.78	0.50
0.326	290.71	0.41	0.41	320.11	1.31	0.70	282.38	0.43	0.38	405.21	0.78	0.50
0.349	298.15	0.42	0.42	320.76	1.31	0.71	286.54	0.44	0.39	405.98	0.78	0.50
0.374	304.84	0.43	0.43	321.01	1.31	0.71	290.34	0.45	0.40	406.39	0.78	0.50
0.401	310.73	0.44	0.44	321.01	1.31	0.71	293.89	0.45	0.40	406.44	0.78	0.50
0.43	315.76	0.45	0.44	320.85	1.31	0.71	297.24	0.46	0.40	406.15	0.78	0.50
0.461	319.89	0.45	0.45	320.54	1.31	0.71	300.42	0.46	0.41	405.55	0.78	0.50
0.494	323.08	0.46	0.46	320.03	1.31	0.70	303.42	0.47	0.41	404.68	0.78	0.50
0.53	325.31	0.46	0.46	319.26	1.31	0.70	306.19	0.47	0.42	403.60	0.78	0.50
0.568	326.61	0.46	0.46	318.16	1.30	0.70	308.66	0.47	0.42	402.41	0.77	0.50
0.608	327.00	0.46	0.46	316.71	1.30	0.70	310.77	0.48	0.42	401.16	0.77	0.50
0.652	326.56	0.46	0.46	314.91	1.29	0.69	312.44	0.48	0.43	399.90	0.77	0.49
0.699	325.37	0.46	0.46	312.82	1.28	0.69	313.62	0.48	0.43	398.61	0.77	0.49
0.749	323.53	0.46	0.46	310.49	1.27	0.68	314.26	0.48	0.43	397.25	0.76	0.49
0.803	321.12	0.45	0.45	307.97	1.26	0.68	314.33	0.48	0.43	395.72	0.76	0.49
0.861	318.19	0.45	0.45	305.28	1.25	0.67	313.84	0.48	0.43	393.94	0.76	0.49
0.923	314.81	0.44	0.44	302.40	1.24	0.67	312.84	0.48	0.43	391.81	0.75	0.48
0.989	310.99	0.44	0.44	299.28	1.22	0.66	311.41	0.48	0.42	389.28	0.75	0.48
1.06	306.78	0.43	0.43	295.86	1.21	0.65	309.67	0.48	0.42	386.35	0.74	0.48
1.136	302.22	0.43	0.43	292.08	1.19	0.64	307.77	0.47	0.42	383.04	0.74	0.47
1.218	297.38	0.42	0.42	287.92	1.18	0.63	305.81	0.47	0.42	379.40	0.73	0.47
1.306	292.30	0.41	0.41	283.39	1.16	0.62	303.86	0.47	0.41	375.50	0.72	0.46
1.399	287.06	0.41	0.40	278.55	1.14	0.61	301.89	0.46	0.41	371.38	0.71	0.46
1.5	281.74	0.40	0.40	273.47	1.12	0.60	299.79	0.46	0.41	367.09	0.71	0.45

Table F11. Circular velocity curves of the 238 (E1–Sdm) CALIFA galaxies with 75th and 25th percentile uncertainties.

R/R_e	NGC0551			NGC0681			NGC0741			NGC0755		
	V_c	ΔV_c^{75th}	ΔV_c^{25th}									
0.05	61.41	0.21	0.14	133.42	0.50	0.41	422.04	0.56	0.49	15.33	0.06	0.06
0.054	65.22	0.22	0.15	138.13	0.51	0.42	435.61	0.58	0.51	16.22	0.07	0.06
0.057	69.19	0.23	0.15	142.44	0.53	0.44	448.41	0.60	0.52	17.20	0.07	0.07
0.062	73.30	0.25	0.16	146.29	0.54	0.45	460.42	0.61	0.54	18.26	0.08	0.07
0.066	77.53	0.26	0.17	149.62	0.56	0.46	471.64	0.63	0.55	19.40	0.08	0.08
0.071	81.85	0.28	0.18	152.37	0.57	0.47	482.06	0.64	0.56	20.63	0.09	0.08
0.076	86.24	0.29	0.19	154.54	0.58	0.48	491.68	0.66	0.57	21.96	0.09	0.09
0.081	90.66	0.31	0.20	156.16	0.58	0.48	500.47	0.67	0.58	23.37	0.10	0.10
0.087	95.06	0.32	0.21	157.30	0.59	0.48	508.38	0.68	0.59	24.88	0.11	0.10
0.093	99.40	0.34	0.22	158.08	0.59	0.49	515.34	0.69	0.60	26.49	0.12	0.11
0.1	103.60	0.35	0.23	158.65	0.59	0.49	521.25	0.70	0.61	28.20	0.12	0.12
0.107	107.60	0.36	0.24	159.16	0.59	0.49	526.07	0.70	0.61	30.00	0.13	0.13
0.115	111.35	0.38	0.25	159.78	0.59	0.49	529.81	0.71	0.62	31.91	0.14	0.13
0.123	114.77	0.39	0.26	160.63	0.60	0.49	532.60	0.71	0.62	33.91	0.15	0.14
0.132	117.80	0.40	0.26	161.80	0.60	0.50	534.64	0.71	0.62	36.00	0.16	0.15
0.142	120.38	0.41	0.27	163.31	0.61	0.50	536.23	0.72	0.63	38.19	0.17	0.16
0.152	122.50	0.42	0.27	165.13	0.61	0.51	537.69	0.72	0.63	40.47	0.18	0.17
0.163	124.14	0.42	0.28	167.18	0.62	0.51	539.29	0.72	0.63	42.83	0.19	0.18
0.174	125.33	0.43	0.28	169.37	0.63	0.52	541.22	0.72	0.63	45.26	0.20	0.19
0.187	126.13	0.43	0.28	171.58	0.64	0.53	543.51	0.73	0.64	47.75	0.21	0.20
0.2	126.64	0.43	0.28	173.68	0.65	0.53	546.06	0.73	0.64	50.29	0.23	0.21
0.215	126.99	0.43	0.28	175.58	0.65	0.54	548.66	0.73	0.64	52.87	0.24	0.22
0.23	127.31	0.43	0.28	177.16	0.66	0.55	551.03	0.74	0.64	55.47	0.25	0.24
0.247	127.74	0.43	0.29	178.37	0.66	0.55	552.91	0.74	0.65	58.09	0.26	0.25
0.265	128.38	0.44	0.29	179.16	0.67	0.55	554.09	0.74	0.65	60.70	0.27	0.26
0.284	129.31	0.44	0.29	179.54	0.67	0.55	554.44	0.74	0.65	63.31	0.28	0.27
0.304	130.56	0.44	0.29	179.58	0.67	0.55	553.93	0.74	0.65	65.92	0.30	0.28
0.326	132.10	0.45	0.30	179.37	0.67	0.55	552.61	0.74	0.65	68.52	0.31	0.29
0.349	133.92	0.45	0.30	179.06	0.67	0.55	550.60	0.73	0.64	71.14	0.32	0.30
0.374	135.95	0.46	0.30	178.83	0.67	0.55	548.05	0.73	0.64	73.80	0.33	0.31
0.401	138.17	0.47	0.31	178.84	0.67	0.55	545.10	0.73	0.64	76.53	0.34	0.33
0.43	140.52	0.48	0.31	179.22	0.67	0.55	541.86	0.72	0.63	79.35	0.36	0.34
0.461	143.01	0.49	0.32	180.08	0.67	0.55	538.41	0.72	0.63	82.32	0.37	0.35
0.494	145.61	0.49	0.33	181.43	0.68	0.56	534.82	0.71	0.62	85.44	0.38	0.36
0.53	148.35	0.50	0.33	183.25	0.68	0.56	531.15	0.71	0.62	88.74	0.40	0.38
0.568	151.25	0.51	0.34	185.46	0.69	0.57	527.44	0.70	0.62	92.21	0.41	0.39
0.608	154.32	0.52	0.34	187.95	0.70	0.58	523.78	0.70	0.61	95.84	0.43	0.41
0.652	157.61	0.53	0.35	190.60	0.71	0.59	520.20	0.69	0.61	99.59	0.45	0.42
0.699	161.11	0.55	0.36	193.27	0.72	0.60	516.71	0.69	0.60	103.43	0.47	0.44
0.749	164.83	0.56	0.37	195.85	0.73	0.60	513.24	0.68	0.60	107.29	0.48	0.46
0.803	168.78	0.57	0.38	198.20	0.74	0.61	509.67	0.68	0.60	111.10	0.50	0.47
0.861	172.92	0.59	0.39	200.23	0.75	0.62	505.84	0.68	0.59	114.80	0.52	0.49
0.923	177.22	0.60	0.40	201.84	0.75	0.62	501.58	0.67	0.59	118.31	0.53	0.50
0.989	181.63	0.62	0.41	202.98	0.76	0.63	496.78	0.66	0.58	121.52	0.55	0.52
1.06	186.05	0.63	0.42	203.62	0.76	0.63	491.39	0.66	0.57	124.35	0.56	0.53
1.136	190.39	0.65	0.43	203.77	0.76	0.63	485.46	0.65	0.57	126.70	0.57	0.54
1.218	194.50	0.66	0.43	203.46	0.76	0.63	479.10	0.64	0.56	128.47	0.58	0.55
1.306	198.24	0.67	0.44	202.72	0.75	0.62	472.43	0.63	0.55	129.61	0.58	0.55
1.399	201.43	0.68	0.45	201.61	0.75	0.62	465.60	0.62	0.54	130.06	0.58	0.55
1.5	203.90	0.69	0.46	200.15	0.75	0.62	458.70	0.61	0.54	129.81	0.58	0.55

Table F12. Circular velocity curves of the 238 (E1–Sdm) CALIFA galaxies with 75th and 25th percentile uncertainties.

R/R_e	NGC0768			NGC0774			NGC0776			NGC0781		
	V_c	ΔV_c^{75th}	ΔV_c^{25th}									
0.05	46.98	0.14	0.12	53.38	0.15	0.07	106.02	0.55	0.40	44.69	0.09	0.08
0.054	50.24	0.15	0.13	57.08	0.16	0.08	112.02	0.58	0.43	47.66	0.10	0.09
0.057	53.72	0.16	0.13	61.04	0.17	0.08	118.13	0.61	0.45	50.82	0.10	0.09
0.062	57.43	0.17	0.14	65.25	0.18	0.09	124.30	0.64	0.47	54.18	0.11	0.10
0.066	61.37	0.18	0.15	69.74	0.20	0.10	130.45	0.67	0.50	57.74	0.12	0.11
0.071	65.56	0.19	0.16	74.52	0.21	0.10	136.53	0.70	0.52	61.50	0.12	0.11
0.076	70.01	0.20	0.18	79.60	0.22	0.11	142.43	0.73	0.54	65.48	0.13	0.12
0.081	74.72	0.22	0.19	84.99	0.24	0.12	148.07	0.76	0.56	69.66	0.14	0.13
0.087	79.71	0.23	0.20	90.69	0.26	0.12	153.34	0.79	0.58	74.04	0.15	0.14
0.093	84.97	0.25	0.21	96.73	0.27	0.13	158.12	0.82	0.60	78.63	0.16	0.15
0.1	90.51	0.26	0.23	103.09	0.29	0.14	162.30	0.84	0.62	83.40	0.17	0.16
0.107	96.33	0.28	0.24	109.79	0.31	0.15	165.78	0.86	0.63	88.34	0.18	0.17
0.115	102.41	0.30	0.26	116.82	0.33	0.16	168.47	0.87	0.64	93.44	0.19	0.17
0.123	108.76	0.32	0.27	124.17	0.35	0.17	170.30	0.88	0.65	98.67	0.20	0.18
0.132	115.35	0.33	0.29	131.83	0.37	0.18	171.25	0.88	0.65	104.00	0.21	0.19
0.142	122.17	0.35	0.31	139.78	0.40	0.19	171.32	0.88	0.65	109.39	0.22	0.21
0.152	129.16	0.37	0.32	147.98	0.42	0.20	170.59	0.88	0.65	114.80	0.23	0.22
0.163	136.31	0.40	0.34	156.40	0.44	0.21	169.18	0.87	0.64	120.19	0.25	0.23
0.174	143.54	0.42	0.36	164.98	0.47	0.23	167.22	0.86	0.64	125.49	0.26	0.24
0.187	150.81	0.44	0.38	173.65	0.49	0.24	164.91	0.85	0.63	130.67	0.27	0.25
0.2	158.03	0.46	0.40	182.35	0.52	0.25	162.42	0.84	0.62	135.65	0.28	0.25
0.215	165.11	0.48	0.42	190.97	0.54	0.26	159.90	0.82	0.61	140.39	0.29	0.26
0.23	171.97	0.50	0.43	199.42	0.56	0.27	157.46	0.81	0.60	144.84	0.30	0.27
0.247	178.50	0.52	0.45	207.58	0.59	0.28	155.19	0.80	0.59	148.97	0.31	0.28
0.265	184.59	0.54	0.46	215.33	0.61	0.29	153.12	0.79	0.58	152.73	0.31	0.29
0.284	190.15	0.55	0.48	222.56	0.63	0.30	151.27	0.78	0.58	156.12	0.32	0.29
0.304	195.09	0.57	0.49	229.15	0.65	0.31	149.67	0.77	0.57	159.12	0.33	0.30
0.326	199.34	0.58	0.50	235.01	0.67	0.32	148.31	0.77	0.56	161.74	0.33	0.30
0.349	202.87	0.59	0.51	240.08	0.68	0.33	147.17	0.76	0.56	164.00	0.34	0.31
0.374	205.70	0.60	0.52	244.35	0.69	0.33	146.22	0.75	0.56	165.92	0.34	0.31
0.401	207.88	0.60	0.52	247.85	0.70	0.34	145.42	0.75	0.55	167.54	0.34	0.31
0.43	209.52	0.61	0.53	250.68	0.71	0.34	144.70	0.75	0.55	168.92	0.35	0.32
0.461	210.79	0.61	0.53	252.97	0.72	0.35	144.01	0.74	0.55	170.10	0.35	0.32
0.494	211.86	0.62	0.53	254.92	0.72	0.35	143.29	0.74	0.55	171.16	0.35	0.32
0.53	212.92	0.62	0.54	256.70	0.73	0.35	142.52	0.74	0.54	172.13	0.35	0.32
0.568	214.15	0.62	0.54	258.51	0.73	0.35	141.67	0.73	0.54	173.04	0.35	0.32
0.608	215.65	0.63	0.54	260.44	0.74	0.36	140.76	0.73	0.54	173.90	0.36	0.33
0.652	217.49	0.63	0.55	262.53	0.74	0.36	139.83	0.72	0.53	174.68	0.36	0.33
0.699	219.67	0.64	0.55	264.72	0.75	0.36	138.94	0.72	0.53	175.32	0.36	0.33
0.749	222.12	0.64	0.56	266.91	0.76	0.36	138.16	0.71	0.53	175.76	0.36	0.33
0.803	224.74	0.65	0.57	268.90	0.76	0.37	137.57	0.71	0.52	175.94	0.36	0.33
0.861	227.43	0.66	0.57	270.53	0.77	0.37	137.25	0.71	0.52	175.84	0.36	0.33
0.923	230.03	0.67	0.58	271.60	0.77	0.37	137.23	0.71	0.52	175.45	0.36	0.33
0.989	232.44	0.67	0.58	271.96	0.77	0.37	137.53	0.71	0.52	174.80	0.36	0.33
1.06	234.53	0.68	0.59	271.50	0.77	0.37	138.15	0.71	0.53	173.96	0.36	0.33
1.136	236.22	0.69	0.59	270.14	0.76	0.37	139.04	0.72	0.53	172.99	0.35	0.32
1.218	237.46	0.69	0.60	267.87	0.76	0.37	140.15	0.72	0.53	171.98	0.35	0.32
1.306	238.23	0.69	0.60	264.74	0.75	0.36	141.39	0.73	0.54	170.98	0.35	0.32
1.399	238.58	0.69	0.60	260.84	0.74	0.36	142.67	0.74	0.54	170.03	0.35	0.32
1.5	238.57	0.69	0.60	256.34	0.73	0.35	143.89	0.74	0.55	169.11	0.35	0.32

Table F13. Circular velocity curves of the 238 (E1–Sdm) CALIFA galaxies with 75th and 25th percentile uncertainties.

R/R_e	NGC0810			NGC0932			NGC1056			NGC1060		
	V_c	ΔV_c^{75th}	ΔV_c^{25th}									
0.05	145.82	0.28	0.35	142.98	0.30	0.21	68.39	0.31	0.20	315.97	1.17	0.64
0.054	155.79	0.30	0.37	151.29	0.32	0.22	71.62	0.33	0.21	332.90	1.24	0.68
0.057	166.36	0.32	0.40	159.81	0.34	0.23	74.82	0.34	0.22	350.03	1.30	0.71
0.062	177.56	0.34	0.42	168.47	0.36	0.24	77.94	0.36	0.23	367.25	1.36	0.75
0.066	189.40	0.37	0.45	177.21	0.38	0.26	80.94	0.37	0.24	384.41	1.43	0.78
0.071	201.88	0.39	0.48	185.96	0.40	0.27	83.81	0.38	0.25	401.39	1.49	0.82
0.076	215.02	0.42	0.51	194.61	0.41	0.28	86.50	0.40	0.25	418.03	1.55	0.85
0.081	228.80	0.44	0.55	203.06	0.43	0.29	89.00	0.41	0.26	434.19	1.61	0.88
0.087	243.21	0.47	0.58	211.21	0.45	0.31	91.32	0.42	0.27	449.73	1.67	0.91
0.093	258.22	0.50	0.62	218.92	0.47	0.32	93.47	0.43	0.27	464.51	1.72	0.94
0.1	273.78	0.53	0.65	226.09	0.48	0.33	95.51	0.44	0.28	478.40	1.78	0.97
0.107	289.85	0.56	0.69	232.61	0.50	0.34	97.51	0.45	0.29	491.27	1.82	1.00
0.115	306.32	0.59	0.73	238.39	0.51	0.34	99.57	0.46	0.29	503.01	1.87	1.02
0.123	323.10	0.63	0.77	243.36	0.52	0.35	101.81	0.47	0.30	513.53	1.91	1.04
0.132	340.06	0.66	0.81	247.49	0.53	0.36	104.34	0.48	0.31	522.74	1.94	1.06
0.142	357.04	0.69	0.85	250.80	0.53	0.36	107.27	0.49	0.32	530.60	1.97	1.08
0.152	373.85	0.72	0.89	253.34	0.54	0.37	110.67	0.51	0.33	537.13	1.99	1.09
0.163	390.28	0.76	0.93	255.19	0.54	0.37	114.56	0.53	0.34	542.39	2.01	1.10
0.174	406.09	0.79	0.97	256.45	0.55	0.37	118.93	0.55	0.35	546.53	2.03	1.11
0.187	421.05	0.82	1.00	257.25	0.55	0.37	123.73	0.57	0.36	549.77	2.04	1.12
0.2	434.89	0.84	1.04	257.69	0.55	0.37	128.89	0.59	0.38	552.36	2.05	1.12
0.215	447.39	0.87	1.07	257.85	0.55	0.37	134.32	0.62	0.40	554.52	2.06	1.13
0.23	458.33	0.89	1.09	257.81	0.55	0.37	139.93	0.64	0.41	556.44	2.07	1.13
0.247	467.58	0.91	1.11	257.61	0.55	0.37	145.62	0.67	0.43	558.17	2.07	1.13
0.265	475.07	0.92	1.13	257.30	0.55	0.37	151.28	0.70	0.45	559.66	2.08	1.14
0.284	480.84	0.93	1.15	256.92	0.55	0.37	156.80	0.72	0.46	560.76	2.08	1.14
0.304	485.06	0.94	1.16	256.50	0.55	0.37	162.06	0.75	0.48	561.29	2.08	1.14
0.326	488.00	0.95	1.16	256.07	0.55	0.37	166.93	0.77	0.49	561.09	2.08	1.14
0.349	490.01	0.95	1.17	255.62	0.54	0.37	171.28	0.79	0.51	560.05	2.08	1.14
0.374	491.45	0.95	1.17	255.12	0.54	0.37	174.98	0.81	0.52	558.17	2.07	1.13
0.401	492.66	0.96	1.17	254.54	0.54	0.37	177.94	0.82	0.53	555.49	2.06	1.13
0.43	493.86	0.96	1.18	253.85	0.54	0.37	180.07	0.83	0.53	552.08	2.05	1.12
0.461	495.11	0.96	1.18	252.99	0.54	0.37	181.30	0.83	0.54	547.98	2.03	1.11
0.494	496.30	0.96	1.18	251.95	0.54	0.36	181.66	0.84	0.54	543.23	2.02	1.10
0.53	497.22	0.96	1.19	250.70	0.53	0.36	181.17	0.83	0.53	537.81	2.00	1.09
0.568	497.59	0.96	1.19	249.22	0.53	0.36	179.97	0.83	0.53	531.74	1.97	1.08
0.608	497.19	0.96	1.19	247.49	0.53	0.36	178.19	0.82	0.53	525.09	1.95	1.07
0.652	495.88	0.96	1.18	245.48	0.52	0.36	176.05	0.81	0.52	518.03	1.92	1.05
0.699	493.63	0.96	1.18	243.17	0.52	0.35	173.72	0.80	0.51	510.80	1.90	1.04
0.749	490.51	0.95	1.17	240.57	0.51	0.35	171.37	0.79	0.51	503.72	1.87	1.02
0.803	486.68	0.94	1.16	237.70	0.51	0.34	169.11	0.78	0.50	497.05	1.85	1.01
0.861	482.30	0.94	1.15	234.65	0.50	0.34	166.98	0.77	0.49	491.00	1.82	1.00
0.923	477.54	0.93	1.14	231.53	0.49	0.34	164.95	0.76	0.49	485.58	1.80	0.99
0.989	472.54	0.92	1.13	228.47	0.49	0.33	162.98	0.75	0.48	480.69	1.78	0.98
1.06	467.40	0.91	1.11	225.64	0.48	0.33	161.00	0.74	0.48	476.07	1.77	0.97
1.136	462.17	0.90	1.10	223.16	0.48	0.32	158.97	0.73	0.47	471.42	1.75	0.96
1.218	456.94	0.89	1.09	221.13	0.47	0.32	156.87	0.72	0.46	466.47	1.73	0.95
1.306	451.73	0.88	1.08	219.60	0.47	0.32	154.71	0.71	0.46	461.00	1.71	0.94
1.399	446.60	0.87	1.06	218.56	0.47	0.32	152.49	0.70	0.45	454.90	1.69	0.92
1.5	441.54	0.86	1.05	217.95	0.46	0.32	150.22	0.69	0.44	448.17	1.66	0.91

Table F14. Circular velocity curves of the 238 (E1–Sdm) CALIFA galaxies with 75th and 25th percentile uncertainties.

R/R_e	NGC1167			NGC1349			NGC1542			NGC1645		
	V_c	ΔV_c^{75th}	ΔV_c^{25th}									
0.05	201.54	0.30	0.30	173.32	0.49	0.54	39.34	0.17	0.12	112.47	0.14	0.13
0.054	212.57	0.32	0.31	183.47	0.52	0.58	42.02	0.18	0.13	120.08	0.15	0.14
0.057	223.75	0.34	0.33	193.89	0.55	0.61	44.88	0.19	0.14	128.15	0.16	0.15
0.062	234.99	0.36	0.34	204.51	0.58	0.64	47.93	0.21	0.15	136.68	0.18	0.16
0.066	246.19	0.37	0.36	215.25	0.61	0.68	51.18	0.22	0.16	145.67	0.19	0.17
0.071	257.25	0.39	0.38	226.02	0.64	0.71	54.63	0.24	0.17	155.14	0.20	0.18
0.076	268.05	0.41	0.39	236.72	0.67	0.74	58.29	0.25	0.18	165.07	0.21	0.19
0.081	278.48	0.42	0.41	247.22	0.70	0.78	62.16	0.27	0.19	175.45	0.23	0.20
0.087	288.44	0.44	0.42	257.39	0.73	0.81	66.25	0.29	0.21	186.28	0.24	0.21
0.093	297.83	0.45	0.44	267.09	0.75	0.84	70.56	0.31	0.22	197.50	0.25	0.22
0.1	306.58	0.46	0.45	276.20	0.78	0.87	75.08	0.33	0.23	209.10	0.27	0.24
0.107	314.67	0.48	0.46	284.57	0.80	0.90	79.82	0.35	0.25	221.00	0.28	0.25
0.115	322.08	0.49	0.47	292.13	0.83	0.92	84.76	0.37	0.26	233.14	0.30	0.27
0.123	328.84	0.50	0.48	298.78	0.84	0.94	89.90	0.39	0.28	245.44	0.32	0.28
0.132	335.01	0.51	0.49	304.50	0.86	0.96	95.20	0.41	0.30	257.78	0.33	0.29
0.142	340.65	0.52	0.50	309.32	0.87	0.97	100.66	0.44	0.31	270.04	0.35	0.31
0.152	345.83	0.52	0.51	313.30	0.88	0.99	106.23	0.46	0.33	282.08	0.36	0.32
0.163	350.57	0.53	0.51	316.55	0.89	1.00	111.87	0.49	0.35	293.76	0.38	0.33
0.174	354.89	0.54	0.52	319.21	0.90	1.00	117.54	0.51	0.37	304.90	0.39	0.35
0.187	358.78	0.54	0.53	321.40	0.91	1.01	123.16	0.54	0.38	315.33	0.41	0.36
0.2	362.19	0.55	0.53	323.21	0.91	1.02	128.69	0.56	0.40	324.90	0.42	0.37
0.215	365.10	0.55	0.54	324.70	0.92	1.02	134.03	0.58	0.42	333.43	0.43	0.38
0.23	367.50	0.56	0.54	325.84	0.92	1.02	139.10	0.61	0.43	340.81	0.44	0.39
0.247	369.44	0.56	0.54	326.59	0.92	1.03	143.83	0.63	0.45	346.93	0.45	0.40
0.265	370.97	0.56	0.54	326.85	0.92	1.03	148.12	0.64	0.46	351.72	0.45	0.40
0.284	372.21	0.56	0.55	326.54	0.92	1.03	151.90	0.66	0.47	355.17	0.46	0.40
0.304	373.26	0.56	0.55	325.64	0.92	1.02	155.10	0.67	0.48	357.32	0.46	0.41
0.326	374.19	0.57	0.55	324.16	0.92	1.02	157.70	0.69	0.49	358.25	0.46	0.41
0.349	375.02	0.57	0.55	322.19	0.91	1.01	159.68	0.69	0.50	358.07	0.46	0.41
0.374	375.74	0.57	0.55	319.90	0.90	1.01	161.11	0.70	0.50	356.94	0.46	0.41
0.401	376.26	0.57	0.55	317.47	0.90	1.00	162.05	0.71	0.50	355.03	0.46	0.40
0.43	376.47	0.57	0.55	315.10	0.89	0.99	162.66	0.71	0.51	352.49	0.45	0.40
0.461	376.27	0.57	0.55	312.99	0.88	0.98	163.10	0.71	0.51	349.45	0.45	0.40
0.494	375.58	0.57	0.55	311.28	0.88	0.98	163.58	0.71	0.51	346.03	0.44	0.39
0.53	374.41	0.57	0.55	310.06	0.88	0.98	164.29	0.71	0.51	342.27	0.44	0.39
0.568	372.80	0.56	0.55	309.35	0.87	0.97	165.38	0.72	0.51	338.17	0.43	0.39
0.608	370.91	0.56	0.54	309.14	0.87	0.97	166.95	0.73	0.52	333.75	0.43	0.38
0.652	368.90	0.56	0.54	309.35	0.87	0.97	169.02	0.74	0.53	329.01	0.42	0.37
0.699	366.98	0.55	0.54	309.88	0.88	0.97	171.56	0.75	0.53	324.01	0.42	0.37
0.749	365.29	0.55	0.54	310.61	0.88	0.98	174.46	0.76	0.54	318.84	0.41	0.36
0.803	363.93	0.55	0.53	311.39	0.88	0.98	177.59	0.77	0.55	313.67	0.40	0.36
0.861	362.89	0.55	0.53	312.07	0.88	0.98	180.81	0.79	0.56	308.64	0.40	0.35
0.923	362.07	0.55	0.53	312.52	0.88	0.98	183.94	0.80	0.57	303.88	0.39	0.35
0.989	361.30	0.55	0.53	312.63	0.88	0.98	186.83	0.81	0.58	299.49	0.38	0.34
1.06	360.40	0.55	0.53	312.32	0.88	0.98	189.32	0.82	0.59	295.51	0.38	0.34
1.136	359.20	0.54	0.53	311.56	0.88	0.98	191.26	0.83	0.59	291.91	0.38	0.33
1.218	357.56	0.54	0.52	310.35	0.88	0.98	192.52	0.84	0.60	288.65	0.37	0.33
1.306	355.45	0.54	0.52	308.74	0.87	0.97	193.01	0.84	0.60	285.65	0.37	0.33
1.399	352.87	0.53	0.52	306.78	0.87	0.97	192.67	0.84	0.60	282.82	0.36	0.32
1.5	349.91	0.53	0.51	304.54	0.86	0.96	191.51	0.83	0.60	280.07	0.36	0.32

Table F15. Circular velocity curves of the 238 (E1–Sdm) CALIFA galaxies with 75th and 25th percentile uncertainties.

R/R_e	NGC1677			NGC2253			NGC2347			NGC2410		
	V_c	ΔV_c^{75th}	ΔV_c^{25th}									
0.05	26.61	0.17	0.16	99.15	0.34	0.22	129.81	0.31	0.48	83.12	0.13	0.12
0.054	28.25	0.19	0.17	105.83	0.37	0.24	134.76	0.32	0.50	88.63	0.14	0.13
0.057	29.99	0.20	0.18	112.90	0.39	0.25	139.75	0.33	0.52	94.45	0.15	0.14
0.062	31.84	0.21	0.19	120.36	0.42	0.27	144.79	0.35	0.54	100.57	0.16	0.14
0.066	33.79	0.23	0.20	128.22	0.44	0.29	149.86	0.36	0.55	106.98	0.17	0.15
0.071	35.85	0.24	0.22	136.48	0.47	0.31	154.96	0.37	0.57	113.68	0.18	0.16
0.076	38.00	0.26	0.23	145.13	0.50	0.32	160.05	0.38	0.59	120.66	0.19	0.17
0.081	40.25	0.27	0.25	154.15	0.53	0.34	165.08	0.39	0.61	127.89	0.21	0.18
0.087	42.59	0.29	0.26	163.53	0.57	0.37	169.99	0.41	0.63	135.34	0.22	0.19
0.093	44.99	0.31	0.28	173.23	0.60	0.39	174.72	0.42	0.65	142.97	0.23	0.21
0.1	47.46	0.33	0.29	183.20	0.63	0.41	179.22	0.43	0.66	150.73	0.24	0.22
0.107	49.96	0.34	0.31	193.39	0.67	0.43	183.43	0.44	0.68	158.56	0.26	0.23
0.115	52.49	0.36	0.32	203.71	0.70	0.46	187.35	0.45	0.69	166.37	0.27	0.24
0.123	55.02	0.38	0.34	214.09	0.74	0.48	190.99	0.46	0.71	174.08	0.28	0.25
0.132	57.51	0.40	0.35	224.41	0.78	0.50	194.42	0.46	0.72	181.60	0.29	0.26
0.142	59.95	0.41	0.37	234.55	0.81	0.52	197.73	0.47	0.73	188.79	0.31	0.27
0.152	62.30	0.43	0.38	244.36	0.84	0.55	201.02	0.48	0.74	195.56	0.32	0.28
0.163	64.54	0.44	0.40	253.69	0.88	0.57	204.45	0.49	0.76	201.78	0.33	0.29
0.174	66.63	0.46	0.41	262.37	0.91	0.59	208.14	0.50	0.77	207.33	0.33	0.30
0.187	68.55	0.47	0.42	270.25	0.93	0.60	212.19	0.51	0.79	212.13	0.34	0.30
0.2	70.31	0.48	0.43	277.16	0.96	0.62	216.67	0.52	0.80	216.10	0.35	0.31
0.215	71.89	0.50	0.44	282.97	0.98	0.63	221.60	0.53	0.82	219.23	0.35	0.31
0.23	73.32	0.51	0.45	287.58	0.99	0.64	226.96	0.54	0.84	221.55	0.36	0.32
0.247	74.63	0.52	0.46	290.93	1.01	0.65	232.70	0.56	0.86	223.14	0.36	0.32
0.265	75.88	0.52	0.47	293.03	1.01	0.66	238.73	0.57	0.88	224.15	0.36	0.32
0.284	77.11	0.53	0.48	293.92	1.02	0.66	244.93	0.58	0.91	224.78	0.36	0.32
0.304	78.40	0.54	0.49	293.72	1.02	0.66	251.19	0.60	0.93	225.24	0.36	0.32
0.326	79.80	0.55	0.49	292.57	1.01	0.65	257.35	0.61	0.95	225.75	0.36	0.32
0.349	81.34	0.56	0.50	290.66	1.01	0.65	263.28	0.63	0.98	226.45	0.37	0.33
0.374	83.06	0.57	0.51	288.13	1.00	0.64	268.79	0.64	1.00	227.44	0.37	0.33
0.401	84.94	0.59	0.53	285.13	0.99	0.64	273.70	0.65	1.01	228.72	0.37	0.33
0.43	86.97	0.60	0.54	281.75	0.97	0.63	277.85	0.66	1.03	230.20	0.37	0.33
0.461	89.12	0.62	0.55	278.08	0.96	0.62	281.07	0.67	1.04	231.75	0.37	0.33
0.494	91.36	0.63	0.57	274.16	0.95	0.61	283.24	0.68	1.05	233.19	0.38	0.33
0.53	93.68	0.65	0.58	270.05	0.93	0.60	284.31	0.68	1.05	234.34	0.38	0.34
0.568	96.06	0.66	0.59	265.79	0.92	0.59	284.27	0.68	1.05	235.03	0.38	0.34
0.608	98.50	0.68	0.61	261.42	0.90	0.58	283.24	0.68	1.05	235.13	0.38	0.34
0.652	101.01	0.70	0.63	256.97	0.89	0.57	281.39	0.67	1.04	234.56	0.38	0.34
0.699	103.58	0.72	0.64	252.41	0.87	0.56	279.01	0.67	1.03	233.30	0.38	0.34
0.749	106.21	0.73	0.66	247.73	0.86	0.55	276.41	0.66	1.02	231.39	0.37	0.33
0.803	108.88	0.75	0.67	242.86	0.84	0.54	273.91	0.65	1.01	228.96	0.37	0.33
0.861	111.53	0.77	0.69	237.77	0.82	0.53	271.74	0.65	1.01	226.19	0.37	0.32
0.923	114.12	0.79	0.71	232.41	0.80	0.52	270.04	0.64	1.00	223.29	0.36	0.32
0.989	116.55	0.81	0.72	226.83	0.78	0.51	268.81	0.64	1.00	220.52	0.36	0.32
1.06	118.74	0.82	0.74	221.07	0.76	0.49	267.92	0.64	0.99	218.07	0.35	0.31
1.136	120.59	0.83	0.75	215.25	0.74	0.48	267.15	0.64	0.99	216.11	0.35	0.31
1.218	122.01	0.84	0.76	209.51	0.72	0.47	266.27	0.64	0.99	214.71	0.35	0.31
1.306	122.92	0.85	0.76	203.98	0.71	0.46	265.03	0.63	0.98	213.86	0.35	0.31
1.399	123.28	0.85	0.76	198.76	0.69	0.44	263.25	0.63	0.98	213.51	0.34	0.31
1.5	123.05	0.85	0.76	193.89	0.67	0.43	260.81	0.62	0.97	213.52	0.34	0.31

Table F16. Circular velocity curves of the 238 (E1–Sdm) CALIFA galaxies with 75th and 25th percentile uncertainties.

R/R_e	NGC2449			NGC2476			NGC2481			NGC2486		
	V_c	ΔV_c^{75th}	ΔV_c^{25th}									
0.05	91.43	0.16	0.13	92.68	0.30	0.26	66.05	0.13	0.10	296.98	0.87	0.81
0.054	96.97	0.17	0.13	98.94	0.32	0.28	70.47	0.13	0.11	297.08	0.87	0.81
0.057	102.71	0.18	0.14	105.57	0.34	0.30	75.17	0.14	0.12	295.68	0.86	0.81
0.062	108.62	0.19	0.15	112.58	0.36	0.32	80.16	0.15	0.13	293.00	0.86	0.80
0.066	114.67	0.20	0.16	119.99	0.38	0.34	85.44	0.16	0.13	289.41	0.85	0.79
0.071	120.84	0.21	0.17	127.78	0.41	0.36	91.02	0.18	0.14	285.33	0.83	0.78
0.076	127.07	0.22	0.18	135.96	0.43	0.39	96.90	0.19	0.15	281.24	0.82	0.77
0.081	133.32	0.23	0.19	144.52	0.46	0.41	103.08	0.20	0.16	277.56	0.81	0.76
0.087	139.55	0.24	0.19	153.45	0.49	0.44	109.56	0.21	0.17	274.60	0.80	0.75
0.093	145.68	0.25	0.20	162.72	0.52	0.46	116.31	0.22	0.18	272.51	0.80	0.75
0.1	151.67	0.26	0.21	172.29	0.55	0.49	123.33	0.24	0.20	271.28	0.79	0.74
0.107	157.45	0.27	0.22	182.12	0.58	0.52	130.60	0.25	0.21	270.78	0.79	0.74
0.115	162.98	0.28	0.23	192.16	0.62	0.55	138.07	0.27	0.22	270.81	0.79	0.74
0.123	168.20	0.29	0.23	202.32	0.65	0.58	145.72	0.28	0.23	271.17	0.79	0.74
0.132	173.09	0.30	0.24	212.54	0.68	0.61	153.49	0.30	0.24	271.69	0.79	0.75
0.142	177.62	0.30	0.25	222.69	0.71	0.63	161.33	0.31	0.26	272.25	0.80	0.75
0.152	181.77	0.31	0.25	232.68	0.75	0.66	169.17	0.33	0.27	272.76	0.80	0.75
0.163	185.55	0.32	0.26	242.38	0.78	0.69	176.94	0.34	0.28	273.15	0.80	0.75
0.174	188.96	0.32	0.26	251.65	0.81	0.72	184.56	0.36	0.29	273.38	0.80	0.75
0.187	192.01	0.33	0.27	260.38	0.83	0.74	191.95	0.37	0.30	273.40	0.80	0.75
0.2	194.73	0.33	0.27	268.45	0.86	0.76	199.02	0.39	0.32	273.15	0.80	0.75
0.215	197.12	0.34	0.27	275.74	0.88	0.79	205.71	0.40	0.33	272.57	0.80	0.75
0.23	199.18	0.34	0.28	282.21	0.90	0.80	211.94	0.41	0.34	271.55	0.79	0.74
0.247	200.94	0.34	0.28	287.83	0.92	0.82	217.68	0.42	0.35	270.03	0.79	0.74
0.265	202.40	0.35	0.28	292.61	0.94	0.83	222.87	0.43	0.35	267.93	0.78	0.73
0.284	203.59	0.35	0.28	296.63	0.95	0.84	227.51	0.44	0.36	265.23	0.77	0.73
0.304	204.55	0.35	0.28	300.00	0.96	0.85	231.59	0.45	0.37	261.94	0.76	0.72
0.326	205.32	0.35	0.29	302.85	0.97	0.86	235.12	0.46	0.37	258.15	0.75	0.71
0.349	205.95	0.35	0.29	305.31	0.98	0.87	238.11	0.46	0.38	253.95	0.74	0.70
0.374	206.47	0.35	0.29	307.46	0.98	0.88	240.57	0.47	0.38	249.50	0.73	0.68
0.401	206.90	0.35	0.29	309.32	0.99	0.88	242.51	0.47	0.38	244.92	0.72	0.67
0.43	207.24	0.35	0.29	310.83	1.00	0.89	243.93	0.47	0.39	240.36	0.70	0.66
0.461	207.48	0.35	0.29	311.87	1.00	0.89	244.84	0.47	0.39	235.89	0.69	0.65
0.494	207.61	0.35	0.29	312.29	1.00	0.89	245.27	0.48	0.39	231.59	0.68	0.64
0.53	207.60	0.35	0.29	311.91	1.00	0.89	245.28	0.48	0.39	227.45	0.66	0.62
0.568	207.48	0.35	0.29	310.61	0.99	0.88	244.94	0.47	0.39	223.49	0.65	0.61
0.608	207.30	0.35	0.29	308.33	0.99	0.88	244.32	0.47	0.39	219.68	0.64	0.60
0.652	207.13	0.35	0.29	305.08	0.98	0.87	243.50	0.47	0.39	216.00	0.63	0.59
0.699	207.08	0.35	0.29	300.99	0.96	0.86	242.56	0.47	0.38	212.46	0.62	0.58
0.749	207.24	0.35	0.29	296.26	0.95	0.84	241.54	0.47	0.38	209.07	0.61	0.57
0.803	207.71	0.35	0.29	291.16	0.93	0.83	240.46	0.47	0.38	205.87	0.60	0.56
0.861	208.56	0.36	0.29	286.00	0.92	0.81	239.35	0.46	0.38	202.92	0.59	0.56
0.923	209.79	0.36	0.29	281.05	0.90	0.80	238.24	0.46	0.38	200.30	0.58	0.55
0.989	211.37	0.36	0.29	276.54	0.89	0.79	237.14	0.46	0.38	198.09	0.58	0.54
1.06	213.22	0.36	0.30	272.62	0.87	0.78	236.08	0.46	0.37	196.38	0.57	0.54
1.136	215.23	0.37	0.30	269.31	0.86	0.77	235.09	0.46	0.37	195.20	0.57	0.54
1.218	217.26	0.37	0.30	266.58	0.85	0.76	234.15	0.45	0.37	194.59	0.57	0.53
1.306	219.12	0.37	0.31	264.31	0.85	0.75	233.25	0.45	0.37	194.53	0.57	0.53
1.399	220.67	0.38	0.31	262.37	0.84	0.75	232.32	0.45	0.37	194.99	0.57	0.53
1.5	221.71	0.38	0.31	260.59	0.83	0.74	231.29	0.45	0.37	195.90	0.57	0.54

Table F17. Circular velocity curves of the 238 (E1–Sdm) CALIFA galaxies with 75th and 25th percentile uncertainties.

R/R_e	NGC2553			NGC2554			NGC2592			NGC2604		
	V_c	ΔV_c^{75th}	ΔV_c^{25th}									
0.05	89.83	0.21	0.21	186.52	0.25	0.19	79.94	0.07	0.07	41.29	0.21	0.20
0.054	95.83	0.23	0.23	197.96	0.26	0.20	85.37	0.08	0.08	43.34	0.22	0.21
0.057	102.17	0.24	0.24	209.80	0.28	0.21	91.15	0.09	0.08	45.38	0.23	0.22
0.062	108.87	0.26	0.26	222.00	0.29	0.23	97.30	0.09	0.09	47.40	0.24	0.23
0.066	115.92	0.28	0.27	234.50	0.31	0.24	103.83	0.10	0.10	49.37	0.25	0.24
0.071	123.32	0.29	0.29	247.19	0.32	0.25	110.74	0.10	0.10	51.27	0.26	0.25
0.076	131.07	0.31	0.31	259.99	0.34	0.26	118.04	0.11	0.11	53.08	0.27	0.25
0.081	139.16	0.33	0.33	272.76	0.36	0.28	125.75	0.12	0.12	54.77	0.28	0.26
0.087	147.57	0.35	0.35	285.36	0.37	0.29	133.85	0.13	0.12	56.34	0.29	0.27
0.093	156.29	0.37	0.37	297.61	0.39	0.30	142.34	0.13	0.13	57.77	0.29	0.28
0.1	165.29	0.40	0.39	309.33	0.41	0.32	151.22	0.14	0.14	59.06	0.30	0.28
0.107	174.53	0.42	0.41	320.32	0.42	0.33	160.45	0.15	0.15	60.23	0.31	0.29
0.115	183.97	0.44	0.44	330.39	0.43	0.34	170.02	0.16	0.16	61.29	0.31	0.29
0.123	193.57	0.46	0.46	339.32	0.45	0.35	179.89	0.17	0.17	62.26	0.32	0.30
0.132	203.26	0.49	0.48	346.96	0.46	0.35	190.00	0.18	0.18	63.18	0.32	0.30
0.142	212.99	0.51	0.50	353.18	0.46	0.36	200.29	0.19	0.19	64.08	0.33	0.31
0.152	222.67	0.53	0.53	357.88	0.47	0.36	210.68	0.20	0.19	64.96	0.33	0.31
0.163	232.23	0.56	0.55	361.09	0.47	0.37	221.09	0.21	0.20	65.84	0.33	0.32
0.174	241.59	0.58	0.57	362.87	0.48	0.37	231.41	0.22	0.21	66.72	0.34	0.32
0.187	250.65	0.60	0.59	363.39	0.48	0.37	241.51	0.23	0.22	67.57	0.34	0.32
0.2	259.33	0.62	0.61	362.89	0.48	0.37	251.29	0.24	0.23	68.38	0.35	0.33
0.215	267.53	0.64	0.63	361.65	0.48	0.37	260.60	0.25	0.24	69.12	0.35	0.33
0.23	275.17	0.66	0.65	359.94	0.47	0.37	269.33	0.25	0.25	69.78	0.35	0.34
0.247	282.18	0.68	0.67	358.04	0.47	0.36	277.36	0.26	0.26	70.34	0.36	0.34
0.265	288.50	0.69	0.68	356.12	0.47	0.36	284.59	0.27	0.26	70.81	0.36	0.34
0.284	294.12	0.70	0.70	354.29	0.47	0.36	290.95	0.27	0.27	71.21	0.36	0.34
0.304	299.04	0.72	0.71	352.58	0.46	0.36	296.41	0.28	0.27	71.57	0.36	0.34
0.326	303.30	0.73	0.72	350.96	0.46	0.36	300.97	0.28	0.28	71.94	0.37	0.35
0.349	306.96	0.73	0.73	349.35	0.46	0.36	304.66	0.29	0.28	72.36	0.37	0.35
0.374	310.07	0.74	0.74	347.67	0.46	0.35	307.53	0.29	0.28	72.88	0.37	0.35
0.401	312.67	0.75	0.74	345.85	0.45	0.35	309.64	0.29	0.29	73.55	0.37	0.35
0.43	314.78	0.75	0.75	343.86	0.45	0.35	311.06	0.29	0.29	74.38	0.38	0.36
0.461	316.36	0.76	0.75	341.69	0.45	0.35	311.85	0.29	0.29	75.41	0.38	0.36
0.494	317.35	0.76	0.75	339.39	0.45	0.35	312.05	0.29	0.29	76.64	0.39	0.37
0.53	317.70	0.76	0.75	336.99	0.44	0.34	311.70	0.29	0.29	78.07	0.40	0.38
0.568	317.33	0.76	0.75	334.58	0.44	0.34	310.85	0.29	0.29	79.71	0.41	0.38
0.608	316.22	0.76	0.75	332.20	0.44	0.34	309.57	0.29	0.29	81.55	0.41	0.39
0.652	314.40	0.75	0.75	329.89	0.43	0.34	307.94	0.29	0.28	83.59	0.43	0.40
0.699	311.93	0.75	0.74	327.67	0.43	0.33	306.06	0.29	0.28	85.83	0.44	0.41
0.749	308.94	0.74	0.73	325.51	0.43	0.33	304.04	0.29	0.28	88.26	0.45	0.42
0.803	305.54	0.73	0.72	323.41	0.43	0.33	301.92	0.28	0.28	90.87	0.46	0.44
0.861	301.85	0.72	0.72	321.35	0.42	0.33	299.74	0.28	0.28	93.62	0.48	0.45
0.923	297.95	0.71	0.71	319.33	0.42	0.33	297.47	0.28	0.28	96.48	0.49	0.46
0.989	293.88	0.70	0.70	317.34	0.42	0.32	295.06	0.28	0.27	99.40	0.51	0.48
1.06	289.66	0.69	0.69	315.38	0.41	0.32	292.45	0.28	0.27	102.33	0.52	0.49
1.136	285.30	0.68	0.68	313.44	0.41	0.32	289.59	0.27	0.27	105.20	0.54	0.51
1.218	280.84	0.67	0.67	311.50	0.41	0.32	286.45	0.27	0.27	107.93	0.55	0.52
1.306	276.33	0.66	0.66	309.50	0.41	0.32	283.04	0.27	0.26	110.47	0.56	0.53
1.399	271.86	0.65	0.64	307.37	0.40	0.31	279.42	0.26	0.26	112.73	0.57	0.54
1.5	267.53	0.64	0.63	305.04	0.40	0.31	275.63	0.26	0.26	114.66	0.58	0.55

Table F18. Circular velocity curves of the 238 (E1–Sdm) CALIFA galaxies with 75th and 25th percentile uncertainties.

R/R_e	NGC2639			NGC2730			NGC2880			NGC2906		
	V_c	ΔV_c^{75th}	ΔV_c^{25th}									
0.05	106.10	0.14	0.28	29.29	0.13	0.09	106.32	0.12	0.10	116.87	0.23	0.20
0.054	112.92	0.14	0.30	31.22	0.14	0.10	112.91	0.12	0.11	122.40	0.24	0.21
0.057	120.05	0.15	0.32	33.27	0.15	0.10	119.75	0.13	0.11	127.83	0.25	0.22
0.062	127.50	0.16	0.34	35.44	0.16	0.11	126.85	0.14	0.12	133.10	0.26	0.22
0.066	135.25	0.17	0.36	37.72	0.17	0.12	134.15	0.15	0.13	138.14	0.27	0.23
0.071	143.27	0.18	0.38	40.13	0.18	0.12	141.62	0.16	0.13	142.87	0.28	0.24
0.076	151.54	0.19	0.40	42.65	0.19	0.13	149.22	0.16	0.14	147.23	0.29	0.25
0.081	160.01	0.20	0.42	45.29	0.20	0.14	156.89	0.17	0.15	151.16	0.30	0.25
0.087	168.64	0.22	0.45	48.02	0.22	0.15	164.55	0.18	0.16	154.61	0.30	0.26
0.093	177.36	0.23	0.47	50.86	0.23	0.16	172.13	0.19	0.16	157.54	0.31	0.27
0.1	186.12	0.24	0.49	53.77	0.24	0.17	179.54	0.20	0.17	159.96	0.31	0.27
0.107	194.84	0.25	0.52	56.75	0.26	0.18	186.70	0.20	0.18	161.87	0.32	0.27
0.115	203.45	0.26	0.54	59.78	0.27	0.19	193.50	0.21	0.18	163.31	0.32	0.28
0.123	211.87	0.27	0.56	62.82	0.28	0.20	199.87	0.22	0.19	164.34	0.32	0.28
0.132	220.05	0.28	0.58	65.84	0.30	0.21	205.73	0.23	0.19	165.03	0.32	0.28
0.142	227.92	0.29	0.61	68.82	0.31	0.22	211.03	0.23	0.20	165.46	0.33	0.28
0.152	235.45	0.30	0.63	71.70	0.32	0.22	215.71	0.24	0.20	165.73	0.33	0.28
0.163	242.62	0.31	0.64	74.45	0.34	0.23	219.80	0.24	0.21	165.93	0.33	0.28
0.174	249.46	0.32	0.66	77.03	0.35	0.24	223.30	0.24	0.21	166.17	0.33	0.28
0.187	256.01	0.33	0.68	79.39	0.36	0.25	226.27	0.25	0.21	166.53	0.33	0.28
0.2	262.33	0.34	0.70	81.49	0.37	0.25	228.79	0.25	0.22	167.07	0.33	0.28
0.215	268.48	0.34	0.71	83.31	0.38	0.26	230.93	0.25	0.22	167.84	0.33	0.28
0.23	274.51	0.35	0.73	84.84	0.38	0.27	232.75	0.26	0.22	168.80	0.33	0.28
0.247	280.46	0.36	0.74	86.07	0.39	0.27	234.31	0.26	0.22	169.90	0.33	0.29
0.265	286.31	0.37	0.76	87.04	0.39	0.27	235.63	0.26	0.22	171.05	0.34	0.29
0.284	291.99	0.37	0.78	87.81	0.40	0.27	236.69	0.26	0.22	172.12	0.34	0.29
0.304	297.42	0.38	0.79	88.45	0.40	0.28	237.48	0.26	0.22	173.03	0.34	0.29
0.326	302.47	0.39	0.80	89.05	0.40	0.28	237.97	0.26	0.22	173.67	0.34	0.29
0.349	307.03	0.39	0.82	89.74	0.41	0.28	238.15	0.26	0.22	174.00	0.34	0.29
0.374	311.02	0.40	0.83	90.61	0.41	0.28	238.03	0.26	0.22	174.02	0.34	0.29
0.401	314.40	0.40	0.83	91.75	0.42	0.29	237.64	0.26	0.22	173.77	0.34	0.29
0.43	317.16	0.41	0.84	93.25	0.42	0.29	237.02	0.26	0.22	173.33	0.34	0.29
0.461	319.38	0.41	0.85	95.14	0.43	0.30	236.23	0.26	0.22	172.84	0.34	0.29
0.494	321.15	0.41	0.85	97.46	0.44	0.30	235.30	0.26	0.22	172.43	0.34	0.29
0.53	322.63	0.41	0.86	100.19	0.45	0.31	234.26	0.26	0.22	172.25	0.34	0.29
0.568	323.95	0.41	0.86	103.35	0.47	0.32	233.09	0.26	0.22	172.43	0.34	0.29
0.608	325.27	0.42	0.86	106.89	0.48	0.33	231.77	0.25	0.22	173.05	0.34	0.29
0.652	326.70	0.42	0.87	110.80	0.50	0.35	230.30	0.25	0.22	174.19	0.34	0.29
0.699	328.32	0.42	0.87	115.02	0.52	0.36	228.63	0.25	0.22	175.88	0.35	0.30
0.749	330.16	0.42	0.88	119.52	0.54	0.37	226.78	0.25	0.21	178.11	0.35	0.30
0.803	332.16	0.42	0.88	124.23	0.56	0.39	224.73	0.25	0.21	180.87	0.36	0.31
0.861	334.20	0.43	0.89	129.07	0.58	0.40	222.51	0.24	0.21	184.10	0.36	0.31
0.923	336.13	0.43	0.89	133.97	0.61	0.42	220.13	0.24	0.21	187.72	0.37	0.32
0.989	337.72	0.43	0.90	138.83	0.63	0.43	217.64	0.24	0.21	191.64	0.38	0.32
1.06	338.74	0.43	0.90	143.53	0.65	0.45	215.08	0.24	0.20	195.71	0.39	0.33
1.136	338.99	0.43	0.90	147.96	0.67	0.46	212.50	0.23	0.20	199.80	0.39	0.34
1.218	338.30	0.43	0.90	151.97	0.69	0.48	209.98	0.23	0.20	203.73	0.40	0.34
1.306	336.58	0.43	0.89	155.43	0.70	0.49	207.57	0.23	0.20	207.32	0.41	0.35
1.399	333.81	0.43	0.89	158.20	0.72	0.49	205.32	0.23	0.19	210.38	0.41	0.36
1.5	330.04	0.42	0.88	160.13	0.73	0.50	203.24	0.22	0.19	212.73	0.42	0.36

Table F19. Circular velocity curves of the 238 (E1–Sdm) CALIFA galaxies with 75th and 25th percentile uncertainties.

R/R_e	NGC2916			NGC2918			NGC3057			NGC3106		
	V_c	ΔV_c^{75th}	ΔV_c^{25th}									
0.05	110.07	0.12	0.12	95.75	0.15	0.12	23.97	0.18	0.18	205.63	0.36	0.36
0.054	116.01	0.13	0.12	102.36	0.16	0.12	25.19	0.19	0.19	216.26	0.38	0.38
0.057	122.02	0.14	0.13	109.40	0.17	0.13	26.43	0.21	0.20	226.86	0.40	0.40
0.062	128.04	0.14	0.13	116.88	0.18	0.14	27.67	0.22	0.21	237.30	0.42	0.42
0.066	134.02	0.15	0.14	124.81	0.19	0.15	28.92	0.23	0.22	247.46	0.44	0.44
0.071	139.91	0.16	0.15	133.21	0.20	0.16	30.16	0.24	0.23	257.16	0.45	0.46
0.076	145.63	0.16	0.15	142.09	0.22	0.17	31.38	0.25	0.24	266.24	0.47	0.47
0.081	151.14	0.17	0.16	151.46	0.23	0.18	32.56	0.26	0.25	274.54	0.49	0.49
0.087	156.37	0.17	0.16	161.32	0.25	0.19	33.70	0.27	0.25	281.90	0.50	0.50
0.093	161.27	0.18	0.17	171.67	0.26	0.21	34.79	0.28	0.26	288.18	0.51	0.51
0.1	165.80	0.19	0.17	182.51	0.28	0.22	35.83	0.28	0.27	293.29	0.52	0.52
0.107	169.95	0.19	0.18	193.80	0.30	0.23	36.83	0.29	0.28	297.18	0.53	0.53
0.115	173.69	0.19	0.18	205.52	0.31	0.25	37.79	0.30	0.29	299.89	0.53	0.53
0.123	177.04	0.20	0.19	217.63	0.33	0.26	38.74	0.31	0.29	301.50	0.53	0.53
0.132	180.00	0.20	0.19	230.08	0.35	0.28	39.67	0.32	0.30	302.21	0.53	0.54
0.142	182.57	0.20	0.19	242.80	0.37	0.29	40.62	0.32	0.31	302.24	0.53	0.54
0.152	184.75	0.21	0.19	255.69	0.39	0.31	41.60	0.33	0.32	301.85	0.53	0.54
0.163	186.54	0.21	0.20	268.65	0.41	0.32	42.61	0.34	0.32	301.30	0.53	0.53
0.174	187.91	0.21	0.20	281.57	0.43	0.34	43.66	0.35	0.33	300.77	0.53	0.53
0.187	188.82	0.21	0.20	294.31	0.45	0.36	44.74	0.36	0.34	300.37	0.53	0.53
0.2	189.25	0.21	0.20	306.72	0.47	0.37	45.82	0.37	0.35	300.12	0.53	0.53
0.215	189.21	0.21	0.20	318.64	0.49	0.39	46.90	0.38	0.36	299.99	0.53	0.53
0.23	188.72	0.21	0.20	329.94	0.50	0.40	47.95	0.38	0.37	299.88	0.53	0.53
0.247	187.87	0.21	0.20	340.48	0.52	0.41	48.96	0.39	0.37	299.72	0.53	0.53
0.265	186.76	0.21	0.20	350.14	0.53	0.42	49.91	0.40	0.38	299.42	0.53	0.53
0.284	185.56	0.21	0.20	358.85	0.55	0.43	50.81	0.41	0.39	298.92	0.53	0.53
0.304	184.41	0.21	0.19	366.59	0.56	0.44	51.66	0.41	0.39	298.16	0.53	0.53
0.326	183.46	0.20	0.19	373.39	0.57	0.45	52.49	0.42	0.40	297.10	0.53	0.53
0.349	182.82	0.20	0.19	379.34	0.58	0.46	53.32	0.43	0.41	295.70	0.52	0.52
0.374	182.57	0.20	0.19	384.56	0.59	0.46	54.20	0.43	0.41	293.94	0.52	0.52
0.401	182.75	0.20	0.19	389.21	0.59	0.47	55.17	0.44	0.42	291.84	0.52	0.52
0.43	183.35	0.20	0.19	393.43	0.60	0.48	56.26	0.45	0.43	289.43	0.51	0.51
0.461	184.38	0.21	0.19	397.34	0.61	0.48	57.49	0.46	0.44	286.76	0.51	0.51
0.494	185.83	0.21	0.20	400.99	0.61	0.48	58.88	0.47	0.45	283.86	0.50	0.50
0.53	187.68	0.21	0.20	404.35	0.62	0.49	60.43	0.48	0.46	280.77	0.50	0.50
0.568	189.97	0.21	0.20	407.34	0.62	0.49	62.14	0.50	0.48	277.47	0.49	0.49
0.608	192.69	0.22	0.20	409.82	0.63	0.50	63.98	0.51	0.49	273.95	0.48	0.49
0.652	195.86	0.22	0.21	411.67	0.63	0.50	65.93	0.53	0.50	270.17	0.48	0.48
0.699	199.48	0.22	0.21	412.74	0.63	0.50	67.98	0.55	0.52	266.10	0.47	0.47
0.749	203.52	0.23	0.21	412.96	0.63	0.50	70.09	0.56	0.54	261.78	0.46	0.46
0.803	207.90	0.23	0.22	412.29	0.63	0.50	72.25	0.58	0.55	257.27	0.45	0.46
0.861	212.55	0.24	0.22	410.76	0.63	0.50	74.42	0.60	0.57	252.69	0.45	0.45
0.923	217.32	0.24	0.23	408.43	0.62	0.49	76.57	0.61	0.59	248.20	0.44	0.44
0.989	222.07	0.25	0.23	405.37	0.62	0.49	78.67	0.63	0.60	243.94	0.43	0.43
1.06	226.63	0.25	0.24	401.67	0.61	0.49	80.68	0.65	0.62	240.04	0.42	0.43
1.136	230.80	0.26	0.24	397.37	0.61	0.48	82.56	0.66	0.63	236.54	0.42	0.42
1.218	234.40	0.26	0.25	392.52	0.60	0.47	84.27	0.68	0.64	233.44	0.41	0.41
1.306	237.24	0.27	0.25	387.13	0.59	0.47	85.78	0.69	0.66	230.66	0.41	0.41
1.399	239.17	0.27	0.25	381.27	0.58	0.46	87.04	0.70	0.67	228.08	0.40	0.40
1.5	240.05	0.27	0.25	374.99	0.57	0.45	88.04	0.71	0.67	225.59	0.40	0.40

Table F20. Circular velocity curves of the 238 (E1–Sdm) CALIFA galaxies with 75th and 25th percentile uncertainties.

R/R_e	NGC3160			NGC3300			NGC3381			NGC3615		
	V_c	ΔV_c^{75th}	ΔV_c^{25th}									
0.05	92.37	0.21	0.25	72.53	0.16	0.10	54.22	0.40	0.32	240.93	0.83	0.59
0.054	98.02	0.23	0.27	77.37	0.17	0.10	53.56	0.39	0.32	255.52	0.88	0.62
0.057	103.88	0.24	0.28	82.50	0.18	0.11	52.93	0.39	0.31	270.60	0.93	0.66
0.062	109.92	0.25	0.30	87.92	0.19	0.12	52.35	0.38	0.31	286.08	0.99	0.70
0.066	116.11	0.27	0.32	93.62	0.20	0.13	51.84	0.38	0.31	301.88	1.04	0.74
0.071	122.42	0.28	0.33	99.61	0.22	0.13	51.42	0.38	0.30	317.87	1.09	0.78
0.076	128.80	0.30	0.35	105.88	0.23	0.14	51.07	0.37	0.30	333.91	1.15	0.82
0.081	135.20	0.31	0.37	112.43	0.24	0.15	50.81	0.37	0.30	349.85	1.20	0.85
0.087	141.55	0.33	0.38	119.23	0.26	0.16	50.62	0.37	0.30	365.47	1.26	0.89
0.093	147.79	0.34	0.40	126.27	0.27	0.17	50.49	0.37	0.30	380.57	1.31	0.93
0.1	153.85	0.35	0.42	133.51	0.29	0.18	50.42	0.37	0.30	394.92	1.36	0.97
0.107	159.66	0.37	0.43	140.92	0.31	0.19	50.42	0.37	0.30	408.29	1.41	1.00
0.115	165.16	0.38	0.45	148.45	0.32	0.20	50.50	0.37	0.30	420.45	1.45	1.03
0.123	170.29	0.39	0.46	156.04	0.34	0.21	50.65	0.37	0.30	431.20	1.48	1.05
0.132	175.01	0.40	0.48	163.63	0.36	0.22	50.90	0.37	0.30	440.40	1.52	1.08
0.142	179.32	0.41	0.49	171.15	0.37	0.23	51.25	0.38	0.30	447.96	1.54	1.09
0.152	183.24	0.42	0.50	178.51	0.39	0.24	51.70	0.38	0.31	453.90	1.56	1.11
0.163	186.81	0.43	0.51	185.63	0.40	0.25	52.27	0.38	0.31	458.32	1.58	1.12
0.174	190.11	0.44	0.52	192.43	0.42	0.26	52.95	0.39	0.31	461.43	1.59	1.13
0.187	193.24	0.45	0.53	198.82	0.43	0.27	53.72	0.40	0.32	463.51	1.60	1.13
0.2	196.31	0.45	0.53	204.72	0.45	0.27	54.58	0.40	0.32	464.86	1.60	1.14
0.215	199.41	0.46	0.54	210.07	0.46	0.28	55.50	0.41	0.33	465.75	1.60	1.14
0.23	202.61	0.47	0.55	214.82	0.47	0.29	56.45	0.42	0.34	466.37	1.61	1.14
0.247	205.95	0.47	0.56	218.92	0.48	0.29	57.40	0.42	0.34	466.79	1.61	1.14
0.265	209.40	0.48	0.57	222.35	0.48	0.30	58.32	0.43	0.35	466.95	1.61	1.14
0.284	212.91	0.49	0.58	225.12	0.49	0.30	59.18	0.44	0.35	466.71	1.61	1.14
0.304	216.40	0.50	0.59	227.22	0.50	0.30	59.97	0.44	0.36	465.90	1.60	1.14
0.326	219.72	0.51	0.60	228.70	0.50	0.31	60.68	0.45	0.36	464.41	1.60	1.13
0.349	222.77	0.51	0.61	229.59	0.50	0.31	61.32	0.45	0.36	462.19	1.59	1.13
0.374	225.41	0.52	0.61	229.95	0.50	0.31	61.93	0.46	0.37	459.29	1.58	1.12
0.401	227.53	0.52	0.62	229.87	0.50	0.31	62.53	0.46	0.37	455.85	1.57	1.11
0.43	229.08	0.53	0.62	229.44	0.50	0.31	63.20	0.47	0.38	452.04	1.56	1.10
0.461	230.03	0.53	0.63	228.76	0.50	0.31	63.96	0.47	0.38	448.00	1.54	1.09
0.494	230.43	0.53	0.63	227.91	0.50	0.31	64.88	0.48	0.39	443.84	1.53	1.08
0.53	230.39	0.53	0.63	226.95	0.49	0.30	65.97	0.49	0.39	439.58	1.51	1.07
0.568	230.10	0.53	0.63	225.92	0.49	0.30	67.24	0.50	0.40	435.16	1.50	1.06
0.608	229.75	0.53	0.62	224.84	0.49	0.30	68.67	0.51	0.41	430.51	1.48	1.05
0.652	229.57	0.53	0.62	223.70	0.49	0.30	70.21	0.52	0.42	425.50	1.47	1.04
0.699	229.76	0.53	0.62	222.53	0.49	0.30	71.81	0.53	0.43	420.08	1.45	1.03
0.749	230.47	0.53	0.63	221.36	0.48	0.30	73.40	0.54	0.44	414.25	1.43	1.01
0.803	231.77	0.53	0.63	220.23	0.48	0.30	74.93	0.55	0.45	408.09	1.41	1.00
0.861	233.66	0.54	0.63	219.22	0.48	0.29	76.33	0.56	0.45	401.73	1.38	0.98
0.923	236.08	0.54	0.64	218.37	0.48	0.29	77.56	0.57	0.46	395.30	1.36	0.97
0.989	238.88	0.55	0.65	217.74	0.47	0.29	78.58	0.58	0.47	388.94	1.34	0.95
1.06	241.90	0.56	0.66	217.35	0.47	0.29	79.35	0.59	0.47	382.71	1.32	0.94
1.136	244.97	0.56	0.67	217.23	0.47	0.29	79.88	0.59	0.48	376.64	1.30	0.92
1.218	247.87	0.57	0.67	217.36	0.47	0.29	80.15	0.59	0.48	370.67	1.28	0.91
1.306	250.40	0.58	0.68	217.75	0.47	0.29	80.19	0.59	0.48	364.76	1.26	0.89
1.399	252.35	0.58	0.69	218.35	0.48	0.29	80.03	0.59	0.48	358.83	1.24	0.88
1.5	253.55	0.58	0.69	219.11	0.48	0.29	79.69	0.59	0.47	352.83	1.22	0.86

Table F21. Circular velocity curves of the 238 (E1–Sdm) CALIFA galaxies with 75th and 25th percentile uncertainties.

R/R_e	NGC3811			NGC3815			NGC3994			NGC4003		
	V_c	ΔV_c^{75th}	ΔV_c^{25th}									
0.05	171.24	0.32	0.27	54.22	0.11	0.10	71.71	0.22	0.18	170.63	0.53	0.45
0.054	179.48	0.34	0.28	57.75	0.12	0.10	76.59	0.24	0.19	174.74	0.55	0.47
0.057	187.54	0.35	0.29	61.48	0.12	0.11	81.80	0.26	0.20	178.17	0.56	0.47
0.062	195.28	0.37	0.30	65.40	0.13	0.12	87.33	0.27	0.22	180.88	0.57	0.48
0.066	202.55	0.38	0.31	69.51	0.14	0.12	93.19	0.29	0.23	182.90	0.57	0.49
0.071	209.19	0.39	0.32	73.79	0.15	0.13	99.40	0.31	0.25	184.27	0.58	0.49
0.076	215.03	0.40	0.33	78.23	0.16	0.14	105.96	0.33	0.27	185.11	0.58	0.49
0.081	219.88	0.41	0.34	82.82	0.17	0.15	112.87	0.36	0.28	185.59	0.58	0.49
0.087	223.58	0.42	0.35	87.54	0.18	0.16	120.13	0.38	0.30	185.91	0.58	0.50
0.093	225.98	0.42	0.35	92.35	0.19	0.17	127.74	0.40	0.32	186.27	0.58	0.50
0.1	226.97	0.43	0.35	97.22	0.20	0.17	135.68	0.43	0.34	186.88	0.59	0.50
0.107	226.52	0.42	0.35	102.10	0.21	0.18	143.94	0.46	0.36	187.91	0.59	0.50
0.115	224.65	0.42	0.35	106.95	0.22	0.19	152.48	0.48	0.38	189.47	0.59	0.50
0.123	221.48	0.42	0.34	111.68	0.23	0.20	161.25	0.51	0.41	191.61	0.60	0.51
0.132	217.25	0.41	0.34	116.25	0.24	0.21	170.22	0.54	0.43	194.34	0.61	0.52
0.142	212.25	0.40	0.33	120.58	0.25	0.22	179.31	0.57	0.45	197.62	0.62	0.53
0.152	206.86	0.39	0.32	124.59	0.25	0.22	188.44	0.60	0.47	201.36	0.63	0.54
0.163	201.47	0.38	0.31	128.21	0.26	0.23	197.50	0.62	0.50	205.46	0.64	0.55
0.174	196.42	0.37	0.30	131.38	0.27	0.24	206.39	0.65	0.52	209.83	0.66	0.56
0.187	191.96	0.36	0.30	134.06	0.27	0.24	214.97	0.68	0.54	214.31	0.67	0.57
0.2	188.20	0.35	0.29	136.22	0.28	0.24	223.10	0.71	0.56	218.78	0.69	0.58
0.215	185.15	0.35	0.29	137.89	0.28	0.25	230.62	0.73	0.58	223.09	0.70	0.59
0.23	182.69	0.34	0.28	139.12	0.28	0.25	237.39	0.75	0.60	227.09	0.71	0.61
0.247	180.69	0.34	0.28	140.01	0.29	0.25	243.25	0.77	0.61	230.66	0.72	0.61
0.265	178.98	0.34	0.28	140.71	0.29	0.25	248.08	0.78	0.63	233.68	0.73	0.62
0.284	177.44	0.33	0.28	141.38	0.29	0.25	251.80	0.80	0.63	236.05	0.74	0.63
0.304	175.97	0.33	0.27	142.21	0.29	0.26	254.37	0.80	0.64	237.72	0.75	0.63
0.326	174.49	0.33	0.27	143.37	0.29	0.26	255.84	0.81	0.64	238.66	0.75	0.64
0.349	172.99	0.32	0.27	144.98	0.30	0.26	256.33	0.81	0.65	238.91	0.75	0.64
0.374	171.49	0.32	0.27	147.11	0.30	0.26	256.02	0.81	0.65	238.53	0.75	0.64
0.401	170.02	0.32	0.26	149.78	0.31	0.27	255.21	0.81	0.64	237.63	0.75	0.63
0.43	168.68	0.32	0.26	152.93	0.31	0.28	254.20	0.80	0.64	236.33	0.74	0.63
0.461	167.56	0.31	0.26	156.51	0.32	0.28	253.32	0.80	0.64	234.78	0.74	0.63
0.494	166.76	0.31	0.26	160.40	0.33	0.29	252.84	0.80	0.64	233.10	0.73	0.62
0.53	166.37	0.31	0.26	164.50	0.34	0.30	252.96	0.80	0.64	231.39	0.73	0.62
0.568	166.44	0.31	0.26	168.69	0.34	0.30	253.77	0.80	0.64	229.73	0.72	0.61
0.608	167.00	0.31	0.26	172.86	0.35	0.31	255.27	0.81	0.64	228.16	0.72	0.61
0.652	168.02	0.32	0.26	176.90	0.36	0.32	257.37	0.81	0.65	226.70	0.71	0.60
0.699	169.45	0.32	0.26	180.69	0.37	0.33	259.91	0.82	0.66	225.32	0.71	0.60
0.749	171.23	0.32	0.27	184.16	0.38	0.33	262.76	0.83	0.66	224.03	0.70	0.60
0.803	173.25	0.33	0.27	187.21	0.38	0.34	265.73	0.84	0.67	222.80	0.70	0.59
0.861	175.39	0.33	0.27	189.80	0.39	0.34	268.67	0.85	0.68	221.61	0.69	0.59
0.923	177.54	0.33	0.28	191.90	0.39	0.35	271.45	0.86	0.68	220.47	0.69	0.59
0.989	179.55	0.34	0.28	193.50	0.40	0.35	273.93	0.87	0.69	219.39	0.69	0.58
1.06	181.29	0.34	0.28	194.63	0.40	0.35	276.02	0.87	0.70	218.39	0.68	0.58
1.136	182.62	0.34	0.28	195.34	0.40	0.35	277.65	0.88	0.70	217.50	0.68	0.58
1.218	183.41	0.34	0.28	195.65	0.40	0.35	278.74	0.88	0.70	216.73	0.68	0.58
1.306	183.58	0.34	0.28	195.63	0.40	0.35	279.26	0.88	0.70	216.06	0.68	0.58
1.399	183.05	0.34	0.28	195.29	0.40	0.35	279.13	0.88	0.70	215.45	0.68	0.57
1.5	181.79	0.34	0.28	194.67	0.40	0.35	278.30	0.88	0.70	214.79	0.67	0.57

Table F22. Circular velocity curves of the 238 (E1–Sdm) CALIFA galaxies with 75th and 25th percentile uncertainties.

R/R_e	NGC4047			NGC4149			NGC4185			NGC4210		
	V_c	ΔV_c^{75th}	ΔV_c^{25th}									
0.05	76.98	0.25	0.17	57.28	0.15	0.13	84.39	0.26	0.16	74.34	0.13	0.11
0.054	81.38	0.27	0.18	61.03	0.16	0.14	88.31	0.27	0.17	78.67	0.14	0.12
0.057	85.87	0.28	0.19	64.97	0.17	0.15	92.38	0.29	0.18	83.12	0.14	0.13
0.062	90.42	0.30	0.20	69.12	0.18	0.16	96.58	0.30	0.18	87.65	0.15	0.13
0.066	95.01	0.31	0.21	73.46	0.19	0.17	100.89	0.31	0.19	92.22	0.16	0.14
0.071	99.58	0.33	0.22	77.99	0.20	0.18	105.27	0.33	0.20	96.80	0.17	0.15
0.076	104.09	0.34	0.23	82.69	0.22	0.19	109.65	0.34	0.21	101.34	0.18	0.15
0.081	108.48	0.36	0.24	87.56	0.23	0.20	113.97	0.35	0.22	105.77	0.18	0.16
0.087	112.71	0.37	0.25	92.55	0.24	0.21	118.14	0.37	0.23	110.02	0.19	0.17
0.093	116.72	0.38	0.26	97.66	0.26	0.23	122.07	0.38	0.23	114.04	0.20	0.17
0.1	120.47	0.39	0.27	102.84	0.27	0.24	125.66	0.39	0.24	117.74	0.20	0.18
0.107	123.93	0.41	0.28	108.04	0.28	0.25	128.83	0.40	0.25	121.06	0.21	0.18
0.115	127.10	0.42	0.29	113.23	0.30	0.26	131.51	0.41	0.25	123.92	0.22	0.19
0.123	130.00	0.43	0.29	118.33	0.31	0.27	133.62	0.41	0.26	126.29	0.22	0.19
0.132	132.68	0.44	0.30	123.30	0.32	0.28	135.13	0.42	0.26	128.12	0.22	0.20
0.142	135.25	0.44	0.30	128.06	0.34	0.30	136.05	0.42	0.26	129.41	0.22	0.20
0.152	137.84	0.45	0.31	132.56	0.35	0.31	136.42	0.42	0.26	130.16	0.23	0.20
0.163	140.60	0.46	0.32	136.73	0.36	0.32	136.34	0.42	0.26	130.42	0.23	0.20
0.174	143.68	0.47	0.32	140.52	0.37	0.32	135.94	0.42	0.26	130.25	0.23	0.20
0.187	147.24	0.48	0.33	143.90	0.38	0.33	135.40	0.42	0.26	129.72	0.23	0.20
0.2	151.38	0.50	0.34	146.85	0.39	0.34	134.93	0.42	0.26	128.91	0.22	0.20
0.215	156.15	0.51	0.35	149.38	0.39	0.34	134.72	0.42	0.26	127.88	0.22	0.20
0.23	161.53	0.53	0.36	151.52	0.40	0.35	134.91	0.42	0.26	126.70	0.22	0.19
0.247	167.48	0.55	0.38	153.32	0.40	0.35	135.59	0.42	0.26	125.41	0.22	0.19
0.265	173.89	0.57	0.39	154.84	0.41	0.36	136.79	0.42	0.26	124.07	0.22	0.19
0.284	180.65	0.59	0.41	156.14	0.41	0.36	138.47	0.43	0.27	122.74	0.21	0.19
0.304	187.64	0.62	0.42	157.27	0.41	0.36	140.54	0.44	0.27	121.49	0.21	0.19
0.326	194.73	0.64	0.44	158.26	0.42	0.37	142.91	0.44	0.27	120.43	0.21	0.18
0.349	201.78	0.66	0.45	159.15	0.42	0.37	145.48	0.45	0.28	119.66	0.21	0.18
0.374	208.68	0.68	0.47	159.92	0.42	0.37	148.15	0.46	0.28	119.26	0.21	0.18
0.401	215.27	0.71	0.48	160.59	0.42	0.37	150.84	0.47	0.29	119.31	0.21	0.18
0.43	221.45	0.73	0.50	161.18	0.42	0.37	153.50	0.48	0.29	119.87	0.21	0.18
0.461	227.09	0.74	0.51	161.72	0.43	0.37	156.09	0.48	0.30	120.96	0.21	0.18
0.494	232.11	0.76	0.52	162.29	0.43	0.37	158.61	0.49	0.30	122.61	0.21	0.19
0.53	236.45	0.78	0.53	162.97	0.43	0.38	161.08	0.50	0.31	124.80	0.22	0.19
0.568	240.10	0.79	0.54	163.82	0.43	0.38	163.56	0.51	0.31	127.54	0.22	0.19
0.608	243.07	0.80	0.55	164.93	0.43	0.38	166.15	0.52	0.32	130.79	0.23	0.20
0.652	245.45	0.81	0.55	166.32	0.44	0.38	168.92	0.52	0.32	134.53	0.23	0.21
0.699	247.33	0.81	0.56	168.02	0.44	0.39	171.98	0.53	0.33	138.72	0.24	0.21
0.749	248.87	0.82	0.56	169.99	0.45	0.39	175.40	0.54	0.34	143.31	0.25	0.22
0.803	250.19	0.82	0.56	172.19	0.45	0.40	179.21	0.56	0.34	148.23	0.26	0.23
0.861	251.42	0.82	0.57	174.56	0.46	0.40	183.40	0.57	0.35	153.42	0.27	0.23
0.923	252.66	0.83	0.57	177.03	0.47	0.41	187.91	0.58	0.36	158.77	0.28	0.24
0.989	253.94	0.83	0.57	179.51	0.47	0.41	192.64	0.60	0.37	164.21	0.29	0.25
1.06	255.27	0.84	0.57	181.94	0.48	0.42	197.44	0.61	0.38	169.61	0.29	0.26
1.136	256.59	0.84	0.58	184.22	0.48	0.43	202.14	0.63	0.39	174.85	0.30	0.27
1.218	257.81	0.85	0.58	186.29	0.49	0.43	206.57	0.64	0.40	179.81	0.31	0.27
1.306	258.77	0.85	0.58	188.03	0.49	0.43	210.54	0.65	0.40	184.34	0.32	0.28
1.399	259.31	0.85	0.58	189.35	0.50	0.44	213.84	0.66	0.41	188.28	0.33	0.29
1.5	259.22	0.85	0.58	190.14	0.50	0.44	216.28	0.67	0.41	191.49	0.33	0.29

Table F23. Circular velocity curves of the 238 (E1–Sdm) CALIFA galaxies with 75th and 25th percentile uncertainties.

R/R_e	NGC4470			NGC4644			NGC4711			NGC4816		
	V_c	ΔV_c^{75th}	ΔV_c^{25th}									
0.05	23.42	0.16	0.10	44.59	0.07	0.08	38.69	0.09	0.08	364.02	0.47	0.47
0.054	23.56	0.16	0.10	47.62	0.08	0.08	41.10	0.09	0.09	371.09	0.48	0.48
0.057	23.60	0.16	0.10	50.84	0.08	0.09	43.63	0.10	0.09	377.20	0.49	0.49
0.062	23.54	0.16	0.10	54.27	0.09	0.09	46.26	0.11	0.10	382.41	0.50	0.49
0.066	23.41	0.16	0.10	57.91	0.10	0.10	48.99	0.11	0.10	386.77	0.50	0.50
0.071	23.23	0.16	0.10	61.76	0.10	0.11	51.80	0.12	0.11	390.36	0.51	0.50
0.076	23.04	0.16	0.10	65.83	0.11	0.11	54.68	0.13	0.12	393.22	0.51	0.51
0.081	22.86	0.16	0.10	70.12	0.12	0.12	57.60	0.13	0.12	395.36	0.51	0.51
0.087	22.74	0.16	0.10	74.63	0.12	0.13	60.54	0.14	0.13	396.79	0.52	0.51
0.093	22.70	0.16	0.10	79.35	0.13	0.14	63.48	0.15	0.14	397.54	0.52	0.51
0.1	22.77	0.16	0.10	84.28	0.14	0.14	66.38	0.15	0.14	397.63	0.52	0.51
0.107	22.96	0.16	0.10	89.40	0.15	0.15	69.20	0.16	0.15	397.16	0.52	0.51
0.115	23.28	0.17	0.10	94.70	0.16	0.16	71.90	0.17	0.15	396.25	0.52	0.51
0.123	23.74	0.17	0.10	100.15	0.17	0.17	74.44	0.17	0.16	395.03	0.51	0.51
0.132	24.34	0.18	0.11	105.72	0.18	0.18	76.78	0.18	0.16	393.61	0.51	0.51
0.142	25.08	0.18	0.11	111.36	0.19	0.19	78.88	0.18	0.17	392.06	0.51	0.51
0.152	25.96	0.19	0.11	117.03	0.20	0.20	80.73	0.19	0.17	390.41	0.51	0.50
0.163	26.97	0.20	0.12	122.67	0.20	0.21	82.31	0.19	0.18	388.64	0.51	0.50
0.174	28.13	0.21	0.12	128.20	0.21	0.22	83.63	0.19	0.18	386.71	0.50	0.50
0.187	29.41	0.22	0.13	133.55	0.22	0.23	84.71	0.20	0.18	384.60	0.50	0.50
0.2	30.83	0.23	0.14	138.64	0.23	0.24	85.62	0.20	0.18	382.31	0.50	0.49
0.215	32.38	0.24	0.14	143.38	0.24	0.25	86.44	0.20	0.18	379.86	0.49	0.49
0.23	34.06	0.25	0.15	147.67	0.25	0.25	87.24	0.20	0.19	377.30	0.49	0.49
0.247	35.85	0.26	0.16	151.45	0.25	0.26	88.13	0.20	0.19	374.67	0.49	0.48
0.265	37.77	0.28	0.17	154.64	0.26	0.27	89.21	0.21	0.19	371.99	0.48	0.48
0.284	39.79	0.29	0.18	157.21	0.26	0.27	90.53	0.21	0.19	369.29	0.48	0.48
0.304	41.91	0.31	0.19	159.16	0.27	0.27	92.13	0.21	0.20	366.54	0.48	0.47
0.326	44.12	0.33	0.20	160.53	0.27	0.28	94.02	0.22	0.20	363.73	0.47	0.47
0.349	46.42	0.34	0.21	161.41	0.27	0.28	96.19	0.22	0.21	360.81	0.47	0.47
0.374	48.80	0.36	0.22	161.95	0.27	0.28	98.60	0.23	0.21	357.77	0.47	0.46
0.401	51.25	0.38	0.23	162.33	0.27	0.28	101.21	0.23	0.22	354.61	0.46	0.46
0.43	53.76	0.40	0.24	162.73	0.27	0.28	103.99	0.24	0.22	351.37	0.46	0.45
0.461	56.32	0.42	0.25	163.36	0.27	0.28	106.91	0.25	0.23	348.09	0.45	0.45
0.494	58.94	0.44	0.26	164.37	0.27	0.28	109.96	0.25	0.23	344.86	0.45	0.45
0.53	61.61	0.46	0.28	165.86	0.28	0.28	113.13	0.26	0.24	341.74	0.44	0.44
0.568	64.33	0.48	0.29	167.86	0.28	0.29	116.44	0.27	0.25	338.81	0.44	0.44
0.608	67.12	0.50	0.30	170.33	0.28	0.29	119.91	0.28	0.26	336.14	0.44	0.43
0.652	69.98	0.52	0.31	173.19	0.29	0.30	123.55	0.29	0.26	333.76	0.43	0.43
0.699	72.92	0.54	0.33	176.33	0.29	0.30	127.40	0.29	0.27	331.68	0.43	0.43
0.749	75.94	0.56	0.34	179.61	0.30	0.31	131.46	0.30	0.28	329.85	0.43	0.43
0.803	79.04	0.58	0.35	182.89	0.31	0.31	135.72	0.31	0.29	328.19	0.43	0.42
0.861	82.19	0.61	0.37	186.00	0.31	0.32	140.16	0.32	0.30	326.58	0.42	0.42
0.923	85.38	0.63	0.38	188.81	0.32	0.32	144.70	0.33	0.31	324.89	0.42	0.42
0.989	88.55	0.66	0.40	191.16	0.32	0.33	149.27	0.35	0.32	323.00	0.42	0.42
1.06	91.64	0.68	0.41	192.94	0.32	0.33	153.75	0.36	0.33	320.82	0.42	0.41
1.136	94.57	0.70	0.42	194.04	0.32	0.33	158.00	0.37	0.34	318.29	0.41	0.41
1.218	97.26	0.72	0.44	194.41	0.32	0.33	161.90	0.37	0.35	315.38	0.41	0.41
1.306	99.63	0.74	0.45	194.03	0.32	0.33	165.30	0.38	0.35	312.11	0.41	0.40
1.399	101.61	0.75	0.46	192.95	0.32	0.33	168.05	0.39	0.36	308.57	0.40	0.40
1.5	103.11	0.76	0.46	191.28	0.32	0.33	170.03	0.39	0.36	304.84	0.40	0.39

Table F24. Circular velocity curves of the 238 (E1–Sdm) CALIFA galaxies with 75th and 25th percentile uncertainties.

R/R_e	NGC4956			NGC4961			NGC5000			NGC5029		
	V_c	ΔV_c^{75th}	ΔV_c^{25th}									
0.05	67.04	0.13	0.11	34.61	0.12	0.11	38.96	0.12	0.11	239.35	0.32	0.31
0.054	71.64	0.14	0.12	36.83	0.13	0.12	41.35	0.12	0.12	253.00	0.34	0.33
0.057	76.53	0.15	0.13	39.17	0.13	0.13	43.84	0.13	0.13	266.94	0.36	0.35
0.062	81.73	0.16	0.13	41.64	0.14	0.14	46.43	0.14	0.13	281.05	0.38	0.37
0.066	87.25	0.17	0.14	44.24	0.15	0.15	49.10	0.15	0.14	295.22	0.40	0.39
0.071	93.10	0.19	0.15	46.97	0.16	0.16	51.84	0.16	0.15	309.31	0.42	0.40
0.076	99.29	0.20	0.16	49.82	0.17	0.17	54.64	0.17	0.16	323.16	0.44	0.42
0.081	105.81	0.21	0.17	52.78	0.18	0.18	57.48	0.17	0.17	336.59	0.46	0.44
0.087	112.68	0.23	0.19	55.84	0.19	0.19	60.34	0.18	0.17	349.43	0.47	0.46
0.093	119.88	0.24	0.20	58.99	0.21	0.20	63.21	0.19	0.18	361.50	0.49	0.47
0.1	127.41	0.26	0.21	62.21	0.22	0.21	66.05	0.20	0.19	372.60	0.51	0.49
0.107	135.26	0.27	0.22	65.47	0.23	0.22	68.86	0.21	0.20	382.60	0.52	0.50
0.115	143.41	0.29	0.24	68.76	0.24	0.23	71.61	0.22	0.21	391.39	0.53	0.51
0.123	151.82	0.30	0.25	72.03	0.25	0.24	74.29	0.23	0.21	398.89	0.54	0.52
0.132	160.45	0.32	0.26	75.28	0.26	0.25	76.89	0.23	0.22	405.13	0.55	0.53
0.142	169.25	0.34	0.28	78.46	0.27	0.26	79.41	0.24	0.23	410.16	0.56	0.54
0.152	178.15	0.36	0.29	81.54	0.29	0.27	81.86	0.25	0.24	414.14	0.56	0.54
0.163	187.08	0.37	0.31	84.51	0.30	0.28	84.25	0.26	0.24	417.26	0.57	0.55
0.174	195.95	0.39	0.32	87.35	0.31	0.29	86.60	0.26	0.25	419.74	0.57	0.55
0.187	204.65	0.41	0.34	90.06	0.32	0.30	88.90	0.27	0.26	421.80	0.57	0.55
0.2	213.07	0.43	0.35	92.66	0.32	0.31	91.18	0.28	0.26	423.59	0.57	0.55
0.215	221.09	0.44	0.36	95.18	0.33	0.32	93.43	0.28	0.27	425.23	0.58	0.56
0.23	228.60	0.46	0.38	97.69	0.34	0.33	95.64	0.29	0.28	426.76	0.58	0.56
0.247	235.48	0.47	0.39	100.27	0.35	0.34	97.76	0.30	0.28	428.15	0.58	0.56
0.265	241.64	0.48	0.40	103.02	0.36	0.35	99.78	0.30	0.29	429.39	0.58	0.56
0.284	247.00	0.50	0.41	106.01	0.37	0.36	101.64	0.31	0.29	430.42	0.58	0.56
0.304	251.53	0.50	0.41	109.33	0.38	0.37	103.31	0.31	0.30	431.25	0.58	0.56
0.326	255.24	0.51	0.42	113.03	0.40	0.38	104.77	0.32	0.30	431.88	0.59	0.57
0.349	258.17	0.52	0.43	117.12	0.41	0.39	106.02	0.32	0.31	432.36	0.59	0.57
0.374	260.40	0.52	0.43	121.56	0.43	0.41	107.06	0.33	0.31	432.72	0.59	0.57
0.401	262.06	0.53	0.43	126.31	0.44	0.43	107.95	0.33	0.31	432.97	0.59	0.57
0.43	263.29	0.53	0.43	131.27	0.46	0.44	108.74	0.33	0.31	433.06	0.59	0.57
0.461	264.20	0.53	0.44	136.34	0.48	0.46	109.51	0.33	0.32	432.93	0.59	0.57
0.494	264.91	0.53	0.44	141.40	0.50	0.48	110.35	0.34	0.32	432.50	0.59	0.57
0.53	265.48	0.53	0.44	146.34	0.51	0.49	111.33	0.34	0.32	431.69	0.59	0.57
0.568	265.95	0.53	0.44	151.03	0.53	0.51	112.50	0.34	0.33	430.45	0.58	0.56
0.608	266.33	0.53	0.44	155.34	0.54	0.52	113.90	0.35	0.33	428.78	0.58	0.56
0.652	266.59	0.53	0.44	159.14	0.56	0.54	115.52	0.35	0.33	426.70	0.58	0.56
0.699	266.74	0.53	0.44	162.29	0.57	0.55	117.34	0.36	0.34	424.27	0.58	0.56
0.749	266.77	0.53	0.44	164.69	0.58	0.55	119.30	0.36	0.35	421.54	0.57	0.55
0.803	266.69	0.53	0.44	166.24	0.58	0.56	121.35	0.37	0.35	418.56	0.57	0.55
0.861	266.51	0.53	0.44	166.88	0.58	0.56	123.40	0.38	0.36	415.30	0.56	0.54
0.923	266.27	0.53	0.44	166.61	0.58	0.56	125.37	0.38	0.36	411.72	0.56	0.54
0.989	265.94	0.53	0.44	165.47	0.58	0.56	127.18	0.39	0.37	407.73	0.55	0.53
1.06	265.52	0.53	0.44	163.61	0.57	0.55	128.76	0.39	0.37	403.28	0.55	0.53
1.136	264.95	0.53	0.44	161.19	0.56	0.54	130.04	0.40	0.38	398.32	0.54	0.52
1.218	264.17	0.53	0.44	158.46	0.55	0.53	130.96	0.40	0.38	392.87	0.53	0.51
1.306	263.10	0.53	0.43	155.67	0.55	0.52	131.48	0.40	0.38	387.04	0.52	0.51
1.399	261.70	0.52	0.43	153.07	0.54	0.52	131.60	0.40	0.38	381.00	0.52	0.50
1.5	259.92	0.52	0.43	150.81	0.53	0.51	131.31	0.40	0.38	374.95	0.51	0.49

Table F25. Circular velocity curves of the 238 (E1–Sdm) CALIFA galaxies with 75th and 25th percentile uncertainties.

R/R_e	NGC5056			NGC5218			NGC5378			NGC5480		
	V_c	ΔV_c^{75th}	ΔV_c^{25th}									
0.05	69.17	0.12	0.10	25.86	0.11	0.05	139.64	0.34	0.31	92.24	0.41	0.29
0.054	73.52	0.13	0.10	27.61	0.12	0.05	146.98	0.36	0.33	93.07	0.41	0.29
0.057	78.06	0.14	0.11	29.49	0.13	0.06	154.33	0.38	0.35	94.17	0.42	0.30
0.062	82.78	0.15	0.12	31.52	0.14	0.06	161.61	0.40	0.36	95.53	0.43	0.30
0.066	87.65	0.16	0.12	33.70	0.15	0.07	168.72	0.41	0.38	97.09	0.43	0.31
0.071	92.66	0.17	0.13	36.03	0.16	0.07	175.57	0.43	0.39	98.77	0.44	0.31
0.076	97.77	0.17	0.14	38.53	0.17	0.08	182.03	0.45	0.41	100.48	0.45	0.32
0.081	102.94	0.18	0.15	41.20	0.19	0.08	187.99	0.46	0.42	102.12	0.45	0.32
0.087	108.13	0.19	0.15	44.06	0.20	0.09	193.33	0.47	0.43	103.63	0.46	0.33
0.093	113.27	0.20	0.16	47.11	0.21	0.09	197.96	0.49	0.45	104.93	0.47	0.33
0.1	118.31	0.21	0.17	50.37	0.23	0.10	201.79	0.50	0.45	105.98	0.47	0.34
0.107	123.17	0.22	0.18	53.84	0.24	0.11	204.77	0.50	0.46	106.75	0.48	0.34
0.115	127.77	0.23	0.18	57.53	0.26	0.11	206.88	0.51	0.47	107.23	0.48	0.34
0.123	132.04	0.24	0.19	61.46	0.28	0.12	208.18	0.51	0.47	107.44	0.48	0.34
0.132	135.88	0.24	0.19	65.64	0.30	0.13	208.75	0.51	0.47	107.40	0.48	0.34
0.142	139.24	0.25	0.20	70.06	0.32	0.14	208.72	0.51	0.47	107.16	0.48	0.34
0.152	142.05	0.25	0.20	74.75	0.34	0.15	208.26	0.51	0.47	106.77	0.48	0.34
0.163	144.27	0.26	0.21	79.70	0.36	0.16	207.52	0.51	0.47	106.27	0.47	0.34
0.174	145.91	0.26	0.21	84.91	0.39	0.17	206.67	0.51	0.46	105.70	0.47	0.33
0.187	147.00	0.26	0.21	90.40	0.41	0.18	205.81	0.51	0.46	105.11	0.47	0.33
0.2	147.61	0.26	0.21	96.16	0.44	0.19	205.01	0.50	0.46	104.53	0.47	0.33
0.215	147.88	0.26	0.21	102.18	0.47	0.20	204.33	0.50	0.46	103.96	0.46	0.33
0.23	147.94	0.26	0.21	108.46	0.49	0.21	203.79	0.50	0.46	103.45	0.46	0.33
0.247	147.97	0.26	0.21	114.98	0.52	0.23	203.43	0.50	0.46	103.01	0.46	0.33
0.265	148.14	0.26	0.21	121.72	0.56	0.24	203.26	0.50	0.46	102.66	0.46	0.32
0.284	148.59	0.27	0.21	128.66	0.59	0.25	203.30	0.50	0.46	102.42	0.46	0.32
0.304	149.42	0.27	0.21	135.78	0.62	0.27	203.53	0.50	0.46	102.30	0.46	0.32
0.326	150.71	0.27	0.21	143.04	0.65	0.28	203.88	0.50	0.46	102.31	0.46	0.32
0.349	152.46	0.27	0.22	150.40	0.69	0.30	204.23	0.50	0.46	102.47	0.46	0.32
0.374	154.67	0.28	0.22	157.81	0.72	0.31	204.43	0.50	0.46	102.82	0.46	0.33
0.401	157.29	0.28	0.22	165.24	0.75	0.33	204.32	0.50	0.46	103.37	0.46	0.33
0.43	160.26	0.29	0.23	172.63	0.79	0.34	203.74	0.50	0.46	104.18	0.46	0.33
0.461	163.50	0.29	0.23	179.93	0.82	0.36	202.60	0.50	0.46	105.27	0.47	0.33
0.494	166.94	0.30	0.24	187.10	0.85	0.37	200.85	0.49	0.45	106.68	0.48	0.34
0.53	170.47	0.30	0.24	194.07	0.89	0.38	198.52	0.49	0.45	108.42	0.48	0.34
0.568	174.02	0.31	0.25	200.79	0.92	0.40	195.70	0.48	0.44	110.50	0.49	0.35
0.608	177.47	0.32	0.25	207.17	0.95	0.41	192.58	0.47	0.43	112.89	0.50	0.36
0.652	180.75	0.32	0.26	213.15	0.97	0.42	189.37	0.46	0.43	115.56	0.52	0.37
0.699	183.79	0.33	0.26	218.61	1.00	0.43	186.32	0.46	0.42	118.45	0.53	0.38
0.749	186.53	0.33	0.27	223.43	1.02	0.44	183.66	0.45	0.41	121.50	0.54	0.39
0.803	188.94	0.34	0.27	227.48	1.04	0.45	181.57	0.45	0.41	124.61	0.56	0.40
0.861	191.01	0.34	0.27	230.62	1.05	0.46	180.16	0.44	0.41	127.69	0.57	0.40
0.923	192.76	0.34	0.27	232.72	1.06	0.46	179.47	0.44	0.40	130.64	0.58	0.41
0.989	194.22	0.35	0.28	233.70	1.07	0.46	179.45	0.44	0.40	133.34	0.59	0.42
1.06	195.44	0.35	0.28	233.51	1.07	0.46	180.02	0.44	0.40	135.67	0.61	0.43
1.136	196.43	0.35	0.28	232.22	1.06	0.46	181.07	0.44	0.41	137.50	0.61	0.44
1.218	197.21	0.35	0.28	229.93	1.05	0.45	182.49	0.45	0.41	138.73	0.62	0.44
1.306	197.78	0.35	0.28	226.88	1.04	0.45	184.15	0.45	0.41	139.26	0.62	0.44
1.399	198.11	0.35	0.28	223.32	1.02	0.44	185.92	0.46	0.42	139.00	0.62	0.44
1.5	198.15	0.35	0.28	219.55	1.00	0.43	187.68	0.46	0.42	137.93	0.62	0.44

Table F26. Circular velocity curves of the 238 (E1–Sdm) CALIFA galaxies with 75th and 25th percentile uncertainties.

R/R_e	NGC5485			NGC5520			NGC5614			NGC5630		
	V_c	ΔV_c^{75th}	ΔV_c^{25th}									
0.05	217.52	0.27	0.31	84.94	0.20	0.16	111.82	0.22	0.19	33.22	0.12	0.11
0.054	222.44	0.28	0.32	88.68	0.21	0.17	119.18	0.24	0.20	34.98	0.13	0.11
0.057	227.12	0.28	0.32	92.32	0.22	0.17	126.92	0.25	0.21	36.76	0.13	0.12
0.062	231.63	0.29	0.33	95.80	0.23	0.18	135.05	0.27	0.22	38.56	0.14	0.13
0.066	236.05	0.29	0.34	99.09	0.23	0.19	143.56	0.28	0.24	40.34	0.15	0.13
0.071	240.44	0.30	0.34	102.15	0.24	0.19	152.42	0.30	0.25	42.10	0.15	0.14
0.076	244.81	0.30	0.35	104.95	0.25	0.20	161.62	0.32	0.27	43.81	0.16	0.14
0.081	249.13	0.31	0.36	107.50	0.25	0.20	171.12	0.34	0.28	45.45	0.17	0.15
0.087	253.35	0.31	0.36	109.79	0.26	0.21	180.87	0.36	0.30	47.00	0.17	0.15
0.093	257.36	0.32	0.37	111.87	0.26	0.21	190.82	0.38	0.32	48.45	0.18	0.16
0.1	261.08	0.32	0.37	113.81	0.27	0.21	200.89	0.40	0.33	49.79	0.18	0.16
0.107	264.43	0.33	0.38	115.70	0.27	0.22	211.00	0.42	0.35	51.02	0.19	0.17
0.115	267.36	0.33	0.38	117.66	0.28	0.22	221.04	0.44	0.37	52.15	0.19	0.17
0.123	269.88	0.33	0.38	119.79	0.28	0.22	230.90	0.46	0.38	53.21	0.20	0.18
0.132	272.03	0.34	0.39	122.22	0.29	0.23	240.46	0.48	0.40	54.24	0.20	0.18
0.142	273.92	0.34	0.39	125.04	0.30	0.23	249.57	0.49	0.41	55.29	0.20	0.18
0.152	275.71	0.34	0.39	128.29	0.30	0.24	258.12	0.51	0.43	56.41	0.21	0.19
0.163	277.56	0.34	0.40	132.03	0.31	0.25	265.95	0.53	0.44	57.66	0.21	0.19
0.174	279.64	0.35	0.40	136.24	0.32	0.26	272.98	0.54	0.45	59.09	0.22	0.19
0.187	282.07	0.35	0.40	140.89	0.33	0.26	279.10	0.55	0.46	60.73	0.22	0.20
0.2	284.92	0.35	0.41	145.95	0.35	0.27	284.29	0.56	0.47	62.59	0.23	0.21
0.215	288.20	0.36	0.41	151.35	0.36	0.28	288.52	0.57	0.48	64.65	0.24	0.21
0.23	291.84	0.36	0.42	157.01	0.37	0.29	291.86	0.58	0.49	66.91	0.25	0.22
0.247	295.71	0.37	0.42	162.84	0.39	0.31	294.38	0.58	0.49	69.33	0.26	0.23
0.265	299.67	0.37	0.43	168.74	0.40	0.32	296.20	0.59	0.49	71.86	0.27	0.24
0.284	303.52	0.38	0.43	174.59	0.41	0.33	297.45	0.59	0.49	74.47	0.28	0.25
0.304	307.09	0.38	0.44	180.24	0.43	0.34	298.24	0.59	0.50	77.10	0.29	0.25
0.326	310.20	0.38	0.44	185.57	0.44	0.35	298.68	0.59	0.50	79.72	0.29	0.26
0.349	312.72	0.39	0.45	190.41	0.45	0.36	298.81	0.59	0.50	82.29	0.30	0.27
0.374	314.54	0.39	0.45	194.62	0.46	0.37	298.67	0.59	0.50	84.77	0.31	0.28
0.401	315.60	0.39	0.45	198.04	0.47	0.37	298.28	0.59	0.50	87.13	0.32	0.29
0.43	315.89	0.39	0.45	200.54	0.48	0.38	297.68	0.59	0.49	89.35	0.33	0.29
0.461	315.47	0.39	0.45	202.02	0.48	0.38	296.91	0.59	0.49	91.44	0.34	0.30
0.494	314.42	0.39	0.45	202.44	0.48	0.38	296.06	0.59	0.49	93.40	0.35	0.31
0.53	312.84	0.39	0.45	201.80	0.48	0.38	295.20	0.58	0.49	95.28	0.35	0.31
0.568	310.84	0.39	0.44	200.16	0.48	0.38	294.42	0.58	0.49	97.14	0.36	0.32
0.608	308.48	0.38	0.44	197.70	0.47	0.37	293.77	0.58	0.49	99.03	0.37	0.33
0.652	305.83	0.38	0.44	194.64	0.46	0.37	293.25	0.58	0.49	101.03	0.37	0.33
0.699	302.90	0.38	0.43	191.23	0.45	0.36	292.81	0.58	0.49	103.21	0.38	0.34
0.749	299.72	0.37	0.43	187.77	0.45	0.35	292.34	0.58	0.49	105.60	0.39	0.35
0.803	296.35	0.37	0.42	184.49	0.44	0.35	291.74	0.58	0.48	108.23	0.40	0.36
0.861	292.88	0.36	0.42	181.58	0.43	0.34	290.87	0.57	0.48	111.07	0.41	0.37
0.923	289.42	0.36	0.41	179.12	0.43	0.34	289.64	0.57	0.48	114.07	0.42	0.38
0.989	286.09	0.35	0.41	177.11	0.42	0.33	288.01	0.57	0.48	117.17	0.43	0.39
1.06	282.98	0.35	0.40	175.50	0.42	0.33	285.96	0.57	0.48	120.29	0.45	0.40
1.136	280.10	0.35	0.40	174.17	0.41	0.33	283.57	0.56	0.47	123.32	0.46	0.41
1.218	277.40	0.34	0.40	173.05	0.41	0.33	280.93	0.56	0.47	126.20	0.47	0.42
1.306	274.78	0.34	0.39	172.04	0.41	0.32	278.18	0.55	0.46	128.81	0.48	0.42
1.399	272.07	0.34	0.39	171.07	0.41	0.32	275.44	0.54	0.46	131.09	0.49	0.43
1.5	269.12	0.33	0.38	170.08	0.40	0.32	272.83	0.54	0.45	132.95	0.49	0.44

Table F27. Circular velocity curves of the 238 (E1–Sdm) CALIFA galaxies with 75th and 25th percentile uncertainties.

R/R_e	NGC5633			NGC5657			NGC5682			NGC5720		
	V_c	ΔV_c^{75th}	ΔV_c^{25th}									
0.05	27.69	0.09	0.11	43.14	0.07	0.07	28.90	0.16	0.15	269.03	0.43	0.50
0.054	29.39	0.09	0.12	46.08	0.08	0.07	30.84	0.18	0.16	272.87	0.43	0.51
0.057	31.20	0.10	0.13	49.22	0.08	0.08	32.92	0.19	0.17	275.27	0.44	0.51
0.062	33.12	0.11	0.14	52.56	0.09	0.08	35.13	0.20	0.18	276.20	0.44	0.51
0.066	35.15	0.11	0.15	56.13	0.10	0.09	37.49	0.22	0.19	275.75	0.44	0.51
0.071	37.29	0.12	0.16	59.93	0.10	0.10	40.00	0.23	0.21	274.12	0.44	0.51
0.076	39.53	0.13	0.17	63.96	0.11	0.10	42.66	0.25	0.22	271.60	0.43	0.50
0.081	41.87	0.14	0.18	68.23	0.12	0.11	45.47	0.26	0.24	268.60	0.43	0.50
0.087	44.30	0.14	0.19	72.74	0.12	0.12	48.45	0.28	0.25	265.54	0.42	0.49
0.093	46.82	0.15	0.20	77.51	0.13	0.13	51.58	0.30	0.27	262.84	0.42	0.49
0.1	49.41	0.16	0.21	82.53	0.14	0.13	54.88	0.32	0.29	260.82	0.41	0.48
0.107	52.07	0.17	0.22	87.79	0.15	0.14	58.32	0.34	0.31	259.66	0.41	0.48
0.115	54.78	0.18	0.23	93.30	0.16	0.15	61.92	0.36	0.32	259.36	0.41	0.48
0.123	57.53	0.19	0.24	99.04	0.17	0.16	65.66	0.38	0.34	259.79	0.41	0.48
0.132	60.31	0.20	0.26	104.99	0.18	0.17	69.53	0.40	0.36	260.72	0.41	0.48
0.142	63.11	0.21	0.27	111.14	0.19	0.18	73.50	0.43	0.39	261.90	0.42	0.49
0.152	65.92	0.21	0.28	117.46	0.20	0.19	77.57	0.45	0.41	263.08	0.42	0.49
0.163	68.74	0.22	0.29	123.91	0.21	0.20	81.70	0.47	0.43	264.04	0.42	0.49
0.174	71.55	0.23	0.30	130.43	0.22	0.21	85.86	0.50	0.45	264.62	0.42	0.49
0.187	74.37	0.24	0.32	136.99	0.23	0.22	90.01	0.52	0.47	264.71	0.42	0.49
0.2	77.19	0.25	0.33	143.52	0.24	0.23	94.11	0.55	0.49	264.23	0.42	0.49
0.215	80.02	0.26	0.34	149.95	0.26	0.24	98.13	0.57	0.52	263.19	0.42	0.49
0.23	82.87	0.27	0.35	156.20	0.27	0.25	102.00	0.59	0.54	261.61	0.42	0.48
0.247	85.74	0.28	0.36	162.20	0.28	0.26	105.70	0.61	0.56	259.56	0.41	0.48
0.265	88.65	0.29	0.38	167.87	0.29	0.27	109.16	0.63	0.57	257.13	0.41	0.48
0.284	91.61	0.30	0.39	173.15	0.30	0.28	112.36	0.65	0.59	254.40	0.40	0.47
0.304	94.62	0.31	0.40	177.97	0.30	0.29	115.27	0.67	0.61	251.47	0.40	0.47
0.326	97.70	0.32	0.42	182.30	0.31	0.30	117.86	0.68	0.62	248.40	0.40	0.46
0.349	100.88	0.33	0.43	186.10	0.32	0.30	120.14	0.70	0.63	245.25	0.39	0.45
0.374	104.19	0.34	0.44	189.38	0.32	0.31	122.09	0.71	0.64	242.11	0.39	0.45
0.401	107.69	0.35	0.46	192.16	0.33	0.31	123.72	0.72	0.65	239.05	0.38	0.44
0.43	111.42	0.36	0.47	194.47	0.33	0.32	125.05	0.73	0.66	236.19	0.38	0.44
0.461	115.44	0.38	0.49	196.35	0.33	0.32	126.08	0.73	0.66	233.65	0.37	0.43
0.494	119.80	0.39	0.51	197.85	0.34	0.32	126.81	0.74	0.67	231.56	0.37	0.43
0.53	124.51	0.41	0.53	198.98	0.34	0.32	127.26	0.74	0.67	230.02	0.37	0.43
0.568	129.60	0.42	0.55	199.78	0.34	0.33	127.43	0.74	0.67	229.13	0.36	0.42
0.608	135.05	0.44	0.57	200.28	0.34	0.33	127.37	0.74	0.67	228.92	0.36	0.42
0.652	140.82	0.46	0.60	200.51	0.34	0.33	127.15	0.74	0.67	229.41	0.37	0.43
0.699	146.88	0.48	0.62	200.50	0.34	0.33	126.86	0.74	0.67	230.57	0.37	0.43
0.749	153.13	0.50	0.65	200.31	0.34	0.33	126.61	0.73	0.67	232.33	0.37	0.43
0.803	159.51	0.52	0.68	199.97	0.34	0.33	126.54	0.73	0.67	234.61	0.37	0.43
0.861	165.89	0.54	0.71	199.51	0.34	0.33	126.73	0.74	0.67	237.29	0.38	0.44
0.923	172.18	0.56	0.73	198.90	0.34	0.32	127.26	0.74	0.67	240.22	0.38	0.45
0.989	178.21	0.58	0.76	198.10	0.34	0.32	128.13	0.74	0.67	243.27	0.39	0.45
1.06	183.86	0.60	0.78	197.01	0.34	0.32	129.33	0.75	0.68	246.24	0.39	0.46
1.136	188.95	0.62	0.80	195.56	0.33	0.32	130.77	0.76	0.69	248.96	0.40	0.46
1.218	193.32	0.63	0.82	193.66	0.33	0.32	132.35	0.77	0.70	251.25	0.40	0.47
1.306	196.80	0.64	0.84	191.26	0.33	0.31	133.96	0.78	0.70	252.93	0.40	0.47
1.399	199.22	0.65	0.85	188.35	0.32	0.31	135.46	0.79	0.71	253.85	0.40	0.47
1.5	200.46	0.66	0.85	184.99	0.32	0.30	136.72	0.79	0.72	253.92	0.40	0.47

Table F28. Circular velocity curves of the 238 (E1–Sdm) CALIFA galaxies with 75th and 25th percentile uncertainties.

R/R_e	NGC5732			NGC5784			NGC5876			NGC5888		
	V_c	ΔV_c^{75th}	ΔV_c^{25th}									
0.05	35.54	0.19	0.16	159.10	0.17	0.15	89.31	0.11	0.12	108.22	0.12	0.10
0.054	37.89	0.20	0.17	169.54	0.18	0.16	95.47	0.12	0.13	115.02	0.13	0.11
0.057	40.40	0.21	0.18	180.53	0.19	0.17	102.03	0.13	0.14	122.11	0.14	0.11
0.062	43.05	0.23	0.20	192.04	0.20	0.18	109.01	0.14	0.15	129.46	0.15	0.12
0.066	45.86	0.24	0.21	204.06	0.22	0.19	116.42	0.14	0.16	137.05	0.16	0.13
0.071	48.83	0.26	0.22	216.58	0.23	0.20	124.27	0.15	0.17	144.84	0.17	0.14
0.076	51.94	0.27	0.24	229.54	0.24	0.22	132.58	0.16	0.18	152.78	0.17	0.14
0.081	55.21	0.29	0.25	242.89	0.26	0.23	141.35	0.18	0.19	160.82	0.18	0.15
0.087	58.63	0.31	0.27	256.56	0.27	0.24	150.60	0.19	0.20	168.89	0.19	0.16
0.093	62.18	0.33	0.29	270.45	0.29	0.26	160.31	0.20	0.22	176.91	0.20	0.17
0.1	65.86	0.35	0.30	284.45	0.30	0.27	170.49	0.21	0.23	184.80	0.21	0.17
0.107	69.64	0.37	0.32	298.42	0.31	0.28	181.11	0.23	0.24	192.45	0.22	0.18
0.115	73.51	0.39	0.34	312.20	0.33	0.30	192.15	0.24	0.26	199.78	0.23	0.19
0.123	77.44	0.41	0.36	325.60	0.34	0.31	203.58	0.25	0.27	206.68	0.24	0.19
0.132	81.40	0.43	0.37	338.41	0.36	0.32	215.34	0.27	0.29	213.07	0.24	0.20
0.142	85.35	0.45	0.39	350.42	0.37	0.33	227.37	0.28	0.31	218.90	0.25	0.21
0.152	89.25	0.47	0.41	361.41	0.38	0.34	239.58	0.30	0.32	224.11	0.26	0.21
0.163	93.04	0.49	0.43	371.16	0.39	0.35	251.87	0.31	0.34	228.71	0.26	0.21
0.174	96.69	0.51	0.44	379.47	0.40	0.36	264.13	0.33	0.36	232.73	0.27	0.22
0.187	100.13	0.53	0.46	386.22	0.41	0.37	276.22	0.34	0.37	236.25	0.27	0.22
0.2	103.32	0.55	0.48	391.31	0.41	0.37	287.99	0.36	0.39	239.35	0.27	0.22
0.215	106.23	0.56	0.49	394.73	0.42	0.37	299.26	0.37	0.40	242.14	0.28	0.23
0.23	108.82	0.58	0.50	396.57	0.42	0.38	309.87	0.39	0.42	244.74	0.28	0.23
0.247	111.10	0.59	0.51	397.00	0.42	0.38	319.66	0.40	0.43	247.19	0.28	0.23
0.265	113.09	0.60	0.52	396.27	0.42	0.38	328.47	0.41	0.44	249.50	0.28	0.23
0.284	114.83	0.61	0.53	394.67	0.42	0.37	336.18	0.42	0.45	251.63	0.29	0.24
0.304	116.40	0.62	0.54	392.49	0.41	0.37	342.73	0.43	0.46	253.49	0.29	0.24
0.326	117.90	0.63	0.54	389.98	0.41	0.37	348.09	0.43	0.47	254.97	0.29	0.24
0.349	119.45	0.63	0.55	387.35	0.41	0.37	352.32	0.44	0.48	255.96	0.29	0.24
0.374	121.16	0.64	0.56	384.68	0.41	0.36	355.53	0.44	0.48	256.40	0.29	0.24
0.401	123.13	0.65	0.57	382.04	0.40	0.36	357.88	0.45	0.48	256.28	0.29	0.24
0.43	125.41	0.67	0.58	379.40	0.40	0.36	359.58	0.45	0.48	255.68	0.29	0.24
0.461	128.02	0.68	0.59	376.77	0.40	0.36	360.78	0.45	0.49	254.74	0.29	0.24
0.494	130.94	0.70	0.60	374.14	0.39	0.35	361.63	0.45	0.49	253.67	0.29	0.24
0.53	134.11	0.71	0.62	371.51	0.39	0.35	362.18	0.45	0.49	252.73	0.29	0.24
0.568	137.45	0.73	0.63	368.92	0.39	0.35	362.38	0.45	0.49	252.16	0.29	0.24
0.608	140.87	0.75	0.65	366.39	0.39	0.35	362.10	0.45	0.49	252.21	0.29	0.24
0.652	144.27	0.77	0.66	363.90	0.38	0.34	361.17	0.45	0.49	253.01	0.29	0.24
0.699	147.54	0.78	0.68	361.43	0.38	0.34	359.39	0.45	0.48	254.66	0.29	0.24
0.749	150.61	0.80	0.69	358.90	0.38	0.34	356.58	0.44	0.48	257.13	0.29	0.24
0.803	153.38	0.81	0.71	356.20	0.38	0.34	352.66	0.44	0.48	260.36	0.30	0.24
0.861	155.78	0.83	0.72	353.23	0.37	0.33	347.57	0.43	0.47	264.21	0.30	0.25
0.923	157.79	0.84	0.73	349.88	0.37	0.33	341.41	0.42	0.46	268.55	0.31	0.25
0.989	159.39	0.85	0.73	346.08	0.36	0.33	334.34	0.42	0.45	273.19	0.31	0.26
1.06	160.61	0.85	0.74	341.83	0.36	0.32	326.60	0.41	0.44	277.99	0.32	0.26
1.136	161.50	0.86	0.74	337.16	0.36	0.32	318.50	0.40	0.43	282.75	0.32	0.27
1.218	162.14	0.86	0.75	332.18	0.35	0.31	310.34	0.39	0.42	287.31	0.33	0.27
1.306	162.63	0.86	0.75	327.02	0.34	0.31	302.42	0.38	0.41	291.50	0.33	0.27
1.399	163.04	0.87	0.75	321.84	0.34	0.30	294.95	0.37	0.40	295.17	0.34	0.28
1.5	163.44	0.87	0.75	316.79	0.33	0.30	288.09	0.36	0.39	298.16	0.34	0.28

Table F29. Circular velocity curves of the 238 (E1–Sdm) CALIFA galaxies with 75th and 25th percentile uncertainties.

R/R_e	NGC5908			NGC5971			NGC5980			NGC5987		
	V_c	ΔV_c^{75th}	ΔV_c^{25th}									
0.05	165.56	0.20	0.16	74.61	0.26	0.19	53.22	0.13	0.09	236.21	0.44	0.26
0.054	173.07	0.21	0.17	79.48	0.28	0.20	56.77	0.14	0.09	245.26	0.45	0.27
0.057	180.35	0.22	0.17	84.60	0.30	0.21	60.53	0.15	0.10	253.72	0.47	0.28
0.062	187.28	0.22	0.18	89.97	0.32	0.23	64.50	0.16	0.10	261.43	0.48	0.29
0.066	193.75	0.23	0.19	95.58	0.33	0.24	68.68	0.17	0.11	268.28	0.50	0.29
0.071	199.64	0.24	0.19	101.43	0.36	0.25	73.08	0.18	0.12	274.14	0.51	0.30
0.076	204.84	0.25	0.20	107.48	0.38	0.27	77.68	0.19	0.13	278.96	0.52	0.31
0.081	209.27	0.25	0.20	113.73	0.40	0.29	82.48	0.20	0.13	282.73	0.52	0.31
0.087	212.86	0.26	0.20	120.14	0.42	0.30	87.47	0.21	0.14	285.48	0.53	0.31
0.093	215.61	0.26	0.21	126.67	0.44	0.32	92.65	0.22	0.15	287.34	0.53	0.31
0.1	217.57	0.26	0.21	133.27	0.47	0.33	97.97	0.24	0.16	288.48	0.53	0.32
0.107	218.83	0.26	0.21	139.89	0.49	0.35	103.44	0.25	0.17	289.10	0.54	0.32
0.115	219.58	0.26	0.21	146.46	0.51	0.37	109.00	0.26	0.18	289.41	0.54	0.32
0.123	220.03	0.26	0.21	152.90	0.54	0.38	114.64	0.28	0.19	289.60	0.54	0.32
0.132	220.44	0.26	0.21	159.16	0.56	0.40	120.31	0.29	0.19	289.77	0.54	0.32
0.142	221.04	0.26	0.21	165.13	0.58	0.41	125.97	0.31	0.20	289.97	0.54	0.32
0.152	222.05	0.27	0.21	170.75	0.60	0.43	131.58	0.32	0.21	290.18	0.54	0.32
0.163	223.63	0.27	0.21	175.95	0.62	0.44	137.10	0.33	0.22	290.31	0.54	0.32
0.174	225.83	0.27	0.22	180.66	0.63	0.45	142.47	0.35	0.23	290.29	0.54	0.32
0.187	228.66	0.27	0.22	184.83	0.65	0.46	147.68	0.36	0.24	290.02	0.54	0.32
0.2	232.05	0.28	0.22	188.45	0.66	0.47	152.68	0.37	0.25	289.47	0.54	0.32
0.215	235.92	0.28	0.23	191.50	0.67	0.48	157.46	0.38	0.25	288.65	0.54	0.32
0.23	240.14	0.29	0.23	194.00	0.68	0.49	162.00	0.39	0.26	287.64	0.53	0.31
0.247	244.61	0.29	0.23	196.00	0.69	0.49	166.29	0.40	0.27	286.53	0.53	0.31
0.265	249.23	0.30	0.24	197.52	0.69	0.50	170.32	0.41	0.28	285.43	0.53	0.31
0.284	253.91	0.30	0.24	198.63	0.70	0.50	174.07	0.42	0.28	284.47	0.53	0.31
0.304	258.60	0.31	0.25	199.39	0.70	0.50	177.54	0.43	0.29	283.69	0.53	0.31
0.326	263.24	0.32	0.25	199.86	0.70	0.50	180.72	0.44	0.29	283.11	0.52	0.31
0.349	267.82	0.32	0.26	200.10	0.70	0.50	183.58	0.45	0.30	282.68	0.52	0.31
0.374	272.30	0.33	0.26	200.18	0.70	0.50	186.14	0.45	0.30	282.31	0.52	0.31
0.401	276.67	0.33	0.27	200.19	0.70	0.50	188.43	0.46	0.30	281.86	0.52	0.31
0.43	280.88	0.34	0.27	200.18	0.70	0.50	190.50	0.46	0.31	281.21	0.52	0.31
0.461	284.88	0.34	0.27	200.20	0.70	0.50	192.45	0.47	0.31	280.27	0.52	0.31
0.494	288.60	0.35	0.28	200.27	0.70	0.50	194.41	0.47	0.31	278.96	0.52	0.31
0.53	291.94	0.35	0.28	200.39	0.70	0.50	196.48	0.48	0.32	277.30	0.51	0.30
0.568	294.84	0.35	0.28	200.52	0.70	0.50	198.80	0.48	0.32	275.32	0.51	0.30
0.608	297.24	0.36	0.29	200.62	0.70	0.50	201.41	0.49	0.33	273.11	0.51	0.30
0.652	299.14	0.36	0.29	200.63	0.70	0.50	204.36	0.50	0.33	270.81	0.50	0.30
0.699	300.59	0.36	0.29	200.51	0.70	0.50	207.60	0.50	0.34	268.54	0.50	0.29
0.749	301.68	0.36	0.29	200.24	0.70	0.50	211.05	0.51	0.34	266.43	0.49	0.29
0.803	302.55	0.36	0.29	199.78	0.70	0.50	214.61	0.52	0.35	264.55	0.49	0.29
0.861	303.33	0.36	0.29	199.12	0.70	0.50	218.14	0.53	0.35	262.91	0.49	0.29
0.923	304.13	0.36	0.29	198.22	0.70	0.50	221.52	0.54	0.36	261.49	0.48	0.29
0.989	305.00	0.37	0.29	197.06	0.69	0.50	224.65	0.55	0.36	260.18	0.48	0.28
1.06	305.94	0.37	0.29	195.62	0.69	0.49	227.44	0.55	0.37	258.87	0.48	0.28
1.136	306.86	0.37	0.29	193.89	0.68	0.49	229.84	0.56	0.37	257.39	0.48	0.28
1.218	307.64	0.37	0.30	191.89	0.67	0.48	231.81	0.56	0.37	255.63	0.47	0.28
1.306	308.15	0.37	0.30	189.67	0.67	0.48	233.34	0.57	0.38	253.48	0.47	0.28
1.399	308.23	0.37	0.30	187.31	0.66	0.47	234.44	0.57	0.38	250.87	0.47	0.27
1.5	307.75	0.37	0.30	184.93	0.65	0.46	235.10	0.57	0.38	247.80	0.46	0.27

Table F30. Circular velocity curves of the 238 (E1–Sdm) CALIFA galaxies with 75th and 25th percentile uncertainties.

R/R_e	NGC6020			NGC6021			NGC6032			NGC6060		
	V_c	ΔV_c^{75th}	ΔV_c^{25th}									
0.05	186.22	0.53	0.39	88.01	0.20	0.18	48.82	0.48	0.22	132.28	0.26	0.23
0.054	196.88	0.57	0.41	94.06	0.22	0.19	51.44	0.50	0.23	139.68	0.28	0.24
0.057	207.77	0.60	0.43	100.50	0.23	0.20	54.08	0.53	0.24	147.19	0.29	0.25
0.062	218.81	0.63	0.46	107.33	0.25	0.21	56.72	0.56	0.25	154.78	0.31	0.26
0.066	229.91	0.66	0.48	114.58	0.26	0.23	59.33	0.58	0.26	162.37	0.32	0.28
0.071	240.95	0.69	0.50	122.25	0.28	0.24	61.89	0.61	0.27	169.88	0.34	0.29
0.076	251.82	0.72	0.53	130.35	0.30	0.26	64.35	0.63	0.28	177.24	0.35	0.30
0.081	262.37	0.75	0.55	138.90	0.32	0.28	66.70	0.65	0.29	184.36	0.37	0.31
0.087	272.47	0.78	0.57	147.88	0.34	0.30	68.88	0.68	0.30	191.14	0.38	0.33
0.093	281.97	0.81	0.59	157.29	0.36	0.31	70.89	0.70	0.31	197.50	0.40	0.34
0.1	290.73	0.83	0.61	167.13	0.38	0.33	72.70	0.71	0.32	203.37	0.41	0.35
0.107	298.65	0.86	0.62	177.37	0.41	0.36	74.30	0.73	0.33	208.66	0.42	0.36
0.115	305.63	0.88	0.64	187.98	0.43	0.38	75.69	0.74	0.33	213.33	0.43	0.36
0.123	311.65	0.89	0.65	198.91	0.46	0.40	76.90	0.75	0.34	217.35	0.43	0.37
0.132	316.70	0.91	0.66	210.11	0.48	0.42	77.95	0.76	0.34	220.69	0.44	0.38
0.142	320.87	0.92	0.67	221.52	0.51	0.44	78.88	0.77	0.35	223.33	0.45	0.38
0.152	324.27	0.93	0.68	233.03	0.54	0.47	79.74	0.78	0.35	225.26	0.45	0.38
0.163	327.03	0.94	0.68	244.56	0.56	0.49	80.56	0.79	0.36	226.47	0.45	0.39
0.174	329.30	0.95	0.69	255.98	0.59	0.51	81.36	0.80	0.36	226.93	0.45	0.39
0.187	331.20	0.95	0.69	267.15	0.61	0.54	82.15	0.81	0.36	226.60	0.45	0.39
0.2	332.79	0.96	0.70	277.95	0.64	0.56	82.91	0.81	0.37	225.46	0.45	0.38
0.215	334.08	0.96	0.70	288.22	0.66	0.58	83.62	0.82	0.37	223.51	0.45	0.38
0.23	335.02	0.96	0.70	297.82	0.68	0.60	84.24	0.83	0.37	220.82	0.44	0.38
0.247	335.57	0.96	0.70	306.62	0.70	0.61	84.75	0.83	0.38	217.49	0.44	0.37
0.265	335.71	0.96	0.70	314.51	0.72	0.63	85.11	0.84	0.38	213.74	0.43	0.36
0.284	335.45	0.96	0.70	321.42	0.74	0.64	85.35	0.84	0.38	209.78	0.42	0.36
0.304	334.86	0.96	0.70	327.31	0.75	0.66	85.49	0.84	0.38	205.87	0.41	0.35
0.326	334.02	0.96	0.70	332.22	0.76	0.67	85.57	0.84	0.38	202.23	0.40	0.34
0.349	333.05	0.96	0.70	336.19	0.77	0.67	85.68	0.84	0.38	199.00	0.40	0.34
0.374	332.00	0.95	0.69	339.33	0.78	0.68	85.91	0.84	0.38	196.27	0.39	0.33
0.401	330.88	0.95	0.69	341.76	0.78	0.68	86.33	0.85	0.38	194.03	0.39	0.33
0.43	329.66	0.95	0.69	343.60	0.79	0.69	87.04	0.85	0.39	192.27	0.38	0.33
0.461	328.28	0.94	0.69	344.95	0.79	0.69	88.08	0.86	0.39	190.94	0.38	0.33
0.494	326.64	0.94	0.68	345.89	0.79	0.69	89.49	0.88	0.40	190.04	0.38	0.32
0.53	324.70	0.93	0.68	346.44	0.80	0.69	91.27	0.90	0.40	189.60	0.38	0.32
0.568	322.42	0.93	0.67	346.61	0.80	0.69	93.39	0.92	0.41	189.67	0.38	0.32
0.608	319.82	0.92	0.67	346.39	0.80	0.69	95.83	0.94	0.42	190.31	0.38	0.32
0.652	316.93	0.91	0.66	345.79	0.79	0.69	98.53	0.97	0.44	191.57	0.38	0.33
0.699	313.81	0.90	0.66	344.79	0.79	0.69	101.44	1.00	0.45	193.48	0.39	0.33
0.749	310.49	0.89	0.65	343.38	0.79	0.69	104.48	1.03	0.46	196.04	0.39	0.33
0.803	307.01	0.88	0.64	341.57	0.78	0.68	107.59	1.06	0.48	199.21	0.40	0.34
0.861	303.37	0.87	0.63	339.33	0.78	0.68	110.69	1.09	0.49	202.93	0.41	0.35
0.923	299.56	0.86	0.63	336.66	0.77	0.67	113.68	1.12	0.50	207.10	0.41	0.35
0.989	295.59	0.85	0.62	333.55	0.77	0.67	116.48	1.14	0.52	211.59	0.42	0.36
1.06	291.46	0.84	0.61	330.02	0.76	0.66	118.99	1.17	0.53	216.28	0.43	0.37
1.136	287.16	0.82	0.60	326.10	0.75	0.65	121.13	1.19	0.54	220.98	0.44	0.38
1.218	282.72	0.81	0.59	321.86	0.74	0.64	122.80	1.21	0.54	225.53	0.45	0.38
1.306	278.14	0.80	0.58	317.40	0.73	0.64	123.94	1.22	0.55	229.72	0.46	0.39
1.399	273.41	0.79	0.57	312.84	0.72	0.63	124.50	1.22	0.55	233.37	0.47	0.40
1.5	268.54	0.77	0.56	308.30	0.71	0.62	124.44	1.22	0.55	236.26	0.47	0.40

Table F31. Circular velocity curves of the 238 (E1–Sdm) CALIFA galaxies with 75th and 25th percentile uncertainties.

R/R_e	NGC6063			NGC6081			NGC6125			NGC6132		
	V_c	ΔV_c^{75th}	ΔV_c^{25th}									
0.05	44.72	0.10	0.09	121.23	0.25	0.22	342.28	0.47	0.33	71.97	0.15	0.17
0.054	46.62	0.10	0.10	129.04	0.27	0.23	360.01	0.50	0.34	74.82	0.16	0.17
0.057	48.48	0.10	0.10	137.24	0.29	0.24	377.69	0.52	0.36	77.48	0.16	0.18
0.062	50.28	0.11	0.11	145.80	0.31	0.26	395.11	0.54	0.38	79.89	0.17	0.18
0.066	52.01	0.11	0.11	154.70	0.32	0.28	412.02	0.57	0.39	81.98	0.17	0.19
0.071	53.66	0.11	0.11	163.92	0.34	0.29	428.14	0.59	0.41	83.70	0.18	0.19
0.076	55.23	0.12	0.12	173.41	0.36	0.31	443.19	0.61	0.42	85.01	0.18	0.20
0.081	56.74	0.12	0.12	183.14	0.38	0.33	456.86	0.63	0.44	85.86	0.18	0.20
0.087	58.19	0.12	0.12	193.03	0.40	0.34	468.87	0.65	0.45	86.25	0.18	0.20
0.093	59.60	0.13	0.13	203.01	0.43	0.36	478.96	0.66	0.46	86.19	0.18	0.20
0.1	61.00	0.13	0.13	213.00	0.45	0.38	486.94	0.67	0.47	85.74	0.18	0.20
0.107	62.41	0.13	0.13	222.89	0.47	0.40	492.71	0.68	0.47	85.01	0.18	0.20
0.115	63.83	0.14	0.13	232.58	0.49	0.41	496.28	0.68	0.48	84.13	0.18	0.19
0.123	65.27	0.14	0.14	241.94	0.51	0.43	497.81	0.69	0.48	83.27	0.18	0.19
0.132	66.72	0.14	0.14	250.87	0.53	0.45	497.62	0.69	0.48	82.60	0.18	0.19
0.142	68.17	0.15	0.14	259.25	0.54	0.46	496.12	0.68	0.47	82.28	0.18	0.19
0.152	69.59	0.15	0.15	266.99	0.56	0.48	493.81	0.68	0.47	82.44	0.18	0.19
0.163	70.97	0.15	0.15	274.03	0.57	0.49	491.16	0.68	0.47	83.16	0.18	0.19
0.174	72.30	0.16	0.15	280.33	0.59	0.50	488.54	0.67	0.47	84.45	0.18	0.20
0.187	73.56	0.16	0.15	285.92	0.60	0.51	486.15	0.67	0.47	86.31	0.18	0.20
0.2	74.78	0.16	0.16	290.84	0.61	0.52	484.00	0.67	0.46	88.68	0.19	0.20
0.215	75.98	0.16	0.16	295.21	0.62	0.53	481.91	0.66	0.46	91.52	0.19	0.21
0.23	77.20	0.17	0.16	299.12	0.63	0.53	479.63	0.66	0.46	94.80	0.20	0.22
0.247	78.50	0.17	0.17	302.70	0.63	0.54	476.92	0.66	0.46	98.45	0.21	0.23
0.265	79.92	0.17	0.17	306.03	0.64	0.55	473.61	0.65	0.45	102.44	0.22	0.24
0.284	81.51	0.18	0.17	309.15	0.65	0.55	469.67	0.65	0.45	106.72	0.23	0.25
0.304	83.31	0.18	0.18	312.03	0.65	0.56	465.19	0.64	0.45	111.25	0.24	0.26
0.326	85.33	0.18	0.18	314.59	0.66	0.56	460.34	0.63	0.44	115.96	0.25	0.27
0.349	87.57	0.19	0.18	316.74	0.66	0.56	455.34	0.63	0.44	120.81	0.26	0.28
0.374	90.02	0.19	0.19	318.35	0.67	0.57	450.38	0.62	0.43	125.71	0.27	0.29
0.401	92.66	0.20	0.20	319.36	0.67	0.57	445.60	0.61	0.43	130.61	0.28	0.30
0.43	95.47	0.21	0.20	319.70	0.67	0.57	441.03	0.61	0.42	135.44	0.29	0.31
0.461	98.42	0.21	0.21	319.39	0.67	0.57	436.64	0.60	0.42	140.12	0.30	0.32
0.494	101.51	0.22	0.21	318.46	0.67	0.57	432.37	0.60	0.41	144.58	0.31	0.33
0.53	104.73	0.22	0.22	316.98	0.66	0.56	428.11	0.59	0.41	148.78	0.32	0.34
0.568	108.08	0.23	0.23	315.06	0.66	0.56	423.82	0.58	0.41	152.67	0.33	0.35
0.608	111.59	0.24	0.23	312.80	0.66	0.56	419.46	0.58	0.40	156.23	0.33	0.36
0.652	115.27	0.25	0.24	310.26	0.65	0.55	415.01	0.57	0.40	159.48	0.34	0.37
0.699	119.14	0.26	0.25	307.49	0.65	0.55	410.43	0.57	0.39	162.45	0.35	0.38
0.749	123.23	0.26	0.26	304.50	0.64	0.54	405.71	0.56	0.39	165.21	0.35	0.38
0.803	127.53	0.27	0.27	301.27	0.63	0.54	400.82	0.55	0.38	167.85	0.36	0.39
0.861	132.03	0.28	0.28	297.77	0.62	0.53	395.71	0.55	0.38	170.47	0.36	0.39
0.923	136.69	0.29	0.29	293.98	0.62	0.52	390.41	0.54	0.37	173.15	0.37	0.40
0.989	141.44	0.30	0.30	289.93	0.61	0.52	384.92	0.53	0.37	175.92	0.37	0.41
1.06	146.22	0.31	0.31	285.65	0.60	0.51	379.31	0.52	0.36	178.77	0.38	0.41
1.136	150.91	0.32	0.32	281.25	0.59	0.50	373.60	0.51	0.36	181.64	0.39	0.42
1.218	155.39	0.33	0.33	276.82	0.58	0.49	367.83	0.51	0.35	184.40	0.39	0.43
1.306	159.53	0.34	0.34	272.49	0.57	0.49	361.98	0.50	0.35	186.89	0.40	0.43
1.399	163.21	0.35	0.34	268.41	0.56	0.48	355.97	0.49	0.34	188.95	0.40	0.44
1.5	166.27	0.36	0.35	264.69	0.56	0.47	349.73	0.48	0.33	190.42	0.41	0.44

Table F32. Circular velocity curves of the 238 (E1–Sdm) CALIFA galaxies with 75th and 25th percentile uncertainties.

R/R_e	NGC6146			NGC6150			NGC6168			NGC6173		
	V_c	ΔV_c^{75th}	ΔV_c^{25th}									
0.05	215.97	0.44	0.32	124.85	0.17	0.18	12.14	0.05	0.05	374.42	0.53	0.51
0.054	229.86	0.46	0.34	133.16	0.19	0.19	12.85	0.06	0.05	390.04	0.55	0.54
0.057	244.39	0.49	0.36	141.92	0.20	0.20	13.63	0.06	0.06	404.89	0.58	0.56
0.062	259.53	0.52	0.38	151.13	0.21	0.21	14.48	0.07	0.06	418.71	0.60	0.57
0.066	275.26	0.55	0.41	160.81	0.23	0.23	15.40	0.07	0.07	431.27	0.61	0.59
0.071	291.50	0.59	0.43	170.92	0.24	0.24	16.40	0.08	0.07	442.33	0.63	0.61
0.076	308.18	0.62	0.46	181.46	0.25	0.25	17.48	0.09	0.08	451.70	0.64	0.62
0.081	325.20	0.66	0.48	192.40	0.27	0.27	18.65	0.09	0.08	459.28	0.65	0.63
0.087	342.43	0.69	0.51	203.69	0.29	0.29	19.90	0.10	0.09	465.05	0.66	0.64
0.093	359.72	0.73	0.53	215.29	0.30	0.30	21.25	0.11	0.09	469.10	0.67	0.64
0.1	376.89	0.76	0.56	227.13	0.32	0.32	22.69	0.11	0.10	471.63	0.67	0.65
0.107	393.72	0.79	0.58	239.13	0.34	0.34	24.23	0.12	0.11	472.96	0.67	0.65
0.115	409.99	0.83	0.61	251.19	0.35	0.35	25.88	0.13	0.12	473.48	0.67	0.65
0.123	425.45	0.86	0.63	263.21	0.37	0.37	27.64	0.14	0.13	473.57	0.67	0.65
0.132	439.84	0.89	0.65	275.06	0.39	0.39	29.52	0.15	0.13	473.59	0.67	0.65
0.142	452.92	0.91	0.67	286.62	0.40	0.40	31.51	0.16	0.14	473.75	0.67	0.65
0.152	464.46	0.94	0.69	297.76	0.42	0.42	33.63	0.17	0.15	474.13	0.67	0.65
0.163	474.30	0.96	0.70	308.34	0.43	0.43	35.88	0.18	0.16	474.67	0.67	0.65
0.174	482.35	0.97	0.71	318.27	0.45	0.45	38.25	0.19	0.17	475.21	0.68	0.65
0.187	488.61	0.99	0.72	327.46	0.46	0.46	40.76	0.21	0.19	475.54	0.68	0.65
0.2	493.18	0.99	0.73	335.86	0.47	0.47	43.40	0.22	0.20	475.49	0.68	0.65
0.215	496.29	1.00	0.73	343.48	0.48	0.48	46.17	0.23	0.21	474.92	0.68	0.65
0.23	498.25	1.00	0.74	350.34	0.49	0.49	49.08	0.25	0.22	473.79	0.67	0.65
0.247	499.41	1.01	0.74	356.55	0.50	0.50	52.10	0.26	0.24	472.12	0.67	0.65
0.265	500.13	1.01	0.74	362.19	0.51	0.51	55.25	0.28	0.25	469.97	0.67	0.65
0.284	500.68	1.01	0.74	367.36	0.52	0.52	58.51	0.30	0.27	467.42	0.66	0.64
0.304	501.21	1.01	0.74	372.16	0.52	0.52	61.86	0.31	0.28	464.50	0.66	0.64
0.326	501.73	1.01	0.74	376.59	0.53	0.53	65.30	0.33	0.30	461.22	0.66	0.63
0.349	502.13	1.01	0.74	380.63	0.53	0.53	68.80	0.35	0.31	457.54	0.65	0.63
0.374	502.21	1.01	0.74	384.19	0.54	0.54	72.34	0.37	0.33	453.40	0.64	0.62
0.401	501.74	1.01	0.74	387.17	0.54	0.54	75.90	0.39	0.35	448.74	0.64	0.62
0.43	500.53	1.01	0.74	389.47	0.55	0.55	79.45	0.40	0.36	443.57	0.63	0.61
0.461	498.45	1.00	0.74	391.06	0.55	0.55	82.97	0.42	0.38	438.00	0.62	0.60
0.494	495.45	1.00	0.73	391.94	0.55	0.55	86.44	0.44	0.40	432.20	0.61	0.59
0.53	491.58	0.99	0.73	392.24	0.55	0.55	89.84	0.46	0.41	426.40	0.61	0.59
0.568	486.93	0.98	0.72	392.13	0.55	0.55	93.15	0.47	0.43	420.86	0.60	0.58
0.608	481.63	0.97	0.71	391.80	0.55	0.55	96.39	0.49	0.44	415.77	0.59	0.57
0.652	475.84	0.96	0.70	391.47	0.55	0.55	99.54	0.51	0.45	411.23	0.58	0.56
0.699	469.69	0.95	0.70	391.28	0.55	0.55	102.64	0.52	0.47	407.23	0.58	0.56
0.749	463.29	0.93	0.69	391.30	0.55	0.55	105.69	0.54	0.48	403.64	0.57	0.55
0.803	456.74	0.92	0.68	391.47	0.55	0.55	108.73	0.55	0.50	400.24	0.57	0.55
0.861	450.14	0.91	0.67	391.67	0.55	0.55	111.76	0.57	0.51	396.77	0.56	0.54
0.923	443.58	0.89	0.66	391.69	0.55	0.55	114.77	0.58	0.52	392.97	0.56	0.54
0.989	437.18	0.88	0.65	391.34	0.55	0.55	117.76	0.60	0.54	388.62	0.55	0.53
1.06	431.04	0.87	0.64	390.42	0.55	0.55	120.65	0.61	0.55	383.56	0.55	0.53
1.136	425.23	0.86	0.63	388.79	0.55	0.55	123.37	0.63	0.56	377.75	0.54	0.52
1.218	419.76	0.85	0.62	386.39	0.54	0.54	125.81	0.64	0.58	371.22	0.53	0.51
1.306	414.58	0.84	0.61	383.23	0.54	0.54	127.88	0.65	0.58	364.12	0.52	0.50
1.399	409.57	0.83	0.61	379.38	0.53	0.53	129.46	0.66	0.59	356.71	0.51	0.49
1.5	404.55	0.82	0.60	374.95	0.53	0.53	130.46	0.66	0.60	349.25	0.50	0.48

Table F33. Circular velocity curves of the 238 (E1–Sdm) CALIFA galaxies with 75th and 25th percentile uncertainties.

R/R_e	NGC6186			NGC6278			NGC6301			NGC6310		
	V_c	ΔV_c^{75th}	ΔV_c^{25th}									
0.05	108.50	0.32	0.28	88.67	0.12	0.14	69.73	0.10	0.08	80.50	0.14	0.15
0.054	110.85	0.33	0.29	94.71	0.13	0.15	73.75	0.11	0.09	85.30	0.15	0.16
0.057	112.66	0.34	0.29	101.11	0.14	0.16	77.86	0.12	0.09	90.25	0.16	0.16
0.062	113.90	0.34	0.30	107.90	0.15	0.17	82.04	0.12	0.10	95.32	0.17	0.17
0.066	114.56	0.34	0.30	115.09	0.16	0.18	86.25	0.13	0.10	100.48	0.18	0.18
0.071	114.66	0.34	0.30	122.67	0.17	0.20	90.45	0.13	0.11	105.69	0.19	0.19
0.076	114.29	0.34	0.30	130.66	0.18	0.21	94.59	0.14	0.11	110.90	0.20	0.20
0.081	113.57	0.34	0.30	139.05	0.20	0.22	98.63	0.15	0.12	116.06	0.20	0.21
0.087	112.66	0.34	0.29	147.84	0.21	0.24	102.50	0.15	0.12	121.10	0.21	0.22
0.093	111.79	0.33	0.29	157.01	0.22	0.25	106.16	0.16	0.13	125.97	0.22	0.23
0.1	111.14	0.33	0.29	166.54	0.24	0.27	109.56	0.16	0.13	130.58	0.23	0.24
0.107	110.89	0.33	0.29	176.40	0.25	0.28	112.64	0.17	0.13	134.89	0.24	0.25
0.115	111.18	0.33	0.29	186.54	0.26	0.30	115.40	0.17	0.14	138.82	0.24	0.25
0.123	112.04	0.33	0.29	196.91	0.28	0.32	117.81	0.18	0.14	142.33	0.25	0.26
0.132	113.47	0.34	0.30	207.44	0.29	0.33	119.90	0.18	0.14	145.39	0.26	0.27
0.142	115.38	0.34	0.30	218.05	0.31	0.35	121.72	0.18	0.14	147.99	0.26	0.27
0.152	117.69	0.35	0.31	228.64	0.32	0.37	123.35	0.18	0.15	150.17	0.27	0.27
0.163	120.29	0.36	0.31	239.10	0.34	0.38	124.88	0.19	0.15	151.97	0.27	0.28
0.174	123.05	0.37	0.32	249.32	0.35	0.40	126.43	0.19	0.15	153.45	0.27	0.28
0.187	125.87	0.38	0.33	259.16	0.37	0.42	128.10	0.19	0.15	154.70	0.27	0.28
0.2	128.65	0.38	0.34	268.50	0.38	0.43	129.96	0.19	0.15	155.80	0.28	0.28
0.215	131.28	0.39	0.34	277.21	0.39	0.44	132.04	0.20	0.16	156.81	0.28	0.29
0.23	133.65	0.40	0.35	285.20	0.40	0.46	134.35	0.20	0.16	157.76	0.28	0.29
0.247	135.67	0.41	0.35	292.36	0.41	0.47	136.85	0.20	0.16	158.65	0.28	0.29
0.265	137.26	0.41	0.36	298.63	0.42	0.48	139.48	0.21	0.17	159.45	0.28	0.29
0.284	138.37	0.41	0.36	304.00	0.43	0.49	142.20	0.21	0.17	160.11	0.28	0.29
0.304	138.96	0.42	0.36	308.46	0.44	0.49	144.98	0.22	0.17	160.58	0.28	0.29
0.326	139.05	0.42	0.36	312.06	0.44	0.50	147.84	0.22	0.18	160.84	0.28	0.29
0.349	138.68	0.41	0.36	314.84	0.45	0.50	150.82	0.22	0.18	160.87	0.28	0.29
0.374	137.94	0.41	0.36	316.86	0.45	0.51	154.00	0.23	0.18	160.70	0.28	0.29
0.401	136.93	0.41	0.36	318.18	0.45	0.51	157.47	0.23	0.19	160.40	0.28	0.29
0.43	135.80	0.41	0.35	318.84	0.45	0.51	161.31	0.24	0.19	160.06	0.28	0.29
0.461	134.68	0.40	0.35	318.88	0.45	0.51	165.63	0.25	0.20	159.82	0.28	0.29
0.494	133.69	0.40	0.35	318.37	0.45	0.51	170.47	0.25	0.20	159.81	0.28	0.29
0.53	132.92	0.40	0.35	317.38	0.45	0.51	175.87	0.26	0.21	160.17	0.28	0.29
0.568	132.40	0.40	0.35	316.01	0.45	0.51	181.79	0.27	0.22	161.01	0.28	0.29
0.608	132.17	0.40	0.34	314.39	0.45	0.50	188.20	0.28	0.22	162.40	0.29	0.30
0.652	132.20	0.40	0.34	312.68	0.44	0.50	195.02	0.29	0.23	164.37	0.29	0.30
0.699	132.47	0.40	0.35	311.01	0.44	0.50	202.17	0.30	0.24	166.91	0.29	0.31
0.749	132.94	0.40	0.35	309.44	0.44	0.50	209.55	0.31	0.25	169.96	0.30	0.31
0.803	133.57	0.40	0.35	307.99	0.44	0.49	217.06	0.32	0.26	173.44	0.31	0.32
0.861	134.34	0.40	0.35	306.62	0.43	0.49	224.62	0.33	0.27	177.27	0.31	0.32
0.923	135.20	0.40	0.35	305.18	0.43	0.49	232.12	0.35	0.28	181.31	0.32	0.33
0.989	136.12	0.41	0.36	303.54	0.43	0.49	239.45	0.36	0.28	185.44	0.33	0.34
1.06	137.04	0.41	0.36	301.50	0.43	0.48	246.52	0.37	0.29	189.50	0.33	0.35
1.136	137.93	0.41	0.36	298.92	0.42	0.48	253.20	0.38	0.30	193.33	0.34	0.35
1.218	138.69	0.41	0.36	295.68	0.42	0.47	259.37	0.39	0.31	196.75	0.35	0.36
1.306	139.26	0.42	0.36	291.75	0.41	0.47	264.86	0.39	0.31	199.59	0.35	0.37
1.399	139.52	0.42	0.36	287.17	0.41	0.46	269.53	0.40	0.32	201.68	0.36	0.37
1.5	139.39	0.42	0.36	282.07	0.40	0.45	273.17	0.41	0.32	202.86	0.36	0.37

Table F34. Circular velocity curves of the 238 (E1–Sdm) CALIFA galaxies with 75th and 25th percentile uncertainties.

R/R_e	NGC6314			NGC6478			NGC6497			NGC6515		
	V_c	ΔV_c^{75th}	ΔV_c^{25th}									
0.05	94.99	0.30	0.19	147.34	0.18	0.21	389.35	0.43	0.46	161.85	0.29	0.26
0.054	101.35	0.32	0.20	155.90	0.19	0.22	391.98	0.43	0.46	171.72	0.31	0.28
0.057	108.06	0.34	0.22	164.65	0.20	0.24	391.98	0.43	0.46	181.92	0.33	0.29
0.062	115.13	0.36	0.23	173.53	0.21	0.25	389.32	0.43	0.46	192.43	0.35	0.31
0.066	122.56	0.38	0.25	182.46	0.22	0.26	384.11	0.42	0.45	203.17	0.37	0.33
0.071	130.35	0.41	0.26	191.34	0.23	0.27	376.64	0.41	0.45	214.07	0.39	0.34
0.076	138.49	0.43	0.28	200.05	0.24	0.29	367.42	0.40	0.43	225.05	0.40	0.36
0.081	146.95	0.46	0.30	208.47	0.25	0.30	357.07	0.39	0.42	235.99	0.42	0.38
0.087	155.71	0.49	0.31	216.43	0.26	0.31	346.35	0.38	0.41	246.77	0.44	0.40
0.093	164.73	0.51	0.33	223.79	0.27	0.32	336.00	0.37	0.40	257.26	0.46	0.41
0.1	173.97	0.54	0.35	230.35	0.28	0.33	326.65	0.36	0.39	267.30	0.48	0.43
0.107	183.36	0.57	0.37	235.97	0.29	0.34	318.73	0.35	0.38	276.75	0.50	0.45
0.115	192.83	0.60	0.39	240.46	0.29	0.35	312.43	0.34	0.37	285.45	0.51	0.46
0.123	202.29	0.63	0.41	243.71	0.30	0.35	307.72	0.34	0.36	293.26	0.53	0.47
0.132	211.64	0.66	0.43	245.63	0.30	0.35	304.43	0.33	0.36	300.09	0.54	0.48
0.142	220.76	0.69	0.44	246.19	0.30	0.35	302.32	0.33	0.36	305.86	0.55	0.49
0.152	229.54	0.72	0.46	245.44	0.30	0.35	301.15	0.33	0.36	310.56	0.56	0.50
0.163	237.85	0.74	0.48	243.53	0.30	0.35	300.72	0.33	0.36	314.24	0.57	0.51
0.174	245.56	0.77	0.49	240.69	0.29	0.35	300.84	0.33	0.36	317.01	0.57	0.51
0.187	252.56	0.79	0.51	237.20	0.29	0.34	301.36	0.33	0.36	319.03	0.57	0.51
0.2	258.76	0.81	0.52	233.39	0.28	0.34	302.16	0.33	0.36	320.51	0.58	0.52
0.215	264.09	0.82	0.53	229.59	0.28	0.33	303.12	0.33	0.36	321.64	0.58	0.52
0.23	268.52	0.84	0.54	226.05	0.27	0.32	304.16	0.33	0.36	322.59	0.58	0.52
0.247	272.08	0.85	0.55	222.94	0.27	0.32	305.21	0.33	0.36	323.48	0.58	0.52
0.265	274.81	0.86	0.55	220.32	0.27	0.32	306.19	0.34	0.36	324.36	0.58	0.52
0.284	276.81	0.86	0.56	218.20	0.26	0.31	307.04	0.34	0.36	325.19	0.59	0.52
0.304	278.19	0.87	0.56	216.52	0.26	0.31	307.68	0.34	0.36	325.91	0.59	0.52
0.326	279.07	0.87	0.56	215.24	0.26	0.31	308.00	0.34	0.36	326.43	0.59	0.52
0.349	279.56	0.87	0.56	214.33	0.26	0.31	307.90	0.34	0.36	326.66	0.59	0.53
0.374	279.74	0.87	0.56	213.80	0.26	0.31	307.28	0.34	0.36	326.52	0.59	0.53
0.401	279.69	0.87	0.56	213.69	0.26	0.31	306.05	0.34	0.36	325.97	0.59	0.52
0.43	279.45	0.87	0.56	214.06	0.26	0.31	304.18	0.33	0.36	325.00	0.58	0.52
0.461	279.04	0.87	0.56	214.97	0.26	0.31	301.66	0.33	0.36	323.61	0.58	0.52
0.494	278.47	0.87	0.56	216.48	0.26	0.31	298.54	0.33	0.35	321.84	0.58	0.52
0.53	277.74	0.87	0.56	218.62	0.27	0.31	294.95	0.32	0.35	319.75	0.58	0.51
0.568	276.79	0.86	0.56	221.43	0.27	0.32	291.01	0.32	0.34	317.42	0.57	0.51
0.608	275.53	0.86	0.55	224.92	0.27	0.32	286.88	0.31	0.34	314.91	0.57	0.51
0.652	273.87	0.86	0.55	229.07	0.28	0.33	282.73	0.31	0.33	312.33	0.56	0.50
0.699	271.69	0.85	0.55	233.82	0.28	0.34	278.67	0.31	0.33	309.73	0.56	0.50
0.749	268.92	0.84	0.54	239.09	0.29	0.34	274.82	0.30	0.33	307.19	0.55	0.49
0.803	265.55	0.83	0.53	244.75	0.30	0.35	271.27	0.30	0.32	304.72	0.55	0.49
0.861	261.63	0.82	0.53	250.65	0.30	0.36	268.06	0.29	0.32	302.33	0.54	0.49
0.923	257.29	0.80	0.52	256.60	0.31	0.37	265.21	0.29	0.31	299.99	0.54	0.48
0.989	252.70	0.79	0.51	262.38	0.32	0.38	262.76	0.29	0.31	297.63	0.54	0.48
1.06	248.06	0.77	0.50	267.77	0.33	0.38	260.68	0.29	0.31	295.22	0.53	0.47
1.136	243.54	0.76	0.49	272.52	0.33	0.39	258.98	0.28	0.31	292.69	0.53	0.47
1.218	239.27	0.75	0.48	276.41	0.34	0.40	257.65	0.28	0.30	290.00	0.52	0.47
1.306	235.32	0.74	0.47	279.20	0.34	0.40	256.68	0.28	0.30	287.10	0.52	0.46
1.399	231.73	0.72	0.47	280.69	0.34	0.40	256.09	0.28	0.30	283.98	0.51	0.46
1.5	228.47	0.71	0.46	280.74	0.34	0.40	255.85	0.28	0.30	280.61	0.51	0.45

Table F35. Circular velocity curves of the 238 (E1–Sdm) CALIFA galaxies with 75th and 25th percentile uncertainties.

R/R_e	NGC6762			NGC6941			NGC6945			NGC6978		
	V_c	ΔV_c^{75th}	ΔV_c^{25th}									
0.05	24.37	0.04	0.05	132.45	0.21	0.17	104.35	0.16	0.11	91.28	0.10	0.13
0.054	25.91	0.04	0.05	139.84	0.22	0.18	111.01	0.17	0.12	96.94	0.11	0.14
0.057	27.59	0.04	0.06	147.35	0.23	0.18	117.98	0.18	0.13	102.83	0.11	0.15
0.062	29.40	0.05	0.06	154.91	0.24	0.19	125.24	0.19	0.14	108.92	0.12	0.15
0.066	31.35	0.05	0.07	162.46	0.26	0.20	132.78	0.21	0.15	115.19	0.13	0.16
0.071	33.46	0.05	0.07	169.91	0.27	0.21	140.56	0.22	0.15	121.60	0.13	0.17
0.076	35.71	0.06	0.08	177.18	0.28	0.22	148.55	0.23	0.16	128.12	0.14	0.18
0.081	38.13	0.06	0.08	184.17	0.29	0.23	156.71	0.24	0.17	134.70	0.15	0.19
0.087	40.73	0.07	0.09	190.78	0.30	0.24	164.97	0.26	0.18	141.27	0.16	0.20
0.093	43.50	0.07	0.10	196.93	0.31	0.25	173.26	0.27	0.19	147.78	0.16	0.21
0.1	46.46	0.08	0.10	202.54	0.32	0.25	181.52	0.28	0.20	154.17	0.17	0.22
0.107	49.61	0.08	0.11	207.56	0.33	0.26	189.64	0.29	0.21	160.35	0.18	0.23
0.115	52.96	0.09	0.12	211.96	0.33	0.27	197.53	0.31	0.22	166.27	0.18	0.24
0.123	56.52	0.09	0.13	215.74	0.34	0.27	205.10	0.32	0.22	171.86	0.19	0.24
0.132	60.30	0.10	0.14	218.98	0.35	0.27	212.25	0.33	0.23	177.09	0.20	0.25
0.142	64.30	0.11	0.14	221.76	0.35	0.28	218.88	0.34	0.24	181.93	0.20	0.26
0.152	68.51	0.11	0.15	224.19	0.35	0.28	224.93	0.35	0.25	186.37	0.21	0.26
0.163	72.96	0.12	0.16	226.41	0.36	0.28	230.33	0.36	0.25	190.45	0.21	0.27
0.174	77.62	0.13	0.17	228.52	0.36	0.29	235.06	0.37	0.26	194.22	0.21	0.28
0.187	82.50	0.14	0.19	230.60	0.36	0.29	239.14	0.37	0.26	197.75	0.22	0.28
0.2	87.59	0.15	0.20	232.66	0.37	0.29	242.59	0.38	0.27	201.13	0.22	0.29
0.215	92.87	0.15	0.21	234.65	0.37	0.29	245.47	0.38	0.27	204.41	0.23	0.29
0.23	98.32	0.16	0.22	236.48	0.37	0.30	247.86	0.39	0.27	207.64	0.23	0.30
0.247	103.92	0.17	0.23	237.99	0.38	0.30	249.82	0.39	0.27	210.82	0.23	0.30
0.265	109.64	0.18	0.25	239.03	0.38	0.30	251.40	0.39	0.28	213.92	0.24	0.30
0.284	115.43	0.19	0.26	239.46	0.38	0.30	252.62	0.39	0.28	216.86	0.24	0.31
0.304	121.24	0.20	0.27	239.12	0.38	0.30	253.50	0.39	0.28	219.58	0.24	0.31
0.326	127.01	0.21	0.29	237.96	0.38	0.30	253.99	0.39	0.28	221.98	0.25	0.32
0.349	132.69	0.22	0.30	235.95	0.37	0.30	254.10	0.40	0.28	224.03	0.25	0.32
0.374	138.19	0.23	0.31	233.16	0.37	0.29	253.82	0.39	0.28	225.68	0.25	0.32
0.401	143.44	0.24	0.32	229.75	0.36	0.29	253.18	0.39	0.28	226.94	0.25	0.32
0.43	148.38	0.25	0.33	225.95	0.36	0.28	252.22	0.39	0.28	227.85	0.25	0.32
0.461	152.92	0.25	0.34	222.06	0.35	0.28	251.03	0.39	0.27	228.47	0.25	0.32
0.494	157.03	0.26	0.35	218.38	0.34	0.27	249.70	0.39	0.27	228.85	0.25	0.33
0.53	160.66	0.27	0.36	215.19	0.34	0.27	248.32	0.39	0.27	229.08	0.25	0.33
0.568	163.82	0.27	0.37	212.68	0.34	0.27	246.97	0.38	0.27	229.21	0.25	0.33
0.608	166.53	0.28	0.37	210.94	0.33	0.26	245.72	0.38	0.27	229.32	0.25	0.33
0.652	168.85	0.28	0.38	209.96	0.33	0.26	244.60	0.38	0.27	229.51	0.25	0.33
0.699	170.88	0.28	0.38	209.63	0.33	0.26	243.63	0.38	0.27	229.86	0.25	0.33
0.749	172.74	0.29	0.39	209.83	0.33	0.26	242.80	0.38	0.27	230.51	0.26	0.33
0.803	174.52	0.29	0.39	210.41	0.33	0.26	242.06	0.38	0.26	231.55	0.26	0.33
0.861	176.33	0.29	0.40	211.27	0.33	0.27	241.33	0.38	0.26	233.08	0.26	0.33
0.923	178.21	0.30	0.40	212.32	0.33	0.27	240.52	0.37	0.26	235.12	0.26	0.33
0.989	180.14	0.30	0.41	213.51	0.34	0.27	239.53	0.37	0.26	237.63	0.26	0.34
1.06	182.06	0.30	0.41	214.82	0.34	0.27	238.26	0.37	0.26	240.49	0.27	0.34
1.136	183.85	0.31	0.41	216.22	0.34	0.27	236.64	0.37	0.26	243.52	0.27	0.35
1.218	185.35	0.31	0.42	217.70	0.34	0.27	234.66	0.36	0.26	246.50	0.27	0.35
1.306	186.41	0.31	0.42	219.26	0.35	0.28	232.33	0.36	0.25	249.19	0.28	0.35
1.399	186.87	0.31	0.42	220.83	0.35	0.28	229.75	0.36	0.25	251.36	0.28	0.36
1.5	186.61	0.31	0.42	222.35	0.35	0.28	227.02	0.35	0.25	252.79	0.28	0.36

Table F36. Circular velocity curves of the 238 (E1–Sdm) CALIFA galaxies with 75th and 25th percentile uncertainties.

R/R_e	NGC7025			NGC7047			NGC7194			NGC7311		
	V_c	ΔV_c^{75th}	ΔV_c^{25th}									
0.05	128.91	0.16	0.12	65.03	0.14	0.15	191.71	0.47	0.35	90.88	0.18	0.17
0.054	137.49	0.17	0.13	69.21	0.15	0.16	204.18	0.50	0.37	97.02	0.19	0.19
0.057	146.54	0.18	0.14	73.59	0.16	0.17	217.26	0.53	0.40	103.52	0.20	0.20
0.062	156.07	0.20	0.15	78.17	0.17	0.19	230.94	0.56	0.42	110.39	0.22	0.21
0.066	166.07	0.21	0.16	82.93	0.18	0.20	245.19	0.59	0.45	117.63	0.23	0.23
0.071	176.54	0.22	0.17	87.86	0.19	0.21	259.97	0.63	0.48	125.25	0.24	0.24
0.076	187.46	0.24	0.18	92.95	0.21	0.22	275.22	0.67	0.51	133.25	0.26	0.26
0.081	198.79	0.25	0.19	98.16	0.22	0.23	290.86	0.71	0.53	141.61	0.28	0.27
0.087	210.52	0.27	0.20	103.47	0.23	0.25	306.80	0.74	0.56	150.31	0.29	0.29
0.093	222.59	0.28	0.22	108.84	0.24	0.26	322.91	0.78	0.59	159.35	0.31	0.31
0.1	234.93	0.30	0.23	114.21	0.25	0.27	339.05	0.82	0.62	168.67	0.33	0.32
0.107	247.48	0.31	0.24	119.55	0.26	0.28	355.03	0.86	0.65	178.24	0.35	0.34
0.115	260.15	0.33	0.25	124.78	0.28	0.30	370.67	0.90	0.68	188.00	0.37	0.36
0.123	272.85	0.34	0.26	129.84	0.29	0.31	385.73	0.94	0.71	197.88	0.39	0.38
0.132	285.45	0.36	0.28	134.65	0.30	0.32	399.99	0.97	0.73	207.81	0.41	0.40
0.142	297.85	0.38	0.29	139.13	0.31	0.33	413.22	1.00	0.76	217.68	0.43	0.42
0.152	309.94	0.39	0.30	143.19	0.32	0.34	425.17	1.03	0.78	227.41	0.45	0.44
0.163	321.59	0.41	0.31	146.76	0.33	0.35	435.66	1.06	0.80	236.86	0.46	0.45
0.174	332.71	0.42	0.32	149.73	0.33	0.36	444.52	1.08	0.82	245.94	0.48	0.47
0.187	343.22	0.43	0.33	152.03	0.34	0.36	451.69	1.10	0.83	254.52	0.50	0.49
0.2	353.04	0.45	0.34	153.60	0.34	0.36	457.15	1.11	0.84	262.50	0.51	0.50
0.215	362.14	0.46	0.35	154.39	0.34	0.37	461.01	1.12	0.85	269.80	0.53	0.52
0.23	370.49	0.47	0.36	154.41	0.34	0.37	463.47	1.12	0.85	276.33	0.54	0.53
0.247	378.08	0.48	0.37	153.70	0.34	0.36	464.78	1.13	0.85	282.07	0.55	0.54
0.265	384.90	0.49	0.37	152.36	0.34	0.36	465.25	1.13	0.85	287.00	0.56	0.55
0.284	390.94	0.49	0.38	150.58	0.33	0.36	465.17	1.13	0.85	291.14	0.57	0.56
0.304	396.17	0.50	0.38	148.60	0.33	0.35	464.75	1.13	0.85	294.53	0.58	0.57
0.326	400.55	0.51	0.39	146.71	0.33	0.35	464.11	1.13	0.85	297.24	0.58	0.57
0.349	404.03	0.51	0.39	145.20	0.32	0.34	463.27	1.12	0.85	299.34	0.59	0.57
0.374	406.60	0.51	0.39	144.34	0.32	0.34	462.15	1.12	0.85	300.89	0.59	0.58
0.401	408.25	0.52	0.40	144.32	0.32	0.34	460.63	1.12	0.85	301.97	0.59	0.58
0.43	409.03	0.52	0.40	145.26	0.32	0.34	458.58	1.11	0.84	302.65	0.59	0.58
0.461	409.05	0.52	0.40	147.17	0.33	0.35	455.92	1.11	0.84	303.02	0.59	0.58
0.494	408.40	0.52	0.40	150.01	0.33	0.36	452.65	1.10	0.83	303.14	0.59	0.58
0.53	407.23	0.51	0.39	153.70	0.34	0.36	448.82	1.09	0.82	303.11	0.59	0.58
0.568	405.65	0.51	0.39	158.15	0.35	0.38	444.56	1.08	0.82	302.96	0.59	0.58
0.608	403.76	0.51	0.39	163.28	0.36	0.39	440.03	1.07	0.81	302.71	0.59	0.58
0.652	401.61	0.51	0.39	168.99	0.37	0.40	435.38	1.06	0.80	302.33	0.59	0.58
0.699	399.21	0.50	0.39	175.19	0.39	0.42	430.69	1.05	0.79	301.73	0.59	0.58
0.749	396.52	0.50	0.38	181.78	0.40	0.43	426.02	1.03	0.78	300.81	0.59	0.58
0.803	393.53	0.50	0.38	188.64	0.42	0.45	421.33	1.02	0.77	299.46	0.59	0.57
0.861	390.19	0.49	0.38	195.66	0.43	0.46	416.55	1.01	0.76	297.61	0.58	0.57
0.923	386.50	0.49	0.37	202.68	0.45	0.48	411.58	1.00	0.76	295.22	0.58	0.57
0.989	382.51	0.48	0.37	209.56	0.46	0.50	406.35	0.99	0.75	292.33	0.57	0.56
1.06	378.31	0.48	0.37	216.10	0.48	0.51	400.85	0.97	0.74	289.06	0.57	0.55
1.136	374.03	0.47	0.36	222.14	0.49	0.53	395.08	0.96	0.73	285.58	0.56	0.55
1.218	369.81	0.47	0.36	227.47	0.50	0.54	389.13	0.94	0.71	282.14	0.55	0.54
1.306	365.78	0.46	0.35	231.89	0.51	0.55	383.07	0.93	0.70	278.97	0.55	0.54
1.399	362.02	0.46	0.35	235.20	0.52	0.56	376.99	0.91	0.69	276.26	0.54	0.53
1.5	358.53	0.45	0.35	237.26	0.53	0.56	370.92	0.90	0.68	274.13	0.54	0.53

Table F37. Circular velocity curves of the 238 (E1–Sdm) CALIFA galaxies with 75th and 25th percentile uncertainties.

R/R_e	NGC7321			NGC7364			NGC7466			NGC7489		
	V_c	ΔV_c^{75th}	ΔV_c^{25th}									
0.05	148.18	0.25	0.18	105.71	0.18	0.22	81.45	0.12	0.13	63.12	0.19	0.15
0.054	149.30	0.25	0.18	112.72	0.19	0.23	86.85	0.13	0.14	66.51	0.21	0.16
0.057	149.92	0.25	0.18	120.12	0.20	0.25	92.55	0.14	0.15	69.91	0.22	0.16
0.062	150.20	0.25	0.18	127.90	0.21	0.27	98.55	0.15	0.16	73.31	0.23	0.17
0.066	150.36	0.25	0.18	136.06	0.23	0.28	104.83	0.15	0.17	76.65	0.24	0.18
0.071	150.63	0.26	0.18	144.58	0.24	0.30	111.40	0.16	0.18	79.89	0.25	0.19
0.076	151.28	0.26	0.18	153.45	0.26	0.32	118.23	0.17	0.19	82.98	0.26	0.19
0.081	152.51	0.26	0.19	162.63	0.27	0.34	125.31	0.18	0.20	85.87	0.27	0.20
0.087	154.50	0.26	0.19	172.10	0.29	0.36	132.61	0.20	0.21	88.51	0.27	0.21
0.093	157.29	0.27	0.19	181.79	0.30	0.38	140.07	0.21	0.23	90.84	0.28	0.21
0.1	160.88	0.27	0.20	191.63	0.32	0.40	147.66	0.22	0.24	92.83	0.29	0.22
0.107	165.18	0.28	0.20	201.54	0.34	0.42	155.30	0.23	0.25	94.45	0.29	0.22
0.115	170.07	0.29	0.21	211.43	0.35	0.44	162.92	0.24	0.26	95.68	0.30	0.22
0.123	175.41	0.30	0.21	221.15	0.37	0.46	170.41	0.25	0.28	96.56	0.30	0.23
0.132	181.06	0.31	0.22	230.59	0.38	0.48	177.68	0.26	0.29	97.11	0.30	0.23
0.142	186.87	0.32	0.23	239.59	0.40	0.50	184.59	0.27	0.30	97.42	0.30	0.23
0.152	192.70	0.33	0.23	247.98	0.41	0.52	191.03	0.28	0.31	97.57	0.30	0.23
0.163	198.40	0.34	0.24	255.59	0.43	0.53	196.85	0.29	0.32	97.69	0.30	0.23
0.174	203.82	0.35	0.25	262.27	0.44	0.55	201.93	0.30	0.33	97.88	0.30	0.23
0.187	208.81	0.35	0.25	267.87	0.45	0.56	206.12	0.30	0.33	98.26	0.30	0.23
0.2	213.24	0.36	0.26	272.29	0.45	0.57	209.35	0.31	0.34	98.91	0.31	0.23
0.215	216.98	0.37	0.26	275.50	0.46	0.57	211.54	0.31	0.34	99.89	0.31	0.23
0.23	219.96	0.37	0.27	277.52	0.46	0.58	212.69	0.31	0.34	101.24	0.31	0.24
0.247	222.13	0.38	0.27	278.47	0.46	0.58	212.83	0.31	0.35	102.97	0.32	0.24
0.265	223.48	0.38	0.27	278.58	0.46	0.58	212.09	0.31	0.34	105.07	0.32	0.25
0.284	224.10	0.38	0.27	278.16	0.46	0.58	210.66	0.31	0.34	107.54	0.33	0.25
0.304	224.11	0.38	0.27	277.56	0.46	0.58	208.75	0.31	0.34	110.35	0.34	0.26
0.326	223.70	0.38	0.27	277.17	0.46	0.58	206.65	0.31	0.34	113.49	0.35	0.27
0.349	223.08	0.38	0.27	277.30	0.46	0.58	204.60	0.30	0.33	116.93	0.36	0.27
0.374	222.48	0.38	0.27	278.16	0.46	0.58	202.82	0.30	0.33	120.64	0.37	0.28
0.401	222.11	0.38	0.27	279.81	0.47	0.58	201.49	0.30	0.33	124.61	0.39	0.29
0.43	222.16	0.38	0.27	282.19	0.47	0.59	200.68	0.30	0.33	128.80	0.40	0.30
0.461	222.73	0.38	0.27	285.13	0.48	0.59	200.41	0.30	0.32	133.19	0.41	0.31
0.494	223.88	0.38	0.27	288.39	0.48	0.60	200.66	0.30	0.33	137.75	0.43	0.32
0.53	225.63	0.38	0.27	291.73	0.49	0.61	201.33	0.30	0.33	142.46	0.44	0.33
0.568	227.94	0.39	0.28	294.92	0.49	0.61	202.35	0.30	0.33	147.25	0.46	0.34
0.608	230.74	0.39	0.28	297.75	0.50	0.62	203.61	0.30	0.33	152.10	0.47	0.36
0.652	233.91	0.40	0.28	300.05	0.50	0.62	204.99	0.30	0.33	156.92	0.49	0.37
0.699	237.34	0.40	0.29	301.69	0.50	0.63	206.38	0.30	0.33	161.66	0.50	0.38
0.749	240.88	0.41	0.29	302.55	0.50	0.63	207.68	0.31	0.34	166.20	0.51	0.39
0.803	244.39	0.41	0.30	302.55	0.50	0.63	208.82	0.31	0.34	170.47	0.53	0.40
0.861	247.74	0.42	0.30	301.65	0.50	0.63	209.75	0.31	0.34	174.37	0.54	0.41
0.923	250.80	0.43	0.31	299.84	0.50	0.62	210.44	0.31	0.34	177.82	0.55	0.42
0.989	253.49	0.43	0.31	297.16	0.50	0.62	210.92	0.31	0.34	180.74	0.56	0.42
1.06	255.75	0.43	0.31	293.69	0.49	0.61	211.24	0.31	0.34	183.08	0.57	0.43
1.136	257.55	0.44	0.31	289.56	0.48	0.60	211.48	0.31	0.34	184.81	0.57	0.43
1.218	258.91	0.44	0.32	284.95	0.48	0.59	211.75	0.31	0.34	185.95	0.58	0.43
1.306	259.87	0.44	0.32	280.10	0.47	0.58	212.12	0.31	0.34	186.49	0.58	0.44
1.399	260.50	0.44	0.32	275.25	0.46	0.57	212.65	0.31	0.34	186.50	0.58	0.44
1.5	260.85	0.44	0.32	270.58	0.45	0.56	213.36	0.31	0.35	186.03	0.58	0.43

Table F38. Circular velocity curves of the 238 (E1–Sdm) CALIFA galaxies with 75th and 25th percentile uncertainties.

R/R_e	NGC7549			NGC7550			NGC7562			NGC7563		
	V_c	ΔV_c^{75th}	ΔV_c^{25th}									
0.05	75.45	0.20	0.18	247.24	0.41	0.40	173.73	0.46	0.19	86.10	0.10	0.10
0.054	80.50	0.22	0.19	261.28	0.43	0.43	184.72	0.49	0.21	91.98	0.10	0.10
0.057	85.84	0.23	0.21	275.60	0.45	0.45	196.18	0.52	0.22	98.23	0.11	0.11
0.062	91.48	0.25	0.22	290.06	0.48	0.47	208.09	0.55	0.23	104.86	0.12	0.12
0.066	97.40	0.26	0.23	304.55	0.50	0.50	220.40	0.58	0.25	111.88	0.13	0.13
0.071	103.61	0.28	0.25	318.89	0.53	0.52	233.06	0.62	0.26	119.31	0.13	0.13
0.076	110.11	0.30	0.26	332.93	0.55	0.54	245.99	0.65	0.28	127.14	0.14	0.14
0.081	116.87	0.31	0.28	346.45	0.57	0.57	259.10	0.69	0.29	135.38	0.15	0.15
0.087	123.87	0.33	0.30	359.24	0.59	0.59	272.28	0.72	0.31	144.02	0.16	0.16
0.093	131.10	0.35	0.31	371.10	0.61	0.61	285.41	0.76	0.32	153.07	0.17	0.17
0.1	138.51	0.37	0.33	381.82	0.63	0.62	298.33	0.79	0.33	162.49	0.18	0.18
0.107	146.05	0.39	0.35	391.22	0.64	0.64	310.88	0.82	0.35	172.27	0.19	0.19
0.115	153.67	0.41	0.37	399.17	0.66	0.65	322.89	0.86	0.36	182.38	0.21	0.21
0.123	161.30	0.43	0.39	405.59	0.67	0.66	334.19	0.89	0.38	192.77	0.22	0.22
0.132	168.86	0.45	0.41	410.50	0.68	0.67	344.61	0.91	0.39	203.39	0.23	0.23
0.142	176.25	0.47	0.42	414.00	0.68	0.68	354.00	0.94	0.40	214.17	0.24	0.24
0.152	183.38	0.49	0.44	416.29	0.69	0.68	362.27	0.96	0.41	225.04	0.25	0.25
0.163	190.14	0.51	0.46	417.67	0.69	0.68	369.35	0.98	0.41	235.91	0.27	0.27
0.174	196.43	0.53	0.47	418.45	0.69	0.68	375.27	1.00	0.42	246.69	0.28	0.28
0.187	202.15	0.54	0.49	419.00	0.69	0.68	380.11	1.01	0.43	257.27	0.29	0.29
0.2	207.22	0.56	0.50	419.63	0.69	0.69	384.03	1.02	0.43	267.58	0.30	0.30
0.215	211.58	0.57	0.51	420.59	0.69	0.69	387.24	1.03	0.43	277.50	0.31	0.31
0.23	215.19	0.58	0.52	422.05	0.70	0.69	389.94	1.03	0.44	286.98	0.32	0.32
0.247	218.06	0.59	0.52	424.07	0.70	0.69	392.35	1.04	0.44	295.96	0.33	0.33
0.265	220.23	0.59	0.53	426.63	0.70	0.70	394.61	1.05	0.44	304.40	0.34	0.34
0.284	221.80	0.60	0.53	429.65	0.71	0.70	396.75	1.05	0.45	312.32	0.35	0.35
0.304	222.87	0.60	0.54	432.99	0.71	0.71	398.75	1.06	0.45	319.73	0.36	0.36
0.326	223.60	0.60	0.54	436.50	0.72	0.71	400.47	1.06	0.45	326.68	0.37	0.37
0.349	224.11	0.60	0.54	439.98	0.73	0.72	401.78	1.07	0.45	333.23	0.38	0.38
0.374	224.54	0.60	0.54	443.27	0.73	0.72	402.52	1.07	0.45	339.42	0.38	0.38
0.401	225.01	0.60	0.54	446.19	0.74	0.73	402.59	1.07	0.45	345.28	0.39	0.39
0.43	225.60	0.61	0.54	448.62	0.74	0.73	401.96	1.07	0.45	350.80	0.40	0.40
0.461	226.37	0.61	0.54	450.50	0.74	0.74	400.67	1.06	0.45	355.95	0.40	0.40
0.494	227.35	0.61	0.55	451.78	0.74	0.74	398.85	1.06	0.45	360.65	0.41	0.41
0.53	228.55	0.61	0.55	452.49	0.75	0.74	396.67	1.05	0.45	364.80	0.41	0.41
0.568	229.99	0.62	0.55	452.65	0.75	0.74	394.34	1.05	0.44	368.28	0.41	0.42
0.608	231.62	0.62	0.56	452.31	0.75	0.74	392.02	1.04	0.44	370.98	0.42	0.42
0.652	233.42	0.63	0.56	451.50	0.74	0.74	389.83	1.03	0.44	372.76	0.42	0.42
0.699	235.30	0.63	0.56	450.21	0.74	0.74	387.79	1.03	0.44	373.54	0.42	0.42
0.749	237.16	0.64	0.57	448.42	0.74	0.73	385.85	1.02	0.43	373.24	0.42	0.42
0.803	238.87	0.64	0.57	446.08	0.74	0.73	383.87	1.02	0.43	371.82	0.42	0.42
0.861	240.29	0.64	0.58	443.17	0.73	0.72	381.70	1.01	0.43	369.30	0.42	0.42
0.923	241.27	0.65	0.58	439.67	0.72	0.72	379.19	1.01	0.43	365.75	0.41	0.41
0.989	241.67	0.65	0.58	435.63	0.72	0.71	376.21	1.00	0.42	361.24	0.41	0.41
1.06	241.39	0.65	0.58	431.11	0.71	0.70	372.71	0.99	0.42	355.91	0.40	0.40
1.136	240.38	0.65	0.58	426.20	0.70	0.70	368.70	0.98	0.41	349.90	0.39	0.40
1.218	238.65	0.64	0.57	420.94	0.69	0.69	364.26	0.97	0.41	343.33	0.39	0.39
1.306	236.24	0.63	0.57	415.36	0.68	0.68	359.53	0.95	0.40	336.36	0.38	0.38
1.399	233.30	0.63	0.56	409.44	0.67	0.67	354.65	0.94	0.40	329.16	0.37	0.37
1.5	229.98	0.62	0.55	403.12	0.66	0.66	349.78	0.93	0.39	321.89	0.36	0.36

Table F39. Circular velocity curves of the 238 (E1-Sdm) CALIFA galaxies with 75th and 25th percentile uncertainties.

R/R_e	NGC7591			NGC7608			NGC7611			NGC7619		
	V_c	ΔV_c^{75th}	ΔV_c^{25th}									
0.05	56.35	0.09	0.09	41.52	0.17	0.20	135.68	0.64	0.59	384.27	0.53	0.42
0.054	60.16	0.10	0.10	43.54	0.17	0.21	144.84	0.68	0.63	398.70	0.55	0.44
0.057	64.20	0.10	0.10	45.54	0.18	0.22	154.55	0.73	0.68	412.35	0.57	0.45
0.062	68.47	0.11	0.11	47.50	0.19	0.23	164.80	0.78	0.72	425.06	0.59	0.47
0.066	72.99	0.12	0.12	49.39	0.20	0.24	175.60	0.83	0.77	436.74	0.61	0.48
0.071	77.75	0.13	0.12	51.17	0.21	0.24	186.97	0.88	0.82	447.31	0.62	0.49
0.076	82.75	0.13	0.13	52.84	0.21	0.25	198.87	0.94	0.87	456.78	0.63	0.50
0.081	88.00	0.14	0.14	54.35	0.22	0.26	211.31	1.00	0.93	465.17	0.64	0.51
0.087	93.48	0.15	0.15	55.68	0.22	0.27	224.25	1.06	0.98	472.58	0.66	0.52
0.093	99.18	0.16	0.16	56.83	0.23	0.27	237.65	1.12	1.04	479.10	0.66	0.53
0.1	105.10	0.17	0.17	57.79	0.23	0.28	251.46	1.19	1.10	484.83	0.67	0.53
0.107	111.20	0.18	0.18	58.56	0.24	0.28	265.59	1.26	1.16	489.86	0.68	0.54
0.115	117.47	0.19	0.19	59.18	0.24	0.28	279.94	1.32	1.23	494.24	0.69	0.55
0.123	123.86	0.20	0.20	59.66	0.24	0.29	294.41	1.39	1.29	497.97	0.69	0.55
0.132	130.35	0.21	0.21	60.05	0.24	0.29	308.85	1.46	1.35	501.05	0.69	0.55
0.142	136.88	0.22	0.22	60.39	0.24	0.29	323.08	1.53	1.42	503.46	0.70	0.56
0.152	143.42	0.23	0.23	60.72	0.24	0.29	336.92	1.59	1.48	505.18	0.70	0.56
0.163	149.92	0.24	0.24	61.06	0.25	0.29	350.16	1.66	1.54	506.24	0.70	0.56
0.174	156.32	0.25	0.25	61.44	0.25	0.29	362.58	1.71	1.59	506.68	0.70	0.56
0.187	162.58	0.26	0.26	61.84	0.25	0.30	373.96	1.77	1.64	506.55	0.70	0.56
0.2	168.66	0.27	0.27	62.28	0.25	0.30	384.07	1.82	1.68	505.93	0.70	0.56
0.215	174.54	0.28	0.28	62.74	0.25	0.30	392.72	1.86	1.72	504.88	0.70	0.56
0.23	180.20	0.29	0.29	63.23	0.25	0.30	399.78	1.89	1.75	503.45	0.70	0.56
0.247	185.63	0.30	0.30	63.75	0.26	0.31	405.16	1.92	1.78	501.63	0.70	0.55
0.265	190.84	0.31	0.31	64.34	0.26	0.31	408.84	1.93	1.79	499.42	0.69	0.55
0.284	195.83	0.32	0.31	65.01	0.26	0.31	410.90	1.94	1.80	496.73	0.69	0.55
0.304	200.62	0.33	0.32	65.83	0.27	0.32	411.49	1.95	1.80	493.51	0.68	0.54
0.326	205.19	0.33	0.33	66.83	0.27	0.32	410.83	1.94	1.80	489.67	0.68	0.54
0.349	209.52	0.34	0.34	68.07	0.27	0.33	409.16	1.93	1.79	485.20	0.67	0.54
0.374	213.57	0.35	0.34	69.58	0.28	0.33	406.70	1.92	1.78	480.09	0.67	0.53
0.401	217.27	0.35	0.35	71.39	0.29	0.34	403.63	1.91	1.77	474.40	0.66	0.52
0.43	220.54	0.36	0.35	73.49	0.30	0.35	400.02	1.89	1.75	468.23	0.65	0.52
0.461	223.31	0.36	0.36	75.89	0.31	0.36	395.89	1.87	1.74	461.69	0.64	0.51
0.494	225.51	0.37	0.36	78.58	0.32	0.38	391.21	1.85	1.72	454.89	0.63	0.50
0.53	227.06	0.37	0.36	81.52	0.33	0.39	385.92	1.82	1.69	447.96	0.62	0.49
0.568	227.91	0.37	0.37	84.68	0.34	0.41	380.02	1.80	1.67	440.99	0.61	0.49
0.608	228.03	0.37	0.37	88.03	0.36	0.42	373.56	1.77	1.64	434.07	0.60	0.48
0.652	227.40	0.37	0.36	91.53	0.37	0.44	366.68	1.73	1.61	427.26	0.59	0.47
0.699	226.06	0.37	0.36	95.13	0.38	0.46	359.61	1.70	1.58	420.60	0.58	0.46
0.749	224.09	0.36	0.36	98.77	0.40	0.47	352.60	1.67	1.55	414.08	0.57	0.46
0.803	221.61	0.36	0.36	102.41	0.41	0.49	345.93	1.64	1.52	407.68	0.57	0.45
0.861	218.81	0.36	0.35	105.97	0.43	0.51	339.82	1.61	1.49	401.35	0.56	0.44
0.923	215.89	0.35	0.35	109.41	0.44	0.52	334.48	1.58	1.47	395.05	0.55	0.44
0.989	213.04	0.35	0.34	112.66	0.45	0.54	330.00	1.56	1.45	388.73	0.54	0.43
1.06	210.43	0.34	0.34	115.65	0.47	0.55	326.41	1.54	1.43	382.41	0.53	0.42
1.136	208.18	0.34	0.33	118.31	0.48	0.57	323.70	1.53	1.42	376.15	0.52	0.41
1.218	206.35	0.34	0.33	120.59	0.49	0.58	321.79	1.52	1.41	370.02	0.51	0.41
1.306	204.95	0.33	0.33	122.42	0.49	0.59	320.56	1.52	1.41	364.12	0.50	0.40
1.399	203.92	0.33	0.33	123.75	0.50	0.59	319.86	1.51	1.40	358.52	0.50	0.40
1.5	203.18	0.33	0.33	124.51	0.50	0.60	319.52	1.51	1.40	353.22	0.49	0.39

Table F40. Circular velocity curves of the 238 (E1–Sdm) CALIFA galaxies with 75th and 25th percentile uncertainties.

R/R_e	NGC7623			NGC7625			NGC7631			NGC7653		
	V_c	ΔV_c^{75th}	ΔV_c^{25th}									
0.05	80.29	0.12	0.28	61.35	0.26	0.22	53.32	0.08	0.07	65.45	0.21	0.12
0.054	85.79	0.13	0.30	63.36	0.27	0.23	56.82	0.08	0.07	69.74	0.23	0.13
0.057	91.64	0.14	0.32	65.23	0.28	0.24	60.52	0.09	0.08	74.26	0.24	0.14
0.062	97.85	0.15	0.34	66.95	0.29	0.24	64.41	0.09	0.08	79.00	0.26	0.15
0.066	104.43	0.16	0.36	68.53	0.30	0.25	68.48	0.10	0.09	83.98	0.27	0.16
0.071	111.39	0.17	0.38	69.99	0.30	0.25	72.74	0.11	0.09	89.17	0.29	0.17
0.076	118.74	0.18	0.41	71.39	0.31	0.26	77.18	0.11	0.10	94.57	0.31	0.18
0.081	126.49	0.20	0.44	72.79	0.32	0.27	81.77	0.12	0.10	100.16	0.33	0.19
0.087	134.63	0.21	0.47	74.26	0.32	0.27	86.49	0.13	0.11	105.91	0.35	0.20
0.093	143.16	0.22	0.49	75.91	0.33	0.28	91.33	0.13	0.11	111.81	0.37	0.21
0.1	152.07	0.24	0.53	77.82	0.34	0.28	96.24	0.14	0.12	117.81	0.39	0.23
0.107	161.33	0.25	0.56	80.05	0.35	0.29	101.19	0.15	0.13	123.87	0.41	0.24
0.115	170.92	0.26	0.59	82.64	0.36	0.30	106.13	0.15	0.13	129.96	0.43	0.25
0.123	180.80	0.28	0.63	85.61	0.37	0.31	111.00	0.16	0.14	136.01	0.44	0.26
0.132	190.93	0.30	0.66	88.94	0.39	0.33	115.73	0.17	0.15	141.97	0.46	0.27
0.142	201.23	0.31	0.70	92.58	0.40	0.34	120.26	0.17	0.15	147.79	0.48	0.28
0.152	211.64	0.33	0.73	96.48	0.42	0.35	124.51	0.18	0.16	153.41	0.50	0.29
0.163	222.06	0.34	0.77	100.60	0.44	0.37	128.42	0.19	0.16	158.78	0.52	0.30
0.174	232.40	0.36	0.80	104.86	0.46	0.38	131.92	0.19	0.17	163.86	0.54	0.31
0.187	242.55	0.38	0.84	109.22	0.48	0.40	134.96	0.20	0.17	168.61	0.55	0.32
0.2	252.38	0.39	0.87	113.62	0.50	0.42	137.50	0.20	0.17	173.01	0.57	0.33
0.215	261.76	0.40	0.91	117.99	0.51	0.43	139.55	0.20	0.18	177.05	0.58	0.34
0.23	270.58	0.42	0.94	122.29	0.53	0.45	141.14	0.20	0.18	180.71	0.59	0.35
0.247	278.71	0.43	0.96	126.46	0.55	0.46	142.34	0.21	0.18	183.99	0.60	0.35
0.265	286.06	0.44	0.99	130.48	0.57	0.48	143.24	0.21	0.18	186.88	0.61	0.36
0.284	292.55	0.45	1.01	134.30	0.59	0.49	143.99	0.21	0.18	189.37	0.62	0.36
0.304	298.13	0.46	1.03	137.92	0.60	0.51	144.73	0.21	0.18	191.45	0.63	0.37
0.326	302.82	0.47	1.05	141.33	0.62	0.52	145.59	0.21	0.18	193.10	0.63	0.37
0.349	306.66	0.47	1.06	144.56	0.63	0.53	146.69	0.21	0.18	194.34	0.64	0.37
0.374	309.74	0.48	1.07	147.61	0.64	0.54	148.10	0.21	0.19	195.20	0.64	0.37
0.401	312.19	0.48	1.08	150.52	0.66	0.55	149.84	0.22	0.19	195.74	0.64	0.38
0.43	314.15	0.49	1.09	153.28	0.67	0.56	151.92	0.22	0.19	196.06	0.64	0.38
0.461	315.72	0.49	1.09	155.88	0.68	0.57	154.30	0.22	0.19	196.27	0.64	0.38
0.494	316.98	0.49	1.10	158.28	0.69	0.58	156.94	0.23	0.20	196.51	0.64	0.38
0.53	317.93	0.49	1.10	160.40	0.70	0.59	159.79	0.23	0.20	196.87	0.64	0.38
0.568	318.55	0.49	1.10	162.13	0.71	0.59	162.79	0.24	0.20	197.45	0.65	0.38
0.608	318.74	0.49	1.10	163.38	0.71	0.60	165.88	0.24	0.21	198.26	0.65	0.38
0.652	318.44	0.49	1.10	164.06	0.72	0.60	168.99	0.24	0.21	199.30	0.65	0.38
0.699	317.56	0.49	1.10	164.13	0.72	0.60	172.05	0.25	0.22	200.49	0.66	0.38
0.749	316.09	0.49	1.09	163.60	0.71	0.60	174.96	0.25	0.22	201.77	0.66	0.39
0.803	314.02	0.49	1.09	162.54	0.71	0.60	177.64	0.26	0.22	203.02	0.66	0.39
0.861	311.39	0.48	1.08	161.09	0.70	0.59	179.99	0.26	0.23	204.15	0.67	0.39
0.923	308.24	0.48	1.07	159.41	0.70	0.58	181.94	0.26	0.23	205.07	0.67	0.39
0.989	304.59	0.47	1.05	157.71	0.69	0.58	183.44	0.27	0.23	205.70	0.67	0.39
1.06	300.46	0.46	1.04	156.18	0.68	0.57	184.50	0.27	0.23	206.00	0.67	0.40
1.136	295.83	0.46	1.02	154.97	0.68	0.57	185.14	0.27	0.23	205.95	0.67	0.40
1.218	290.74	0.45	1.01	154.13	0.67	0.57	185.46	0.27	0.23	205.57	0.67	0.39
1.306	285.21	0.44	0.99	153.64	0.67	0.56	185.55	0.27	0.23	204.89	0.67	0.39
1.399	279.34	0.43	0.97	153.42	0.67	0.56	185.56	0.27	0.23	203.98	0.67	0.39
1.5	273.24	0.42	0.95	153.31	0.67	0.56	185.56	0.27	0.23	202.92	0.66	0.39

Table F41. Circular velocity curves of the 238 (E1–Sdm) CALIFA galaxies with 75th and 25th percentile uncertainties.

R/R_e	NGC7671			NGC7683			NGC7711			NGC7716		
	V_c	ΔV_c^{75th}	ΔV_c^{25th}									
0.05	136.88	0.20	0.16	113.65	0.18	0.21	146.20	0.30	0.17	107.73	0.16	0.14
0.054	146.03	0.21	0.17	121.14	0.19	0.22	155.28	0.32	0.18	113.93	0.17	0.15
0.057	155.69	0.23	0.19	129.03	0.21	0.23	164.73	0.34	0.19	120.29	0.18	0.16
0.062	165.87	0.24	0.20	137.31	0.22	0.25	174.51	0.36	0.21	126.75	0.19	0.17
0.066	176.57	0.26	0.21	145.97	0.23	0.27	184.58	0.38	0.22	133.26	0.20	0.18
0.071	187.77	0.27	0.22	155.01	0.25	0.28	194.88	0.40	0.23	139.76	0.21	0.19
0.076	199.46	0.29	0.24	164.40	0.26	0.30	205.36	0.42	0.24	146.19	0.22	0.20
0.081	211.61	0.31	0.25	174.11	0.28	0.32	215.94	0.45	0.25	152.46	0.22	0.20
0.087	224.17	0.32	0.27	184.09	0.29	0.33	226.52	0.47	0.27	158.50	0.23	0.21
0.093	237.10	0.34	0.28	194.29	0.31	0.35	237.01	0.49	0.28	164.22	0.24	0.22
0.1	250.32	0.36	0.30	204.64	0.33	0.37	247.30	0.51	0.29	169.53	0.25	0.23
0.107	263.73	0.38	0.31	215.06	0.34	0.39	257.26	0.53	0.30	174.36	0.26	0.23
0.115	277.21	0.40	0.33	225.46	0.36	0.41	266.79	0.55	0.31	178.64	0.26	0.24
0.123	290.63	0.42	0.35	235.72	0.38	0.43	275.77	0.57	0.32	182.30	0.27	0.24
0.132	303.84	0.44	0.36	245.72	0.39	0.45	284.12	0.59	0.33	185.33	0.27	0.25
0.142	316.65	0.46	0.38	255.36	0.41	0.46	291.75	0.60	0.34	187.71	0.28	0.25
0.152	328.87	0.48	0.39	264.50	0.42	0.48	298.63	0.62	0.35	189.45	0.28	0.25
0.163	340.31	0.49	0.41	273.04	0.43	0.50	304.74	0.63	0.36	190.58	0.28	0.26
0.174	350.74	0.51	0.42	280.89	0.45	0.51	310.08	0.64	0.36	191.14	0.28	0.26
0.187	360.00	0.52	0.43	287.97	0.46	0.52	314.70	0.65	0.37	191.17	0.28	0.26
0.2	367.92	0.53	0.44	294.26	0.47	0.54	318.62	0.66	0.38	190.71	0.28	0.26
0.215	374.38	0.54	0.45	299.78	0.48	0.55	321.89	0.67	0.38	189.79	0.28	0.25
0.23	379.32	0.55	0.45	304.56	0.49	0.55	324.53	0.67	0.38	188.42	0.28	0.25
0.247	382.77	0.55	0.46	308.69	0.49	0.56	326.52	0.67	0.38	186.63	0.28	0.25
0.265	384.81	0.56	0.46	312.27	0.50	0.57	327.85	0.68	0.39	184.45	0.27	0.25
0.284	385.59	0.56	0.46	315.38	0.50	0.57	328.52	0.68	0.39	181.93	0.27	0.24
0.304	385.31	0.56	0.46	318.11	0.51	0.58	328.53	0.68	0.39	179.16	0.26	0.24
0.326	384.17	0.56	0.46	320.47	0.51	0.58	327.93	0.68	0.39	176.25	0.26	0.24
0.349	382.37	0.55	0.46	322.47	0.51	0.59	326.81	0.68	0.38	173.32	0.26	0.23
0.374	380.07	0.55	0.45	324.09	0.52	0.59	325.28	0.67	0.38	170.52	0.25	0.23
0.401	377.39	0.55	0.45	325.29	0.52	0.59	323.46	0.67	0.38	167.95	0.25	0.23
0.43	374.40	0.54	0.45	326.07	0.52	0.59	321.48	0.66	0.38	165.70	0.24	0.22
0.461	371.20	0.54	0.44	326.45	0.52	0.59	319.42	0.66	0.38	163.80	0.24	0.22
0.494	367.85	0.53	0.44	326.47	0.52	0.59	317.33	0.66	0.37	162.24	0.24	0.22
0.53	364.43	0.53	0.43	326.21	0.52	0.59	315.26	0.65	0.37	160.99	0.24	0.22
0.568	361.03	0.52	0.43	325.73	0.52	0.59	313.22	0.65	0.37	160.01	0.24	0.21
0.608	357.72	0.52	0.43	325.06	0.52	0.59	311.21	0.64	0.37	159.23	0.23	0.21
0.652	354.53	0.51	0.42	324.24	0.52	0.59	309.22	0.64	0.36	158.59	0.23	0.21
0.699	351.50	0.51	0.42	323.23	0.51	0.59	307.24	0.63	0.36	158.03	0.23	0.21
0.749	348.65	0.50	0.42	321.99	0.51	0.59	305.21	0.63	0.36	157.49	0.23	0.21
0.803	346.02	0.50	0.41	320.49	0.51	0.58	303.08	0.63	0.36	156.94	0.23	0.21
0.861	343.64	0.50	0.41	318.68	0.51	0.58	300.77	0.62	0.35	156.31	0.23	0.21
0.923	341.55	0.49	0.41	316.52	0.50	0.58	298.21	0.62	0.35	155.57	0.23	0.21
0.989	339.75	0.49	0.40	314.01	0.50	0.57	295.35	0.61	0.35	154.70	0.23	0.21
1.06	338.23	0.49	0.40	311.15	0.50	0.57	292.16	0.60	0.34	153.67	0.23	0.21
1.136	336.92	0.49	0.40	307.98	0.49	0.56	288.66	0.60	0.34	152.49	0.23	0.20
1.218	335.73	0.49	0.40	304.55	0.49	0.55	284.92	0.59	0.34	151.15	0.22	0.20
1.306	334.54	0.48	0.40	300.97	0.48	0.55	281.03	0.58	0.33	149.70	0.22	0.20
1.399	333.22	0.48	0.40	297.32	0.47	0.54	277.10	0.57	0.33	148.18	0.22	0.20
1.5	331.65	0.48	0.40	293.71	0.47	0.53	273.22	0.56	0.32	146.60	0.22	0.20

Table F42. Circular velocity curves of the 238 (E1–Sdm) CALIFA galaxies with 75th and 25th percentile uncertainties.

R/R_e	NGC7722			NGC7738			NGC7787			NGC7819		
	V_c	ΔV_c^{75th}	ΔV_c^{25th}									
0.05	179.83	0.44	0.40	110.69	0.28	0.30	72.50	0.32	0.32	94.26	0.26	0.24
0.054	190.21	0.47	0.42	117.53	0.30	0.32	77.29	0.34	0.34	99.22	0.27	0.25
0.057	200.83	0.49	0.45	124.64	0.32	0.34	82.34	0.36	0.36	104.21	0.29	0.27
0.062	211.62	0.52	0.47	131.97	0.33	0.36	87.65	0.39	0.38	109.17	0.30	0.28
0.066	222.49	0.55	0.50	139.50	0.35	0.38	93.22	0.41	0.41	114.07	0.31	0.29
0.071	233.36	0.57	0.52	147.18	0.37	0.40	99.03	0.44	0.43	118.85	0.33	0.31
0.076	244.10	0.60	0.54	154.94	0.39	0.42	105.08	0.46	0.46	123.46	0.34	0.32
0.081	254.59	0.62	0.57	162.71	0.41	0.44	111.34	0.49	0.49	127.86	0.35	0.33
0.087	264.70	0.65	0.59	170.41	0.43	0.46	117.79	0.52	0.52	131.99	0.36	0.34
0.093	274.30	0.67	0.61	177.93	0.45	0.48	124.39	0.55	0.55	135.82	0.37	0.35
0.1	283.27	0.69	0.63	185.17	0.47	0.50	131.08	0.58	0.58	139.35	0.38	0.36
0.107	291.48	0.71	0.65	191.98	0.49	0.52	137.83	0.61	0.60	142.56	0.39	0.37
0.115	298.84	0.73	0.67	198.26	0.50	0.54	144.55	0.64	0.63	145.46	0.40	0.37
0.123	305.32	0.75	0.68	203.86	0.52	0.55	151.16	0.67	0.66	148.09	0.41	0.38
0.132	310.87	0.76	0.69	208.67	0.53	0.57	157.59	0.69	0.69	150.47	0.41	0.39
0.142	315.54	0.77	0.70	212.59	0.54	0.58	163.72	0.72	0.72	152.63	0.42	0.39
0.152	319.36	0.78	0.71	215.55	0.55	0.59	169.45	0.75	0.74	154.57	0.43	0.40
0.163	322.42	0.79	0.72	217.54	0.55	0.59	174.68	0.77	0.77	156.27	0.43	0.40
0.174	324.80	0.80	0.72	218.57	0.55	0.59	179.31	0.79	0.79	157.70	0.43	0.41
0.187	326.57	0.80	0.73	218.74	0.55	0.59	183.25	0.81	0.80	158.79	0.44	0.41
0.2	327.80	0.80	0.73	218.22	0.55	0.59	186.44	0.82	0.82	159.45	0.44	0.41
0.215	328.53	0.81	0.73	217.20	0.55	0.59	188.85	0.83	0.83	159.62	0.44	0.41
0.23	328.81	0.81	0.73	215.91	0.55	0.59	190.50	0.84	0.84	159.24	0.44	0.41
0.247	328.74	0.81	0.73	214.57	0.54	0.58	191.44	0.84	0.84	158.28	0.44	0.41
0.265	328.43	0.80	0.73	213.38	0.54	0.58	191.77	0.84	0.84	156.76	0.43	0.40
0.284	328.01	0.80	0.73	212.47	0.54	0.58	191.61	0.84	0.84	154.74	0.43	0.40
0.304	327.61	0.80	0.73	211.90	0.54	0.58	191.11	0.84	0.84	152.33	0.42	0.39
0.326	327.33	0.80	0.73	211.67	0.54	0.58	190.40	0.84	0.84	149.67	0.41	0.38
0.349	327.16	0.80	0.73	211.73	0.54	0.58	189.59	0.83	0.83	146.92	0.41	0.38
0.374	327.01	0.80	0.73	211.99	0.54	0.58	188.75	0.83	0.83	144.21	0.40	0.37
0.401	326.74	0.80	0.73	212.35	0.54	0.58	187.92	0.83	0.82	141.64	0.39	0.36
0.43	326.14	0.80	0.73	212.71	0.54	0.58	187.13	0.82	0.82	139.28	0.38	0.36
0.461	325.05	0.80	0.72	212.98	0.54	0.58	186.39	0.82	0.82	137.14	0.38	0.35
0.494	323.36	0.79	0.72	213.09	0.54	0.58	185.76	0.82	0.82	135.21	0.37	0.35
0.53	321.06	0.79	0.71	213.01	0.54	0.58	185.27	0.82	0.81	133.48	0.37	0.34
0.568	318.23	0.78	0.71	212.71	0.54	0.58	184.98	0.81	0.81	131.94	0.36	0.34
0.608	315.01	0.77	0.70	212.23	0.54	0.58	184.91	0.81	0.81	130.63	0.36	0.34
0.652	311.64	0.76	0.69	211.62	0.54	0.58	185.05	0.81	0.81	129.59	0.36	0.33
0.699	308.30	0.76	0.69	210.97	0.53	0.57	185.38	0.82	0.81	128.87	0.36	0.33
0.749	305.17	0.75	0.68	210.33	0.53	0.57	185.82	0.82	0.82	128.51	0.35	0.33
0.803	302.34	0.74	0.67	209.80	0.53	0.57	186.29	0.82	0.82	128.54	0.35	0.33
0.861	299.82	0.73	0.67	209.39	0.53	0.57	186.70	0.82	0.82	128.98	0.36	0.33
0.923	297.55	0.73	0.66	209.11	0.53	0.57	186.95	0.82	0.82	129.81	0.36	0.33
0.989	295.43	0.72	0.66	208.94	0.53	0.57	186.97	0.82	0.82	130.99	0.36	0.34
1.06	293.39	0.72	0.65	208.81	0.53	0.57	186.70	0.82	0.82	132.47	0.37	0.34
1.136	291.37	0.71	0.65	208.66	0.53	0.57	186.13	0.82	0.82	134.18	0.37	0.34
1.218	289.35	0.71	0.64	208.43	0.53	0.57	185.26	0.82	0.81	136.02	0.38	0.35
1.306	287.34	0.70	0.64	208.06	0.53	0.57	184.11	0.81	0.81	137.89	0.38	0.35
1.399	285.36	0.70	0.64	207.54	0.53	0.56	182.72	0.80	0.80	139.68	0.39	0.36
1.5	283.41	0.69	0.63	206.86	0.52	0.56	181.15	0.80	0.80	141.25	0.39	0.36

Table F43. Circular velocity curves of the 238 (E1-Sdm) CALIFA galaxies with 75th and 25th percentile uncertainties.

R/R_e	NGC7824			UGC00005			UGC00029			UGC00036		
	V_c	ΔV_c^{75th}	ΔV_c^{25th}	V_c	ΔV_c^{75th}	ΔV_c^{25th}	V_c	ΔV_c^{75th}	ΔV_c^{25th}	V_c	ΔV_c^{75th}	ΔV_c^{25th}
0.05	131.51	0.34	0.30	45.15	0.06	0.06	222.29	1.08	0.96	107.04	0.20	0.22
0.054	140.48	0.36	0.32	48.14	0.07	0.06	233.89	1.14	1.01	113.85	0.21	0.23
0.057	149.99	0.38	0.34	51.31	0.07	0.07	245.52	1.19	1.06	120.97	0.22	0.25
0.062	160.06	0.41	0.36	54.65	0.08	0.07	257.06	1.25	1.11	128.38	0.24	0.26
0.066	170.69	0.44	0.38	58.17	0.08	0.08	268.37	1.30	1.16	136.05	0.25	0.28
0.071	181.90	0.47	0.41	61.86	0.09	0.08	279.34	1.36	1.21	143.97	0.27	0.29
0.076	193.68	0.50	0.44	65.72	0.09	0.09	289.80	1.41	1.25	152.08	0.28	0.31
0.081	206.03	0.53	0.46	69.76	0.10	0.09	299.64	1.46	1.30	160.34	0.30	0.33
0.087	218.93	0.56	0.49	73.96	0.11	0.10	308.72	1.50	1.34	168.68	0.31	0.34
0.093	232.35	0.59	0.52	78.31	0.11	0.10	316.96	1.54	1.37	177.03	0.33	0.36
0.1	246.25	0.63	0.55	82.80	0.12	0.11	324.28	1.58	1.40	185.31	0.34	0.38
0.107	260.56	0.67	0.59	87.42	0.13	0.12	330.69	1.61	1.43	193.41	0.36	0.39
0.115	275.21	0.70	0.62	92.13	0.13	0.12	336.21	1.63	1.46	201.25	0.37	0.41
0.123	290.09	0.74	0.65	96.91	0.14	0.13	340.93	1.66	1.48	208.72	0.39	0.42
0.132	305.08	0.78	0.69	101.72	0.15	0.13	344.96	1.68	1.49	215.72	0.40	0.44
0.142	320.02	0.82	0.72	106.52	0.15	0.14	348.43	1.69	1.51	222.18	0.41	0.45
0.152	334.73	0.86	0.75	111.26	0.16	0.15	351.45	1.71	1.52	228.04	0.42	0.46
0.163	349.00	0.89	0.78	115.88	0.17	0.15	354.10	1.72	1.53	233.28	0.43	0.47
0.174	362.61	0.93	0.82	120.33	0.17	0.16	356.41	1.73	1.54	237.92	0.44	0.48
0.187	375.30	0.96	0.84	124.54	0.18	0.16	358.35	1.74	1.55	242.05	0.45	0.49
0.2	386.83	0.99	0.87	128.45	0.19	0.17	359.87	1.75	1.56	245.77	0.46	0.50
0.215	396.94	1.02	0.89	132.03	0.19	0.17	360.90	1.75	1.56	249.24	0.46	0.51
0.23	405.40	1.04	0.91	135.23	0.19	0.18	361.40	1.76	1.56	252.63	0.47	0.51
0.247	412.02	1.06	0.93	138.06	0.20	0.18	361.36	1.76	1.56	256.09	0.48	0.52
0.265	416.68	1.07	0.94	140.55	0.20	0.19	360.83	1.75	1.56	259.72	0.48	0.53
0.284	419.36	1.07	0.94	142.77	0.21	0.19	359.88	1.75	1.56	263.55	0.49	0.53
0.304	420.12	1.08	0.94	144.82	0.21	0.19	358.65	1.74	1.55	267.55	0.50	0.54
0.326	419.14	1.07	0.94	146.85	0.21	0.19	357.23	1.74	1.55	271.63	0.50	0.55
0.349	416.71	1.07	0.94	149.02	0.21	0.20	355.75	1.73	1.54	275.67	0.51	0.56
0.374	413.20	1.06	0.93	151.47	0.22	0.20	354.24	1.72	1.53	279.55	0.52	0.57
0.401	409.00	1.05	0.92	154.34	0.22	0.20	352.74	1.71	1.53	283.16	0.53	0.57
0.43	404.49	1.04	0.91	157.72	0.23	0.21	351.22	1.71	1.52	286.43	0.53	0.58
0.461	399.99	1.02	0.90	161.64	0.23	0.21	349.63	1.70	1.51	289.32	0.54	0.59
0.494	395.71	1.01	0.89	166.07	0.24	0.22	347.90	1.69	1.51	291.79	0.54	0.59
0.53	391.76	1.00	0.88	170.97	0.25	0.23	345.99	1.68	1.50	293.86	0.55	0.60
0.568	388.16	0.99	0.87	176.26	0.25	0.23	343.83	1.67	1.49	295.54	0.55	0.60
0.608	384.87	0.99	0.87	181.84	0.26	0.24	341.40	1.66	1.48	296.86	0.55	0.60
0.652	381.80	0.98	0.86	187.63	0.27	0.25	338.71	1.65	1.47	297.86	0.55	0.60
0.699	378.83	0.97	0.85	193.54	0.28	0.26	335.81	1.63	1.45	298.58	0.55	0.61
0.749	375.80	0.96	0.84	199.50	0.29	0.26	332.77	1.62	1.44	299.09	0.56	0.61
0.803	372.54	0.95	0.84	205.45	0.30	0.27	329.69	1.60	1.43	299.46	0.56	0.61
0.861	368.89	0.94	0.83	211.35	0.30	0.28	326.64	1.59	1.41	299.77	0.56	0.61
0.923	364.70	0.93	0.82	217.15	0.31	0.29	323.71	1.57	1.40	300.11	0.56	0.61
0.989	359.87	0.92	0.81	222.83	0.32	0.30	320.91	1.56	1.39	300.55	0.56	0.61
1.06	354.38	0.91	0.80	228.36	0.33	0.30	318.22	1.55	1.38	301.13	0.56	0.61
1.136	348.30	0.89	0.78	233.68	0.34	0.31	315.57	1.53	1.37	301.86	0.56	0.61
1.218	341.77	0.88	0.77	238.72	0.34	0.32	312.89	1.52	1.35	302.72	0.56	0.61
1.306	335.03	0.86	0.75	243.39	0.35	0.32	310.11	1.51	1.34	303.65	0.56	0.62
1.399	328.35	0.84	0.74	247.54	0.36	0.33	307.16	1.49	1.33	304.56	0.57	0.62
1.5	322.02	0.82	0.72	251.00	0.36	0.33	304.03	1.48	1.32	305.34	0.57	0.62

Table F44. Circular velocity curves of the 238 (E1–Sdm) CALIFA galaxies with 75th and 25th percentile uncertainties.

R/R_e	UGC00148			UGC00312			UGC00809			UGC00987		
	V_c	ΔV_c^{75th}	ΔV_c^{25th}									
0.05	40.92	0.17	0.15	62.32	0.24	0.21	10.71	0.04	0.03	67.05	0.20	0.12
0.054	42.79	0.18	0.16	65.21	0.25	0.22	11.33	0.04	0.04	71.55	0.22	0.13
0.057	44.62	0.19	0.16	68.06	0.26	0.23	12.02	0.04	0.04	76.31	0.23	0.14
0.062	46.38	0.20	0.17	70.83	0.27	0.24	12.78	0.05	0.04	81.34	0.25	0.15
0.066	48.07	0.20	0.18	73.51	0.28	0.25	13.60	0.05	0.05	86.63	0.26	0.16
0.071	49.67	0.21	0.18	76.06	0.29	0.26	14.49	0.05	0.05	92.20	0.28	0.17
0.076	51.15	0.22	0.19	78.48	0.30	0.27	15.45	0.06	0.06	98.03	0.30	0.18
0.081	52.51	0.22	0.19	80.78	0.31	0.28	16.50	0.06	0.06	104.11	0.31	0.19
0.087	53.77	0.23	0.20	82.97	0.32	0.28	17.62	0.07	0.06	110.43	0.33	0.20
0.093	54.94	0.23	0.20	85.11	0.32	0.29	18.83	0.07	0.07	116.97	0.35	0.21
0.1	56.05	0.24	0.21	87.26	0.33	0.30	20.14	0.08	0.07	123.70	0.37	0.23
0.107	57.15	0.24	0.21	89.50	0.34	0.31	21.54	0.08	0.08	130.58	0.40	0.24
0.115	58.30	0.25	0.22	91.94	0.35	0.31	23.04	0.09	0.09	137.57	0.42	0.25
0.123	59.55	0.25	0.22	94.67	0.36	0.32	24.66	0.09	0.09	144.60	0.44	0.26
0.132	60.96	0.26	0.23	97.78	0.37	0.33	26.39	0.10	0.10	151.61	0.46	0.28
0.142	62.57	0.27	0.23	101.33	0.39	0.35	28.24	0.11	0.10	158.53	0.48	0.29
0.152	64.37	0.27	0.24	105.35	0.40	0.36	30.23	0.11	0.11	165.26	0.50	0.30
0.163	66.38	0.28	0.25	109.82	0.42	0.37	32.36	0.12	0.12	171.72	0.52	0.31
0.174	68.55	0.29	0.25	114.71	0.44	0.39	34.63	0.13	0.13	177.83	0.54	0.33
0.187	70.86	0.30	0.26	119.97	0.46	0.41	37.06	0.14	0.14	183.48	0.56	0.34
0.2	73.24	0.31	0.27	125.52	0.48	0.43	39.66	0.15	0.15	188.61	0.57	0.34
0.215	75.66	0.32	0.28	131.29	0.50	0.45	42.43	0.16	0.16	193.15	0.58	0.35
0.23	78.08	0.33	0.29	137.20	0.52	0.47	45.38	0.17	0.17	197.08	0.60	0.36
0.247	80.47	0.34	0.30	143.15	0.55	0.49	48.53	0.18	0.18	200.38	0.61	0.37
0.265	82.82	0.35	0.31	149.05	0.57	0.51	51.89	0.20	0.19	203.10	0.61	0.37
0.284	85.11	0.36	0.32	154.79	0.59	0.53	55.45	0.21	0.21	205.30	0.62	0.38
0.304	87.36	0.37	0.32	160.25	0.61	0.55	59.24	0.23	0.22	207.06	0.63	0.38
0.326	89.61	0.38	0.33	165.30	0.63	0.56	63.26	0.24	0.24	208.48	0.63	0.38
0.349	91.90	0.39	0.34	169.80	0.65	0.58	67.51	0.26	0.25	209.64	0.63	0.38
0.374	94.29	0.40	0.35	173.63	0.66	0.59	72.00	0.27	0.27	210.63	0.64	0.39
0.401	96.85	0.41	0.36	176.66	0.67	0.60	76.74	0.29	0.29	211.48	0.64	0.39
0.43	99.66	0.43	0.37	178.81	0.68	0.61	81.73	0.31	0.31	212.23	0.64	0.39
0.461	102.77	0.44	0.38	180.01	0.69	0.61	86.95	0.33	0.32	212.88	0.64	0.39
0.494	106.23	0.45	0.39	180.26	0.69	0.62	92.41	0.35	0.35	213.46	0.65	0.39
0.53	110.06	0.47	0.41	179.62	0.69	0.61	98.09	0.37	0.37	214.01	0.65	0.39
0.568	114.26	0.49	0.42	178.24	0.68	0.61	103.98	0.40	0.39	214.58	0.65	0.39
0.608	118.80	0.51	0.44	176.33	0.67	0.60	110.05	0.42	0.41	215.24	0.65	0.39
0.652	123.64	0.53	0.46	174.18	0.66	0.59	116.26	0.44	0.43	216.06	0.65	0.40
0.699	128.73	0.55	0.48	172.11	0.66	0.59	122.57	0.47	0.46	217.08	0.66	0.40
0.749	133.99	0.57	0.50	170.44	0.65	0.58	128.93	0.49	0.48	218.28	0.66	0.40
0.803	139.34	0.60	0.52	169.41	0.65	0.58	135.27	0.52	0.51	219.62	0.66	0.40
0.861	144.70	0.62	0.54	169.19	0.65	0.58	141.50	0.54	0.53	221.01	0.67	0.40
0.923	149.95	0.64	0.56	169.80	0.65	0.58	147.54	0.56	0.55	222.30	0.67	0.41
0.989	154.97	0.66	0.58	171.20	0.65	0.58	153.28	0.58	0.57	223.35	0.68	0.41
1.06	159.64	0.68	0.59	173.25	0.66	0.59	158.61	0.60	0.59	224.02	0.68	0.41
1.136	163.82	0.70	0.61	175.77	0.67	0.60	163.39	0.62	0.61	224.19	0.68	0.41
1.218	167.38	0.71	0.62	178.59	0.68	0.61	167.51	0.64	0.63	223.76	0.68	0.41
1.306	170.17	0.73	0.63	181.50	0.69	0.62	170.84	0.65	0.64	222.70	0.67	0.41
1.399	172.08	0.74	0.64	184.33	0.70	0.63	173.27	0.66	0.65	220.99	0.67	0.40
1.5	173.02	0.74	0.64	186.89	0.71	0.64	174.71	0.67	0.65	218.69	0.66	0.40

Table F45. Circular velocity curves of the 238 (E1–Sdm) CALIFA galaxies with 75th and 25th percentile uncertainties.

R/R_e	UGC01057			UGC01271			UGC02222			UGC02229		
	V_c	ΔV_c^{75th}	ΔV_c^{25th}									
0.05	48.83	0.16	0.18	138.35	0.49	0.42	88.06	0.21	0.16	141.42	0.27	0.23
0.054	51.96	0.17	0.19	146.02	0.52	0.45	93.73	0.22	0.17	150.38	0.29	0.25
0.057	55.24	0.18	0.21	153.80	0.54	0.47	99.71	0.24	0.18	159.73	0.30	0.27
0.062	58.68	0.19	0.22	161.62	0.57	0.50	106.01	0.25	0.20	169.44	0.32	0.28
0.066	62.24	0.21	0.23	169.41	0.60	0.52	112.61	0.27	0.21	179.48	0.34	0.30
0.071	65.94	0.22	0.25	177.08	0.63	0.54	119.55	0.29	0.22	189.80	0.36	0.32
0.076	69.74	0.23	0.26	184.54	0.65	0.57	126.81	0.30	0.23	200.33	0.38	0.33
0.081	73.63	0.24	0.28	191.68	0.68	0.59	134.40	0.32	0.25	211.01	0.40	0.35
0.087	77.57	0.26	0.29	198.41	0.70	0.61	142.32	0.34	0.26	221.73	0.42	0.37
0.093	81.54	0.27	0.31	204.63	0.73	0.63	150.57	0.36	0.28	232.38	0.44	0.39
0.1	85.48	0.28	0.32	210.27	0.75	0.65	159.13	0.38	0.29	242.83	0.46	0.40
0.107	89.34	0.30	0.34	215.28	0.76	0.66	168.00	0.40	0.31	252.92	0.48	0.42
0.115	93.08	0.31	0.35	219.67	0.78	0.67	177.13	0.43	0.33	262.51	0.50	0.44
0.123	96.62	0.32	0.36	223.47	0.79	0.69	186.48	0.45	0.34	271.42	0.52	0.45
0.132	99.89	0.33	0.38	226.79	0.80	0.70	195.99	0.47	0.36	279.50	0.53	0.46
0.142	102.83	0.34	0.39	229.78	0.81	0.71	205.56	0.49	0.38	286.59	0.55	0.48
0.152	105.37	0.35	0.40	232.62	0.82	0.71	215.11	0.52	0.40	292.58	0.56	0.49
0.163	107.45	0.36	0.41	235.51	0.83	0.72	224.49	0.54	0.41	297.42	0.57	0.49
0.174	109.03	0.36	0.41	238.63	0.85	0.73	233.58	0.56	0.43	301.10	0.57	0.50
0.187	110.09	0.37	0.42	242.08	0.86	0.74	242.22	0.58	0.45	303.72	0.58	0.50
0.2	110.65	0.37	0.42	245.89	0.87	0.75	250.26	0.60	0.46	305.44	0.58	0.51
0.215	110.77	0.37	0.42	250.01	0.89	0.77	257.52	0.62	0.48	306.53	0.58	0.51
0.23	110.54	0.37	0.42	254.29	0.90	0.78	263.87	0.63	0.49	307.29	0.58	0.51
0.247	110.10	0.37	0.42	258.58	0.92	0.79	269.18	0.65	0.50	308.02	0.59	0.51
0.265	109.64	0.36	0.41	262.69	0.93	0.81	273.37	0.66	0.51	308.98	0.59	0.51
0.284	109.32	0.36	0.41	266.48	0.94	0.82	276.40	0.66	0.51	310.33	0.59	0.52
0.304	109.33	0.36	0.41	269.85	0.96	0.83	278.32	0.67	0.51	312.08	0.59	0.52
0.326	109.81	0.36	0.41	272.73	0.97	0.84	279.23	0.67	0.52	314.15	0.60	0.52
0.349	110.86	0.37	0.42	275.12	0.98	0.84	279.30	0.67	0.52	316.34	0.60	0.53
0.374	112.50	0.37	0.42	277.02	0.98	0.85	278.76	0.67	0.52	318.44	0.61	0.53
0.401	114.74	0.38	0.43	278.49	0.99	0.85	277.85	0.67	0.51	320.25	0.61	0.53
0.43	117.54	0.39	0.44	279.57	0.99	0.86	276.80	0.67	0.51	321.63	0.61	0.53
0.461	120.85	0.40	0.46	280.28	0.99	0.86	275.80	0.66	0.51	322.52	0.61	0.54
0.494	124.61	0.41	0.47	280.65	0.99	0.86	274.95	0.66	0.51	322.91	0.61	0.54
0.53	128.75	0.43	0.49	280.65	0.99	0.86	274.26	0.66	0.51	322.87	0.61	0.54
0.568	133.19	0.44	0.50	280.26	0.99	0.86	273.71	0.66	0.51	322.47	0.61	0.54
0.608	137.86	0.46	0.52	279.43	0.99	0.86	273.22	0.66	0.50	321.81	0.61	0.53
0.652	142.67	0.47	0.54	278.15	0.99	0.85	272.73	0.66	0.50	320.92	0.61	0.53
0.699	147.51	0.49	0.56	276.39	0.98	0.85	272.16	0.65	0.50	319.80	0.61	0.53
0.749	152.28	0.51	0.57	274.18	0.97	0.84	271.49	0.65	0.50	318.37	0.61	0.53
0.803	156.88	0.52	0.59	271.54	0.96	0.83	270.72	0.65	0.50	316.50	0.60	0.53
0.861	161.17	0.54	0.61	268.53	0.95	0.82	269.87	0.65	0.50	314.08	0.60	0.52
0.923	165.05	0.55	0.62	265.20	0.94	0.81	268.95	0.65	0.50	310.97	0.59	0.52
0.989	168.41	0.56	0.64	261.65	0.93	0.80	267.95	0.64	0.50	307.13	0.58	0.51
1.06	171.15	0.57	0.65	257.96	0.91	0.79	266.85	0.64	0.49	302.58	0.58	0.50
1.136	173.20	0.58	0.65	254.26	0.90	0.78	265.55	0.64	0.49	297.46	0.57	0.49
1.218	174.52	0.58	0.66	250.64	0.89	0.77	263.96	0.63	0.49	291.96	0.56	0.49
1.306	175.11	0.58	0.66	247.20	0.88	0.76	261.94	0.63	0.48	286.36	0.55	0.48
1.399	175.00	0.58	0.66	244.00	0.86	0.75	259.40	0.62	0.48	280.93	0.53	0.47
1.5	174.27	0.58	0.66	241.04	0.85	0.74	256.25	0.62	0.47	275.89	0.53	0.46

Table F46. Circular velocity curves of the 238 (E1–Sdm) CALIFA galaxies with 75th and 25th percentile uncertainties.

R/R_e	UGC02403			UGC03253			UGC03539			UGC03995		
	V_c	ΔV_c^{75th}	ΔV_c^{25th}									
0.05	78.56	0.33	0.30	87.58	0.16	0.14	34.80	0.13	0.13	188.92	0.39	0.42
0.054	82.51	0.35	0.32	92.90	0.17	0.15	37.12	0.14	0.14	197.16	0.41	0.43
0.057	86.44	0.36	0.33	98.40	0.18	0.15	39.57	0.15	0.15	205.16	0.42	0.45
0.062	90.32	0.38	0.35	104.07	0.20	0.16	42.17	0.16	0.16	212.80	0.44	0.47
0.066	94.09	0.40	0.36	109.88	0.21	0.17	44.92	0.17	0.17	220.02	0.45	0.48
0.071	97.72	0.41	0.38	115.80	0.22	0.18	47.82	0.18	0.18	226.72	0.47	0.50
0.076	101.16	0.43	0.39	121.79	0.23	0.19	50.87	0.19	0.19	232.84	0.48	0.51
0.081	104.38	0.44	0.40	127.79	0.24	0.20	54.07	0.21	0.21	238.34	0.49	0.52
0.087	107.34	0.45	0.42	133.76	0.25	0.21	57.40	0.22	0.22	243.18	0.50	0.54
0.093	110.04	0.46	0.43	139.65	0.26	0.22	60.87	0.23	0.23	247.38	0.51	0.54
0.1	112.48	0.48	0.44	145.39	0.27	0.23	64.47	0.25	0.25	250.92	0.52	0.55
0.107	114.68	0.48	0.44	150.94	0.28	0.24	68.17	0.26	0.26	253.84	0.52	0.56
0.115	116.69	0.49	0.45	156.24	0.29	0.24	71.97	0.27	0.28	256.14	0.53	0.56
0.123	118.55	0.50	0.46	161.27	0.30	0.25	75.85	0.29	0.29	257.83	0.53	0.57
0.132	120.34	0.51	0.47	165.99	0.31	0.26	79.77	0.30	0.31	258.93	0.53	0.57
0.142	122.09	0.52	0.47	170.40	0.32	0.27	83.72	0.32	0.32	259.44	0.53	0.57
0.152	123.85	0.52	0.48	174.51	0.33	0.27	87.65	0.33	0.34	259.41	0.53	0.57
0.163	125.61	0.53	0.49	178.34	0.34	0.28	91.55	0.35	0.35	258.92	0.53	0.57
0.174	127.34	0.54	0.49	181.90	0.34	0.29	95.39	0.36	0.37	258.10	0.53	0.57
0.187	128.99	0.55	0.50	185.23	0.35	0.29	99.12	0.38	0.38	257.10	0.53	0.57
0.2	130.49	0.55	0.51	188.31	0.35	0.30	102.74	0.39	0.39	256.06	0.53	0.56
0.215	131.76	0.56	0.51	191.13	0.36	0.30	106.22	0.41	0.41	255.11	0.52	0.56
0.23	132.73	0.56	0.51	193.65	0.36	0.30	109.56	0.42	0.42	254.33	0.52	0.56
0.247	133.37	0.56	0.52	195.78	0.37	0.31	112.75	0.43	0.43	253.69	0.52	0.56
0.265	133.67	0.56	0.52	197.46	0.37	0.31	115.80	0.44	0.44	253.14	0.52	0.56
0.284	133.68	0.56	0.52	198.61	0.37	0.31	118.72	0.45	0.46	252.56	0.52	0.56
0.304	133.47	0.56	0.52	199.19	0.37	0.31	121.54	0.46	0.47	251.84	0.52	0.55
0.326	133.16	0.56	0.52	199.17	0.37	0.31	124.28	0.48	0.48	250.85	0.52	0.55
0.349	132.90	0.56	0.52	198.59	0.37	0.31	126.96	0.49	0.49	249.53	0.51	0.55
0.374	132.85	0.56	0.52	197.51	0.37	0.31	129.57	0.50	0.50	247.85	0.51	0.55
0.401	133.16	0.56	0.52	196.05	0.37	0.31	132.12	0.51	0.51	245.82	0.51	0.54
0.43	133.95	0.57	0.52	194.36	0.37	0.30	134.59	0.51	0.52	243.54	0.50	0.54
0.461	135.28	0.57	0.52	192.59	0.36	0.30	136.96	0.52	0.53	241.14	0.50	0.53
0.494	137.19	0.58	0.53	190.91	0.36	0.30	139.19	0.53	0.53	238.77	0.49	0.53
0.53	139.67	0.59	0.54	189.47	0.36	0.30	141.23	0.54	0.54	236.60	0.49	0.52
0.568	142.66	0.60	0.55	188.40	0.35	0.30	143.06	0.55	0.55	234.75	0.48	0.52
0.608	146.10	0.62	0.57	187.78	0.35	0.29	144.65	0.55	0.56	233.32	0.48	0.51
0.652	149.90	0.63	0.58	187.66	0.35	0.29	146.01	0.56	0.56	232.35	0.48	0.51
0.699	153.96	0.65	0.60	188.03	0.35	0.29	147.17	0.56	0.56	231.84	0.48	0.51
0.749	158.18	0.67	0.61	188.87	0.36	0.30	148.16	0.57	0.57	231.72	0.48	0.51
0.803	162.43	0.69	0.63	190.13	0.36	0.30	149.06	0.57	0.57	231.96	0.48	0.51
0.861	166.57	0.70	0.65	191.71	0.36	0.30	149.92	0.57	0.58	232.48	0.48	0.51
0.923	170.46	0.72	0.66	193.53	0.36	0.30	150.79	0.58	0.58	233.23	0.48	0.51
0.989	173.95	0.74	0.67	195.49	0.37	0.31	151.70	0.58	0.58	234.16	0.48	0.52
1.06	176.90	0.75	0.69	197.50	0.37	0.31	152.64	0.58	0.59	235.23	0.48	0.52
1.136	179.15	0.76	0.69	199.48	0.38	0.31	153.57	0.59	0.59	236.41	0.49	0.52
1.218	180.57	0.76	0.70	201.35	0.38	0.32	154.46	0.59	0.59	237.68	0.49	0.52
1.306	181.08	0.77	0.70	203.05	0.38	0.32	155.22	0.59	0.60	239.03	0.49	0.53
1.399	180.60	0.76	0.70	204.55	0.38	0.32	155.77	0.60	0.60	240.42	0.49	0.53
1.5	179.14	0.76	0.69	205.83	0.39	0.32	156.05	0.60	0.60	241.82	0.50	0.53

Table F47. Circular velocity curves of the 238 (E1–Sdm) CALIFA galaxies with 75th and 25th percentile uncertainties.

R/R_e	UGC04029			UGC04132			UGC04145			UGC04197		
	V_c	ΔV_c^{75th}	ΔV_c^{25th}									
0.05	87.66	0.25	0.20	60.04	0.11	0.08	17.65	0.03	0.03	92.34	0.15	0.13
0.054	90.69	0.26	0.21	64.06	0.12	0.08	18.73	0.03	0.04	97.61	0.16	0.13
0.057	93.46	0.27	0.22	68.31	0.13	0.09	19.91	0.03	0.04	102.98	0.17	0.14
0.062	95.93	0.27	0.22	72.79	0.14	0.09	21.20	0.04	0.04	108.42	0.18	0.15
0.066	98.07	0.28	0.23	77.51	0.15	0.10	22.59	0.04	0.04	113.88	0.19	0.16
0.071	99.87	0.29	0.23	82.46	0.16	0.10	24.11	0.04	0.05	119.29	0.20	0.16
0.076	101.34	0.29	0.24	87.63	0.17	0.11	25.74	0.05	0.05	124.60	0.20	0.17
0.081	102.52	0.29	0.24	93.01	0.18	0.12	27.50	0.05	0.06	129.74	0.21	0.18
0.087	103.47	0.30	0.24	98.58	0.19	0.12	29.39	0.05	0.06	134.61	0.22	0.19
0.093	104.30	0.30	0.24	104.33	0.20	0.13	31.43	0.06	0.06	139.16	0.23	0.19
0.1	105.10	0.30	0.25	110.22	0.21	0.14	33.61	0.06	0.07	143.28	0.23	0.20
0.107	106.01	0.30	0.25	116.20	0.22	0.15	35.96	0.07	0.07	146.93	0.24	0.20
0.115	107.12	0.31	0.25	122.23	0.23	0.15	38.48	0.07	0.08	150.03	0.25	0.21
0.123	108.52	0.31	0.25	128.25	0.24	0.16	41.18	0.08	0.09	152.58	0.25	0.21
0.132	110.25	0.32	0.26	134.18	0.25	0.17	44.07	0.08	0.09	154.55	0.25	0.21
0.142	112.33	0.32	0.26	139.94	0.27	0.18	47.16	0.09	0.10	155.99	0.26	0.22
0.152	114.71	0.33	0.27	145.44	0.28	0.18	50.47	0.09	0.10	156.97	0.26	0.22
0.163	117.37	0.34	0.27	150.58	0.29	0.19	54.01	0.10	0.11	157.57	0.26	0.22
0.174	120.22	0.34	0.28	155.26	0.29	0.20	57.78	0.11	0.12	157.91	0.26	0.22
0.187	123.21	0.35	0.29	159.38	0.30	0.20	61.81	0.12	0.13	158.11	0.26	0.22
0.2	126.25	0.36	0.30	162.86	0.31	0.21	66.11	0.12	0.14	158.25	0.26	0.22
0.215	129.27	0.37	0.30	165.65	0.31	0.21	70.69	0.13	0.15	158.42	0.26	0.22
0.23	132.21	0.38	0.31	167.71	0.32	0.21	75.56	0.14	0.16	158.63	0.26	0.22
0.247	135.01	0.39	0.32	169.08	0.32	0.21	80.74	0.15	0.17	158.91	0.26	0.22
0.265	137.61	0.39	0.32	169.85	0.32	0.21	86.24	0.16	0.18	159.24	0.26	0.22
0.284	139.98	0.40	0.33	170.16	0.32	0.22	92.07	0.17	0.19	159.62	0.26	0.22
0.304	142.10	0.41	0.33	170.23	0.32	0.22	98.24	0.19	0.20	160.07	0.26	0.22
0.326	143.95	0.41	0.34	170.32	0.32	0.22	104.75	0.20	0.22	160.62	0.26	0.22
0.349	145.56	0.42	0.34	170.71	0.32	0.22	111.61	0.21	0.23	161.31	0.26	0.22
0.374	146.95	0.42	0.34	171.66	0.33	0.22	118.81	0.22	0.25	162.23	0.27	0.22
0.401	148.17	0.42	0.35	173.37	0.33	0.22	126.36	0.24	0.26	163.44	0.27	0.23
0.43	149.26	0.43	0.35	175.97	0.33	0.22	134.24	0.25	0.28	164.99	0.27	0.23
0.461	150.30	0.43	0.35	179.51	0.34	0.23	142.42	0.27	0.30	166.92	0.27	0.23
0.494	151.36	0.43	0.35	183.95	0.35	0.23	150.89	0.28	0.31	169.23	0.28	0.23
0.53	152.50	0.44	0.36	189.22	0.36	0.24	159.59	0.30	0.33	171.87	0.28	0.24
0.568	153.80	0.44	0.36	195.22	0.37	0.25	168.49	0.32	0.35	174.77	0.29	0.24
0.608	155.27	0.44	0.36	201.82	0.38	0.26	177.50	0.34	0.37	177.86	0.29	0.25
0.652	156.95	0.45	0.37	208.90	0.40	0.26	186.56	0.35	0.39	181.01	0.30	0.25
0.699	158.81	0.45	0.37	216.32	0.41	0.27	195.56	0.37	0.41	184.13	0.30	0.25
0.749	160.82	0.46	0.38	223.93	0.42	0.28	204.38	0.39	0.43	187.10	0.31	0.26
0.803	162.92	0.47	0.38	231.56	0.44	0.29	212.89	0.40	0.44	189.83	0.31	0.26
0.861	165.04	0.47	0.39	239.04	0.45	0.30	220.96	0.42	0.46	192.24	0.32	0.27
0.923	167.10	0.48	0.39	246.17	0.47	0.31	228.41	0.43	0.48	194.27	0.32	0.27
0.989	169.00	0.48	0.40	252.75	0.48	0.32	235.10	0.44	0.49	195.90	0.32	0.27
1.06	170.65	0.49	0.40	258.58	0.49	0.33	240.86	0.45	0.50	197.15	0.32	0.27
1.136	171.95	0.49	0.40	263.45	0.50	0.33	245.55	0.46	0.51	198.05	0.32	0.27
1.218	172.83	0.49	0.40	267.20	0.51	0.34	249.06	0.47	0.52	198.68	0.33	0.27
1.306	173.20	0.50	0.41	269.67	0.51	0.34	251.31	0.47	0.52	199.14	0.33	0.28
1.399	173.02	0.50	0.40	270.75	0.51	0.34	252.28	0.48	0.53	199.51	0.33	0.28
1.5	172.30	0.49	0.40	270.42	0.51	0.34	252.02	0.48	0.53	199.87	0.33	0.28

Table F48. Circular velocity curves of the 238 (E1–Sdm) CALIFA galaxies with 75th and 25th percentile uncertainties.

R/R_e	UGC04280			UGC04308			UGC05108			UGC05113		
	V_c	ΔV_c^{75th}	ΔV_c^{25th}									
0.05	51.89	0.10	0.12	54.43	0.20	0.20	231.59	0.62	0.45	96.90	0.22	0.22
0.054	55.24	0.11	0.13	57.49	0.22	0.21	240.27	0.64	0.47	103.45	0.24	0.23
0.057	58.76	0.11	0.14	60.63	0.23	0.22	248.20	0.66	0.48	110.38	0.25	0.25
0.062	62.46	0.12	0.15	63.81	0.24	0.24	255.20	0.68	0.50	117.71	0.27	0.27
0.066	66.33	0.13	0.16	67.03	0.25	0.25	261.03	0.70	0.51	125.43	0.29	0.29
0.071	70.36	0.13	0.17	70.25	0.26	0.26	265.52	0.71	0.52	133.56	0.30	0.30
0.076	74.54	0.14	0.18	73.44	0.28	0.27	268.50	0.72	0.52	142.07	0.32	0.32
0.081	78.85	0.15	0.19	76.58	0.29	0.28	269.86	0.72	0.52	150.97	0.34	0.34
0.087	83.26	0.16	0.20	79.64	0.30	0.30	269.55	0.72	0.52	160.23	0.36	0.36
0.093	87.76	0.17	0.21	82.59	0.31	0.31	267.66	0.72	0.52	169.81	0.39	0.39
0.1	92.30	0.18	0.22	85.39	0.32	0.32	264.36	0.71	0.51	179.69	0.41	0.41
0.107	96.84	0.19	0.23	88.02	0.33	0.33	259.97	0.69	0.51	189.79	0.43	0.43
0.115	101.34	0.19	0.25	90.45	0.34	0.34	254.92	0.68	0.50	200.06	0.46	0.45
0.123	105.74	0.20	0.26	92.66	0.35	0.34	249.71	0.67	0.49	210.40	0.48	0.48
0.132	109.99	0.21	0.27	94.62	0.36	0.35	244.88	0.65	0.48	220.69	0.50	0.50
0.142	114.03	0.22	0.28	96.33	0.36	0.36	240.88	0.64	0.47	230.83	0.53	0.52
0.152	117.81	0.23	0.29	97.77	0.37	0.36	238.05	0.64	0.46	240.65	0.55	0.55
0.163	121.28	0.23	0.29	98.93	0.37	0.37	236.56	0.63	0.46	249.99	0.57	0.57
0.174	124.40	0.24	0.30	99.84	0.38	0.37	236.42	0.63	0.46	258.69	0.59	0.59
0.187	127.15	0.24	0.31	100.50	0.38	0.37	237.55	0.63	0.46	266.55	0.61	0.61
0.2	129.54	0.25	0.31	100.95	0.38	0.37	239.76	0.64	0.47	273.40	0.62	0.62
0.215	131.59	0.25	0.32	101.22	0.38	0.38	242.88	0.65	0.47	279.09	0.64	0.63
0.23	133.36	0.26	0.32	101.34	0.38	0.38	246.73	0.66	0.48	283.48	0.65	0.64
0.247	134.91	0.26	0.33	101.35	0.38	0.38	251.13	0.67	0.49	286.51	0.65	0.65
0.265	136.33	0.26	0.33	101.28	0.38	0.38	255.92	0.68	0.50	288.17	0.66	0.66
0.284	137.68	0.27	0.33	101.16	0.38	0.38	260.92	0.70	0.51	288.54	0.66	0.66
0.304	139.04	0.27	0.34	101.03	0.38	0.37	265.97	0.71	0.52	287.81	0.66	0.65
0.326	140.46	0.27	0.34	100.94	0.38	0.37	270.92	0.72	0.53	286.25	0.65	0.65
0.349	141.94	0.27	0.34	100.95	0.38	0.37	275.63	0.74	0.54	284.17	0.65	0.65
0.374	143.49	0.28	0.35	101.13	0.38	0.38	279.99	0.75	0.54	281.93	0.64	0.64
0.401	145.10	0.28	0.35	101.56	0.38	0.38	283.88	0.76	0.55	279.86	0.64	0.64
0.43	146.77	0.28	0.36	102.31	0.39	0.38	287.24	0.77	0.56	278.20	0.63	0.63
0.461	148.49	0.29	0.36	103.42	0.39	0.38	290.05	0.78	0.56	277.09	0.63	0.63
0.494	150.27	0.29	0.36	104.92	0.40	0.39	292.30	0.78	0.57	276.56	0.63	0.63
0.53	152.13	0.29	0.37	106.80	0.40	0.40	294.06	0.79	0.57	276.51	0.63	0.63
0.568	154.07	0.30	0.37	109.04	0.41	0.40	295.41	0.79	0.57	276.80	0.63	0.63
0.608	156.11	0.30	0.38	111.59	0.42	0.41	296.46	0.79	0.58	277.23	0.63	0.63
0.652	158.24	0.30	0.38	114.42	0.43	0.42	297.33	0.79	0.58	277.61	0.63	0.63
0.699	160.43	0.31	0.39	117.48	0.44	0.44	298.12	0.80	0.58	277.74	0.63	0.63
0.749	162.65	0.31	0.40	120.70	0.46	0.45	298.90	0.80	0.58	277.49	0.63	0.63
0.803	164.85	0.32	0.40	124.05	0.47	0.46	299.69	0.80	0.58	276.72	0.63	0.63
0.861	166.98	0.32	0.41	127.46	0.48	0.47	300.43	0.80	0.58	275.38	0.63	0.63
0.923	169.00	0.33	0.41	130.90	0.49	0.49	301.03	0.80	0.59	273.47	0.62	0.62
0.989	170.88	0.33	0.42	134.32	0.51	0.50	301.36	0.81	0.59	271.04	0.62	0.62
1.06	172.59	0.33	0.42	137.68	0.52	0.51	301.29	0.81	0.59	268.22	0.61	0.61
1.136	174.09	0.34	0.42	140.94	0.53	0.52	300.68	0.80	0.58	265.14	0.60	0.60
1.218	175.37	0.34	0.43	144.06	0.54	0.53	299.47	0.80	0.58	261.95	0.60	0.60
1.306	176.39	0.34	0.43	146.99	0.56	0.55	297.62	0.80	0.58	258.79	0.59	0.59
1.399	177.16	0.34	0.43	149.68	0.57	0.56	295.14	0.79	0.57	255.76	0.58	0.58
1.5	177.64	0.34	0.43	152.06	0.57	0.56	292.12	0.78	0.57	252.88	0.58	0.58

Table F49. Circular velocity curves of the 238 (E1–Sdm) CALIFA galaxies with 75th and 25th percentile uncertainties.

R/R_e	UGC05598			UGC05771			UGC05990			UGC06036		
	V_c	ΔV_c^{75th}	ΔV_c^{25th}									
0.05	32.40	0.20	0.16	212.16	0.46	0.44	12.66	0.06	0.05	108.75	0.12	0.12
0.054	34.57	0.22	0.18	224.75	0.49	0.46	13.00	0.06	0.05	115.92	0.13	0.13
0.057	36.87	0.23	0.19	237.71	0.51	0.49	13.42	0.07	0.06	123.47	0.13	0.14
0.062	39.31	0.25	0.20	250.95	0.54	0.51	13.92	0.08	0.07	131.40	0.14	0.15
0.066	41.89	0.26	0.21	264.41	0.57	0.54	14.50	0.09	0.07	139.70	0.15	0.16
0.071	44.61	0.28	0.23	277.96	0.60	0.57	15.17	0.09	0.08	148.37	0.16	0.17
0.076	47.47	0.30	0.24	291.48	0.63	0.60	15.92	0.10	0.09	157.38	0.17	0.18
0.081	50.48	0.32	0.26	304.84	0.66	0.63	16.77	0.11	0.09	166.71	0.18	0.19
0.087	53.62	0.34	0.28	317.87	0.69	0.65	17.70	0.12	0.10	176.32	0.19	0.20
0.093	56.88	0.36	0.29	330.41	0.71	0.68	18.73	0.13	0.11	186.16	0.20	0.21
0.1	60.26	0.38	0.31	342.28	0.74	0.70	19.86	0.14	0.12	196.18	0.21	0.22
0.107	63.74	0.40	0.33	353.33	0.76	0.72	21.09	0.16	0.13	206.31	0.23	0.23
0.115	67.30	0.43	0.35	363.41	0.78	0.75	22.43	0.17	0.14	216.47	0.24	0.24
0.123	70.91	0.45	0.37	372.41	0.80	0.76	23.87	0.18	0.15	226.57	0.25	0.25
0.132	74.55	0.47	0.38	380.26	0.82	0.78	25.43	0.19	0.16	236.54	0.26	0.26
0.142	78.17	0.50	0.40	386.95	0.84	0.79	27.10	0.21	0.17	246.27	0.27	0.27
0.152	81.72	0.52	0.42	392.51	0.85	0.81	28.89	0.22	0.19	255.68	0.28	0.28
0.163	85.17	0.54	0.44	397.02	0.86	0.81	30.82	0.24	0.20	264.69	0.29	0.29
0.174	88.44	0.56	0.46	400.59	0.87	0.82	32.87	0.26	0.21	273.23	0.30	0.30
0.187	91.49	0.58	0.47	403.35	0.87	0.83	35.05	0.27	0.23	281.26	0.31	0.31
0.2	94.24	0.60	0.49	405.40	0.88	0.83	37.38	0.29	0.25	288.75	0.32	0.32
0.215	96.66	0.61	0.50	406.82	0.88	0.83	39.85	0.31	0.26	295.69	0.32	0.33
0.23	98.68	0.63	0.51	407.68	0.88	0.84	42.46	0.33	0.28	302.08	0.33	0.34
0.247	100.27	0.64	0.52	408.02	0.88	0.84	45.22	0.36	0.30	307.92	0.34	0.34
0.265	101.43	0.64	0.52	407.89	0.88	0.84	48.13	0.38	0.32	313.18	0.34	0.35
0.284	102.17	0.65	0.53	407.39	0.88	0.84	51.18	0.40	0.34	317.85	0.35	0.35
0.304	102.55	0.65	0.53	406.66	0.88	0.83	54.37	0.43	0.36	321.85	0.35	0.36
0.326	102.66	0.65	0.53	405.83	0.88	0.83	57.69	0.46	0.38	325.11	0.36	0.36
0.349	102.63	0.65	0.53	405.03	0.87	0.83	61.13	0.48	0.41	327.55	0.36	0.36
0.374	102.60	0.65	0.53	404.33	0.87	0.83	64.68	0.51	0.43	329.10	0.36	0.37
0.401	102.74	0.65	0.53	403.71	0.87	0.83	68.32	0.54	0.45	329.75	0.36	0.37
0.43	103.17	0.65	0.53	403.09	0.87	0.83	72.02	0.57	0.48	329.52	0.36	0.37
0.461	104.01	0.66	0.54	402.31	0.87	0.83	75.75	0.60	0.50	328.50	0.36	0.37
0.494	105.33	0.67	0.54	401.21	0.87	0.82	79.48	0.63	0.53	326.81	0.36	0.36
0.53	107.16	0.68	0.55	399.63	0.86	0.82	83.15	0.66	0.55	324.60	0.36	0.36
0.568	109.47	0.70	0.56	397.46	0.86	0.82	86.73	0.69	0.58	322.01	0.35	0.36
0.608	112.23	0.71	0.58	394.65	0.85	0.81	90.15	0.71	0.60	319.15	0.35	0.36
0.652	115.39	0.73	0.59	391.23	0.85	0.80	93.36	0.74	0.62	316.09	0.35	0.35
0.699	118.87	0.75	0.61	387.32	0.84	0.79	96.29	0.76	0.64	312.87	0.34	0.35
0.749	122.61	0.78	0.63	383.07	0.83	0.79	98.88	0.78	0.66	309.52	0.34	0.34
0.803	126.53	0.80	0.65	378.68	0.82	0.78	101.08	0.80	0.67	306.06	0.33	0.34
0.861	130.54	0.83	0.67	374.32	0.81	0.77	102.84	0.82	0.68	302.55	0.33	0.34
0.923	134.55	0.85	0.69	370.13	0.80	0.76	104.13	0.83	0.69	299.05	0.33	0.33
0.989	138.45	0.88	0.71	366.18	0.79	0.75	104.95	0.83	0.70	295.65	0.32	0.33
1.06	142.14	0.90	0.73	362.44	0.78	0.74	105.30	0.83	0.70	292.44	0.32	0.33
1.136	145.50	0.92	0.75	358.83	0.78	0.74	105.23	0.83	0.70	289.48	0.32	0.32
1.218	148.43	0.94	0.77	355.19	0.77	0.73	104.79	0.83	0.70	286.81	0.31	0.32
1.306	150.84	0.96	0.78	351.36	0.76	0.72	104.05	0.82	0.69	284.45	0.31	0.32
1.399	152.61	0.97	0.79	347.21	0.75	0.71	103.11	0.82	0.69	282.39	0.31	0.31
1.5	153.70	0.98	0.79	342.66	0.74	0.70	102.05	0.81	0.68	280.59	0.31	0.31

Table F50. Circular velocity curves of the 238 (E1–Sdm) CALIFA galaxies with 75th and 25th percentile uncertainties.

R/R_e	UGC06312			UGC07012			UGC07145			UGC08107		
	V_c	ΔV_c^{75th}	ΔV_c^{25th}									
0.05	116.11	0.23	0.21	32.33	0.15	0.13	40.78	0.17	0.15	72.89	0.11	0.14
0.054	123.68	0.24	0.22	34.44	0.16	0.13	43.49	0.18	0.16	77.94	0.12	0.15
0.057	131.63	0.26	0.24	36.68	0.17	0.14	46.36	0.19	0.17	83.31	0.13	0.16
0.062	139.96	0.27	0.25	39.06	0.18	0.15	49.38	0.21	0.18	89.02	0.14	0.17
0.066	148.64	0.29	0.27	41.58	0.19	0.16	52.57	0.22	0.19	95.08	0.15	0.18
0.071	157.66	0.31	0.28	44.24	0.20	0.18	55.91	0.23	0.20	101.50	0.16	0.20
0.076	166.97	0.33	0.30	47.04	0.22	0.19	59.40	0.25	0.22	108.29	0.17	0.22
0.081	176.55	0.34	0.32	49.97	0.23	0.20	63.03	0.26	0.23	115.47	0.18	0.22
0.087	186.33	0.36	0.34	53.03	0.24	0.21	66.80	0.28	0.24	123.03	0.19	0.24
0.093	196.23	0.38	0.35	56.22	0.26	0.22	70.68	0.30	0.26	130.98	0.20	0.25
0.1	206.17	0.40	0.37	59.51	0.27	0.24	74.66	0.31	0.27	139.30	0.22	0.27
0.107	216.05	0.42	0.39	62.91	0.29	0.25	78.72	0.33	0.29	147.99	0.23	0.28
0.115	225.74	0.44	0.41	66.38	0.31	0.27	82.80	0.35	0.30	157.03	0.25	0.30
0.123	235.11	0.46	0.42	69.91	0.32	0.28	86.89	0.36	0.32	166.38	0.26	0.32
0.132	244.02	0.48	0.44	73.46	0.34	0.29	90.94	0.38	0.33	176.01	0.28	0.34
0.142	252.32	0.49	0.46	77.02	0.36	0.31	94.89	0.40	0.35	185.87	0.29	0.36
0.152	259.86	0.51	0.47	80.55	0.37	0.32	98.69	0.41	0.36	195.89	0.31	0.38
0.163	266.51	0.52	0.48	84.00	0.39	0.34	102.29	0.43	0.37	205.99	0.32	0.40
0.174	272.17	0.53	0.49	87.35	0.40	0.35	105.64	0.44	0.39	216.08	0.34	0.42
0.187	276.79	0.54	0.50	90.57	0.42	0.36	108.68	0.45	0.40	226.05	0.35	0.43
0.2	280.34	0.55	0.51	93.61	0.43	0.38	111.39	0.47	0.41	235.78	0.37	0.45
0.215	282.89	0.55	0.51	96.46	0.45	0.39	113.74	0.48	0.42	245.15	0.38	0.47
0.23	284.56	0.56	0.51	99.11	0.46	0.40	115.76	0.48	0.42	254.02	0.40	0.49
0.247	285.52	0.56	0.52	101.55	0.47	0.41	117.46	0.49	0.43	262.27	0.41	0.50
0.265	285.96	0.56	0.52	103.80	0.48	0.42	118.93	0.50	0.44	269.79	0.42	0.52
0.284	286.07	0.56	0.52	105.89	0.49	0.42	120.28	0.50	0.44	276.48	0.43	0.53
0.304	286.00	0.56	0.52	107.84	0.50	0.43	121.61	0.51	0.45	282.29	0.44	0.54
0.326	285.83	0.56	0.52	109.69	0.51	0.44	123.08	0.51	0.45	287.20	0.45	0.55
0.349	285.57	0.56	0.52	111.48	0.52	0.45	124.79	0.52	0.46	291.26	0.46	0.56
0.374	285.17	0.56	0.51	113.23	0.53	0.45	126.85	0.53	0.46	294.56	0.46	0.57
0.401	284.57	0.56	0.51	114.98	0.53	0.46	129.30	0.54	0.47	297.21	0.47	0.57
0.43	283.72	0.55	0.51	116.74	0.54	0.47	132.15	0.55	0.48	299.38	0.47	0.58
0.461	282.60	0.55	0.51	118.53	0.55	0.48	135.38	0.57	0.50	301.23	0.47	0.58
0.494	281.23	0.55	0.51	120.40	0.56	0.48	138.91	0.58	0.51	302.93	0.47	0.58
0.53	279.68	0.55	0.50	122.36	0.57	0.49	142.68	0.60	0.52	304.61	0.48	0.59
0.568	277.99	0.54	0.50	124.45	0.58	0.50	146.60	0.61	0.54	306.40	0.48	0.59
0.608	276.22	0.54	0.50	126.69	0.59	0.51	150.58	0.63	0.55	308.40	0.48	0.59
0.652	274.38	0.54	0.50	129.08	0.60	0.52	154.53	0.65	0.57	310.71	0.49	0.60
0.699	272.44	0.53	0.49	131.59	0.61	0.53	158.39	0.66	0.58	313.38	0.49	0.60
0.749	270.39	0.53	0.49	134.17	0.62	0.54	162.10	0.68	0.59	316.46	0.50	0.61
0.803	268.21	0.52	0.48	136.75	0.63	0.55	165.61	0.69	0.61	319.92	0.50	0.62
0.861	265.91	0.52	0.48	139.22	0.65	0.56	168.89	0.71	0.62	323.71	0.51	0.62
0.923	263.54	0.52	0.48	141.48	0.66	0.57	171.97	0.72	0.63	327.68	0.51	0.63
0.989	261.16	0.51	0.47	143.40	0.67	0.58	174.84	0.73	0.64	331.66	0.52	0.64
1.06	258.83	0.51	0.47	144.89	0.67	0.58	177.55	0.74	0.65	335.42	0.52	0.65
1.136	256.59	0.50	0.46	145.84	0.68	0.58	180.14	0.75	0.66	338.75	0.53	0.65
1.218	254.45	0.50	0.46	146.18	0.68	0.59	182.64	0.76	0.67	341.46	0.53	0.66
1.306	252.37	0.49	0.46	145.85	0.68	0.58	185.05	0.77	0.68	343.39	0.54	0.66
1.399	250.25	0.49	0.45	144.86	0.67	0.58	187.34	0.78	0.69	344.43	0.54	0.66
1.5	247.99	0.48	0.45	143.24	0.66	0.57	189.43	0.79	0.69	344.56	0.54	0.66

Table F51. Circular velocity curves of the 238 (E1–Sdm) CALIFA galaxies with 75th and 25th percentile uncertainties.

R/R_e	UGC08231			UGC08234			UGC08733			UGC08778		
	V_c	ΔV_c^{75th}	ΔV_c^{25th}									
0.05	29.85	0.13	0.13	84.89	0.28	0.18	40.72	0.16	0.16	33.30	0.10	0.08
0.054	31.80	0.14	0.14	90.77	0.30	0.19	42.49	0.17	0.16	35.50	0.11	0.09
0.057	33.87	0.14	0.14	97.02	0.32	0.20	44.25	0.18	0.17	37.86	0.12	0.09
0.062	36.08	0.15	0.15	103.66	0.34	0.22	45.99	0.19	0.18	40.36	0.12	0.10
0.066	38.41	0.17	0.17	110.72	0.36	0.23	47.72	0.19	0.18	43.01	0.13	0.10
0.071	40.88	0.18	0.18	118.20	0.39	0.25	49.44	0.20	0.19	45.81	0.14	0.11
0.076	43.49	0.19	0.19	126.12	0.41	0.26	51.16	0.21	0.20	48.77	0.15	0.12
0.081	46.22	0.20	0.20	134.48	0.44	0.28	52.88	0.22	0.20	51.88	0.16	0.13
0.087	49.09	0.21	0.21	143.29	0.47	0.30	54.63	0.22	0.21	55.14	0.17	0.13
0.093	52.08	0.23	0.23	152.55	0.50	0.32	56.39	0.23	0.22	58.54	0.18	0.14
0.1	55.19	0.24	0.24	162.26	0.53	0.34	58.18	0.24	0.22	62.08	0.19	0.15
0.107	58.41	0.25	0.25	172.39	0.56	0.36	59.98	0.24	0.23	65.74	0.20	0.16
0.115	61.73	0.27	0.27	182.92	0.60	0.38	61.78	0.25	0.24	69.50	0.22	0.17
0.123	65.14	0.28	0.28	193.83	0.63	0.41	63.54	0.26	0.25	73.34	0.23	0.18
0.132	68.63	0.30	0.30	205.05	0.67	0.43	65.24	0.27	0.25	77.24	0.24	0.19
0.142	72.18	0.31	0.31	216.54	0.71	0.45	66.85	0.27	0.26	81.15	0.25	0.20
0.152	75.78	0.33	0.33	228.21	0.74	0.48	68.32	0.28	0.26	85.04	0.26	0.21
0.163	79.42	0.35	0.35	239.95	0.78	0.50	69.64	0.28	0.27	88.86	0.28	0.22
0.174	83.08	0.36	0.36	251.67	0.82	0.53	70.80	0.29	0.27	92.55	0.29	0.23
0.187	86.78	0.38	0.38	263.21	0.86	0.55	71.80	0.29	0.28	96.07	0.30	0.24
0.2	90.50	0.39	0.39	274.44	0.90	0.57	72.64	0.30	0.28	99.34	0.31	0.24
0.215	94.27	0.41	0.41	285.17	0.93	0.60	73.36	0.30	0.28	102.32	0.32	0.25
0.23	98.11	0.43	0.43	295.25	0.96	0.62	73.99	0.30	0.29	104.94	0.33	0.26
0.247	102.03	0.45	0.45	304.49	0.99	0.64	74.60	0.30	0.29	107.18	0.33	0.26
0.265	106.06	0.46	0.46	312.73	1.02	0.66	75.25	0.31	0.29	109.02	0.34	0.27
0.284	110.23	0.48	0.48	319.84	1.04	0.67	76.00	0.31	0.29	110.45	0.34	0.27
0.304	114.54	0.50	0.50	325.72	1.06	0.68	76.91	0.31	0.30	111.52	0.35	0.27
0.326	118.98	0.52	0.52	330.32	1.08	0.69	78.02	0.32	0.30	112.29	0.35	0.28
0.349	123.52	0.54	0.54	333.68	1.09	0.70	79.36	0.32	0.31	112.87	0.35	0.28
0.374	128.12	0.56	0.56	335.89	1.10	0.70	80.93	0.33	0.31	113.37	0.35	0.28
0.401	132.68	0.58	0.58	337.10	1.10	0.71	82.71	0.34	0.32	113.95	0.35	0.28
0.43	137.14	0.60	0.60	337.55	1.10	0.71	84.70	0.35	0.33	114.71	0.36	0.28
0.461	141.40	0.62	0.62	337.46	1.10	0.71	86.85	0.36	0.34	115.77	0.36	0.28
0.494	145.37	0.63	0.63	337.07	1.10	0.71	89.15	0.36	0.35	117.20	0.36	0.29
0.53	148.98	0.65	0.65	336.54	1.10	0.70	91.55	0.37	0.35	119.01	0.37	0.29
0.568	152.20	0.66	0.66	336.00	1.10	0.70	94.02	0.38	0.36	121.20	0.38	0.30
0.608	154.99	0.68	0.68	335.49	1.09	0.70	96.55	0.39	0.37	123.73	0.38	0.30
0.652	157.38	0.69	0.69	334.96	1.09	0.70	99.11	0.41	0.38	126.55	0.39	0.31
0.699	159.42	0.70	0.70	334.36	1.09	0.70	101.69	0.42	0.39	129.60	0.40	0.32
0.749	161.21	0.70	0.70	333.57	1.09	0.70	104.28	0.43	0.40	132.83	0.41	0.33
0.803	162.87	0.71	0.71	332.49	1.08	0.70	106.88	0.44	0.41	136.17	0.42	0.33
0.861	164.56	0.72	0.72	331.02	1.08	0.69	109.49	0.45	0.42	139.57	0.43	0.34
0.923	166.41	0.73	0.73	329.09	1.07	0.69	112.10	0.46	0.43	142.98	0.44	0.35
0.989	168.51	0.74	0.74	326.66	1.07	0.68	114.70	0.47	0.44	146.35	0.45	0.36
1.06	170.90	0.75	0.75	323.73	1.06	0.68	117.27	0.48	0.45	149.64	0.46	0.37
1.136	173.56	0.76	0.76	320.35	1.04	0.67	119.77	0.49	0.46	152.78	0.47	0.38
1.218	176.39	0.77	0.77	316.59	1.03	0.66	122.15	0.50	0.47	155.72	0.48	0.38
1.306	179.26	0.78	0.78	312.55	1.02	0.65	124.32	0.51	0.48	158.38	0.49	0.39
1.399	181.98	0.79	0.79	308.34	1.01	0.65	126.23	0.52	0.49	160.66	0.50	0.39
1.5	184.36	0.80	0.80	304.08	0.99	0.64	127.79	0.52	0.50	162.45	0.50	0.40

Table F52. Circular velocity curves of the 238 (E1–Sdm) CALIFA galaxies with 75th and 25th percentile uncertainties.

R/R_e	UGC08781			UGC09476			UGC09537			UGC09542		
	V_c	ΔV_c^{75th}	ΔV_c^{25th}									
0.05	85.09	0.32	0.24	51.48	0.11	0.12	156.70	0.49	0.35	48.75	0.15	0.15
0.054	90.76	0.34	0.26	54.50	0.12	0.13	165.84	0.52	0.37	51.43	0.16	0.15
0.057	96.75	0.37	0.28	57.62	0.13	0.14	175.21	0.55	0.39	54.14	0.17	0.16
0.062	103.05	0.39	0.30	60.80	0.13	0.15	184.73	0.57	0.41	56.88	0.18	0.17
0.066	109.66	0.42	0.31	64.03	0.14	0.15	194.32	0.60	0.44	59.60	0.19	0.18
0.071	116.59	0.44	0.33	67.27	0.15	0.16	203.89	0.63	0.46	62.28	0.20	0.19
0.076	123.81	0.47	0.36	70.48	0.15	0.17	213.31	0.66	0.48	64.88	0.21	0.19
0.081	131.31	0.50	0.38	73.63	0.16	0.18	222.47	0.69	0.50	67.37	0.21	0.20
0.087	139.06	0.53	0.40	76.67	0.17	0.19	231.20	0.72	0.52	69.73	0.22	0.21
0.093	147.03	0.56	0.42	79.55	0.17	0.19	239.35	0.74	0.54	71.91	0.23	0.22
0.1	155.18	0.59	0.45	82.20	0.18	0.20	246.74	0.77	0.55	73.90	0.24	0.22
0.107	163.44	0.62	0.47	84.57	0.18	0.20	253.23	0.79	0.57	75.68	0.24	0.23
0.115	171.74	0.65	0.49	86.61	0.19	0.21	258.67	0.80	0.58	77.27	0.25	0.23
0.123	180.02	0.68	0.52	88.27	0.19	0.21	262.93	0.82	0.59	78.68	0.25	0.24
0.132	188.18	0.71	0.54	89.53	0.20	0.22	265.97	0.83	0.60	79.97	0.25	0.24
0.142	196.12	0.75	0.56	90.37	0.20	0.22	267.78	0.83	0.60	81.19	0.26	0.24
0.152	203.72	0.77	0.58	90.81	0.20	0.22	268.45	0.84	0.60	82.45	0.26	0.25
0.163	210.89	0.80	0.61	90.90	0.20	0.22	268.17	0.83	0.60	83.81	0.27	0.25
0.174	217.52	0.83	0.62	90.73	0.20	0.22	267.19	0.83	0.60	85.38	0.27	0.26
0.187	223.49	0.85	0.64	90.41	0.20	0.22	265.85	0.83	0.60	87.20	0.28	0.26
0.2	228.74	0.87	0.66	90.08	0.20	0.22	264.48	0.82	0.59	89.31	0.28	0.27
0.215	233.18	0.89	0.67	89.87	0.20	0.22	263.40	0.82	0.59	91.73	0.29	0.28
0.23	236.79	0.90	0.68	89.90	0.20	0.22	262.84	0.82	0.59	94.41	0.30	0.28
0.247	239.55	0.91	0.69	90.23	0.20	0.22	262.94	0.82	0.59	97.33	0.31	0.29
0.265	241.49	0.92	0.69	90.90	0.20	0.22	263.69	0.82	0.59	100.41	0.32	0.30
0.284	242.67	0.92	0.70	91.88	0.20	0.22	265.00	0.82	0.59	103.59	0.33	0.31
0.304	243.18	0.92	0.70	93.13	0.20	0.23	266.72	0.83	0.60	106.82	0.34	0.32
0.326	243.12	0.92	0.70	94.57	0.21	0.23	268.65	0.84	0.60	110.03	0.35	0.33
0.349	242.65	0.92	0.70	96.16	0.21	0.23	270.63	0.84	0.61	113.18	0.36	0.34
0.374	241.91	0.92	0.69	97.82	0.21	0.24	272.49	0.85	0.61	116.23	0.37	0.35
0.401	241.09	0.92	0.69	99.54	0.22	0.24	274.11	0.85	0.61	119.16	0.38	0.36
0.43	240.35	0.91	0.69	101.28	0.22	0.25	275.40	0.86	0.62	121.97	0.39	0.37
0.461	239.85	0.91	0.69	103.04	0.23	0.25	276.32	0.86	0.62	124.67	0.40	0.37
0.494	239.69	0.91	0.69	104.86	0.23	0.25	276.86	0.86	0.62	127.31	0.41	0.38
0.53	239.91	0.91	0.69	106.77	0.23	0.26	277.03	0.86	0.62	129.96	0.41	0.39
0.568	240.47	0.91	0.69	108.83	0.24	0.26	276.87	0.86	0.62	132.69	0.42	0.40
0.608	241.30	0.92	0.69	111.09	0.24	0.27	276.38	0.86	0.62	135.56	0.43	0.41
0.652	242.26	0.92	0.70	113.60	0.25	0.28	275.55	0.86	0.62	138.64	0.44	0.42
0.699	243.19	0.92	0.70	116.42	0.25	0.28	274.32	0.85	0.61	141.93	0.45	0.43
0.749	243.92	0.93	0.70	119.55	0.26	0.29	272.62	0.85	0.61	145.42	0.46	0.44
0.803	244.33	0.93	0.70	122.99	0.27	0.30	270.36	0.84	0.61	149.06	0.48	0.45
0.861	244.29	0.93	0.70	126.71	0.28	0.31	267.47	0.83	0.60	152.73	0.49	0.46
0.923	243.74	0.93	0.70	130.66	0.29	0.32	263.92	0.82	0.59	156.32	0.50	0.47
0.989	242.69	0.92	0.70	134.74	0.29	0.33	259.77	0.81	0.58	159.68	0.51	0.48
1.06	241.20	0.92	0.69	138.89	0.30	0.34	255.15	0.79	0.57	162.67	0.52	0.49
1.136	239.41	0.91	0.69	142.97	0.31	0.35	250.23	0.78	0.56	165.14	0.53	0.50
1.218	237.49	0.90	0.68	146.87	0.32	0.36	245.25	0.76	0.55	166.98	0.53	0.50
1.306	235.65	0.90	0.68	150.45	0.33	0.36	240.46	0.75	0.54	168.08	0.54	0.50
1.399	234.10	0.89	0.67	153.57	0.34	0.37	236.09	0.73	0.53	168.36	0.54	0.51
1.5	232.94	0.89	0.67	156.09	0.34	0.38	232.29	0.72	0.52	167.80	0.54	0.50

Table F53. Circular velocity curves of the 238 (E1–Sdm) CALIFA galaxies with 75th and 25th percentile uncertainties.

R/R_e	UGC09665			UGC09873			UGC09892			UGC10097		
	V_c	ΔV_c^{75th}	ΔV_c^{25th}									
0.05	29.01	0.11	0.09	104.45	0.38	0.37	65.96	0.25	0.19	225.21	0.28	0.27
0.054	30.89	0.12	0.09	106.25	0.38	0.38	67.58	0.26	0.20	238.95	0.30	0.28
0.057	32.90	0.13	0.10	108.02	0.39	0.38	69.22	0.26	0.20	253.17	0.32	0.30
0.062	35.03	0.14	0.10	109.79	0.40	0.39	70.92	0.27	0.20	267.80	0.34	0.32
0.066	37.29	0.15	0.11	111.56	0.40	0.40	72.74	0.28	0.21	282.78	0.36	0.33
0.071	39.67	0.15	0.12	113.32	0.41	0.40	74.75	0.28	0.22	297.99	0.37	0.35
0.076	42.18	0.16	0.13	115.05	0.42	0.41	76.97	0.29	0.22	313.32	0.39	0.37
0.081	44.81	0.18	0.13	116.69	0.42	0.42	79.41	0.30	0.23	328.63	0.41	0.39
0.087	47.55	0.19	0.14	118.21	0.43	0.42	82.07	0.31	0.24	343.75	0.43	0.40
0.093	50.41	0.20	0.15	119.54	0.43	0.43	84.89	0.32	0.25	358.49	0.45	0.42
0.1	53.36	0.21	0.16	120.66	0.44	0.43	87.83	0.33	0.25	372.67	0.47	0.44
0.107	56.40	0.22	0.17	121.54	0.44	0.43	90.81	0.34	0.26	386.08	0.49	0.45
0.115	59.50	0.23	0.18	122.16	0.44	0.43	93.77	0.35	0.27	398.54	0.50	0.47
0.123	62.64	0.25	0.19	122.52	0.44	0.44	96.63	0.37	0.28	409.86	0.52	0.48
0.132	65.78	0.26	0.20	122.62	0.44	0.44	99.34	0.38	0.29	419.92	0.53	0.49
0.142	68.91	0.27	0.21	122.47	0.44	0.44	101.83	0.39	0.29	428.63	0.54	0.50
0.152	71.97	0.28	0.22	122.09	0.44	0.43	104.05	0.39	0.30	435.98	0.55	0.51
0.163	74.93	0.30	0.23	121.52	0.44	0.43	105.94	0.40	0.31	442.02	0.56	0.52
0.174	77.73	0.31	0.24	120.79	0.44	0.43	107.49	0.41	0.31	446.86	0.56	0.53
0.187	80.32	0.32	0.24	119.95	0.43	0.43	108.66	0.41	0.31	450.69	0.57	0.53
0.2	82.67	0.33	0.25	119.05	0.43	0.42	109.46	0.41	0.32	453.70	0.57	0.53
0.215	84.72	0.33	0.26	118.14	0.43	0.42	109.91	0.42	0.32	456.05	0.57	0.54
0.23	86.44	0.34	0.26	117.26	0.42	0.42	110.06	0.42	0.32	457.89	0.58	0.54
0.247	87.83	0.35	0.27	116.43	0.42	0.41	109.97	0.42	0.32	459.26	0.58	0.54
0.265	88.89	0.35	0.27	115.64	0.42	0.41	109.71	0.42	0.32	460.14	0.58	0.54
0.284	89.64	0.35	0.27	114.88	0.42	0.41	109.41	0.41	0.32	460.48	0.58	0.54
0.304	90.17	0.36	0.27	114.14	0.41	0.41	109.16	0.41	0.32	460.20	0.58	0.54
0.326	90.56	0.36	0.27	113.41	0.41	0.40	109.05	0.41	0.32	459.25	0.58	0.54
0.349	90.93	0.36	0.28	112.69	0.41	0.40	109.17	0.41	0.32	457.61	0.58	0.54
0.374	91.41	0.36	0.28	112.00	0.40	0.40	109.54	0.41	0.32	455.36	0.57	0.54
0.401	92.12	0.36	0.28	111.36	0.40	0.40	110.15	0.42	0.32	452.59	0.57	0.53
0.43	93.16	0.37	0.28	110.84	0.40	0.39	110.97	0.42	0.32	449.46	0.56	0.53
0.461	94.59	0.37	0.29	110.48	0.40	0.39	111.90	0.42	0.32	446.11	0.56	0.53
0.494	96.44	0.38	0.29	110.36	0.40	0.39	112.87	0.43	0.33	442.68	0.56	0.52
0.53	98.71	0.39	0.30	110.52	0.40	0.39	113.80	0.43	0.33	439.25	0.55	0.52
0.568	101.36	0.40	0.31	111.02	0.40	0.40	114.64	0.43	0.33	435.88	0.55	0.51
0.608	104.35	0.41	0.32	111.91	0.40	0.40	115.35	0.44	0.33	432.57	0.54	0.51
0.652	107.61	0.42	0.33	113.20	0.41	0.40	115.93	0.44	0.34	429.31	0.54	0.51
0.699	111.09	0.44	0.34	114.87	0.42	0.41	116.41	0.44	0.34	426.04	0.54	0.50
0.749	114.72	0.45	0.35	116.92	0.42	0.42	116.84	0.44	0.34	422.68	0.53	0.50
0.803	118.41	0.47	0.36	119.30	0.43	0.42	117.31	0.44	0.34	419.16	0.53	0.49
0.861	122.11	0.48	0.37	121.96	0.44	0.43	117.89	0.45	0.34	415.35	0.52	0.49
0.923	125.73	0.50	0.38	124.82	0.45	0.44	118.66	0.45	0.34	411.17	0.52	0.48
0.989	129.20	0.51	0.39	127.80	0.46	0.45	119.69	0.45	0.35	406.53	0.51	0.48
1.06	132.45	0.52	0.40	130.82	0.47	0.47	121.00	0.46	0.35	401.40	0.50	0.47
1.136	135.41	0.53	0.41	133.76	0.48	0.48	122.58	0.46	0.35	395.77	0.50	0.47
1.218	138.03	0.54	0.42	136.52	0.49	0.49	124.39	0.47	0.36	389.71	0.49	0.46
1.306	140.27	0.55	0.42	138.96	0.50	0.49	126.35	0.48	0.37	383.34	0.48	0.45
1.399	142.09	0.56	0.43	140.96	0.51	0.50	128.36	0.49	0.37	376.78	0.47	0.44
1.5	143.49	0.57	0.43	142.40	0.51	0.51	130.32	0.49	0.38	370.16	0.47	0.44

Table F54. Circular velocity curves of the 238 (E1–Sdm) CALIFA galaxies with 75th and 25th percentile uncertainties.

R/R_e	UGC10123			UGC10205			UGC10257			UGC10331		
	V_c	ΔV_c^{75th}	ΔV_c^{25th}									
0.05	28.54	0.06	0.07	109.58	0.12	0.14	53.29	0.16	0.15	25.79	0.18	0.26
0.054	30.49	0.07	0.07	116.57	0.13	0.15	56.06	0.17	0.16	27.51	0.20	0.28
0.057	32.59	0.07	0.08	123.88	0.14	0.16	58.84	0.18	0.17	29.35	0.21	0.30
0.062	34.83	0.08	0.09	131.49	0.14	0.17	61.61	0.19	0.18	31.30	0.23	0.32
0.066	37.23	0.08	0.09	139.38	0.15	0.18	64.34	0.20	0.18	33.37	0.24	0.34
0.071	39.79	0.09	0.10	147.51	0.16	0.19	66.99	0.21	0.19	35.56	0.26	0.37
0.076	42.53	0.09	0.10	155.84	0.17	0.20	69.53	0.21	0.20	37.87	0.27	0.39
0.081	45.44	0.10	0.11	164.32	0.18	0.21	71.93	0.22	0.21	40.31	0.29	0.42
0.087	48.54	0.11	0.12	172.88	0.19	0.22	74.18	0.23	0.21	42.86	0.31	0.44
0.093	51.84	0.11	0.13	181.43	0.20	0.23	76.25	0.24	0.22	45.54	0.33	0.47
0.1	55.33	0.12	0.14	189.89	0.21	0.25	78.14	0.24	0.22	48.32	0.35	0.50
0.107	59.04	0.13	0.15	198.13	0.22	0.26	79.87	0.25	0.23	51.21	0.37	0.53
0.115	62.95	0.14	0.16	206.06	0.23	0.27	81.48	0.25	0.23	54.19	0.39	0.56
0.123	67.08	0.15	0.17	213.54	0.23	0.28	83.01	0.26	0.24	57.24	0.42	0.59
0.132	71.42	0.16	0.18	220.45	0.24	0.28	84.53	0.26	0.24	60.34	0.44	0.63
0.142	75.97	0.17	0.19	226.67	0.25	0.29	86.11	0.27	0.25	63.46	0.46	0.66
0.152	80.73	0.18	0.20	232.10	0.26	0.30	87.82	0.27	0.25	66.58	0.49	0.69
0.163	85.69	0.19	0.21	236.69	0.26	0.31	89.70	0.28	0.26	69.65	0.51	0.72
0.174	90.83	0.20	0.23	240.41	0.26	0.31	91.79	0.28	0.26	72.63	0.53	0.75
0.187	96.12	0.21	0.24	243.29	0.27	0.31	94.06	0.29	0.27	75.46	0.55	0.78
0.2	101.55	0.22	0.25	245.43	0.27	0.32	96.50	0.30	0.28	78.11	0.57	0.81
0.215	107.08	0.23	0.27	247.00	0.27	0.32	99.03	0.31	0.28	80.51	0.59	0.84
0.23	112.66	0.25	0.28	248.20	0.27	0.32	101.58	0.31	0.29	82.60	0.60	0.86
0.247	118.24	0.26	0.29	249.29	0.27	0.32	104.08	0.32	0.30	84.35	0.62	0.88
0.265	123.77	0.27	0.31	250.51	0.28	0.32	106.44	0.33	0.30	85.72	0.63	0.89
0.284	129.18	0.28	0.32	252.08	0.28	0.33	108.60	0.34	0.31	86.68	0.63	0.90
0.304	134.39	0.29	0.33	254.18	0.28	0.33	110.50	0.34	0.32	87.26	0.64	0.91
0.326	139.34	0.31	0.35	256.90	0.28	0.33	112.10	0.35	0.32	87.50	0.64	0.91
0.349	143.95	0.32	0.36	260.28	0.29	0.34	113.38	0.35	0.32	87.46	0.64	0.91
0.374	148.17	0.32	0.37	264.27	0.29	0.34	114.36	0.35	0.33	87.27	0.64	0.91
0.401	151.95	0.33	0.38	268.80	0.30	0.35	115.10	0.36	0.33	87.07	0.64	0.90
0.43	155.27	0.34	0.39	273.77	0.30	0.35	115.68	0.36	0.33	87.00	0.64	0.90
0.461	158.14	0.35	0.39	279.02	0.31	0.36	116.22	0.36	0.33	87.21	0.64	0.91
0.494	160.62	0.35	0.40	284.41	0.31	0.37	116.86	0.36	0.33	87.81	0.64	0.91
0.53	162.80	0.36	0.40	289.78	0.32	0.37	117.73	0.36	0.34	88.87	0.65	0.92
0.568	164.83	0.36	0.41	294.95	0.32	0.38	118.96	0.37	0.34	90.42	0.66	0.94
0.608	166.86	0.37	0.41	299.79	0.33	0.39	120.61	0.37	0.35	92.42	0.67	0.96
0.652	169.05	0.37	0.42	304.14	0.33	0.39	122.72	0.38	0.35	94.83	0.69	0.98
0.699	171.54	0.38	0.43	307.92	0.34	0.40	125.25	0.39	0.36	97.57	0.71	1.01
0.749	174.41	0.38	0.43	311.06	0.34	0.40	128.15	0.40	0.37	100.59	0.73	1.04
0.803	177.67	0.39	0.44	313.54	0.35	0.40	131.34	0.41	0.38	103.80	0.76	1.08
0.861	181.29	0.40	0.45	315.40	0.35	0.41	134.71	0.42	0.39	107.11	0.78	1.11
0.923	185.13	0.41	0.46	316.70	0.35	0.41	138.15	0.43	0.40	110.46	0.81	1.15
0.989	189.03	0.41	0.47	317.52	0.35	0.41	141.54	0.44	0.41	113.73	0.83	1.18
1.06	192.82	0.42	0.48	317.93	0.35	0.41	144.76	0.45	0.41	116.85	0.85	1.21
1.136	196.28	0.43	0.49	317.98	0.35	0.41	147.68	0.46	0.42	119.70	0.87	1.24
1.218	199.23	0.44	0.50	317.68	0.35	0.41	150.19	0.47	0.43	122.20	0.89	1.27
1.306	201.48	0.44	0.50	316.98	0.35	0.41	152.17	0.47	0.44	124.24	0.91	1.29
1.399	202.87	0.44	0.50	315.82	0.35	0.41	153.53	0.48	0.44	125.74	0.92	1.31
1.5	203.25	0.45	0.51	314.11	0.35	0.41	154.19	0.48	0.44	126.63	0.92	1.32

Table F55. Circular velocity curves of the 238 (E1–Sdm) CALIFA galaxies with 75th and 25th percentile uncertainties.

R/R_e	UGC10337			UGC10384			UGC10388			UGC10650		
	V_c	ΔV_c^{75th}	ΔV_c^{25th}									
0.05	88.98	0.17	0.28	74.21	0.25	0.23	63.31	0.12	0.09	41.44	0.45	0.42
0.054	94.57	0.18	0.30	76.78	0.26	0.23	67.65	0.13	0.10	44.21	0.48	0.45
0.057	100.39	0.19	0.31	79.17	0.27	0.24	72.27	0.14	0.11	47.14	0.52	0.48
0.062	106.42	0.21	0.33	81.38	0.28	0.25	77.18	0.15	0.12	50.23	0.55	0.51
0.066	112.64	0.22	0.35	83.40	0.28	0.25	82.39	0.16	0.12	53.50	0.59	0.55
0.071	119.01	0.23	0.37	85.25	0.29	0.26	87.90	0.17	0.13	56.94	0.63	0.58
0.076	125.49	0.24	0.39	86.97	0.29	0.27	93.73	0.18	0.14	60.55	0.67	0.62
0.081	132.03	0.26	0.41	88.63	0.30	0.27	99.88	0.19	0.15	64.31	0.71	0.66
0.087	138.55	0.27	0.43	90.30	0.31	0.28	106.34	0.21	0.16	68.23	0.75	0.70
0.093	144.99	0.28	0.46	92.09	0.31	0.28	113.12	0.22	0.17	72.29	0.80	0.74
0.1	151.23	0.29	0.47	94.08	0.32	0.29	120.21	0.23	0.18	76.46	0.84	0.78
0.107	157.20	0.31	0.49	96.36	0.33	0.29	127.58	0.25	0.19	80.73	0.89	0.83
0.115	162.77	0.32	0.51	98.95	0.34	0.30	135.22	0.26	0.20	85.06	0.94	0.87
0.123	167.83	0.33	0.53	101.87	0.35	0.31	143.08	0.28	0.22	89.42	0.99	0.92
0.132	172.26	0.33	0.54	105.08	0.36	0.32	151.14	0.30	0.23	93.75	1.04	0.96
0.142	175.97	0.34	0.55	108.51	0.37	0.33	159.33	0.31	0.24	98.01	1.08	1.00
0.152	178.87	0.35	0.56	112.07	0.38	0.34	167.58	0.33	0.25	102.13	1.13	1.05
0.163	180.91	0.35	0.57	115.66	0.39	0.35	175.80	0.34	0.26	106.04	1.17	1.09
0.174	182.08	0.35	0.57	119.18	0.40	0.36	183.91	0.36	0.28	109.67	1.21	1.12
0.187	182.44	0.35	0.57	122.53	0.42	0.37	191.78	0.37	0.29	112.94	1.25	1.16
0.2	182.11	0.35	0.57	125.61	0.43	0.38	199.30	0.39	0.30	115.77	1.28	1.19
0.215	181.27	0.35	0.57	128.33	0.43	0.39	206.32	0.40	0.31	118.11	1.31	1.21
0.23	180.16	0.35	0.57	130.60	0.44	0.40	212.72	0.42	0.32	119.90	1.33	1.23
0.247	179.04	0.35	0.56	132.35	0.45	0.40	218.35	0.43	0.33	121.12	1.34	1.24
0.265	178.17	0.35	0.56	133.56	0.45	0.41	223.11	0.44	0.34	121.76	1.35	1.25
0.284	177.79	0.35	0.56	134.22	0.45	0.41	226.90	0.44	0.34	121.87	1.35	1.25
0.304	178.06	0.35	0.56	134.38	0.46	0.41	229.68	0.45	0.35	121.53	1.34	1.25
0.326	179.07	0.35	0.56	134.14	0.45	0.41	231.45	0.45	0.35	120.84	1.34	1.24
0.349	180.84	0.35	0.57	133.63	0.45	0.41	232.29	0.45	0.35	119.94	1.33	1.23
0.374	183.34	0.36	0.58	133.03	0.45	0.41	232.33	0.45	0.35	118.99	1.32	1.22
0.401	186.50	0.36	0.59	132.56	0.45	0.41	231.76	0.45	0.35	118.12	1.31	1.21
0.43	190.23	0.37	0.60	132.40	0.45	0.40	230.82	0.45	0.35	117.44	1.30	1.20
0.461	194.44	0.38	0.61	132.72	0.45	0.41	229.72	0.45	0.35	117.02	1.29	1.20
0.494	199.02	0.39	0.62	133.64	0.45	0.41	228.65	0.45	0.34	116.88	1.29	1.20
0.53	203.88	0.40	0.64	135.23	0.46	0.41	227.74	0.44	0.34	117.02	1.29	1.20
0.568	208.92	0.41	0.66	137.48	0.47	0.42	227.02	0.44	0.34	117.39	1.30	1.20
0.608	214.05	0.42	0.67	140.37	0.48	0.43	226.44	0.44	0.34	117.93	1.30	1.21
0.652	219.20	0.43	0.69	143.84	0.49	0.44	225.89	0.44	0.34	118.57	1.31	1.22
0.699	224.30	0.44	0.70	147.82	0.50	0.45	225.24	0.44	0.34	119.26	1.32	1.22
0.749	229.32	0.45	0.72	152.23	0.52	0.47	224.38	0.44	0.34	119.94	1.33	1.23
0.803	234.23	0.46	0.74	156.97	0.53	0.48	223.19	0.44	0.34	120.60	1.33	1.24
0.861	239.02	0.46	0.75	161.93	0.55	0.50	221.65	0.43	0.33	121.23	1.34	1.24
0.923	243.69	0.47	0.77	167.01	0.57	0.51	219.76	0.43	0.33	121.86	1.35	1.25
0.989	248.22	0.48	0.78	172.08	0.58	0.53	217.59	0.43	0.33	122.52	1.36	1.26
1.06	252.55	0.49	0.79	176.99	0.60	0.54	215.26	0.42	0.32	123.26	1.36	1.26
1.136	256.61	0.50	0.81	181.60	0.62	0.56	212.91	0.42	0.32	124.12	1.37	1.27
1.218	260.23	0.51	0.82	185.74	0.63	0.57	210.70	0.41	0.32	125.11	1.38	1.28
1.306	263.24	0.51	0.83	189.27	0.64	0.58	208.73	0.41	0.31	126.20	1.40	1.29
1.399	265.42	0.52	0.83	192.03	0.65	0.59	207.09	0.40	0.31	127.33	1.41	1.31
1.5	266.54	0.52	0.84	193.88	0.66	0.59	205.78	0.40	0.31	128.41	1.42	1.32

Table F56. Circular velocity curves of the 238 (E1–Sdm) CALIFA galaxies with 75th and 25th percentile uncertainties.

R/R_e	UGC10693			UGC10695			UGC10710			UGC10796		
	V_c	ΔV_c^{75th}	ΔV_c^{25th}									
0.05	229.01	0.59	0.50	197.84	0.36	0.34	110.75	0.24	0.19	63.63	0.50	0.56
0.054	242.13	0.63	0.52	208.10	0.38	0.36	117.28	0.26	0.20	66.37	0.52	0.58
0.057	255.53	0.66	0.55	218.36	0.40	0.38	123.99	0.27	0.21	69.04	0.54	0.61
0.062	269.12	0.70	0.58	228.51	0.42	0.40	130.85	0.29	0.23	71.62	0.56	0.63
0.066	282.79	0.73	0.61	238.44	0.44	0.41	137.80	0.30	0.24	74.07	0.58	0.65
0.071	296.42	0.77	0.64	248.01	0.46	0.43	144.79	0.32	0.25	76.39	0.60	0.67
0.076	309.85	0.80	0.67	257.09	0.47	0.45	151.74	0.33	0.26	78.57	0.62	0.69
0.081	322.94	0.84	0.70	265.56	0.49	0.46	158.60	0.35	0.27	80.61	0.63	0.71
0.087	335.53	0.87	0.73	273.29	0.50	0.47	165.26	0.36	0.28	82.53	0.65	0.73
0.093	347.45	0.90	0.75	280.21	0.52	0.49	171.65	0.38	0.30	84.33	0.66	0.74
0.1	358.55	0.93	0.78	286.26	0.53	0.50	177.68	0.39	0.31	86.04	0.68	0.76
0.107	368.72	0.96	0.80	291.44	0.54	0.50	183.27	0.40	0.32	87.67	0.69	0.77
0.115	377.87	0.98	0.82	295.80	0.55	0.51	188.33	0.41	0.32	89.24	0.70	0.79
0.123	385.95	1.00	0.84	299.44	0.55	0.52	192.83	0.42	0.33	90.75	0.71	0.80
0.132	392.99	1.02	0.85	302.50	0.56	0.52	196.73	0.43	0.34	92.18	0.72	0.81
0.142	399.05	1.03	0.86	305.14	0.56	0.53	200.03	0.44	0.34	93.51	0.73	0.82
0.152	404.23	1.05	0.88	307.51	0.57	0.53	202.77	0.45	0.35	94.72	0.74	0.83
0.163	408.64	1.06	0.89	309.73	0.57	0.54	205.00	0.45	0.35	95.76	0.75	0.84
0.174	412.38	1.07	0.89	311.84	0.57	0.54	206.81	0.46	0.36	96.63	0.76	0.85
0.187	415.48	1.08	0.90	313.83	0.58	0.54	208.28	0.46	0.36	97.31	0.76	0.86
0.2	417.94	1.08	0.91	315.65	0.58	0.55	209.50	0.46	0.36	97.83	0.77	0.86
0.215	419.68	1.09	0.91	317.22	0.58	0.55	210.54	0.46	0.36	98.20	0.77	0.86
0.23	420.59	1.09	0.91	318.47	0.59	0.55	211.46	0.47	0.36	98.47	0.77	0.87
0.247	420.57	1.09	0.91	319.37	0.59	0.55	212.28	0.47	0.37	98.70	0.78	0.87
0.265	419.60	1.09	0.91	319.94	0.59	0.55	213.04	0.47	0.37	98.93	0.78	0.87
0.284	417.73	1.08	0.91	320.22	0.59	0.55	213.75	0.47	0.37	99.20	0.78	0.87
0.304	415.11	1.08	0.90	320.29	0.59	0.55	214.45	0.47	0.37	99.53	0.78	0.88
0.326	411.99	1.07	0.89	320.21	0.59	0.55	215.18	0.47	0.37	99.91	0.78	0.88
0.349	408.66	1.06	0.89	320.02	0.59	0.55	216.00	0.48	0.37	100.32	0.79	0.88
0.374	405.38	1.05	0.88	319.73	0.59	0.55	216.97	0.48	0.37	100.71	0.79	0.89
0.401	402.32	1.04	0.87	319.30	0.59	0.55	218.16	0.48	0.38	101.05	0.79	0.89
0.43	399.56	1.04	0.87	318.66	0.59	0.55	219.61	0.48	0.38	101.29	0.80	0.89
0.461	397.02	1.03	0.86	317.77	0.59	0.55	221.33	0.49	0.38	101.40	0.80	0.89
0.494	394.53	1.02	0.85	316.60	0.58	0.55	223.28	0.49	0.38	101.36	0.80	0.89
0.53	391.88	1.02	0.85	315.17	0.58	0.55	225.39	0.50	0.39	101.17	0.79	0.89
0.568	388.83	1.01	0.84	313.56	0.58	0.54	227.54	0.50	0.39	100.86	0.79	0.89
0.608	385.22	1.00	0.83	311.88	0.57	0.54	229.62	0.51	0.40	100.47	0.79	0.89
0.652	380.96	0.99	0.83	310.23	0.57	0.54	231.51	0.51	0.40	100.07	0.79	0.88
0.699	376.07	0.97	0.81	308.70	0.57	0.53	233.11	0.51	0.40	99.75	0.78	0.88
0.749	370.69	0.96	0.80	307.31	0.57	0.53	234.33	0.52	0.40	99.56	0.78	0.88
0.803	365.01	0.95	0.79	306.02	0.56	0.53	235.16	0.52	0.41	99.59	0.78	0.88
0.861	359.27	0.93	0.78	304.73	0.56	0.53	235.61	0.52	0.41	99.86	0.78	0.88
0.923	353.71	0.92	0.77	303.30	0.56	0.53	235.72	0.52	0.41	100.41	0.79	0.88
0.989	348.47	0.90	0.76	301.57	0.56	0.52	235.59	0.52	0.41	101.23	0.80	0.89
1.06	343.62	0.89	0.74	299.40	0.55	0.52	235.35	0.52	0.41	102.30	0.80	0.90
1.136	339.07	0.88	0.73	296.72	0.55	0.51	235.14	0.52	0.41	103.57	0.81	0.91
1.218	334.69	0.87	0.73	293.51	0.54	0.51	235.08	0.52	0.41	104.98	0.82	0.92
1.306	330.26	0.86	0.72	289.83	0.53	0.50	235.25	0.52	0.41	106.46	0.84	0.94
1.399	325.61	0.84	0.71	285.81	0.53	0.50	235.66	0.52	0.41	107.93	0.85	0.95
1.5	320.62	0.83	0.69	281.61	0.52	0.49	236.24	0.52	0.41	109.30	0.86	0.96

Table F57. Circular velocity curves of the 238 (E1–Sdm) CALIFA galaxies with 75th and 25th percentile uncertainties.

R/R_e	UGC10811			UGC10905			UGC10972			UGC11228		
	V_c	ΔV_c^{75th}	ΔV_c^{25th}									
0.05	122.44	0.34	0.32	122.21	0.16	0.19	109.75	0.29	0.24	127.48	0.42	0.22
0.054	130.05	0.37	0.34	130.57	0.17	0.20	112.93	0.30	0.25	135.60	0.44	0.23
0.057	137.96	0.39	0.36	139.44	0.18	0.22	115.75	0.30	0.26	144.10	0.47	0.25
0.062	146.14	0.41	0.39	148.83	0.19	0.23	118.15	0.31	0.26	152.94	0.50	0.26
0.066	154.56	0.44	0.41	158.75	0.20	0.25	120.13	0.32	0.27	162.12	0.53	0.28
0.071	163.17	0.46	0.43	169.22	0.22	0.26	121.67	0.32	0.27	171.58	0.56	0.30
0.076	171.91	0.48	0.45	180.24	0.23	0.28	122.80	0.32	0.27	181.29	0.59	0.31
0.081	180.71	0.51	0.48	191.80	0.25	0.30	123.54	0.33	0.27	191.18	0.63	0.33
0.087	189.49	0.53	0.50	203.88	0.26	0.32	123.96	0.33	0.28	201.20	0.66	0.35
0.093	198.16	0.56	0.52	216.48	0.28	0.34	124.12	0.33	0.28	211.25	0.69	0.37
0.1	206.61	0.58	0.54	229.54	0.29	0.36	124.07	0.33	0.28	221.24	0.73	0.38
0.107	214.74	0.61	0.57	243.01	0.31	0.38	123.87	0.33	0.28	231.07	0.76	0.40
0.115	222.44	0.63	0.59	256.83	0.33	0.40	123.56	0.33	0.28	240.62	0.79	0.42
0.123	229.61	0.65	0.61	270.90	0.35	0.42	123.17	0.32	0.27	249.80	0.82	0.43
0.132	236.17	0.67	0.62	285.12	0.37	0.44	122.72	0.32	0.27	258.48	0.85	0.45
0.142	242.06	0.68	0.64	299.33	0.38	0.46	122.21	0.32	0.27	266.58	0.87	0.46
0.152	247.28	0.70	0.65	313.38	0.40	0.49	121.64	0.32	0.27	274.03	0.90	0.47
0.163	251.85	0.71	0.66	327.08	0.42	0.51	120.98	0.32	0.27	280.80	0.92	0.49
0.174	255.84	0.72	0.67	340.22	0.44	0.53	120.21	0.32	0.27	286.87	0.94	0.50
0.187	259.37	0.73	0.68	352.56	0.45	0.55	119.32	0.31	0.27	292.29	0.96	0.51
0.2	262.56	0.74	0.69	363.87	0.47	0.56	118.30	0.31	0.26	297.12	0.97	0.51
0.215	265.54	0.75	0.70	373.91	0.48	0.58	117.17	0.31	0.26	301.44	0.99	0.52
0.23	268.40	0.76	0.71	382.46	0.49	0.59	115.97	0.31	0.26	305.34	1.00	0.53
0.247	271.15	0.76	0.71	389.34	0.50	0.60	114.79	0.30	0.26	308.87	1.01	0.53
0.265	273.72	0.77	0.72	394.43	0.51	0.61	113.71	0.30	0.25	312.05	1.02	0.54
0.284	275.97	0.78	0.73	397.69	0.51	0.62	112.85	0.30	0.25	314.83	1.03	0.54
0.304	277.72	0.78	0.73	399.20	0.51	0.62	112.30	0.30	0.25	317.15	1.04	0.55
0.326	278.78	0.79	0.74	399.11	0.51	0.62	112.14	0.30	0.25	318.91	1.05	0.55
0.349	278.98	0.79	0.74	397.70	0.51	0.62	112.43	0.30	0.25	320.00	1.05	0.55
0.374	278.23	0.78	0.73	395.30	0.51	0.61	113.21	0.30	0.25	320.37	1.05	0.55
0.401	276.52	0.78	0.73	392.27	0.50	0.61	114.49	0.30	0.25	319.98	1.05	0.55
0.43	273.93	0.77	0.72	388.92	0.50	0.60	116.27	0.31	0.26	318.86	1.05	0.55
0.461	270.62	0.76	0.71	385.50	0.49	0.60	118.54	0.31	0.26	317.08	1.04	0.55
0.494	266.82	0.75	0.70	382.10	0.49	0.59	121.27	0.32	0.27	314.74	1.03	0.54
0.53	262.80	0.74	0.69	378.71	0.49	0.59	124.44	0.33	0.28	311.97	1.02	0.54
0.568	258.80	0.73	0.68	375.24	0.48	0.58	127.98	0.34	0.28	308.90	1.01	0.53
0.608	255.06	0.72	0.67	371.55	0.48	0.58	131.86	0.35	0.29	305.64	1.00	0.53
0.652	251.73	0.71	0.66	367.52	0.47	0.57	135.99	0.36	0.30	302.31	0.99	0.52
0.699	248.93	0.70	0.66	363.08	0.47	0.56	140.30	0.37	0.31	298.98	0.98	0.52
0.749	246.72	0.70	0.65	358.25	0.46	0.55	144.70	0.38	0.32	295.69	0.97	0.51
0.803	245.09	0.69	0.65	353.13	0.45	0.55	149.09	0.39	0.33	292.44	0.96	0.51
0.861	244.05	0.69	0.64	347.90	0.45	0.54	153.35	0.40	0.34	289.19	0.95	0.50
0.923	243.58	0.69	0.64	342.74	0.44	0.53	157.37	0.41	0.35	285.86	0.94	0.49
0.989	243.64	0.69	0.64	337.85	0.43	0.52	161.01	0.42	0.36	282.37	0.93	0.49
1.06	244.22	0.69	0.64	333.39	0.43	0.52	164.18	0.43	0.37	278.67	0.91	0.48
1.136	245.30	0.69	0.65	329.42	0.42	0.51	166.75	0.44	0.37	274.73	0.90	0.48
1.218	246.83	0.70	0.65	325.93	0.42	0.50	168.63	0.44	0.38	270.58	0.89	0.47
1.306	248.79	0.70	0.66	322.81	0.41	0.50	169.77	0.45	0.38	266.28	0.87	0.46
1.399	251.10	0.71	0.66	319.90	0.41	0.50	170.13	0.45	0.38	261.94	0.86	0.45
1.5	253.69	0.72	0.67	317.02	0.41	0.49	169.75	0.45	0.38	257.64	0.84	0.45

Table F58. Circular velocity curves of the 238 (E1–Sdm) CALIFA galaxies with 75th and 25th percentile uncertainties.

R/R_e	UGC11717			UGC12054			UGC12127			UGC12185		
	V_c	ΔV_c^{75th}	ΔV_c^{25th}									
0.05	99.39	0.41	0.34	17.97	0.12	0.14	366.02	0.64	0.79	58.92	0.16	0.16
0.054	106.08	0.44	0.37	18.97	0.13	0.15	378.90	0.66	0.82	62.90	0.17	0.17
0.057	113.16	0.47	0.39	20.05	0.13	0.16	390.96	0.68	0.84	67.11	0.18	0.18
0.062	120.63	0.50	0.42	21.21	0.14	0.18	402.07	0.70	0.87	71.56	0.20	0.19
0.066	128.49	0.53	0.44	22.45	0.15	0.19	412.11	0.72	0.89	76.26	0.21	0.20
0.071	136.74	0.57	0.47	23.77	0.17	0.20	421.01	0.73	0.91	81.21	0.22	0.22
0.076	145.37	0.60	0.50	25.16	0.18	0.22	428.71	0.74	0.92	86.40	0.24	0.23
0.081	154.37	0.64	0.53	26.62	0.19	0.23	435.17	0.76	0.94	91.83	0.25	0.25
0.087	163.71	0.68	0.57	28.15	0.20	0.24	440.40	0.76	0.95	97.50	0.27	0.26
0.093	173.35	0.72	0.60	29.73	0.21	0.26	444.44	0.77	0.96	103.37	0.28	0.28
0.1	183.24	0.76	0.63	31.37	0.23	0.27	447.37	0.78	0.97	109.45	0.30	0.29
0.107	193.31	0.80	0.67	33.04	0.24	0.29	449.32	0.78	0.97	115.69	0.32	0.31
0.115	203.50	0.84	0.70	34.75	0.25	0.31	450.48	0.78	0.97	122.06	0.34	0.33
0.123	213.70	0.88	0.74	36.47	0.26	0.32	451.06	0.78	0.97	128.53	0.35	0.35
0.132	223.78	0.93	0.77	38.20	0.28	0.34	451.33	0.78	0.97	135.03	0.37	0.36
0.142	233.62	0.97	0.81	39.91	0.29	0.35	451.52	0.78	0.97	141.51	0.39	0.38
0.152	243.07	1.01	0.84	41.58	0.30	0.37	451.80	0.78	0.97	147.90	0.41	0.40
0.163	251.95	1.04	0.87	43.22	0.31	0.38	452.26	0.79	0.98	154.14	0.42	0.41
0.174	260.09	1.08	0.90	44.79	0.33	0.40	452.87	0.79	0.98	160.13	0.44	0.43
0.187	267.32	1.11	0.92	46.29	0.34	0.41	453.54	0.79	0.98	165.82	0.46	0.45
0.2	273.48	1.13	0.95	47.72	0.35	0.42	454.14	0.79	0.98	171.12	0.47	0.46
0.215	278.44	1.15	0.96	49.09	0.36	0.44	454.53	0.79	0.98	175.98	0.48	0.47
0.23	282.12	1.17	0.98	50.41	0.37	0.45	454.63	0.79	0.98	180.34	0.50	0.49
0.247	284.50	1.18	0.98	51.72	0.38	0.46	454.39	0.79	0.98	184.17	0.51	0.50
0.265	285.66	1.18	0.99	53.05	0.39	0.47	453.78	0.79	0.98	187.45	0.52	0.50
0.284	285.76	1.18	0.99	54.45	0.40	0.48	452.80	0.79	0.98	190.21	0.52	0.51
0.304	285.05	1.18	0.99	55.97	0.41	0.50	451.41	0.78	0.97	192.46	0.53	0.52
0.326	283.88	1.17	0.98	57.65	0.42	0.51	449.53	0.78	0.97	194.28	0.53	0.52
0.349	282.63	1.17	0.98	59.53	0.44	0.53	447.07	0.78	0.96	195.75	0.54	0.53
0.374	281.64	1.16	0.97	61.63	0.45	0.55	443.95	0.77	0.96	196.96	0.54	0.53
0.401	281.23	1.16	0.97	63.94	0.47	0.57	440.10	0.76	0.95	198.04	0.54	0.53
0.43	281.57	1.16	0.97	66.47	0.49	0.59	435.54	0.76	0.94	199.14	0.55	0.54
0.461	282.73	1.17	0.98	69.16	0.51	0.62	430.34	0.75	0.93	200.41	0.55	0.54
0.494	284.63	1.18	0.98	72.00	0.53	0.64	424.68	0.74	0.92	201.97	0.56	0.54
0.53	287.12	1.19	0.99	74.94	0.55	0.67	418.78	0.73	0.90	203.94	0.56	0.55
0.568	289.98	1.20	1.00	77.93	0.57	0.69	412.88	0.72	0.89	206.38	0.57	0.56
0.608	292.98	1.21	1.01	80.92	0.59	0.72	407.18	0.71	0.88	209.27	0.58	0.56
0.652	295.86	1.22	1.02	83.86	0.61	0.75	401.78	0.70	0.87	212.56	0.58	0.57
0.699	298.40	1.23	1.03	86.69	0.63	0.77	396.71	0.69	0.86	216.14	0.59	0.58
0.749	300.36	1.24	1.04	89.36	0.65	0.80	391.85	0.68	0.85	219.84	0.60	0.59
0.803	301.58	1.25	1.04	91.80	0.67	0.82	387.03	0.67	0.84	223.50	0.61	0.60
0.861	301.92	1.25	1.04	93.97	0.69	0.84	382.03	0.66	0.82	226.92	0.62	0.61
0.923	301.32	1.25	1.04	95.84	0.70	0.85	376.65	0.65	0.81	229.91	0.63	0.62
0.989	299.79	1.24	1.04	97.37	0.71	0.87	370.76	0.64	0.80	232.27	0.64	0.63
1.06	297.43	1.23	1.03	98.56	0.72	0.88	364.28	0.63	0.79	233.82	0.64	0.63
1.136	294.41	1.22	1.02	99.42	0.73	0.89	357.25	0.62	0.77	234.43	0.64	0.63
1.218	290.93	1.20	1.01	100.00	0.73	0.89	349.78	0.61	0.75	234.01	0.64	0.63
1.306	287.22	1.19	0.99	100.35	0.73	0.89	342.07	0.59	0.74	232.51	0.64	0.63
1.399	283.49	1.17	0.98	100.53	0.74	0.90	334.37	0.58	0.72	230.00	0.63	0.62
1.5	279.88	1.16	0.97	100.61	0.74	0.90	326.91	0.57	0.71	226.62	0.62	0.61

Table F59. Circular velocity curves of the 238 (E1-Sdm) CALIFA galaxies with 75th and 25th percentile uncertainties.

R/R_e	UGC12274			UGC12308			UGC12518			UGC12519		
	V_c	ΔV_c^{75th}	ΔV_c^{25th}									
0.05	105.77	0.29	0.28	37.90	0.21	0.18	25.14	2.81	0.40	36.64	0.15	0.14
0.054	112.59	0.31	0.30	40.34	0.22	0.19	26.78	3.01	0.43	38.90	0.16	0.15
0.057	119.75	0.33	0.32	42.91	0.24	0.21	28.53	3.23	0.46	41.25	0.17	0.16
0.062	127.22	0.35	0.34	45.61	0.25	0.22	30.39	3.46	0.49	43.69	0.18	0.17
0.066	134.99	0.37	0.36	48.44	0.27	0.23	32.38	3.70	0.52	46.21	0.19	0.18
0.071	143.03	0.39	0.38	51.38	0.29	0.25	34.49	3.95	0.56	48.80	0.20	0.19
0.076	151.32	0.41	0.40	54.43	0.30	0.26	36.72	4.22	0.60	51.43	0.21	0.20
0.081	159.81	0.44	0.42	57.58	0.32	0.28	39.08	4.50	0.64	54.09	0.22	0.22
0.087	168.45	0.46	0.45	60.80	0.34	0.29	41.57	4.79	0.68	56.75	0.23	0.23
0.093	177.16	0.48	0.47	64.08	0.36	0.31	44.17	5.10	0.72	59.39	0.24	0.24
0.1	185.88	0.51	0.49	67.38	0.38	0.32	46.90	5.42	0.77	61.98	0.26	0.25
0.107	194.51	0.53	0.52	70.67	0.39	0.34	49.74	5.76	0.82	64.48	0.27	0.26
0.115	202.96	0.55	0.54	73.90	0.41	0.36	52.68	6.10	0.87	66.87	0.28	0.27
0.123	211.12	0.58	0.56	77.05	0.43	0.37	55.71	6.46	0.92	69.12	0.28	0.28
0.132	218.89	0.60	0.58	80.04	0.45	0.39	58.82	6.82	0.97	71.21	0.29	0.28
0.142	226.16	0.62	0.60	82.83	0.46	0.40	61.99	7.19	1.02	73.12	0.30	0.29
0.152	232.86	0.64	0.62	85.37	0.48	0.41	65.19	7.56	1.07	74.87	0.31	0.30
0.163	238.89	0.65	0.63	87.59	0.49	0.42	68.39	7.94	1.13	76.47	0.32	0.31
0.174	244.23	0.67	0.65	89.46	0.50	0.43	71.57	8.31	1.18	77.96	0.32	0.31
0.187	248.86	0.68	0.66	90.93	0.51	0.44	74.70	8.67	1.23	79.41	0.33	0.32
0.2	252.80	0.69	0.67	92.01	0.51	0.44	77.74	9.03	1.28	80.89	0.33	0.32
0.215	256.08	0.70	0.68	92.69	0.52	0.45	80.65	9.37	1.33	82.49	0.34	0.33
0.23	258.79	0.71	0.69	93.03	0.52	0.45	83.41	9.69	1.38	84.29	0.35	0.34
0.247	260.97	0.71	0.69	93.10	0.52	0.45	85.98	9.99	1.42	86.37	0.36	0.34
0.265	262.68	0.72	0.70	93.01	0.52	0.45	88.35	10.27	1.46	88.75	0.37	0.35
0.284	263.94	0.72	0.70	92.89	0.52	0.45	90.50	10.52	1.49	91.46	0.38	0.36
0.304	264.74	0.72	0.70	92.88	0.52	0.45	92.43	10.74	1.52	94.48	0.39	0.38
0.326	265.03	0.72	0.70	93.09	0.52	0.45	94.15	10.94	1.55	97.78	0.40	0.39
0.349	264.78	0.72	0.70	93.61	0.52	0.45	95.66	11.12	1.58	101.29	0.42	0.40
0.374	263.96	0.72	0.70	94.50	0.53	0.46	96.96	11.27	1.60	104.99	0.43	0.42
0.401	262.59	0.72	0.70	95.76	0.54	0.46	98.07	11.40	1.62	108.81	0.45	0.43
0.43	260.75	0.71	0.69	97.35	0.54	0.47	98.97	11.50	1.63	112.71	0.46	0.45
0.461	258.55	0.71	0.69	99.20	0.55	0.48	99.65	11.58	1.64	116.65	0.48	0.47
0.494	256.17	0.70	0.68	101.25	0.57	0.49	100.09	11.63	1.65	120.60	0.50	0.48
0.53	253.82	0.69	0.67	103.41	0.58	0.50	100.28	11.66	1.65	124.55	0.51	0.50
0.568	251.71	0.69	0.67	105.59	0.59	0.51	100.22	11.65	1.65	128.49	0.53	0.51
0.608	250.02	0.68	0.66	107.72	0.60	0.52	99.92	11.61	1.65	132.41	0.55	0.53
0.652	248.91	0.68	0.66	109.70	0.61	0.53	99.43	11.56	1.64	136.34	0.56	0.54
0.699	248.41	0.68	0.66	111.46	0.62	0.54	98.82	11.49	1.63	140.28	0.58	0.56
0.749	248.52	0.68	0.66	112.93	0.63	0.55	98.17	11.41	1.62	144.25	0.59	0.58
0.803	249.15	0.68	0.66	114.08	0.64	0.55	97.59	11.34	1.61	148.25	0.61	0.59
0.861	250.16	0.68	0.66	114.87	0.64	0.55	97.16	11.29	1.60	152.25	0.63	0.61
0.923	251.42	0.69	0.67	115.32	0.64	0.56	96.94	11.27	1.60	156.20	0.64	0.62
0.989	252.76	0.69	0.67	115.45	0.65	0.56	96.97	11.27	1.60	160.02	0.66	0.64
1.06	254.02	0.69	0.67	115.36	0.64	0.56	97.25	11.31	1.60	163.61	0.67	0.65
1.136	255.08	0.70	0.68	115.12	0.64	0.56	97.75	11.36	1.61	166.85	0.69	0.67
1.218	255.82	0.70	0.68	114.87	0.64	0.55	98.39	11.44	1.62	169.59	0.70	0.68
1.306	256.14	0.70	0.68	114.71	0.64	0.55	99.10	11.52	1.64	171.70	0.71	0.69
1.399	255.96	0.70	0.68	114.72	0.64	0.55	99.80	11.60	1.65	173.04	0.71	0.69
1.5	255.23	0.70	0.68	114.95	0.64	0.56	100.39	11.67	1.66	173.51	0.72	0.69

Table F60. Circular velocity curves of the 238 (E1–Sdm) CALIFA galaxies with 75th and 25th percentile uncertainties.

R/R_e	UGC12723			UGC12857		
	V_c	ΔV_c^{75th}	ΔV_c^{25th}	V_c	ΔV_c^{75th}	ΔV_c^{25th}
0.05	9.73	0.03	0.04	14.99	0.08	0.08
0.054	10.28	0.04	0.04	15.82	0.08	0.08
0.057	10.90	0.04	0.04	16.73	0.09	0.09
0.062	11.57	0.04	0.05	17.70	0.10	0.09
0.066	12.30	0.05	0.05	18.73	0.10	0.10
0.071	13.10	0.05	0.06	19.83	0.11	0.11
0.076	13.96	0.05	0.06	21.00	0.12	0.12
0.081	14.90	0.06	0.07	22.23	0.13	0.12
0.087	15.91	0.06	0.07	23.52	0.13	0.13
0.093	17.00	0.07	0.08	24.86	0.14	0.14
0.1	18.17	0.07	0.08	26.27	0.15	0.15
0.107	19.43	0.08	0.09	27.73	0.16	0.16
0.115	20.79	0.08	0.09	29.24	0.17	0.17
0.123	22.24	0.09	0.10	30.80	0.18	0.18
0.132	23.80	0.10	0.11	32.42	0.19	0.18
0.142	25.47	0.10	0.12	34.08	0.20	0.19
0.152	27.26	0.11	0.12	35.80	0.21	0.20
0.163	29.17	0.12	0.13	37.59	0.22	0.22
0.174	31.22	0.13	0.14	39.44	0.23	0.23
0.187	33.41	0.14	0.15	41.37	0.24	0.24
0.2	35.75	0.15	0.16	43.40	0.25	0.25
0.215	38.25	0.16	0.17	45.52	0.27	0.26
0.23	40.91	0.17	0.19	47.76	0.28	0.27
0.247	43.75	0.18	0.20	50.12	0.29	0.29
0.265	46.77	0.19	0.21	52.59	0.31	0.30
0.284	49.98	0.21	0.23	55.17	0.32	0.32
0.304	53.39	0.22	0.24	57.84	0.34	0.33
0.326	57.01	0.23	0.26	60.60	0.36	0.35
0.349	60.84	0.25	0.28	63.41	0.37	0.36
0.374	64.88	0.27	0.30	66.26	0.39	0.38
0.401	69.15	0.28	0.32	69.11	0.41	0.40
0.43	73.63	0.30	0.34	71.96	0.42	0.41
0.461	78.33	0.32	0.36	74.76	0.44	0.43
0.494	83.24	0.34	0.38	77.51	0.46	0.45
0.53	88.35	0.36	0.40	80.19	0.47	0.46
0.568	93.63	0.39	0.43	82.78	0.49	0.48
0.608	99.07	0.41	0.45	85.28	0.50	0.49
0.652	104.64	0.43	0.48	87.69	0.52	0.50
0.699	110.28	0.45	0.50	90.01	0.53	0.52
0.749	115.96	0.48	0.53	92.24	0.54	0.53
0.803	121.59	0.50	0.56	94.40	0.56	0.54
0.861	127.12	0.52	0.58	96.50	0.57	0.56
0.923	132.44	0.54	0.60	98.54	0.58	0.57
0.989	137.46	0.57	0.63	100.51	0.59	0.58
1.06	142.06	0.58	0.65	102.41	0.60	0.59
1.136	146.12	0.60	0.67	104.21	0.61	0.60
1.218	149.53	0.61	0.68	105.88	0.62	0.61
1.306	152.16	0.63	0.70	107.36	0.63	0.62
1.399	153.90	0.63	0.70	108.63	0.64	0.63
1.5	154.66	0.64	0.71	109.65	0.65	0.63

This paper has been typeset from a \TeX / \LaTeX file prepared by the author.